TABLE OF CONTENTS

NOMENCLATURE AND LIST OF ABBREVIATIONS

LANGUAGE

This thesis is written in New Zealand English, which is based on British (rather than US) spelling forms. The exceptions to this are for the spelling of sulfur and its derivatives. "Sulfur", "sulfide", "sulfate' etc... are all spelled with an f, not with a ph, in keeping with mainstream scientific journals.

PLACE NAMES

Where possible, original (Māori) place names are used in this thesis, with their English translations or common Pākeha names given in parentheses in the first instance. The names of towns and cities are an exception to this rule.

SEASONS

New Zealand is in the southern hemisphere, and therefore the seasons are all displaced six months from their northern hemisphere counterparts. In New Zealand, the seasons run:

Summer: December, January, February

Autumn: March, April, May

Winter: June, July, August

Spring: September, October, November

UNITS

All units in this thesis are metric SI units. Aqueous concentrations, unless otherwise specified, were measured in, and are presented as, xg/kg (where x is the appropriate SI prefix (m or μ), which should be assumed to be $xg/kg_{solution}$. For the results for surface waters presented, such concentrations are equivalent to xg/L, but for the results from geothermal brines (where solution density may be greater than 1 kg/L), xg/L is not an appropriate unit. Solid sample concentrations are given as either weight percentages (wt %), or in xg/kg.

CHEMISTRY

Chemical elements are written out in full when first used, and their symbols (initially given in parentheses) are used from then on, except at the start of sentences, where full names are given. This latter rule has not been strictly enforced for compounds and complexes, but they are all written out in full the first time. Unless speciation has been determined, symbols used do not show charge or oxidation state. For ease of reference, a list of the more commonly used names and symbols are given below:

- Antimony (Sb)
- Arsenic (As)
- Chloride (Cl)
- Dissolved oxygen (DO)
- Iron (Fe)
- Manganese (Mn)
- Lithium (Li)
- Oxygen (O)
- Sulfate (SO_4)
- Sulfur (S)
- Bisulfide (HS)
- Hydrogen sulfide (H_2S)
- Stibnite (Sb_2S_3)
- Metal oxy-hydroxide (M-OOH (where M = Fe, Mn or Al)

CHAPTER ONE
INTRODUCTION

> *Of all the Minerals contained within the bowels of the Earth, Antimonium delevereth the greatest praise, for the most excellent medicinall vertues, it containeth for the health and benefit of mankinde.*[1]

Antimony (Sb) is an element situated in Group V on the Periodic Table, and lies fourth in that group behind nitrogen (N), phosphorous (P) and arsenic (As). Antimony is a metalloid, having the physical properties of metals, but differing in its chemical behaviour (Greenwood and Earnshaw, 1984). While Sb has a relatively low profile, especially outside industry and geochemistry, it has a history of human use since at least 4000 B.C. (Polmear, 1998).

Generally, Sb is rare, with an average abundance of just 300 μg/kg in continental crust (0.00003 %), and even less in oceanic crust (Skinner and Porter, 1987; Wedepohl, 1995). Despite its scarcity, exposure to Sb concerns certain researchers because the element has no known biological function and is therefore presumed to be toxic (Filella et al, 2002a). The United States Environmental Protection Agency (USEPA), for example, regards Sb as a priority pollutant (De Gregori et al, 2007).

Given this status, it might be presumed that the behaviour of Sb in the environment is well understood, but this is not the case (Filella et al, 2002a). Such research is sparse, most likely because Sb has not yet been linked to any major environmental contamination events. It took the chronic poisoning of millions of Bangladeshis and Taiwanese to push As into the spotlight, and without a similar crisis, it is difficult to imagine Sb moving to the forefront of any research agendas (Hindmarsh, 2000).

The leaching of Sb from PET (polyethylene terephthalate) plastic water bottles, which will be discussed later in this chapter, may in time prove to be the required incentive. The focus of current research is to understand how Sb behaves in aquatic environments before it becomes a major issue.

[1] Evans, J. (1634) The vniversall medicine: or The vertues of the antimoniall cup. Published by John Haviland, London, 16pp, page 6.

Most of the environmental research regarding Sb has focussed on either emissions from industrial processes (such as the burning of coal, or smelting), or the downstream effects of mining, as Sb is often present as a contaminant in other ore bodies (particularly gold) (Ashley et al, 2007; Ettler et al, 2007; Gibbs et al, 2008; Qi et al, 2008). In New Zealand, the by-products of mining are of considerable local concern, even decades after activities cease. However such sources are unlikely to ever affect the lives of many people, as such mines tend to be in relatively isolated areas (Wilson et al, 2004a).

Another significant source of Sb in New Zealand is the Sb produced from geothermal fluids. The centre of New Zealand's North Island has a large number of geothermal fields, some of which contain significantly elevated concentrations of Sb (Ellis and Mahon, 1977). Increasing pressure to develop sustainable forms of power generation means that an increasing number of the geothermal fields are being exploited, and there is a risk that Sb-bearing waste will eventually contaminate receiving environments such as the Waikato River (the largest river in the North Island).

The purpose of this thesis is to develop an understanding of how geothermally-derived Sb behaves in aqueous environments. The research will begin by examining Sb behaviour in the high temperature fluids used to generate electricity, then in surface geothermal springs and finally in downstream receiving environments.

1.1 BACKGROUND AND RATIONALE

Published research on Sb tends to focus on industrial processes or pharmacological findings. The literature regarding Sb in natural environments is rather limited in comparison. This section provides an overview of the relevant research regarding Sb and includes the history of Sb usage, its chemistry, and what is known about the element's behaviour in the environment.

1.1.1 HISTORY

Antimony has a history of human use dating back to at least 4000 B.C., when it was used in a similar way to mascara (Polmear, 1998). Such a practise is referred to in the Old Testament of the Christian Bible (Kings II 9:30), and Sb is still present in some forms of kohl, a make-up popular throughout the Sub-Continent, the Middle-East and northern Africa (Al-Ashban et al, 2004). The metalloid has been used to tint glass and ceramics (red) for at least as long (Tylenda and Fowler, 2007).

Records from the early Roman Empire (50 A.D.) refer to the element as stibium, from which the symbol Sb is derived from, as did Berzelius in his 1814 "Essay on the Cause of Chemical Proportions, and on Some Circumstances Relating to Them: Together with a Short and Easy Method of Expressing Them" (Leicester and Klickstein, 1952). The reason why the element is now called antimony is debatable, and the name antimony may have arisen from errors in translation. Stibium, the Latin term, became al-athmīd in Arabic, and it has been argued that it was later wrongly translated back from Arabic to antimony (van der Krogt, 2005). Alternatively, antimony may be derived from the Greek *anti* and *monos* (alone), because the element is rarely found in its native state (Polmear, 1998).

Antimony was first isolated by Jaābir ibn Ḥayyaān in the 8th century AD (Jaābir ibn Ḥayyaān, 1678). In the Middle Ages, Sb was considered essential in alchemy, and the metalloid was also highly valued for its supposed medicinal properties (Valentinus[2], 1678). Various forms of Sb were prescribed for a wide range of ailments because the consumption of high dosages of Sb caused almost immediate vomiting and diarrhoea. Antimony was therefore considered to be an excellent purgative (Huxham, 1777). The Roman Emporer Claudius allegedly took advantage of the pergative properties of Sb by drinking from cups made of Sb during banquets (Thomson 1925). Antimony compounds are still used in medicine, particularly for the treatment of leishmeniasis, a tropical parasitic disease, despite its side-effects (Flores et al, 2003).

Chemists have been producing novel antimony compounds since the birth of modern chemistry, and recipes for antimony compounds published in the 1920s cite research dating back to 1760 (Morgan and Davies, 1926). Antimony is now used in a variety of applications, in automotive brakes as a fire retardant (replacing asbestos), replacing lead in pewter and to make bullets, as a semi-conductor and as the catalyst to make PET plastics (Filella et al, 2002b; Shotyk and Krachler, 2007).

Most of the world's plastic bottled water and soft drinks are packaged in PET plastic, and there is a growing body of evidence to suggest that Sb can be leached out of the plastic and into solution. The issue surfaced during an informal presentation at the "1st International workshop on Antimony in the Environment", held in Heidelberg, Germany in 2005, where it was reported that samples of orange juice contained detectable concentrations of Sb (0.5 μg/kg), and that these presumably came from the bottles (rather than the orange juice itself).

[2] There is some dispute as to whether Basil Valentinus actually existed, the name may be a pseudonym for Johann Thöde, a 17th century German chemist (Thomson, 1925).

Since then, Shotyk et al (2006; 2007) and Westerhoff et al (2008) have shown, with time, formerly pristine water can leach enough Sb out of PET bottles to be rendered unfit for drinking purposes, at least according to certain water standards (> 2 μg/kg Sb). The long-term health effects of such exposure are not known. It is recommended that potable-fluid containing PET bottles should be kept at relatively low (< 25 ^{o}C) temperatures when in storage (Westerhoff et al, 2008).

1.1.2 CHEMISTRY

Antimony's basic elemental properties are listed below in Table 1.1. Antimony is the 52nd most abundant element on earth, and has four valence states, -3 (such as stibine, SbH_3, which is gaseous), 0 (native antimony), +3, and +5 (Skinner and Porter, 1987). The two naturally occurring isotopes of Sb, ^{121}Sb and ^{123}Sb are both stable.

Table 1.1 Elemental properties of Sb. Data from Fillela et al (2002b)

Property	Value
Atomic number	51
Ground state electron configuration	[Kr] $4d^{10}\ 5s^2\ 5p^3$
Atomic mass	121.760
Natural isotopes	^{121}Sb (57.21 %) ^{123}Sb (42.79%)

MINERALOGY

Sb is a chalcophilic (sulfur bonding) element, and the most common naturally occurring Sb-bearing mineral is stibnite (Sb_2S_3). Antimony oxides are the next most common, valentinite (Sb_2O_3, rhombic), senarmontite (Sb_2O_3, cubic), and cervantite (Sb_2O_4), followed by the hydroxide stibiconite ($Sb_3O_6.H_2O$) and the alteration product kermesite (Sb_2OS_2) (Wang, 1952). In oxidising and circum-neutral pH waters, such as most fresh water rivers and streams, Sb_2S_3 will more readily dissolve than the oxide minerals, which, because of reaction kinetics, are effectively insoluble in circumneutral pH aqueous conditions (Gayer and Garrett, 1952; Zotov et al, 2003).

Stibnite occurs in two forms, crystalline and amorphous. Crystalline Sb_2S_3 has a metallic lustre and forms in a needle habit, whereas amorphous Sb_2S_3 has a bright red-orange colour. In mineral deposits, crystalline Sb_2S_3 is the most common form, while (natural) amorphous Sb_2S_3 is generally associated with geothermal springs (Van Hinsberg et al, 2003; Wilson and Thomssen, 1985). Images of the two Sb_2S_3 forms are presented in Plate 1.1.

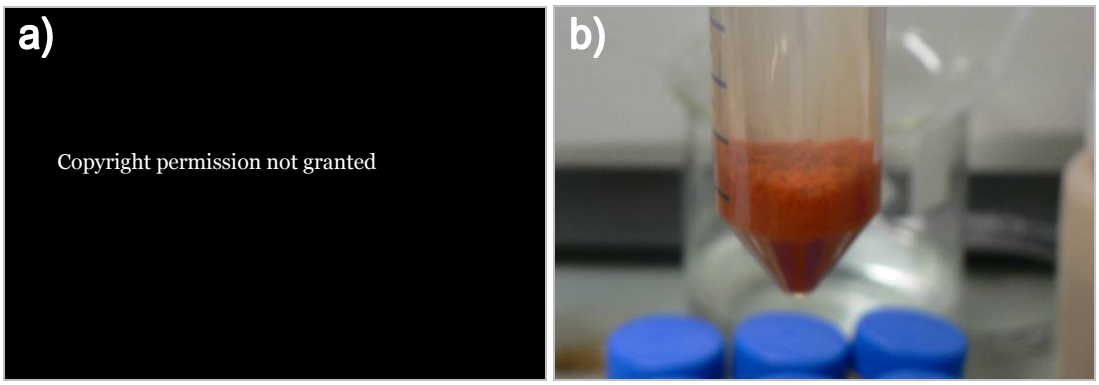

Plate 1.1 Photos of a) crystalline (Auer, 1980) and b) amorphous Sb_2S_3

AQUATIC CHEMISTRY

Dissolved Sb forms a number of species, but the most common are the anionic oxyanions $H_xSbO_3^{(x-3)}$ (Sb^{III}) and $H_xSbO_5^{(x-5)}$ (Sb^{V}). These species are often written as $Sb(OH)_x^{3-x}$ and $Sb(OH)_x^{5-x}$, see Filella (2002a, b) or Spycher and Reed (1989a), but Sb-oxyanions behave like acids, rather than bases, and formulae in this thesis are written in a way that reflects this (Zakaznova-Herzog and Seward, 2006). Antimony is only found as a free ion (as Sb^{III}) in extremely acidic conditions (Filella et al, 2002b). Unlike its Group V counterparts N and As, which are tetrahedral, Sb co-ordinates octahedrally with oxygen (Pauling, 1933). In higher temperature reducing environments, thio-species such as $H_xSb_2S_4^{x-2}$ may become increasingly important (Krupp, 1988). In aerobic freshwaters, Sb is most soluble in neutral or mildly alkaline conditions and less soluble under acidic conditions, differing from heavy metals such as copper. Such heavy metals tend to be present in waters as cations or cationic complexes (e.g. Cu^{2+} or $CuOH^{+}$) and are more soluble in acidic conditions (Filella et al, 2002b).

As a general rule, Sb^{III} is the dominant oxidation state in reducing aqueous environments and Sb^{V} is favoured in oxidising aqueous environments. This means that Sb^{V} is the dominant oxidation state in most surface waters (Filella et al, 2002a). However, thermodynamic data for Sb is incomplete at best. Most of the thermodynamic data for Sb have been collected in highly concentrated solutions (akin to geothermal fluids), which are generally atypical of surface conditions. Furthermore, the majority of the studies have focussed on Sb^{III} species only (Filella et al, 2002b). Nearly all the Sb^{V} acid-base equilibria data, for example, come from a single study by Baes and Mesmer (1976); Sillen and Martell (1964) also provide some data for Sb^{V} hydrolysis.

Kinetic rates of reduction or oxidation are not well understood, and there are reports of Sb^{III} in oxic waters, and of Sb^{V} occurring in anoxic waters (Filella et al, 2002b). Some authors have reported relatively slow redox reaction rates, while others report rapidly occurring redox reaction processes (Belzile et al, 2001; Cutter et al, 2001). Biological processes appear to have a significant influence upon redox reactions, as does the presence or absence of metal-oxyhydroxides (Belzile et al, 2001).

Adsorption onto iron oxy-hydroxides appears to be a critical factor controlling inorganic Sb mobility in freshwater systems, and it has been shown that antimony is much more mobile in low iron systems than in iron-rich systems (Craw et al, 2004). There is also the potential for Sb^{III} to adsorb onto humic acids, with maximum binding at about pH 6 (Buschmann and Sigg, 2004). Overall though, Sb interactions with organic matter are not well understood (Filella et al, 2002b). Ettler et al (2007) have shown that Sb mobility in soil profiles is variable and that the dissolution of Fe-oxyhydroxides in low pH highly organic soils, such as those found in some European forests, may lead to the release of Sb if the soils are disturbed.

Methylated species of Sb, such as $(CH_3)_xSbO(OH)_{3-x}$) can be produced by bacteria and funghi (Jenkins et al, 2002). These biologically produced species are volatile, and have been reported in both fresh and saline natural waters. However, quantifying their presence in aqueous environments is difficult because such species can also be the product of analytical or sampling artefacts (Dodd et al, 1992; Filella et al, 2007; Smith et al, 2002).

TOXICITY

The fact that Sb was used historically as an emetic and a laxative suggests that Sb is toxic to humans, and McCallum (1977) describes a case of mass poisoning in 1929. However, the metalloid's actual toxicity is not well understood, even though Sb has been linked to a variety of illnesses, including cot-death (since disproved), cancer, heart problems and lung disease (McCallum, 2005; Warnock et al, 1995). The mechanism for toxicity appears to involve direct damage to DNA strands, but this has only been proven for stibine (SbH_3) and trimethylstibine ($(CH_3)_3Sb$) species (Andrewes et al, 2004). Babula et al (2008), in a review of the toxicity of uncommon heavy metals (including Sb), found no detailed studies regarding biological uptake, transport or detoxifying mechanisms for Sb.

The amount of Sb required to cause an emetic response is estimated to be between 30-60 mg/L (dependant on body weight), but there is debate about what the threshold for antimony toxicity to humans should be (Tylenda and Fowler, 2007). Researchers such as Lynch et al (1999) suggest that the NOAEL (no observed adverse effect level) for humans is between 50-2500 mg/kg body mass. Others, such as Valli et al (2000) claim the NOAEL threshold is much lower, at about 0.5 mg/kg body mass.

Newton et al (1994) found no evidence that Sb_2O_3 would cause cancer in rats, with Leonard and Gerger (1996) suggesting that, at least when compared to trace elements such as As or chromium (Cr), the carcinogenicity of Sb was insignificant. Kirkland et al (2007) found no evidence that Sb_2O_3 would cause any chromosomal or micronuclei aberrations. Recent claims of a link between Sb (as Sb_2O_3) and cancer in humans typically reference Gebel et al (1997) or Hayes (1997), but neither paper states anything more certain than that further research is required. In contrast, $SbCl_3$ has been demonstrated to be carcinogenic in cultured human bronchial epithelial cells and fibroblasts when they are exposed to Sb concentrations of > 50 μM for longer than four hours (Huang et al, 1998). Dopp et al (2004) reviewed the available data for organo-antimony compound toxicity, and also found insufficient data to make any definite conclusions.

The USEPA drinking water limit is set at the current achievable limit of drinking water treatment systems (6 μg/L), because of a lack of reliable information (USEPA, 2005). In Japan, the drinking water limit is set at 2 μg/L (Westerhoff et al, 2008). New Zealand's Ministry of Health has set the Maximum Allowable Value for Sb in drinking water at 20 μg/L, in line with the World Health Organisation guidelines (Ministry of Health, 2005; Westerhoff et al, 2008).

According to the "Australian and New Zealand Guidelines for Fresh and Marine Water Quality" (ANZECC, 2000), there is insufficient information available regarding the ecological toxicity of antimony, and therefore only interim guidelines of 9 μg/L Sb^{III} for the protection of freshwater aquatic life and 270 μg/L Sb^{III} for the protection of marine aquatic life are listed. There are no ANZECC (2000) guidelines for Sb^{V}, even though it is the dominant species in natural waters (Filella et al, 2002a).

In fish, LeBlanc and Dean (1984) found that Sb concentrations of < 8 µg/L had no effect upon the growth or reproductivity of fathead minnows (*Pimephales promelas*). The median lethal concentration (LC_{50}) of Sb for the freshwater larvae of tilapia (*Oreochromis mossambicus*) was found to be 35.5 mg/L when exposed for 96 hours. For juvenile red seabream (*Pargus major*), a saltwater-dwelling species, the LC_{50} was ~ 15 mg/L Sb^{III} (added as $SbCl_3$) and 6.9 mg/L Sb^{III} (added as potassium antimony tartrate ($C_4H_4O_7SbK$)), but only 0.93 mg/L Sb^{V} (added as $SbCl_5$) for any length of exposure between 24 and 72 hours, suggesting that the Sb^{V} species was more toxic than Sb^{III} (Takayanagi, 2001).

Fjallborg and Dave (2004) found that Sb had no effect on growth of lettuce, oats or radishes, but did find that *Daphnia magna* (a water flea) was adversely affected by concentrations of 5-22 mg/kg (EC_{50}), and concluded animals were more susceptible to Sb than plants. Research in China has suggested that soils enriched in Sb will retard the growth of plants such as rice (He and Yang, 1999).

Antimony-sulfide compounds (Sb_2S_3 and Sb_2S_5) appear to affect the soil microbe communities of certain soils when present in concentrations as low as 125 mg/kg, however this may be due to pH changes, rather than to Sb itself (Hammel et al, 1998). Murata et al (2005) found no evidence that Sb affected soil dehydrogenase activity in a range of soils, but did note that bacterial-colony survival was reduced in the presence of Sb.

1.1.3 ANTIMONY IN THE ENVIRONMENT

Antimony is generally scarce, but it is ubiquitous throughout all four environmental spheres (atmo-, bio-, hydro-, and litho-). Industrial emissions and the degradation of brake pads have led to increased levels in the atmosphere, and there is a large body of research regarding the formation of Sb_2S_3 ore bodies (Gomez et al, 2005; Migdisov and Bychkov, 1998; Nriagu, 1989). More pertinent to this thesis is the research on aqueous Sb and its interaction with soils and biota.

ANTIMONY DISTRIBUTION AND BEHAVIOUR IN THE HYDROSPHERE

In unpolluted areas, concentrations of Sb in freshwaters are typically less than 0.2 µg/kg, and the behaviour of Sb is generally considered to be conservative (Filella et al, 2002a). The world-wide average concentration for seawater is in the range of 0.1-0.2 µg/kg, based on data from various sites in the Atlantic and Pacific Oceans (Cabon and Louis Madec, 2004; Cutter and Cutter, 2006; Ellwood and Maher, 2002; Quentel and Filella, 2002).

Concentrations of Sb are higher in equatorial regions than they are elsewhere in the ocean (Cutter et al, 2001). There is evidence to suggest that in some places the element is scavenged by phytoplankton in a similar way to aluminium, but at a much slower rate, whereas in other areas it behaves conservatively (Cutter and Cutter, 2006).

In estuaries, the only conclusion that has been made is that the behaviour of Sb is dependant on the type of estuary (Filella et al, 2002a). Byrd (1990), for example, reports effectively conservative Sb behaviour in a series of estuaries along the east coast of the USA, and such behaviour was also reported in the Rhine estuary of the Dutch Wadden Sea, but not the Scheldt estuary (which also lies in the Dutch Wadden Sea) (Van der sloot et al, 1989). Migon and Mori (1999) reported an apparent release of Sb from sediments in a Mediterranean estuary.

There are two main types of environment in which concentrations of Sb are elevated: in epithermal or mesothermal ore bodies (and therefore in mines in these deposits), and geothermal environments (Filella et al, 2002a). Most of the literature that considers Sb in natural non-marine waters focuses on these two environment-types or their downstream receiving environments, and both will be discussed later in this chapter.

Outside of mining, Sb appears to demonstrate similar mobility to lead (Pb) and copper (Cu) in the soils of Swiss shooting ranges, although this may simply be because the shot fired contained all three elements and they had not been separated in the soils (Knechtenhofer et al, 2003). Antimony is also associated with Pb in Scottish and Swiss peat bogs, which have accumulated both elements as the result of nearby historic smelting activities (Cloy et al, 2005; Shotyk et al, 1996).

MICRO-BIOTIC INTERACTIONS

Bacterial interactions with Sb have been studied at least since the late 1970s, when the bacterium *Stiobacter senarmontii* was shown to have the ability to oxidise Sb^{III} to Sb^{V}, and that *Staphylococcus aureus* plasmids were shown to be resistant to Sb salts (Summers and Silver, 1978). Methanoarchea, as well as certain bacteria, have the potential to produce methyl-Sb species, but little attention has been given to why (rather than how) organisms use Sb in this manner (Meyer et al, 2007).

Bio-methylated Sb species are presumed to be the products of biological de-toxification, but the details of the specific mechanism(s) are not well-understood, and some researchers consider methylated species to be more toxic than inorganic species (Filella et al, 2002a; Meyer et al, 2007). Andreae et al (1981) argued that bacteria may play a role in the Sb^{III}:Sb^{V} distribution found in river waters and presented a method for detecting and measuring methylated Sb complexes in aqueous samples.

Whether or not bacteria influence Sb speciation has yet to be confirmed, in part because of the problems associated with methyl-Sb analytical methods mentioned earlier (Dodd et al, 1992). Prior to 1981, bio-methylated Sb compounds do not seem to have been discussed in the literature, despite the fact that methods for producing such species in the laboratory have been available since at least 1972 (Andreae et al, 1981; Meinema and Noltes, 1972). Micro-biotic (non-bacterial) organisms that have been shown to accumulate Sb include *Chorella vulgaris* (a freshwater alga) and *Thalassiosira nana* (a marine diatom) (Gebel, 1997; Maeda et al, 1997).

MACRO-BIOTIC UPTAKE

At an abandoned site in England, Li and Thornton (1993) found that the degree of uptake of Sb (and As) by plants corresponded directly to soil concentrations. This was a conclusion also reached by Craw et al (2007) at a mine site in New Zealand. Whether or not antimony is taken up by plants appears to be species specific; there is evidence to show that a species of pondweed (*Potamogetan pectinatus*) will accumulate antimony, whereas other aquatic species, such as arrow-grasses or water milfoils do not (Dodd et al, 1996).

In an abandoned mining area in Spain, *Dittrichia viscose* (False yellowhead) was found to take up Sb from the soil, whereas *Cytisus striatus* (a broom species) appeared to exclude the metalloid (Murciego et al, 2007). Baroni et al (2000) found that the plants species moonwalker (*Achillea ageratum*), ribwort plantain (*Plantago lanceolata*) and maidenstears (*Silene vulgaris*) all accumulate Sb, but that the efficiency of uptake decreased with increasing Sb concentrations in the soil. Elder berries and poplar leaves in urban areas are reported to have higher concentrations of Sb than samples taken from rural areas. This appears related to relative traffic levels (Krachler et al, 1999).

Loccaria amethystine, *Amanita rubescens* and *Lepista nuda* are all mushroom species that accumulate Sb, but do not accumulate other metals such as As or cadmium (Cd) (Kalac and Svoboda, 2000). Other mushroom species exhibit the opposite behaviour.

There is less information available on Sb accumulation by animals. A study of a contaminated site surrounding an antimony smelter in England found no evidence that plants were extracting Sb from soil, but did find elevated levels of Sb in detritivores, who scavenged indiscriminately and therefore occasionally consumed Sb-enriched particulates (Ainsworth et al, 1990a, b). Similar Sb-accumulation by detrital scavengers has been reported in a Corsican estuary (Mori et al, 1999). Elevated Sb concentrations found in earthworms at a former Sb-mine site have also been attributed directly to entrained soil particles, rather than being evidence of bioaccumulation (Gal et al, 2007).

1.1.4 ANTIMONY IN MINING-AFFECTED ENVIRONMENTS

The most comprehensive studies of Sb in the environment to date have come from Australia, where the fate of antimony from a historic mining area has been traced 280 km along the floodplains of the Macleay River, down to the Pacific Ocean (Ashley et al, 2003; Ashley et al, 2007; Tighe et al, 2005a). On the floodplains, 90 % of the sediments contain elevated levels of Sb, averaging about 11 mg/kg compared to background values of about 0.2 mg/kg. On the flood plains, swamp environments were more enriched in Sb than alluvium dominated environments (~13 mg/kg compared to ~10 mg/kg). Variations in Sb concentrations in the region's surface waters ranged from below the detection limit to about 64 μg/kg, suggesting that Sb may be periodically remobilising from the floodplain sediments (Tighe et al, 2005a). Elevated levels of Sb have also been found in a coastal aquifer north of the mouth of the Macleay River (O'Shea et al, 2007).

Kawamoto and Morisawa (2003) have produced a study of Sb at an equally grand scale for the Yoda River in Japan, but this focussed on the influence of sewage treatment plants rather than the effects of mining. The distribution of Sb in mining-affected Japanese river systems have however been reported by other authors, such as Iwashita and Shimamura (2003), who reported Sb concentrations ranging from 0.1 – 13 μg/L in the Sagami River system.

Research at a smaller mining area in northern France, comparing the respective mobilities of As and Sb, has shown that the former is more mobile in reducing environments, whilst the latter is more mobile in oxidising environments, consistent with evidence from industrial smelter sites elsewhere (Casiot et al, 2007; Gál et al, 2006). Flynn et al (2003) argue that remobilisation of Sb from mine site soils is unlikely, and Trois et al (2007) provided evidence that the overall downstream risk of Sb leaching from mine-waste dumps is relatively low if the leachate is acidic.

In New Zealand, Sb is present in most, if not all, of the mesothermal calcareous quartz-schist ore deposits found in the South Island. The results of research on Sb conducted in Marlborough, the West Coast, and Otago are consistent with that produced from the Macleay River region in Australia (Ashley et al, 2003; Ashley et al, 2006; Craw et al, 2004; Wilson et al, 2004b). The mine (and rock) drainage from these areas is circum-neutral, rather than acidic, and Wilson et al (2004a) have shown that Sb is more likely to remobilise from sediments in such environments than from the acidic environments described by Flynn et al (2003) or Trois et al (2007).

1.1.5 ANTIMONY IN GEOTHERMALLY INFLUENCED SYSTEMS

Geothermal environments are another aspect of this research that requires introduction. The key difference between Sb derived from geothermal systems and Sb from other sources, such as mine sites, is not related to Sb itself, but rather to the type of solutions the metalloid is transported in. Geothermal waters differ from mine-derived waters for example, in that the waters draining from mining areas are typically oxidised and only contain elements that have been dissolved as a result of surface weathering processes. In a geothermal system, the fluid may be oxidising or reducing, and element enrichment is highly variable (Nordstrom, 2004).

When host rocks are exposed to geothermally heated fluids, many elements are preferentially leached, enriching the fluids even though the actual elemental content of the rocks may be relatively low (Ellis and Mahon, 1967). The degree of elemental leaching is partially controlled by the temperature of the water, and therefore underground temperatures can be estimated by analysing the chemistry of surface springs, or more accurately, the chemistry of reservoir fluids from wells (Ellis and Mahon, 1977). The type of underlying magma will also influence the chemical composition of high temperature geothermal waters, meaning that, for example, the waters produced from andesitic geothermal systems will differ from those produced from rhyolitic ones (Giggenbach, 1992). Finally, the type of leaching fluid (seawater, groundwater or meteoric waters) is also important. The most important gases in geothermal fluids are carbon dioxide (CO_2) and hydrogen sulfide (H_2S) (Ellis and Mahon, 1977).

There are three major types of geothermal waters: alkali-chloride, bicarbonate and acid-sulfate waters (Ellis and Mahon, 1977). Alkali-chloride waters are typically similar to the high temperature, high pressure fluids, but found at the surface, indicating rapid up-flow conditions. They may be especially enriched in trace elements (Henley and Ellis, 1983), and recent examples have been described by Pope et al (2004), Nordstrom (2005), Simmons et al (1994) and Skalbeck et al (2002). More commonly, the hot rising fluids boil before they reach the surface, and the steam and CO_2 gas can condense to form bicarbonate-rich waters, while the H_2S-gas oxidises in surface waters to create acid-sulfate waters (Henley and Ellis, 1983). These types of waters are not necessarily mutually exclusive. The Wai-O-Tapu geothermal field, for example has springs of all three types (Lloyd, 1959). A cross section of a typical geothermal system, showing all three fluid types, is presented in Figure 1.1.

Geothermal waters typically contain elevated levels of sulfur species, in particular sulfate (SO_4^{2-}) and reduced sulfide species (H_2S, HS^- and S^{2-}), but also other metastable species such as thiosulfate ($S_2O_3^{2-}$) and polythionate ($S_xO_6^{2-}$) can also be present in significant concentrations (Webster, 1987). The latter species do not exist in the deeper high temperature fluids underground, but become increasingly abundant as the fluids reach the surface, cool and sulfide species begin to oxidise, especially in alkaline surface waters (Xu et al, 1998). Sulfur hydrolysis and sulfur-mineral interactions can also induce the formation of the thiosulfate and polythionate species, including thioarsenates (Planer-Friedrich et al, 2007). In some geothermal features at Yellowstone National Park in the U.S.A, thiosulfates and polythionates are the dominant sulfur species in solution (Xu et al, 1998; 2000).

Amorphous (red) Sb_2S_3 mineralisation has been described as a major feature of geothermal environments from such geographically disparate regions as Yellowstone National Park in the United States of America, to Ohāki in New Zealand (Gianella and White, 1947; Ritchie, 1961). Elevated concentrations of Sb in Californian geysers, which range as high as 200 µg/L, are reported by Smith (1987). Stauffer and Thompson (1984) provided data for Sb in Yellowstone Park springs which range in Sb content from 10-170 µg/kg, while concentrations of > 250 µg/kg Sb were reported for a spring in the Steamboat Springs field in Nevada. Stibnite mineralisation at Steamboat Springs was reported at least as early as 1912 (Jones, 1912). Nordstrom et al. (2005) have reported Sb concentrations at other Yellowstone National Park springs, which varied from < 1 µg/L up to 380 µg/L depending upon the nature of the spring being sampled.

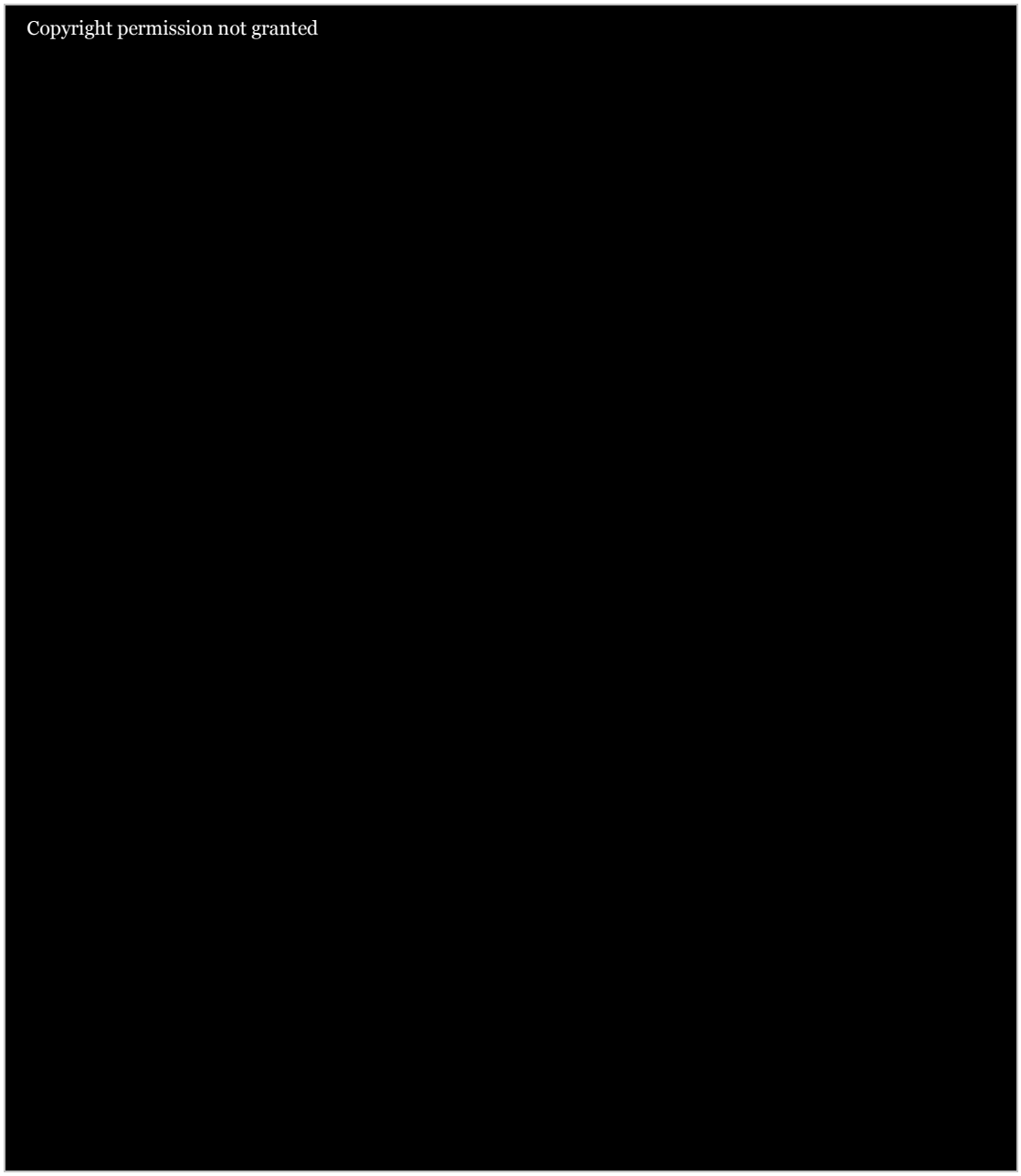

Figure 1.1 A cross-section of a typical geothermal system, showing examples of the various types of fluids that can be produced (Henley and Ellis, 1983).

In Japan, the amount of Sb has been quantified for a number of geothermal systems. For example, Sakamoto et al (1988) reported Sb concentrations between 0.05 and 244 µg/L in springs through Japan and concluded that Sb concentrations were higher in thermal-water-dominated systems than in vapour-dominated systems, while Ujiie-Mikoshiba et al (2006) reported Sb concentrations up to 21.6 wt% in geothermally-derived stream sediments from the northern Honshu region.

Antimony can be used as a tracer element for geothermal systems. Bingqiu et al (1986) for example, have argued that elevated levels of Sb in soils suggest the presence of geothermal areas, as have Lovell et al (1983), who suggested that Sb is a useful tracer of geothermal fluids, at least for the Roosevelt Springs system in Utah.

Geothermal sulfur chemistry is especially important for chalcophilic elements such as Sb and As, and may be able to explain anomalously high concentrations of the metalloids not predicted by their ratios with conservative elements such as chloride (Cl) (Nordstrom et al, 2004). The mix of sulfur species also affects the microbial ecology of any given geothermal feature, which may in turn affect whether, for example, the dominant bacteria are arsenate reducers or arsenite oxidisers (Lloyd and Oremland, 2006; Oremland and Stolz, 2003). While there is little evidence in the literature regarding the microbial ecology aspects of Sb, it may be presumed that, as for As, the type of Sb-utilising bacteria present in a geothermal feature will also be influenced by the system's sulfur-chemistry.

In geothermal systems, thermophilic prokaryotes, especially archaebacteria, can tolerate much higher temperatures than other organisms, with some able to survive in waters warmer than 90 ^{o}C, and are exposed to elevated levels of elements such as As, S and Sb (Hirner et al, 1990). These organisms can congregate to form algal mats, described by Claypool and Kaplan (1974) as "ecological successions". Such mats tend to form in layers, each with distinct microbial communities and chemical zones, and the chemical processes within each zone can be quite disparate. Oremland and Taylor (1978) describe a layer within a marine mat in which both methanogenesis and sulfate-reduction could occur, and there is no reason to suggest that similar seemingly opposing processes could not occur in more hostile environments, such as geothermal ones (Oremland, 1989).

Elevated concentrations of methylated Sb species have been reported in the protokerogen[3] fractions of geothermal mats (Hirner et al, 1998). The presence of methylated species suggests biological uptake, however inorganic Sb-rich particulate inclusion may also be a significant source of Sb in the mats. It is as yet unknown whether the methylated Sb compounds found in New Zealand's geothermal waters are biologically or abiotically produced (Bentley and Chasteen, 2002; Hirner et al, 1990).

In New Zealand, Sb_2S_3 has been found in stromatolites growing in the Waimangu geothermal system, and bacteria within Wai-O-Tapu geothermal field's Champagne Pool may play some role in creating the bright orange Sb_2S_3-rich sinters for which the pool is famous (Jones et al, 2001). Pope et al (2004) suggest that bacteria may play an active role in controlling the concentrations of Sb in geothermal hot spring discharges, and this will be discussed further in Chapter Four.

GEOTHERMAL SYSTEM DEVELOPMENT IN NEW ZEALAND

Most of New Zealand's geothermal systems lie in a geographic area called the Taupo Volcanic Zone (TVZ), shown in Figure 1.2. The TVZ formed 2 million years ago as a result of the collision between the Pacific and Indian-Australian tectonic plates, with the former subducting beneath the latter, a process which has continued through to the present day (Kissling and Weir, 2005). The TVZ is approximately 30 km wide and 150 km long, and produces in excess of 4 GW of energy as heat (Bibby et al, 1995).

Geothermal electricity development began in New Zealand with the commissioning of the Wairakei station in 1958, and geothermal power stations are increasingly important contributors New Zealand's overall power supply (Hunt, 1998). Because of the long-term interest in their development, there is chemical data available for many of the reservoir and surface feature fluids of the various geothermal fields, dating back to the 1960s (for example Ritchie (1961)). Table 1.2 lists the Sb content of selected geothermal reservoir fluids in New Zealand, and it is evident that there is significant variation between systems in both Sb and As concentrations.

[3] Kerogen is a term used to describe sediment containing organic compounds that will yield oil if subjected to increased temperature or pressure (Gillis and Varhaug, 2008). A protokerogen layer therefore is a layer of sediment composed of the precursors of such compounds.

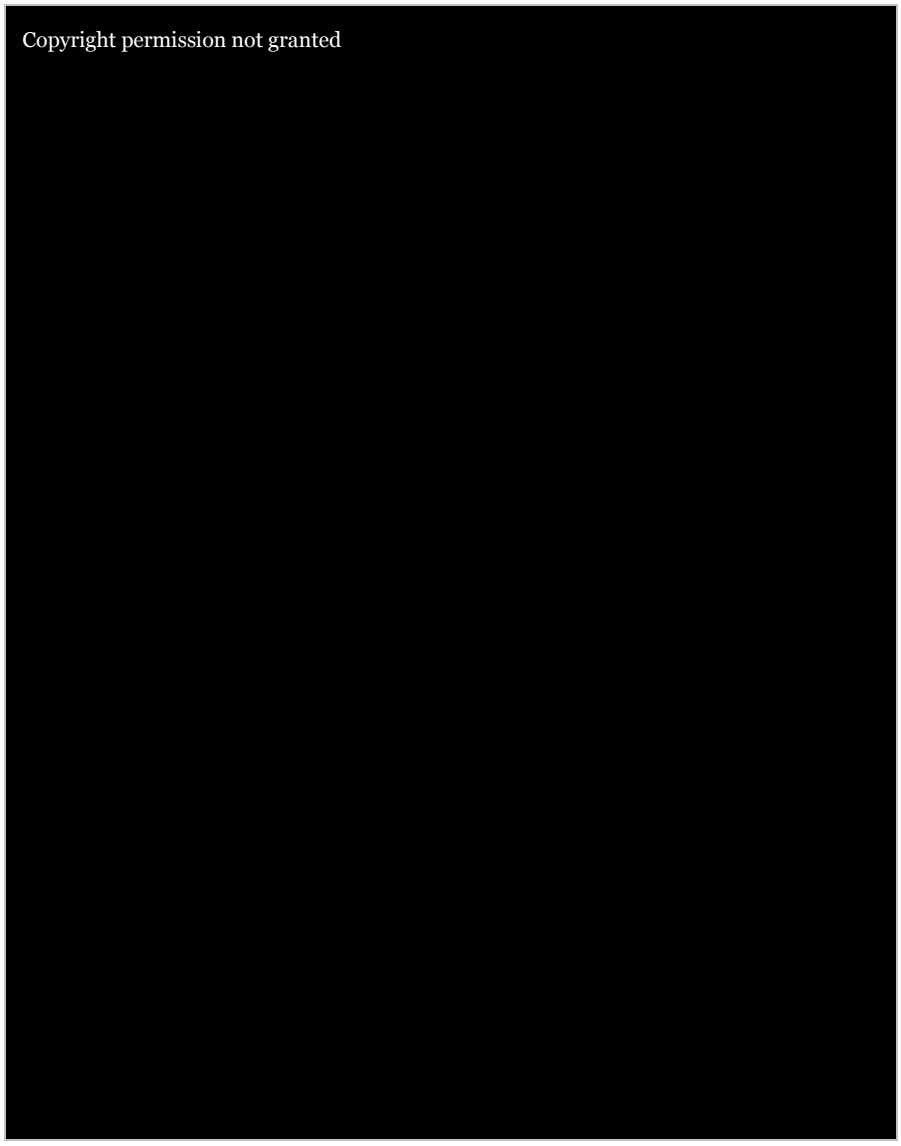

Figure 1.2 Geothermal systems within the Taupo Volcanic Zone of New Zealand (Stewart, 2006)

Table 1.2. Antimony and As concentrations in selected New Zealand geothermal reservoir fluids

Geothermal Field	Sb (µg/kg)	As (µg/kg)
Broadlands (Spycher and Reed, 1989b)	200	5700
Ngawha (Brown and Simmons, 2003))	1700-2000	430-770
Rotokawa (Krupp and Seward, 1990)	800-1800	3000-6800
Wairakei (Weissberg et al, 1979)	100	4700

In fields within the TVZ (Broadlands, Rotokawa and Wairakei in Table 1.2), Sb concentrations are typically at least an order of magnitude lower than for As. However, Sb dominates at Ngawha, the only high temperature geothermal field in New Zealand outside the TVZ. Stibnite precipitation in power station pipelines, also referred to as "scaling", at the Ngawha power station has become an ongoing problem, because as the scale accumulates the amount of fluid that can pass through the pipes is reduced and therefore power generation at the station is inhibited (Dorrington and Brown, 2000). Reyes et al (2002) have described a similar problem at the Rotokawa station. At Rotokawa, Sb_2S_3 is undersaturated in the parent geothermal fluids (Krupp and Seward, 1990), and it appears that the probability of Sb_2S_3 scaling had not been considered to be very likely. Outside New Zealand, two further published papers were found that mentioned Sb_2S_3 scaling: Smith et al (1987) for a power station at the Geysers, California, U.S.A., and Raymond et al (2005) at the Berlin field, El Salvador. Methods for preventing Sb_2S_3 scaling in an exploration well in the Piancastagnaio field (Italy) were presented at the 1995 World Geothermal Conference. It is clear that Sb_2S_3 scaling is becoming a more widespread problem than previous literature had suggested (Cappetti et al, 1995).

Although there is some data for Sb concentrations in selected New Zealand surface geothermal waters (e.g Ritchie, 1961 or Pope et al, 2004), researchers have typically given more attention to the precipitates that form when such fluids discharge at the surface. Prior to development at Rotokawa, Krupp and Seward (1987) described brick red precipitates forming as a result of degassing and cooling processes that contain up to 30 % Sb by weight, and mud surrounding Lake Rotokawa that contained 250-500 tonnes of Sb (Krupp and Seward, 1990). The precipitation from cooling geothermal fluids appears to effectively remove Sb from solution, with Krupp and Seward (1990) suggesting that about 80 % of the dissolved Sb was removed at Rotokawa before the fluids exit the lake.

Similar precipitates have been described at Broadlands and at Wai-O-Tapu's Champagne Pool (Ellis and Mahon, 1977; Weissberg et al, 1979). Pope et al (2004) collected a series of water samples from the discharge of Champagne Pool at Wai-O-Tapu. Antimony concentrations, along with those of several other trace elements, varied significantly over a twenty-four hour period. Antimony concentrations, for example, ranged from < 10 μg/kg at night to 130 μg/kg in the afternoon. The fluctuations in trace metal concentrations were linked to bacterial activity, but the exact processes by which bacteria influenced Sb mobility were not clear.

1.1.6 ARSENIC

No discussion of Sb in the environment would be complete without mentioning As, the element sitting directly above Sb in the Periodic Table. Many studies, including at least one by the author of this thesis, make the claim that aqueous As and Sb behave in a similar manner, for example Wilson et al (2004a). However, in oceans the two exhibit disparate behaviour, and in sub-surface geothermal fluids the two elements have different solubilities and thus behave differently as those fluids cool (Brown and Simmons, 2003; Cutter et al, 2001). Both elements form gaseous hydrides and are analysed using similar methods (e.g. HG-AAS), which may explain why so many studies mention both elements. In most studies that investigate the two metalloids, Sb is normally an auxiliary element, rather than being the focus of the study (e.g. Nimick et al (1998), Ravengai et al (2005) or Stauffer and Thompson (1984)). In geothermal fluids, where both metalloids are present, there is again more information on As, for example Webster and Nordstrom (2003), than there is for Sb.

The bacterial cycling of As has also received more attention than Sb. Stoltz and Oremland (1999) argue that orpiment (As_2S_3) found in geothermal systems, the formation of which is usually attributed to abiotic processes, could also be formed by *Desulfotomaculum auripigmentum*, a bacteria that can reduce both As^V and sulfate as it grows. The ability of *Desulfotomaculum auripigmentum* to precipitate orpiment was demonstrated by Newman et al (1997). *Bacillus selenitireducens*, a bacteria reported in Mono Lake, a reducing, hyper-saline lake in California, U.S.A, has been shown to reduce As^V, and in so doing is perhaps the most important carbon-acceptor in such ecosystems where sulfate is limited (Oremland et al, 2000). The biologically-catalysed production of volatile chloro-arsine and thioarsines has been reported in Yellowstone Park hotsprings (Planer-Friedrich et al, 2006).

Geothermally derived As in New Zealand freshwaters have received some attention, examples include Aggett and Aspell (1977), Robinson et al (1995a), and Webster-Brown and Lane (2005a). In this thesis, one of the objectives was to address the lack of comparable data for Sb, and to determine whether or not Sb and As should ever be considered to behave in a similar manner.

1.2 RESEARCH OBJECTIVES

The purpose of this thesis is to characterise the behaviour and determine the fate of Sb from selected geothermal systems in New Zealand. This understanding should make a significant contribution to our knowledge of how Sb behaves in the environment.

To fulfil this purpose, the following specific objectives have been included:

- To determine factors controlling Sb_2S_3 precipitation at two New Zealand geothermal power stations, using field measurements and geochemically modelled predictions of Sb solubility.
- To investigate whether Sb that has precipitated in surface geothermal features at Wai-O-Tapu and Waimangu can be remobilised, and, if so, to determine the mechanisms and the conditions required for mobility.
- To assess the significance of geothermal Sb contributions to receiving (non-geothermal) environments downstream of Wai-O-Tapu and Waimangu and to determine what, if any, natural processes exist to remove geothermally-derived dissolved Sb.
- To compare the behaviour of geothermal Sb to that observed for geothermal As, and to determine under what circumstances the two metalloids might behave distinctly differently, and when the two might behave in a similar way.

This research was conducted exclusively in the North Island of New Zealand, and apart from the investigation of the Ngawha Power Station, was focussed entirely on the Taupo Volcanic Zone and the Waikato River, which flows north out of Lake Taupo and reaches the ocean 50 km south of Auckland.

1.3 THESIS OUTLINE

This thesis is divided into six chapters, three of which (Chapters Three, Four and Five) form the main body of the thesis and progressively cover: Sb behaviour at high temperatures and high pressures, in surface geothermal features, and in cold receiving freshwaters. Chapters One and Two provide the context for this thesis and Chapter Six gives the overall conclusions. Analytical and experimental data are provided as appendices.

CHAPTER TWO

This chapter provides details of the methods used to collect and analyse the data presented in the following three chapters. Chapter Two includes sampling techniques, analytical procedures, descriptions of the thermodynamic models used, and specific details of experimental processes.

CHAPTER THREE

This chapter focuses on Sb behaviour in high temperature fluids at geothermal power stations and includes a review of the thermodynamic databases used to model Sb behaviour under such conditions. The modelled data was compared to observations at two New Zealand geothermal power stations (Rotokawa and Ngawha) that have Sb_2S_3 actively precipitating in the pipelines.

Research from this chapter was presented orally at the 16th annual Goldschmidt Conference in Melbourne, Australia in 2006, and has since been published as a paper in *Geothermics* (Wilson et al, 2007).

CHAPTER FOUR

In Chapter Four, the research moves from high temperature systems to lower temperature natural surface features. The precipitation and remobilisation (or lack thereof) of Sb is investigated, building upon the research of Pope et al (2004) at the Wai-O-Tapu geothermal area, but expanding the scope to include the behaviour of Sb at the Waimangu geothermal area.

Results from Chapter Four were presented as a poster at the 18th International Symposia on Environmental Biogeochemistry (ISEB) in Taupo, New Zealand in 2007. A manuscript based on the results from this chapter has been submitted to *Chemical Geology*.

CHAPTER FIVE

In this chapter, the eventual fate of Sb produced from geothermal systems and discharged into receiving environments is examined. It examines a range of environments, from small geothermally influenced streams through a major river system (the Waikato River) into an estuary.

Part of this chapter was presented orally at the biannual New Zealand Geochemical Group meeting in Dunedin, New Zealand in 2007, and other results were presented at the 18th annual Goldschmidt Conference in Vancouver, Canada in 2008. It is anticipated that results from this chapter will be published in *Applied Geochemistry* in 2009.

CHAPTER SIX

The aims and objectives of the thesis are revisited in Chapter Six, which presents the overall conclusions of this research. As well as providing an overall summary of the thesis, future research avenues are identified.

CHAPTER TWO
METHODS AND PROTOCOLS

This chapter outlines the sampling protocols and analytical techniques that were employed in this research. Methods specific only to particular aspects of this research, such as the sampling techniques necessary for high temperature geothermal fluid sampling, or adsorption edge experiment details are included.

2.1 SAMPLE COLLECTION

In order to develop an understanding of how Sb behaves in geothermal systems and their receiving environments, a range of samples must be collected: Water, sediment, plants (macrophytes) and algae.

2.1.1 NON-POWERSTATION AQUEOUS SAMPLES

Water samples were collected in 15 or 50 mL polypropylene (PP) vials, 500 mL PP or 500 mL high density polyethylene (HDPE) bottles. Water samples were collected in pairs, with one sample filtered through disposable 0.45 μm Millipore™ filters and the other left unfiltered. Samples for H_2S analysis were collected in 15 mL PP vials. Samples collected at depth from lakes were collected using a purpose-built sampler (Webster 1994).

All re-useable equipment (500 mL bottles, filtration gear, syringes, Teflon beakers etc...) was washed in detergent ($Decon_{90}$™), then rinsed in distilled water and soaked in an acid bath (> 2 M nitric acid) for at least 36 hours, and then rinsed in Milli-Q-water before air-drying and subsequent re-use (Wilson et al, 2004b). Neither lab nor field blanks, collected throughout the research, yielded any evidence of Sb contamination during sampling, nor was there any indication of Sb loss through adsorption onto the sampling vessel. The latter was tested by re-measuring a filtered sample three months after its initial analysis.

2.1.2 POWER STATION FLUIDS

There are a number of complications that arise when sampling geothermal fluids. In particular, such fluids are typically at high temperatures (up to 300 °C), so samples had to be collected using a sealed stainless steel cooling coil, as shown in Plate 2.1. The coil sits in a bucket of cold water, and as the fluid passes through the coil, its temperature is cooled to below boiling point (< 100 °C) and can then be collected safely with no significant vapour loss.

Plate 2.1 Cooling coil used to collect power station fluids, shown with the coil passing through a bucket of cold water before sample collection.

In-line Swagelok® filters were tested, in order to try to determine the relative proportions of dissolved and particulate Sb in solution. The use of a 0.5 µm filter proved unsuccessful, because even when coupled with a 15 µm filter, the 0.5 µm filter would clog, and prevent any flow into the cooling coil. Antimony concentrations measured in samples collected using a 15 µm filter alone were inconsistent, being significantly lower than Sb measured in unfiltered samples at certain collection points, but similar at others. No clear pattern emerged from the results.

Filtering using disposable 0.45 µm filters after collection using a cooling coil was not a practicable option. At the lower collection temperature (typically 40 – 60 °C) Sb_2S_3 is less soluble than it would have been *in-situ* at higher temperatures (Reed and Palandri, 1998). Therefore, the cooled and filtered samples contain less Sb that the fluids they are meant to represent, and the filters contain more Sb than they should. An example of a filter paper from such an exercise is shown in Plate 2.2.

Results for Sb presented for geothermal power station fluids are therefore for "total" Sb, i.e. measured on unfiltered samples. However, it was assumed for modelling purposes that the total Sb concentrations measured were in the dissolved phase. The implications of this assumption are discussed in Chapter Three.

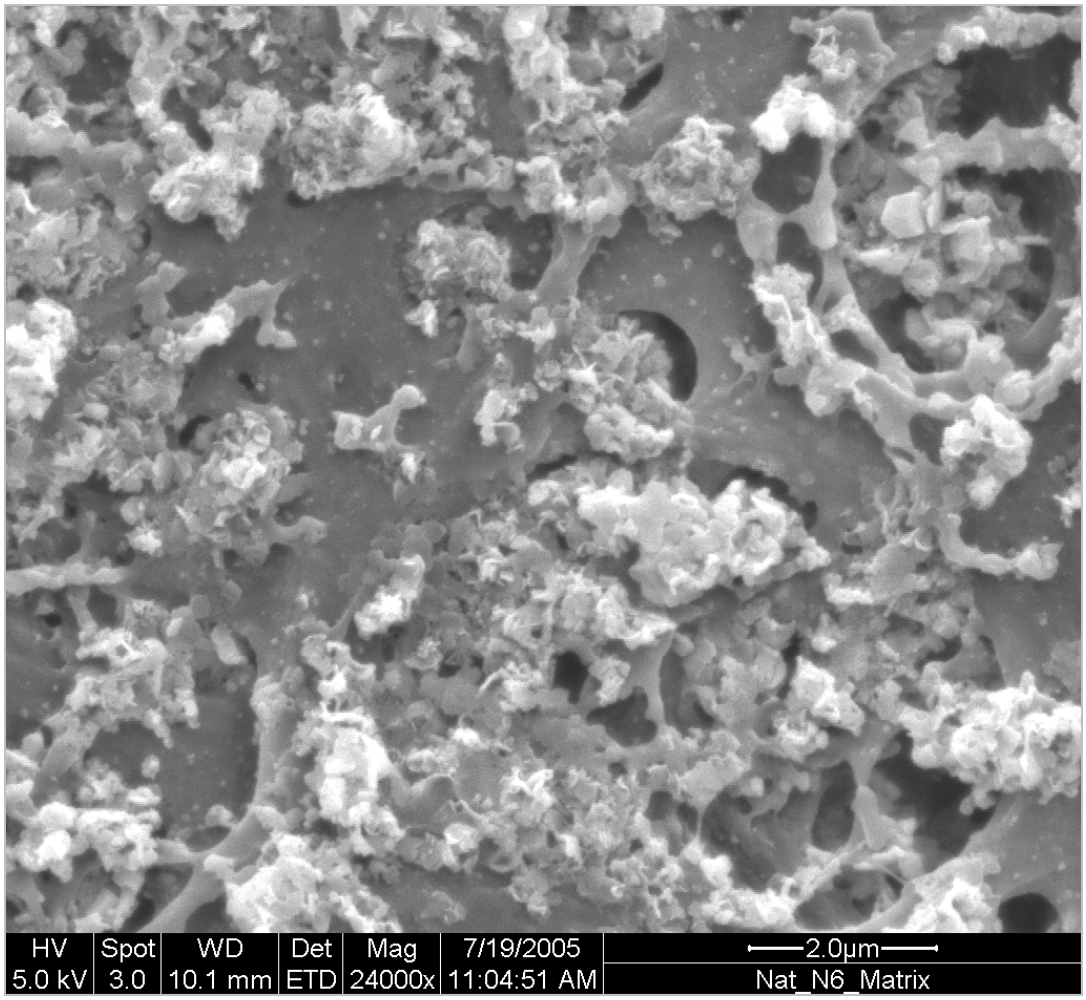

Plate 2.2 Scanning electron microscope (SEM) photo of a 0.45 µm filtered sample from Rotokawa. The precipitates are at least 5 % Sb (by weight).

2.1.3 PRESERVATION

Geothermal fluid samples from the geothermal power stations were preserved in alkali (KOH; pH > 11). As shown in Figure 2.1, the addition of acid (HCl; pH < 2) to these samples suppressed results for Sb. This is because lowering the pH of sulfide-rich samples induced the formation of Sb_2S_3 (Brown and Simmons, 2003). Results for Sb in unpreserved samples were similar to those of samples preserved in alkali, but samples preserved in alkali yielded better recoveries (99-104 %). Samples from the surface discharges of natural geothermal features were not acidified for similar reasons, and because Sb speciation was to be investigated and the addition of alkali increases the rate of oxidation of species in solution, samples were not preserved in alkali either (Pope et al, 2004).

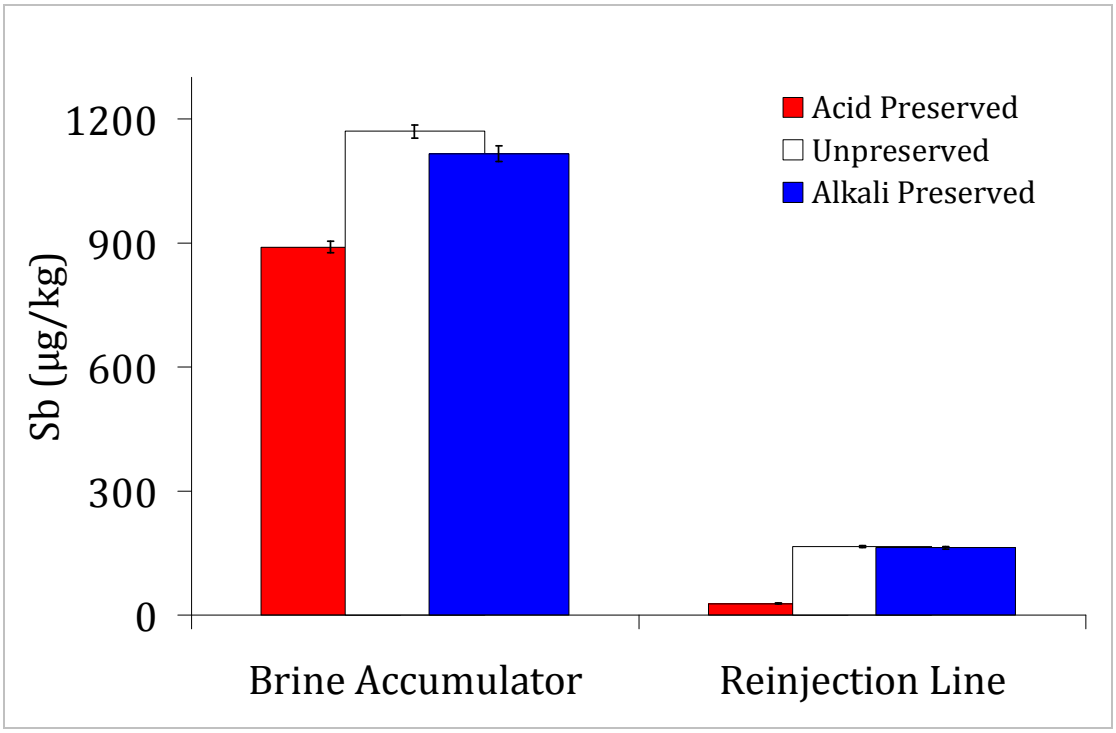

Figure 2.1 Comparison of preservatives used for geothermal fluid samples

Samples for H_2S were preserved using 1 M zinc acetate. However, aqueous samples collected for Sb from receiving environments were not preserved, regardless of whether they were filtered or not. While it is standard practise to acidify freshwater samples for trace metal analyses, Sb is not a metal, nor does it behave like one. Adsorption of Sb onto Fe/Mn/Al-oxyhydroxides can occur, especially in low pH mine drainage, but in circum-neutral waters this does not appear to be a significant process (Aggett and Kriegman, 1987; Ashley et al, 2006; Wilson et al, 2004b). The results of this study also showed that there was little difference between acidified samples and unpreserved samples, as shown in Figure 2.2, and recoveries were comparable.

Leaving samples unpreserved also meant that samples collected at a transition point between natural geothermal system discharges and the receiving environment could be compared to both end members. Consistent protocols could be established, and any interference between preservatives and the analytical method (discussed in Section 2.2.2) could be avoided. Similar results were produced for As with and without acid preservation as well.

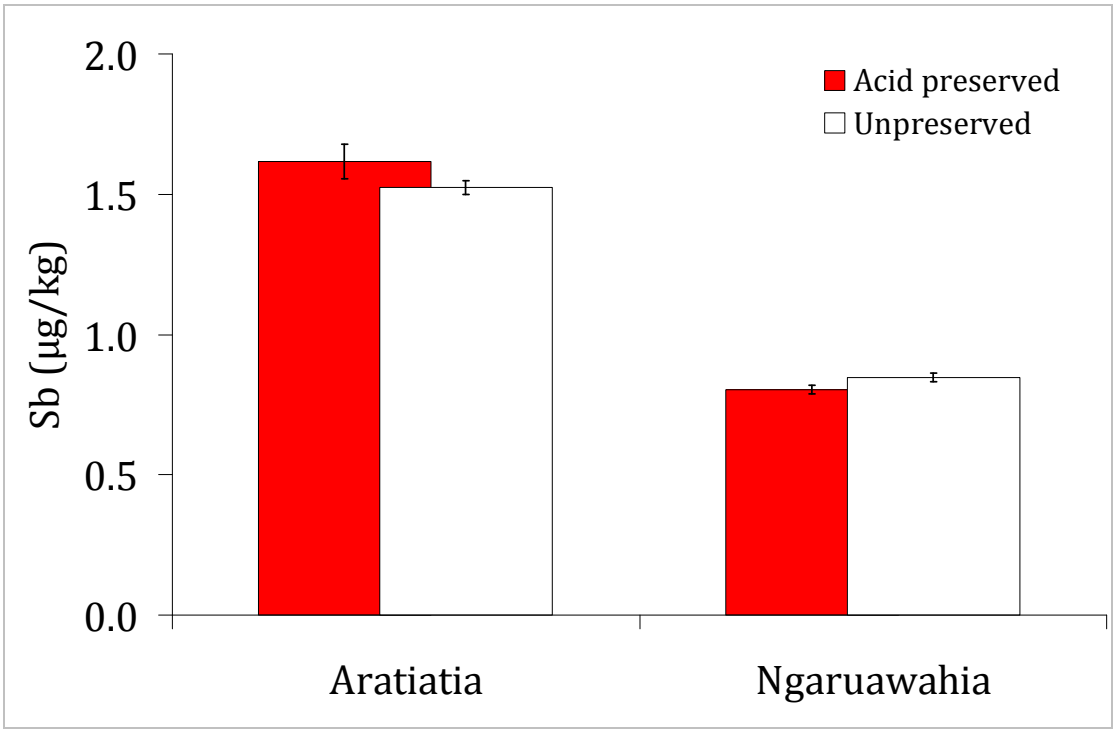

Figure 2.2 Comparison of preserved and unpreserved samples collected from the upper (Aratiatia) and lower (Ngaruawahia) halves of the Waikato River. None of the samples presented were filtered.

Even at low temperatures (-20 °C), adsorption and bacterial activity can potentially distort speciation in samples (de la Calle-Guntinas et al, 1992). De la Calle-Guntinas et al (1992) showed that 1% citric acid (w/v) could preserve Sb^{III} in samples for at least one month at 25°C, and longer at 4 °C, however Sb lasted just as long when no preservative was added. Ariza et al (2000) showed that lactic acid was also a suitable preservative for Sb^{III}, and EDTA has been suggested for As^{III} preservation and therefore may also work for Sb as well (Bednar et al, 2002). The use of preservatives carries with it an increased risk of contamination though, and so it was decided that no preservative would be used (Bornhorst et al, 2005). Instead the technique used was to filter samples (0.45 µm) into 50 mL vials leaving no headspace; this removed most of the bacteria in solution and limited the amount of available atmospheric oxygen. Following collection, all aqueous samples were refrigerated (at 4 °C) as soon as was practically possible.

2.1.4 SEDIMENTS FROM THE WAIKATO RIVER

Two sediment types were collected, suspended particulate material (SPM), and bed sediment. The 0.45 μm nitrocellulose filter papers used to collect SPM were dried initially at 40 °C for 48 hours and then left at room temperature for 4 hours before weighing. The SPM was then collected on to the filter papers by filtering 0.5-2 L of water. These filters were then again dried at 40°C for 48 hours and re-equilibrated at room temperature (for a further 4 hours) before reweighing.

Shallow samples of bed sediment was collected into 250 mL plastic containers and dried in an oven at 60 °C until dry. Samples were then sieved to 63 μm. No other solids were collected.

2.1.5 BIOTA

Algal samples from Waimangu were collected by into 50 mL PP vials by attaching the vials to the end of a pole and scooping the algae out. Combined stem and leaf plant samples from the Waikato hydro-lakes were collected by hand into 250 mL plastic containers (no roots were collected). All biotic samples were rinsed in distilled water in an attempt to remove as much sediment as possible, and then dried at 40 °C until completely dry (up to two weeks), crushed using a pestle and mortar, and then sieved to 0.5 mm.

2.2 CHEMICAL ANALYSES OF WATERS

2.2.1 *IN SITU* ANALYSES

Temperature, conductivity, pH, light and dissolved oxygen (DO) were measured *in situ* using standard portable field meters. Meters used for measuring pH and DO were calibrated at least once daily, conductivity meters were calibrated monthly.

2.2.2 ANTIMONY AND ARSENIC

To determine the amount of Sb and As in aqueous samples, hydride generation coupled with atomic absorption spectroscopy (HG-AAS) was employed. The technique was developed in the early 1970s by Braman et al (1972), but is still widely used, and works by reducing the metalloids from +3 valence states into gaseous hydrides (SbH_3 or AsH_3 in this instance).

Operating conditions for HG-AAS depend upon a variety of variables, which include the pump rate, flame temperature and the length of the reaction loop. For this research a GBC HG3000 continuous-flow hydride generator was employed, coupled to a GBC Avanta Atomic Absorbance Spectrometer. The reducing agent was 0.6 % (w/v) $NaBH_4$ in 0.6 % (w/v) NaOH and the carrier was concentrated HCl. Samples were pre-reduced (to convert metalloids from +5 to +3 states) in 0.5 % KI (w/v) and 2 M HCl. The practical detection limit for Sb was 0.2 µg/kg, but detection limits could be as low as 0.1 µg/kg under optimum conditions. For As the practical detection limit was 0.3 µg/kg. Analytical error was typically < 5 %. Recoveries for Sb ranged from 85-115 %, while As recoveries ranged from 90-110 %.

Over the course of the research, it became increasingly apparent that the presence of nitric acid (HNO_3) in samples interfered with the HG-AAS analyses. This was a particular problem during the analysis of sediment digests (see 2.3.1), which contained aqua-regia residues. The presence of HNO_3 in samples caused excessive bubbling to occur during the hydride generation process, after which the system needed cleaning and re-calibration before further samples could be analysed. Sulfamic acid was touted by Flores et al (2001) as an additive to suppress the formation of nitrogen oxide (NO_x) complexes generated from the HNO_3 in reducing conditions, but the simplest option was to dilute any samples with suspected high nitric acid levels before the pre-reduction step.

SPECIATION

Dissolved Sb^{III} and As^{III} were determined without the pre-reduction step, so as to exclude As^{V} and Sb^{V} from the analyses. A solution of 6 % w/v citric acid was used as a carrier instead of HCl (Andreae et al, 1981). The practical detection limits were 0.3 µg/kg Sb^{III} and 0.5 µg/kg As^{III}.

2.2.3 OTHER ELEMENTS

Iron (Fe) and manganese (Mn) were measured using either flame atomic absorption spectroscopy (FAAS), or graphite furnace coupled with atomic absorption spectroscopy (GF-AAS), depending on the sample concentration. The detection limits for FAAS were 1 mg/kg for Fe and 200 µg/kg for Mn. For GF-AAS analyses, the detection limit was 5 µg/kg for Fe and 1 µg/kg for Mn. The analytical error was < 5 %. In order to analyse sediment digests, which contained 2 M HCl, Mn standards for digest analyses were also made up in 2 M HCl, to account for the formation of Mn-Cl complexes. Recoveries were 100 % for both elements.

Sulfate (SO_4), chloride (Cl), and nitrate (NO_3) concentrations were measured using a Dionex ICS-2000 HPIC with an ASRS Ultra II 2 mm column. Total sulfide concentrations (as H_2S) were measured using the Methylene Blue method, with a detection limit of 0.05 mg/kg total sulfide (APHA, 1998). Lithium (Li) was determined by atomic emission spectroscopy (AES) at 670.7 nm. Measureable concentrations of Li were found in all samples and detection limits for Li were not quantified. Detection limits for AES are relative, and change depending on the concentration of the top standard (which is an arbitrary choice).

2.3 SOLID ANALYSES

In general, sample volumes were too small for non-destructive solid phase analysis (by XRF for example). The exception to this was scanning electron microscope analysis (SEM), which can include a chemical analysis (EDAX). However, SEM-EDAX is only semi-quantitative, with a detection limit of 1 %. SEM images were taken of selected 0.45 μm filter membranes after use.

2.3.1 SEDIMENT DIGESTIONS

Bed sediment and SPM samples were digested using an open hot aqua-regia digestion process, using a method modified from Tighe et al (2004). Microwave digestions are generally the preferred technique for slightly volatile elements such as Sb or As, but SPM samples were sometimes so small (< 10 mg) that the large dilutions required following microwave digestion meant that Sb concentrations in the resulting solutions were below detection limits. The advantage of an open technique was that samples only needed to be diluted up to the amount of solution required for analysis (typically 20 mL for Sb, As, Fe and Mn analyses).

The digestion process involved two steps. First, 20 mL of concentrated aqua regia (15 mL HCl and 5 mL HNO_3) was added to a known amount of sample (typically less than 100 mg) in a polytetrafluroethylene (PTFE) beaker, covered with a PTFE lid, and then boiled down to < 5 mL on a hot plate. Next, 20 mL of 0.1 M aqua regia were added, and the solutions again evaporated to < 5 mL (this time uncovered), left to cool, and then made up to the required volume in 2 M HCl.

Digestion recoveries were tested by using the LKSD set of standard reference materials. For LKSD-2 and LKSD-3, recoveries of 100 ± 10 % for Fe, Mn and As were achieved. Recoveries were not as good for Sb, recoveries ranged from 60% through to 140 %, and overall precision was 25 %. However, there was a lack of practicable alternatives because HNO_3 digests did not work at all, even when sulfamic acid was used, nor did HCl digests (probably because they induced the formation of volatile Sb-Cl species). There were no facilities available at the School of Geology, Geography and Environmental Sciences for HF or $HClO_4$ digests such as those described by Krachler et al (2002), nor was there funding available to send off the large number of prepared samples.

Despite the technique's lack of precision, it was considered good enough to at least determine Sb abundance in sediments to well within an order of magnitude. Results presented have not been corrected, but are rather reflected in error calculations (shown as error bars on graphs where appropriate). Detection limits for the method were dependant on the amount of sediment that could be digested (larger amounts of sediment meant lower detection limits) and the limits of the analytical method[1].

2.3.2 SEQUENTIAL EXTRACTIONS

A sequential extraction procedure was used to determine the availability of Sb in SPM collected from Tuakau Bridge on the Waikato River. The method chosen used a five step process, developed for As by Wenzel et al (2001) and first applied to Sb by Müller et al (2007). The method is summarised in Table 2.1 and was designed to provide an estimate of what may be leached from various solid phases, but it does not account for the organic or sulfur-bound fraction.

Because other studies have reported that organically-bound Sb can account for more than 10 % of the total Sb in sediment (Brannon and Patrick, 1985), a single step extraction using EDTA was also employed. As detailed by Lintschinger et al (1998), this involved shaking a sample in 0.05 M EDTA (pH 7.0) at room temperature for one hour.

[1] For example, if 10 mg of sediment were dissolved, the detection limit for Sb was 400 $\mu g/kg_{sediment}$, based on dilution up to 20 mL after digestion. For 100 mg of sediment, the detection limit for Sb would be 40 $\mu g/kg_{sediment}$.

Table 2.1 Sequential extraction procedure of Müller et al (2007) used for Tuakau SPM

Fraction	Extractant	Conditions
Non-specific sorption	10 mL 0.05 M $(NH_4)_2SO_4$	4 h shaking, 20 ^oC
Specific sorption	10 mL 0.05 M $(NH_4)H_2PO_4$	16 h shaking, 20 ^oC
Amorphous metal oxide bound	10 mL 0.2 M NH_4-oxalate; pH 3.25	Darkness, 6 mL: 4 h shaking, 20 ^oC; 4 mL, 10 min shaking
Crystalline metal oxide bound	6 mL 0.2 M NH_4-oxalate + 0.1 M ascorbic acid; pH 3.25	30 min water bath, 96 ^oC; 4 mL NH_4-oxalate, 10 min shaking in darkness
Residue	Aqua regia	Per digest

The sequential extractions were run in triplicate, together with a blank solution of de-ionised water so that contamination in any of the extractants could be corrected for. The single (EDTA) extraction was performed on a single sample because of a lack of SPM (as will be discussed in Chapter Five).

2.3.3 PLANT DIGESTS

Acid digests of plant (and algae) material could not be analysed using HG-AAS because the organic acids generated during the digestion process caused excess bubbling similar to that produced by residual HNO_3. Therefore, a different digestion was used. Biotic samples were incinerated after being dosed with MgO and $MgNO_3$, based on a method developed by Pahlavanpour et al (1981) and modified by Almela et al (2006). First, 2.5 mL of a solution containing 20 % (w/v) $MgNO_3$ and 2 % (w/v) MgO, along with 5 mL of 50 % (v/v) HNO_3 were added to weighed samples (~ 0.25 g) in 25-50 mL porcelain crucibles. The samples were then dried at 100 ^oC for 4 hours, heated to 200 ^oC for 30 minutes, and then incinerated at 450 ^oC for 10 hours. The ashed samples were then dissolved in 20 mL of 2 M HCl and analysed by HG-AAS.

Recoveries for arsenic were acceptable at 96 ± 17 %. However, for Sb recoveries from the tomato leaf reference standard (NIST-SRM 1573a) used were 185 ± 31 %. Such recoveries suggested that the digestions were contaminated, but the source of the contamination (i.e. the crucibles or one of the reagents) could not be determined. Nonetheless, these recoveries were not so poor that results of the digestion method were worthless. The method did give an indication of the degree of biological uptake, even if the accuracy of the analyses were poor.

2.4 ADSORPTION EXPERIMENTS

Adsorption edge experiments were performed using a method based on that described in Bibby and Webster-Brown (2006). Freeze-dried SPM (collected from Tuakau on the Waikato River) was resuspended in 0.01 M $NaNO_3$ at a concentration of 100 mg/L (typically 30 mg SPM in 300 mL). The solution was then left to re-hydrate at 4 ^{o}C for 48 hours, and then left to equilibrate to 25 ^{o}C (typically 4 hours). The pH of the solution was raised to ~ 10 using NaOH, and constantly mixed using an acid-washed stirrer, before the solution was spiked with Sb (either Sb^{III} or Sb^{V}) to achieve an Sb concentration of 10 µg/kg. This created a similar Sb:SPM ratio to that found in the Waikato River.

Once pH had stabilised, an aliquot (~15 mL) was extracted and then the pH of the bulk solution was lowered by about 0.5 pH units and the process repeated. The end pH was typically ~3. The extracted aliquots were then placed on a mixing wheel, similar to the one shown in Plate 2.3, in a temperature controlled room (25 ^{o}C) and left to rotate in darkness.

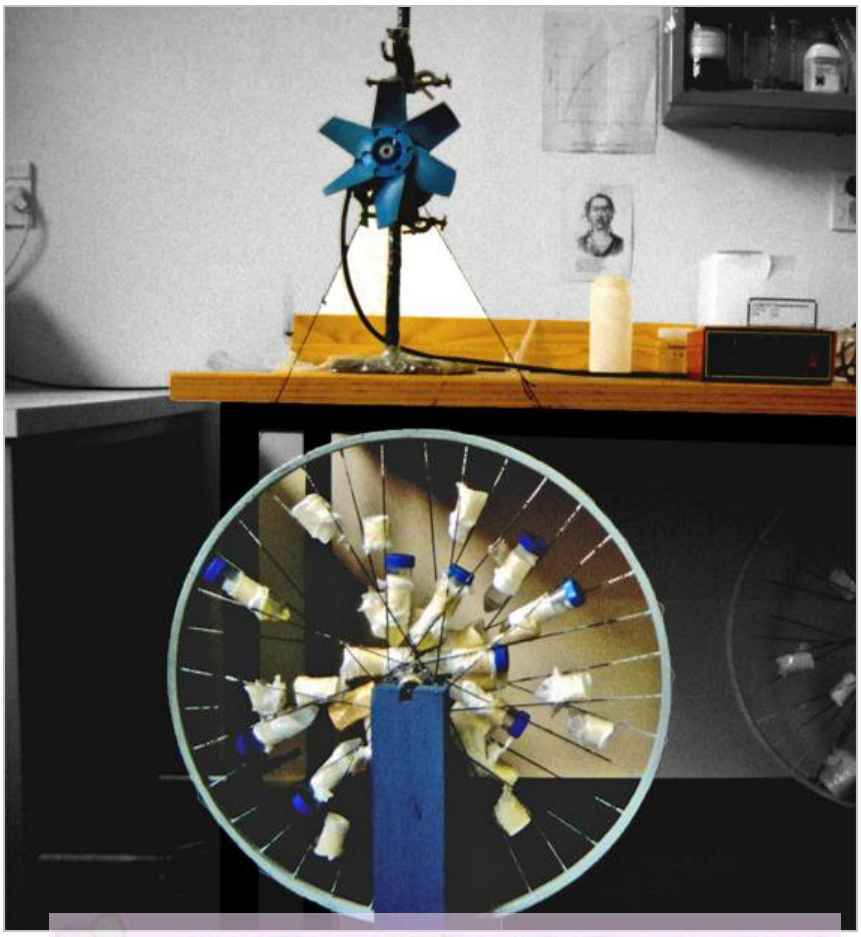

Plate 2.3 Mixing wheel used to maintain sample agitation during adsorption experiments (Photo courtesy of Jenny Webster-Brown)

After 24 hours, the samples were removed from the wheel. Half of each aliquot was filtered (0.45 μm) and the pH was remeasured in the remaining solution to determine the final pH of each sample. Control experiments first without SPM, and then without Sb added, showed that no measurable adsorption onto or release of Sb from the PP vial walls occurred and nor was there removal of Sb through precipitation of Sb solid phases.

2.5 MODELLING METHODS

Geochemical models based on thermodynamic data can be used to predict and to model geochemical processes under thermodynamic equilibrium. In this thesis, four models were used: CHILLER, SOLVEQ and WATCH 2.3 for power stations and PHREEQc for natural geothermal springs and receiving waters. Input data for these models are presented in Appendix I.

2.5.1 GEOTHERMAL FLUID MODELLING

The CHILLER and SOLVEQ programmes (Reed, 1982; Spycher and Reed, 1989b) compute a series of simultaneous and heterogeneous equilibrium calculations at set conditions (i.e. pH, temperature, pressure), and from these predicts the phase distributions and speciation of a wide range of elements. The model can be used to cool, heat, boil, and condense solutions, making it ideal for power station fluid modelling, and the SOLTHERM database associated with the CHILLER/SOLVEQ suite has been designed with geothermal systems in mind (Spycher and Reed, 1989b). Any model prediction is of course dependant upon the quality of the available thermodynamic data, and by necessity assumes a system at equilibrium (Reed, 1982).

Chemical data made available from GEOKEM (a private consulting company) for both Ngawha and Rotokawa power stations were for separate phase analyses (i.e. aqueous and vapour phases). The chemical data provided by GEOKEM were determined by GNS Science, which has ISO17025:2005 accreditation. Analyses were conducted on samples collected separately from those reported in this research.

In order to determine the chemistry of the fluids underground, WATCH 2.3, a computer programme designed to calculate composition and aqueous speciation of geothermal reservoir waters, was used (Arnorsson et al, 1982). WATCH 2.3 uses enthalpy calculations to determine reservoir fluid chemistry, with the only limitation being that the software model assumes that the steam and water are always together. WATCH 2.3 is designed for major ions only, and does not allow for elements such as Sb. The concentrations of elements not included in the WATCH 2.3 calculations were calculated manually based on volumes and dilution factors.

2.5.2 NATURAL SPRINGS AND RECEIVING WATERS MODELLING

PHREEQc is a numerical simulation model designed for low temperature geochemical calculations (Parkhurst and Appelo, 1999). PHREEQc has not been designed to deal with high temperature waters, so was not appropriate for subsurface geothermal fluid modelling, but the model can be used for a number or purposes, including kinetic or speciation calculations, partial redox disequilibria or batch reactions. Like CHILLER and SOLVEQ, the accuracy of PHREEQc is reliant on the quality of the thermodynamic data in the associated databases.

There are several databases included with the PHREEQc software package, and of them, the MINTEQ v.4 database appeared to provide the most suitable data to this study. Based on the findings discussed in Chapter Three, the database was amended to include data from Zotov et al (2003) for Sb_2S_3. The data added to the SOLTHERM and MINTEQ v.4 databases, for SOLVEQ/CHILLER and PHREEQCi respectively, are provided in Appendix I.

CHAPTER THREE
STIBNITE PRECIPITATION IN GEOTHERMAL POWER STATION FLUIDS

In this chapter, the behaviour of antimony in high temperature anoxic geothermal fluids is discussed[5]. Studying elements in subsurface fluids is always problematic for a number of reasons, not the least because any attempt to sample such fluids involves exposing the fluids to the surface, which alters the fluid chemistry (Brown and Simmons, 2003).

Geothermal power stations take fluids from the subsurface geothermal reservoirs and bring them to the surface, changing their nature as little as possible before their energy can be used for power production. Samples of these fluids can be collected enroute through valves connected to the power station pipes so that exposure to the surface environment is minimised. Geothermal power station fluids can therefore be used as proxies for subsurface fluids, and it is fortunate (for this research) that in New Zealand some of the power stations use fluids containing elevated concentrations of Sb.

The two power stations investigated in this chapter, Rotokawa and Ngawha, were chosen because Sb precipitates as Sb_2S_3 within them (Dorrington and Brown, 2000; Reyes et al, 2002). By understanding how and why Sb_2S_3 precipitates in those stations, it is possible to develop an understanding of how Sb behaves in high temperature fluids.

This chapter is unique in the context of this thesis in that As was not investigated. This was because As-bearing minerals were not precipitating in the pipelines of the two power stations, at least not in any significant amount (Ward, 2007).

[5] An abridged version of this chapter has been published as Wilson, N.J, Webster-Brown, J. and Brown, K., 2007. Controls on stibnite precipitation at two New Zealand geothermal power stations. Geothermics, 36(4): 330-347.

3.1 BACKGROUND AND STUDY OBECTIVES

The extraction of geothermal fluids for the generation of power began in New Zealand with the opening of the Wairakei power station in 1958 (Hunt, 1998). The Wairakei station, which is still operative, is now a 200 MW plant that generates electricity predominantly by separating hot steam and using it to directly drive turbines (Bertani, 2005). Ohāki, the third biggest power station in New Zealand, generates power in a similar manner. The hot water, which is separated from the steam before power generation, is either used to run smaller secondary units, or is treated as a waste product (Ellis and Mahon, 1977).

When discharging the cooled geothermal waste, the only practical options are to discharge the fluids at the surface, or to reinject them back into the ground (Rybach, 2003). Reinjection into the parent aquifer minimises the impact of power generation on the surface environment, but the injection of (relatively) cold fluids can potentially hasten the cooling of the sub-surface fluids and reduce the lifetime of the station (DiPippo, 2005). Reinjection outside the geothermal reservoir eliminates the risk of field cooling, but subsidence can occur as there is a net water loss from the parent aquifer (Hole et al, 2007).

Discharging waste into surface waters or shallow groundwaters also occurs. The Wairakei Power Station discharges cooled waste fluids directly into the Waikato River, giving rise to a range of environmental effects related to elevated concentrations of geothermal contaminants (Webster-Brown et al, 2000). The binary power stations at Rotokawa and Ngawha, the two stations used in this research, re-inject the geothermal fluids back into the parent field (Reyes et al, 2002).

The fluids are used quite differently in binary power stations such as Ngawha and Rotokawa. Binary power plants pass geothermal fluids through heat exchangers to vaporise a secondary fluid with a relatively low-boiling point (n-pentane at both power stations described in this chapter), which in turn drive turbines to generate electricity. The secondary fluids are recycled in a closed loop, and spent geothermal water is piped to reinjection wells (DiPippo, 2005). Noncondensible gases are generally the only discharge to the environment.

3.1.1 MINERAL SCALES IN GEOTHERMAL POWER STATIONS

The deposition of mineral scales within power station pipelines is a major hindrance to the extraction of heat from geothermal fluids (Gunnarsson and Arnorsson, 2005). The problems associated with silica and calcite deposits in geothermal power station pipelines are well recognised, but other precipitates, such as sulfide minerals, can also cause similar complications (Azaroual et al, 2004; Ellis and Mahon, 1977; Reyes et al, 2002). Stibnite is one such sulfide, and its formation has developed into an ongoing problem within the heat-exchanger units of the Rotokawa and Ngawha stations (Brown, 2003). This mineral deposition was not predicted by the thermodynamic models used during the development of the two stations, in part because Sb was often not accounted for at all.

There have been few previously reported occurrences of Sb_2S_3 scaling in geothermal power stations. Outside New Zealand, the phenomenon has only been reported in an exploratory well in Italy, and in pipe fragments from the Berlin field, El Salvador (Cappetti et al, 1995; Raymond et al, 2005). In New Zealand, Sb_2S_3 scaling, as well as the precipitation of other minerals, has been described by Reyes et al (2002) at the Rotokawa geothermal power station and by Dorrington and Brown (2000) at the Ngawha geothermal power station. The deposition of the Sb_2S_3-rich scale at Rotokawa is detailed in a recent MSc thesis (Ward, 2007). The scale forming in the OEC 21 heat exchanger is comprised of concentric bands of kaolinite ($Al_2Si_2O_5(OH)_4$) and Sb_2S_3, with telluride and sulfide bands occurring as well. The relative lack of published information regarding this problem is in part because Sb (and therefore Sb_2S_3) is relatively rare, but also because conditions for Sb_2S_3 precipitation appear to be specific and the companies involved (such as Top Energy or Mighty River Power in New Zealand) do not publish.

3.1.2 THE ROTOKAWA AND NGAWHA SITES

There are six commercial geothermal power stations currently operating in New Zealand (Bertani, 2005). Significant Sb_2S_3 scaling is occurring only at binary geothermal power stations such as those built upon the Rotokawa and Ngawha geothermal fields.

ROTOKAWA GEOLOGY

The Rotokawa geothermal field is located in the Taupo Volcanic Zone (TVZ), described in more detail in Chapter One. The Rotokawa power station (and geothermal field) lies about 10 km northeast of Lake Taupo, near the centre of New Zealand's North Island, as shown in Figure 1.2.

Palaeozoic to Mesozoic greywacke forms the basement rock underneath the Rotokawa field, overlain by andesite lava, a series of layered ignimbrites and rhyolite lava, all of which is covered by Holocene tuff and hydrothermal eruption deposits (Krupp et al, 1986). Significant sulfur deposits, containing enriched levels of As and Sb sulfides, as well as gold in ore-grade concentrations, are found around the field's main hot spring area at Lake Rotokawa (Krupp and Seward, 1987).

Fluid in the reservoir exceeds 310 ^{o}C, and contains elevated Au, As, Sb, W, Tl, Hg, Ag, Ge and Ga concentrations (Reyes et al, 2002). Carbon dioxide (CO_2) is the dominant gas, while hydrogen sulfide (H_2S) accounts for 0.5 % by weight of the total gas discharge (Giggenbach, 1995). Geothermal wells have been drilled into two sectors of the field (North and South). Northern wells contain a lower percentage of magmatic derived-fluids and lower concentrations of Cl, Cs and Li (Reyes et al, 2002). All the wells presently used for production are situated in the northern sector.

ROTOKAWA POWER STATION

The Rotokawa power station was commissioned in 1998 by the Mighty River Power company, and is outlined schematically in Figure 3.1. The station is an ORMAT® Geothermal Combined Cycle plant that uses both a steam turbine and a series of binary units to generate up to 34 MW of electricity (Legmann and Sullivan, 2003).

After separation, most (~75 %) of the vapour passes first through a steam turbine generating about 15 MW, and is then split between two heat exchanger units to provide a further 5 MW each (OEC 11 and OEC 12). The bulk (~80 %) of the brine runs through a single heat exchanger unit to generate up to 5 MW (OEC 1). A second heat exchanger unit, installed in 2002, uses the remaining steam and brine to generate an additional 6 MW under optimal conditions (OEC 21, shown in Plate 3.1) (Legmann and Sullivan, 2003). The process condenses the steam phase, and the condensed steam and brine components combine later within the unit, similar to that outlined in Figure 3.2. It is in this mixed-phase heat exchanger that accumulation of Sb_2S_3 scale presents a problem (Ward, 2007).

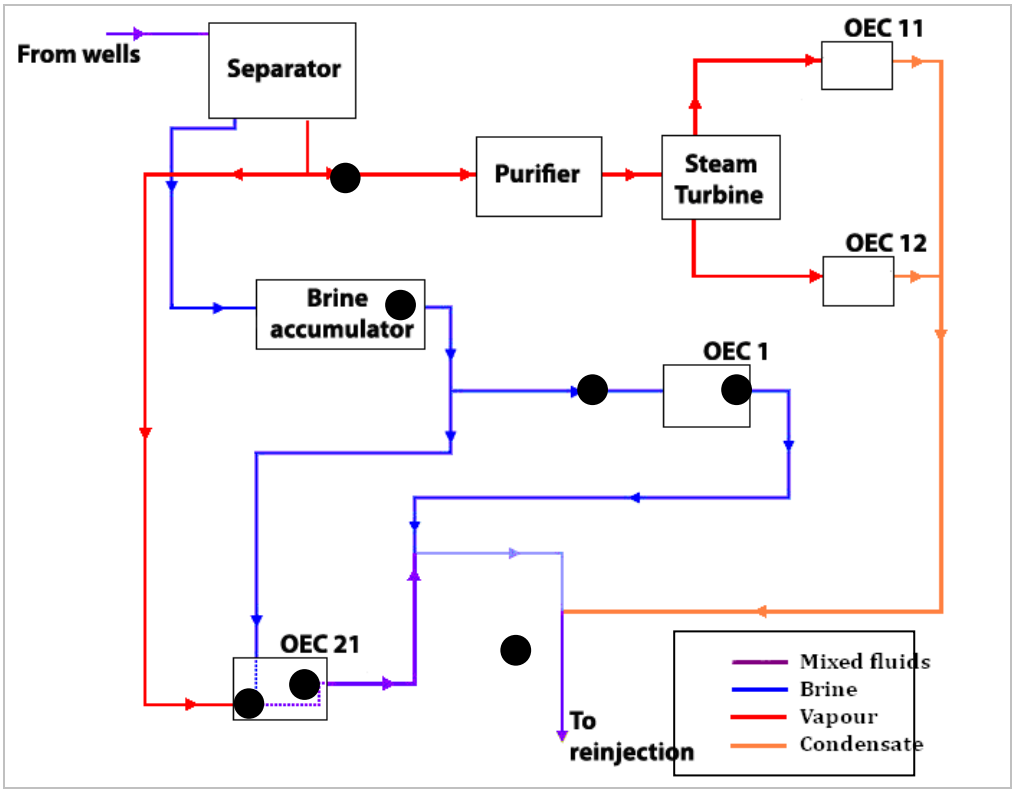

Figure 3.1 Schematic of the Rotokawa power station. Heat exchanger units are abbreviated as HE, and sampling points are shown as black circles.

Plate 3.1 The OEC 21 unit at Rotokawa (Photo courtesy of Kevin Brown)

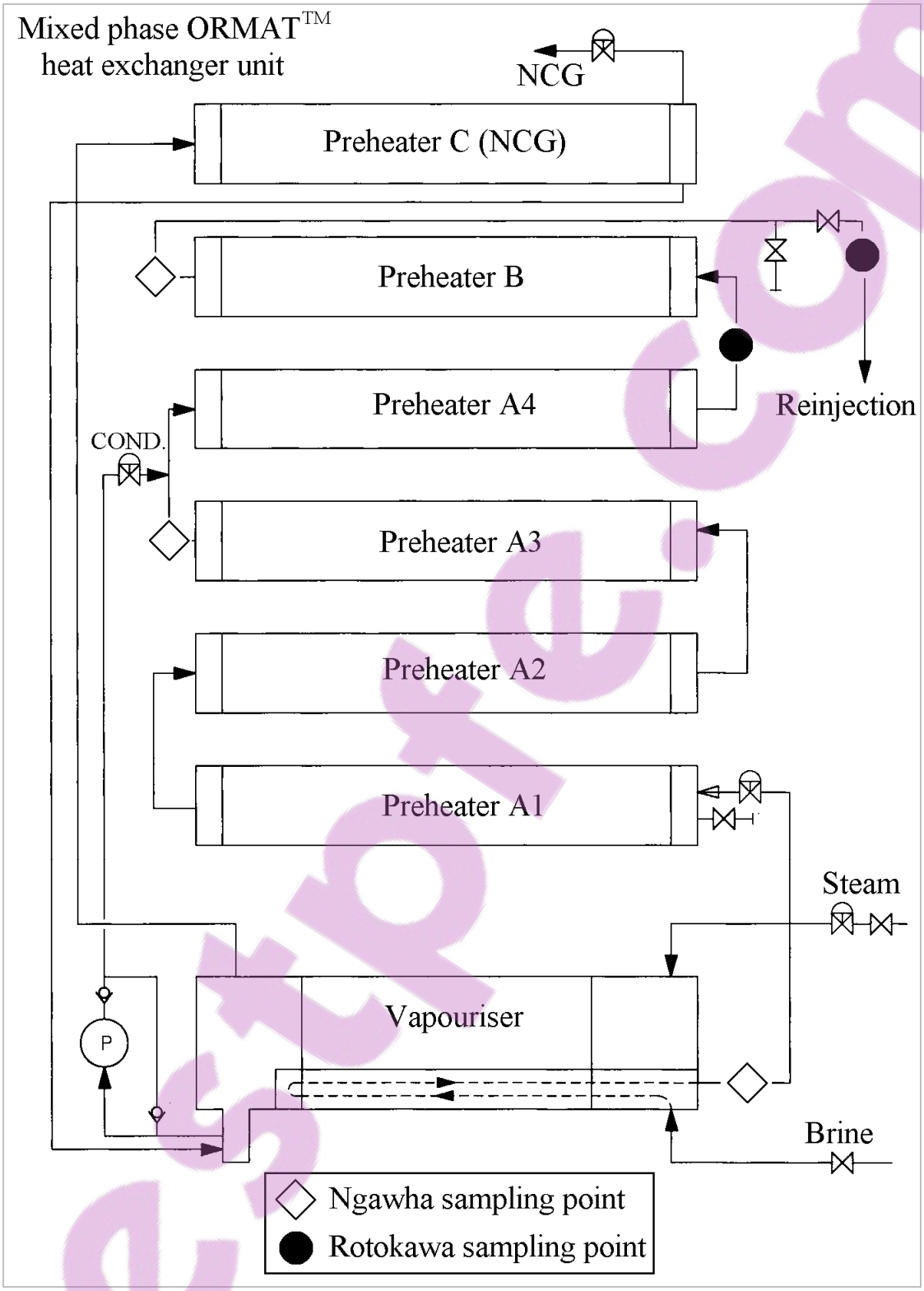

Figure 3.2 A schematic of ORMAT™ heat exchanger units. Rotokawa sampling points are marked with black circles, Ngawha sites by clear diamonds. "NCG" stands for non condensable gases; "COND." is the condensate.

NGAWHA GEOLOGY

The Ngawha geothermal field, also shown in Figure 1.2, has formed in a prehistoric river valley approximately 200 km north-northwest of Auckland, and is the only high temperature geothermal system in New Zealand outside the Taupo Volcanic Zone (Fleming, 1945; Sheppard, 1986). Late Cretaceous-early Tertiary shale and sandstone form the basement rock in the field, which has been overlain since the Pliocene by a series of olivine basalt flows (Fleming, 1945). At some time during these volcanic events, a lake formed within the valley, which subsequently filled with silt and organic-rich sediments. Current hydrothermal activity is most likely a product of basalt intrusions (Ellis and Mahon, 1977; Fleming, 1945). Cinnabar (HgS), marcasite (FeS_2) and native sulfur deposits can be found in eroded lake beds around the hot springs, with minor amounts of alum ($KAl(SO_4)_2$ 12 H_2O), realgar (As_4S_4) and Sb_2S_3 also present (Ellis and Mahon, 1977).

The maximum temperature of the system is about 236 ^oC. All of the energy is derived from a single deep source, and the system has a high gas content (Ellis and Mahon, 1966; Ellis and Mahon, 1977). The fluid within the system has similar Cl, CO_2 and H_2S concentrations to Rotokawa, but the gas phase contains greater fraction of hydrocarbons (2-3 mol % CH_4) (Fleming, 1945; Sheppard, 1986).

NGAWHA POWER STATION

The Ngawha power station, which also became operational in 1998, does not use a steam turbine. Instead the station uses an ORMAT® binary plant that generates 10 MW of electricity from two mixed brine-vapour heat exchanger units, as shown in Figure 3.3 and Plate 3.2. Stibnite scale accumulates in both units, at an approximate rate of 3 tonnes every six months. The configuration of both heat exchanger units is similar to the OEC 21 unit at Rotokawa (Figure 3.2).

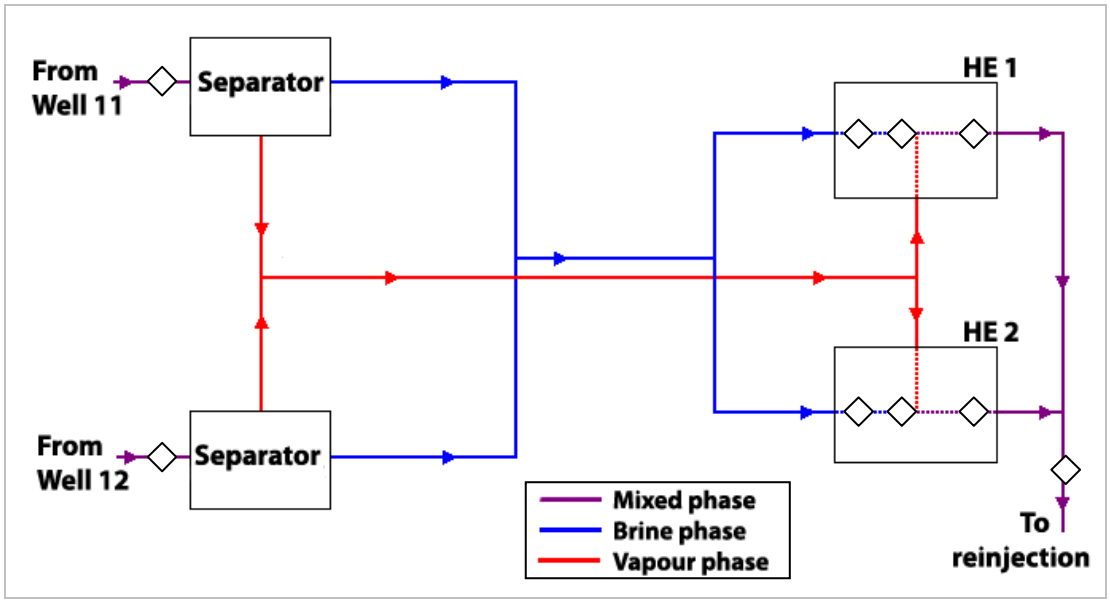

Figure 3.3 Schematic of Ngawha power station. Heat exchanger units are abbreviated as HE, and sampling points are shown as white diamonds.

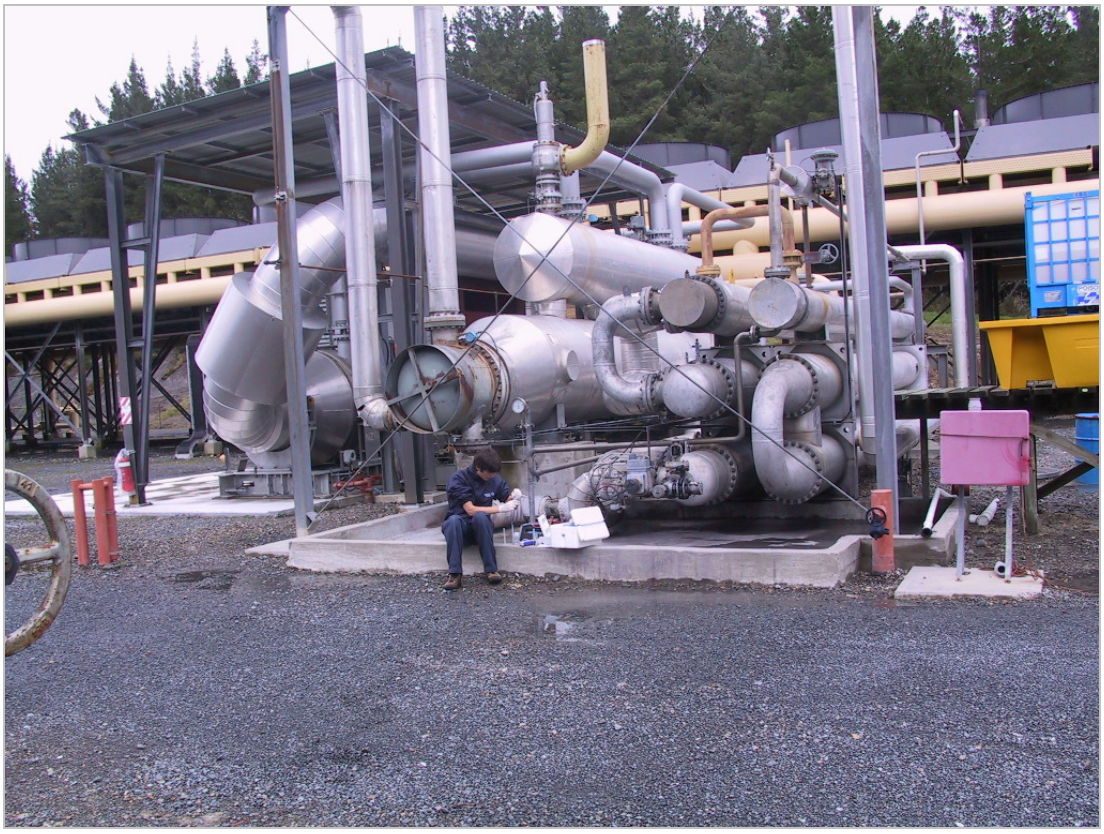

Plate 3.2 The HE 1 unit at Ngawha (Photo courtesy of Kevin Brown).

3.1.3 STUDY OBJECTIVES

The principal purpose of this study was to determine the cause(s) of Sb precipitation as Sb_2S_3 within the Rotokawa and Ngawha power stations. Three objectives were required in order to achieve this:

1. To update the thermodynamic databases in the CHILLER and SOLVEQ models used to predict geothermal fluid behaviour with the most recent reliable solubility data for Sb_2S_3.
2. To measure Sb concentrations in the power station fluids, and then use this data, along with other chemical parameters, to determine where Sb_2S_3 was precipitating, and what was inducing the precipitation.
3. To compare the observed and modelled predictions to determine if Sb behaviour can be reliably predicted.

A secondary aim was to determine the pathways by which Sb travels in geothermal fluids. The hypothesis to be tested in this case was that:

> Antimony is present in both the steam and vapour phases used in the Rotokawa and Ngawha power stations.

3.2 SAMPLING AND ANALYTICAL METHODOLOGY

Both power plants investigated in this study are binary ORMAT™ plants. At both Rotokawa and Ngawha, Sb_2S_3 is being deposited as the geothermal fluids pass through the lines, particularly within certain heat exchanger units, and by sampling at a number of sites along the liquid (brine) lines, it was possible to specifically determine where antimony is being removed from solution using mass-balance calculations. Geothermal fluids discharged from wells are not subject to external influences such as seasonal variation, rainfall, temperature or bacteriological activity, and therefore repetitive sampling was not necessary.

Samples were collected from Rotokawa in August, 2005, and from Ngawha in October, 2005. In order to test reproducibility, samples were collected in triplicate at Rotokawa, and duplicate samples were collected from Well 12 and HE 2 outlet at Ngawha. The specific sampling locations are shown on Figure 3.1 and Figure 3.3. It was not possible to sample before the condensate and brine mixed within the mixed phase heat exchanger unit at Rotokawa, but this was possible at Ngawha (Figure 3.2).

The power station operators supplied physical data for the time of sampling, such as flow rates, pressures and internal temperatures. Mighty River Power provided supplementary chemical data (such as major ion concentrations) for thermodynamic modelling of the Rotokawa station cycle. Top Energy provided these data for the Ngawha station.

3.3 THERMODYNAMIC MODELLING

Data for the solubility of Sb compounds are somewhat limited. For example, in Krupp's (1988) review of data for Sb solubility in sulfur-rich solutions, only four of fifteen published papers included data above 100 °C.

3.3.1 DATA SELECTION

Krupp (1988) proposed that, in high-sulfide systems, thioantimonate species ($H_2Sb_2S_4^o$, $HSb_2S_4^-$, SbS_4^{2-}) would dominate below 100 °C, the complex $Sb_2S_2(OH)_2^o$ becoming prevalent at higher temperatures. While acknowledging that antimonous acid ($H_3SbO_3^o$) and its derivatives were important in sulfur-free systems, Krupp (1988) did not allow for such species to exist in high-sulfide systems. Thioantimonate species data are included in the SOLTHERM database, but these data were derived from Spycher and Reed (1989b).

Natural systems, such as geothermal fluids, tend to have lower total sulfide ($H_2S + HS^-$) concentrations than Krupp used for his calculations, and, when used to model such systems, Krupp's data results in over-estimations of Sb_2S_3 solubility. Spycher and Reed (1989b), when developing the geochemical database SOLTHERM, allowed for the co-existence of both $Sb(OH)_3^o$ and dimeric Sb-S species.

Spycher and Reed (1989a) found that the data from most individual studies were inconsistent. In order to reconcile the available data, they critically evaluated and fitted previously published Sb_2S_3 solubility data, using least square fits and multicomponent equilibrium computations to derive stoichiometries and equilibrium constants. It is Spycher and Reed's (1989a) work that provides the Sb_2S_3 data, as well as some of the arsenic data, for the SOLTHERM database, and for the MINTEQ databases used by PHREEQC, despite some objections from Krupp (1990a, b and the responses from Spycher and Reed (1990a, b)).

More recently, Zotov et al (2003) recalculated solubility data for Sb_2S_3 from the experimental results of a number of studies. The authors recalculated the data in terms of $Sb(OH)_3^o$ (H_3SbO_3) as the dominant dissolved species, according to the reaction:

$$0.5\ Sb_2S_{3(s)} + 3\ H_2O_{(l)} \leftrightarrows Sb(OH)_3^o{}_{(aq)} + 1.5\ H_2S_{(aq)} \qquad (3.1)$$

This reaction as written is independent of pH, but it only holds in conditions in which both H_2S and $Sb(OH)_3^o$ (H_3SbO_3) are not dissociated. When either pH > $pK_{(H_2S)}$ or pH > $pK_{(Sb(OH)_3^o)}$, changes in pH will affect Sb_2S_3 solubility, because H_2S can dissociate to form HS^-, and H_3SbO_3 can either gain or lose hydrogen ions to form $H_4SbO_3^+$ or $H_2SbO_3^-$ (depending upon pH). A similar reaction can be made for arsenious acid equilibria and orpiment (As_2S_3), the arsenic analogue of Sb_2S_3 (Webster, 1990).

When the available data is recalculated in this way, Krupp's (1988) Sb_2S_3 solubility data compared well with thermodynamic data published for Sb_2S_3 solubility by Shikina and Zotov (1999), Akinfiev et al (1993), Shikina and Zotov (1996), Koslov (1982) and Wood et al (1987), and as shown in Figure 3.4. Whether the latter two studies should have been included is questionable. Koslov (1982) did not consider the distribution of H_2S between vapour and liquid phases, therefore overestimating the amount of H_2S available in solution (Zotov et al, 2003). Wood et al's (1987) data were collected in an unusual system that was not necessarily reflective of natural geothermal systems (FeS_2-FeS-Fe_3O_4-ZnS-PbS-Sb_2S_3-Bi_2S_3-Ag_2S-MoS_2 in H_2O-NaCl-CO_2 solutions).

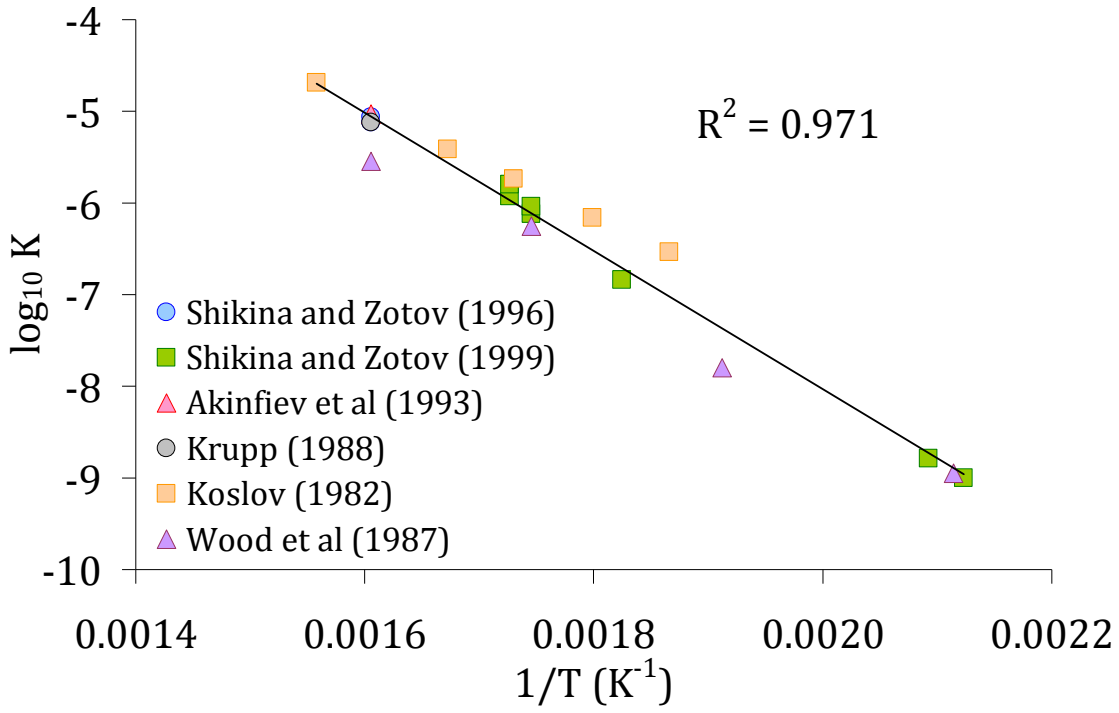

Figure 3.4 Plot of log K vs T^{-1} (in Kelvin) based upon the data presented in Zotov et al (2003).

When plotted alongside the rest of the data, as shown in Figure 3.4, Wood et al's (1987) data fell below the regression line. This indicates Sb_2S_3 in that particular system was more soluble than the rest of the data suggest, but Sb_2S_3 formation in the particular system presented in Wood et al (1987) was possibly limited by competition with other elements (such as Fe) for sulfide complexation. In other systems such competition may not occur to the same extent.

If these two sets of data are removed, a better fit is found for the plot of log K versus T^{-1} (Figure 3.5). The resultant solubility equation for the line of best fit is:

$$\log K = -\frac{7640.3}{T} + 7.213 \qquad (3.2)$$

This equation was used in this study to obtain log K to predict Sb_2S_3 saturation within the Rotokawa and Ngawha systems.

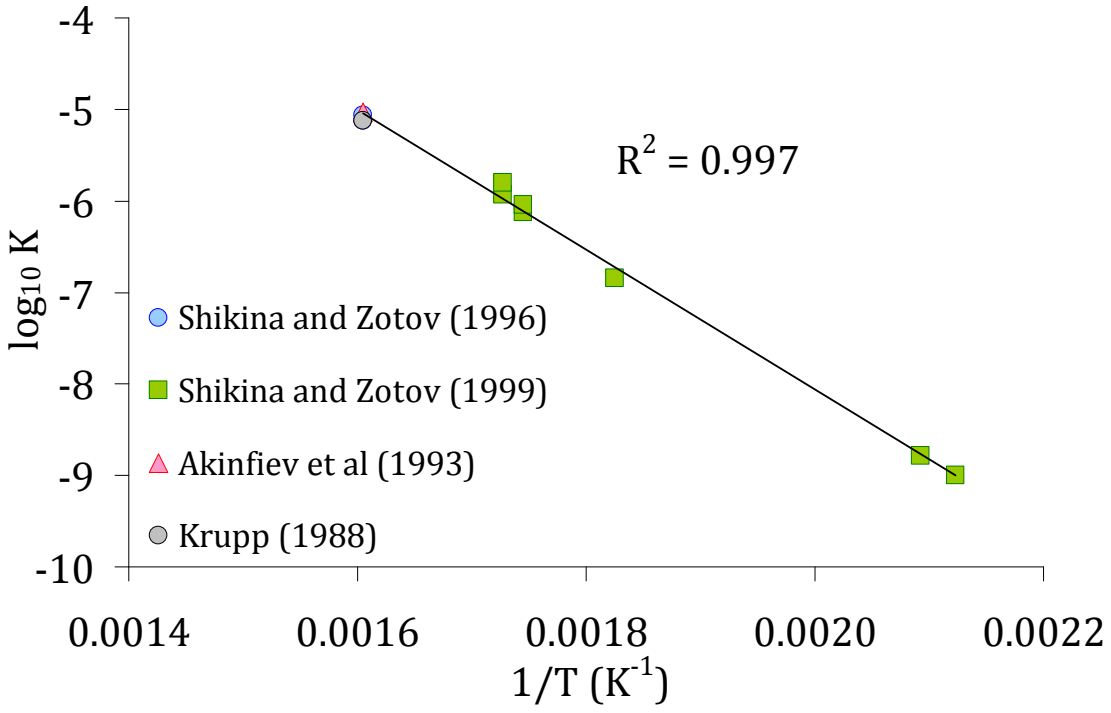

Figure 3.5 Plots of log K vs T^{-1} (in Kelvin) based upon the data presented in Zotov et al (2003), but excluding the data from Wood et al (1987) and Koslov (1982).

According to the Van't Hoff isotherm for a mineral such as Sb_2S_3, a plot of log K vs T^{-1} should be linear - assuming that enthalpy is constant and not a function of temperature (Krauskopf, 1979). Therefore, while Zotov et al (2003) only presented data between 473 and 623 K, data for temperatures < 473 K can be extrapolated.

There is an inherent risk in any such extrapolation that accuracy will be lost outside the known data range. However, the data for Sb_2S_3 solubility contained in SOLTHERM (Reed and Palandri, 1998) also fit a linear relationship when recast in terms of equation 1, so the risk of deteriorating accuracy at lower temperature appears to be minimal. The fit error for equation 2 was 0.085 log (K) units. Experimental errors ranged between 0.05 and 0.2 for the data used to derived equation 3.2.

Kolpakova (1982) determined that pressure was not a significant influence upon the behaviour of Sb in sulfide-rich fluids between 25 and 90 ^oC. This appears to be the case true at higher temperatures as well (Zotov et al, 2003).

3.3.2 MODELLING METHODOLOGY

As explained in Chapter Two, the WATCH 2.3 computer programme (Arnorsson et al, 1982) was used to combine the results of unpublished gas and brine analyses for the RK 5 well at Rotokawa, and for the NG 9 and NG 12 wells at Ngawha. The chemistry of the recombined gas and fluid solutions was then calculated at their respective liquid reservoir temperatures, and then boiled at the temperatures recorded at the power stations for the respective separators (224 ^oC for Rotokawa, 198 ^oC for Ngawha 9, 193 ^oC for Ngawha 12). The CHILLER computer programme (Reed and Palandri, 1998) was used to confirm that flashing did not induce Sb_2S_3 precipitation (because of a decrease in pressure) and to predict the chemistry of the mixed Ngawha condensates.

Output files from WATCH 2.3 were integrated into SOLVEQ (Spycher and Reed, 1989b), which was used to calculate the solubility of Sb_2S_3 at specific temperatures and pH. Measured data for Sb and H_2S concentrations and for pH were used for these predictions. The SOLTHERM database (Reed and Palandri, 1998)) was amended to include Sb_2S_3 solubility data derived from equation 2 for temperatures from 298 K to 623 K. All of the available data for other Sb-minerals, such as $Sb_{(s)}$ and Sb_2O_3 were included, as were the original SOLTHERM database Sb_2S_3 data for comparison.

The assumption that total aqueous Sb concentrations measured in samples are all in the dissolved phase ignores the possibility that colloidal Sb-S material (meta-stibnite) may have formed in solution and carried in suspension. Therefore, measured concentrations may overestimate actual dissolved concentrations of Sb within the power station pipelines.

Overestimations of Sb concentrations are potentially an issue at Ngawha, where (as will be discussed) Sb_2S_3 is oversaturated throughout the heat exchanger units. At Rotokawa, where the models predict that Sb_2S_3 is under-saturated in the heat exchanger units, the presence of colloidal material is effectively irrelevant, at least in terms of modelling results. Regardless, the primary purpose of modelling Sb_2S_3 behaviour at both stations is to determine the cause of Sb_2S_3 scaling at each. The presence or absence of Sb_2S_3 precursors does not influence modelled predictions.

3.4 POWER STATION FLUID CHEMISTRY

The results of geothermal power station fluid sampling are presented in the order that they were sampled. Rotokawa was the first power station studied.

3.4.1 ROTOKAWA

The Sb analyses for samples from the Rotokawa power station are shown in Figure 3.6a, and sample collection parameters presented in Table 3.1. Two of the three samples collected from the brine accumulator appeared to be contaminated, with Sb concentrations of about 1400 µg/kg. These Sb concentrations were significantly higher than the third replicate, which was in better agreement with OEC 1 inlet Sb concentrations. Unlike all other sampling points, the brine accumulator sample valve is located on the underside of the pipeline, and Sb_2S_3 previously precipitated in the valve dead-space may have contaminated the sample when the valve was opened. The two anomalous results were therefore excluded from the data presented. Overall, reproducibility across replicates was satisfactory for unfiltered samples.

Table 3.1 Data measured at the Rotokawa power station. Temperature, pressure and flow data provided courtesy of Mighty River Power.

Sample location	Temp (°C)	pH	Aqueous sulfides (mg/kg H_2S)	Pressure (bar_A)	Flow (T/Hr)	Sb_T (µg/kg)	Sb flux (g/hr)
Steamline	107	4.39	30.6	1.3	148	< 0.2	N/A
Accumulator	224	6.99	12.5	26.0	370	960	355
OEC 1 Inlet	222	6.93	14.2	26.0	291	955	278
OEC 1 Outlet	170	6.62	7.80	18.3	291	159	46.2
OEC 21 Post-mix	160	5.78	32.4	N/M	136	248	33.7
OEC 21 Outlet	151	5.70	29.7	20.0	136	138	18.7
Reinjection	148	5.67	26.8	10.2	574	169	97.0

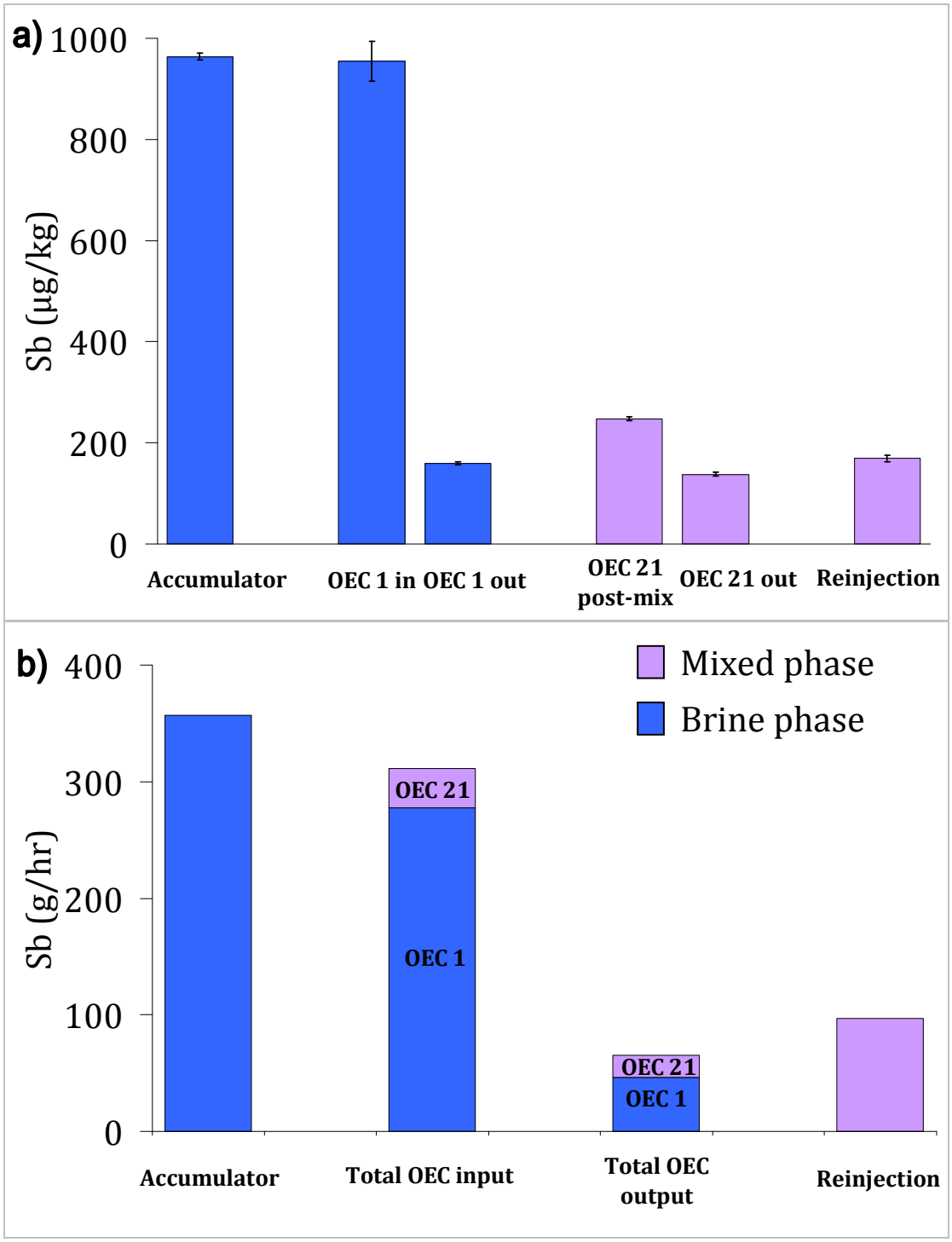

Figure 3.6 Results for the sampling sites at the Rotokawa power station in terms of a) Sb concentrations, and b) Sb flux. Antimony concentration was below detection limit (0.2 µg/kg) in the steam line sample and has been omitted.

Antimony concentrations in the OEC 1 outlet were low relative to the input. This implied that Sb_2S_3 was precipitating within OEC 1. Antimony fluxes were calculated using measured concentration and flow data in order to obtain a more reliable indicator of Sb removal.

When fluxes were compared (Figure 3.6b), this apparent loss in OEC 1 was also evident. In addition, the combined Sb flux output from the OEC units is 33 % less than that in the reinjection line. However, when the power station was shutdown for regular maintenance, while Sb_2S_3 scale was found in OEC 21, no such scale was found in OEC 1. No Sb could be detected in the steam line, so it is unlikely that the "extra" Sb in the reinjection line came from Sb in the vapour phase, and the discrepancy was never resolved. It may reflect an ongoing problem with the OEC 1 outlet sampling site valve.

Based on the Sb analysis of unfiltered samples, the net deposition of Sb in the power station can be calculated as the difference between the incoming flux at the accumulator and the outgoing flux in the reinjection line (Table 3.1). This was 260 g Sb per hour, which equates to 8.7 kg Sb_2S_3 per day or just over 3 tonnes of Sb_2S_3 every year. About ~25 % of the Sb_2S_3 precipitates in OEC 21 (~750 kg per year), if it is assumed (based on the Sb concentrations measured for the brine at the accumulator) the incoming Sb flux for the OEC 21 unit was just under 80 g/hr. The remainder (75 %) of the Sb_2S_3 scale must precipitate in the reinjection line, since the losses calculated for OEC 1 were not reflected in the observed scaling inside the unit, and therefore must be due to sampling problems.

3.4.2 NGAWHA

Antimony concentrations in samples collected from the Ngawha geothermal power station are shown in Figure 3.7a, and along with other sample collection data in Table 3.2. Incoming Ngawha fluids from the two wells have similar Sb concentrations (1600 and 1650 μg kg^{-1} for Wells 9 and 12 respectively), higher than are observed for wells at Rotokawa. These results agree well with unpublished results, which range from 1200 - 1800 μg kg^{-1} for Well 9 and 1000 - 1700 μg kg^{-1} for Well 12 (Brown, K., GEOKEM, Pers. Comm. 10 November, 2005). The results from replicate samples collected from Well 12 and the HE 2 post-condensate sites were consistent, with variation between replicates no greater than analytical variance within the same replicate.

Table 3.2 Data measured at the Ngawha power station. Temperature, pressure and flow data provided courtesy of Top Energy.

Sample location	Temp (°C)	pH	Aqueous sulfides (mg/kg H_2S)	Pressure (bar_A)	Flow (T/Hr)	Sb (µg/kg)	Sb flux (g/hr)
Well 9	198	7.07	15.8	14.5	149	1600	239
Well 12	193	7.09	25.0	13.6	232	1650	383
HE 1 Post-vaporiser	158	6.98	23.2	16.1	191	827	157
HE 1 Pre-mix	106	6.85	23.2	N/M	191	693	133
HE 1 Post-mix	93.8	6.60	21.3	N/M	206	423	86.7
HE 2 Post-vaporiser	158	6.95	13.9	16.0	191	721	138
HE 2 Pre-mix	105	6.85	13.6	N/M	191	676	129
HE 2 Post-mix	93.5	6.83	25.4	N/M	206	537	113
Reinjection	93.1	6.57	23.2	9.7	400	375	150

As shown in Table 3.2, total sulfide concentrations in HE 1 and HE 2 were different (23.2 mg kg^{-1} and 13.9 mg kg^{-1} as H_2S respectively). The observed pH shift following the mixing of brine with condensate in the heat exchanger unit was somewhat smaller in HE 2 (0.12) compared to that in HE 1 (0.25) as well.

A mass-balance calculation, using the flux data presented in Table 3.2 and shown in Figure 3.7b, predicted that the amount of Sb precipitating between the production wells and the reinjection line was 470 g/hr. The majority (430 g/hr) was lost within the two HE units. A loss of 470 g of Sb every hour equates to about 15.8 kg of Sb_2S_3 per day, or 2.9 tonnes of Sb_2S_3 every six months, 90 % of which forms within the HE units. The calculated rate, 2.9 tonnes of Sb_2S_3 per six months, is close to the estimated rate of 3 tonnes per six months based on the amount of Sb_2S_3 removed from these units during mechanical cleaning episodes at the power station (Dorrington and Brown, 2000).

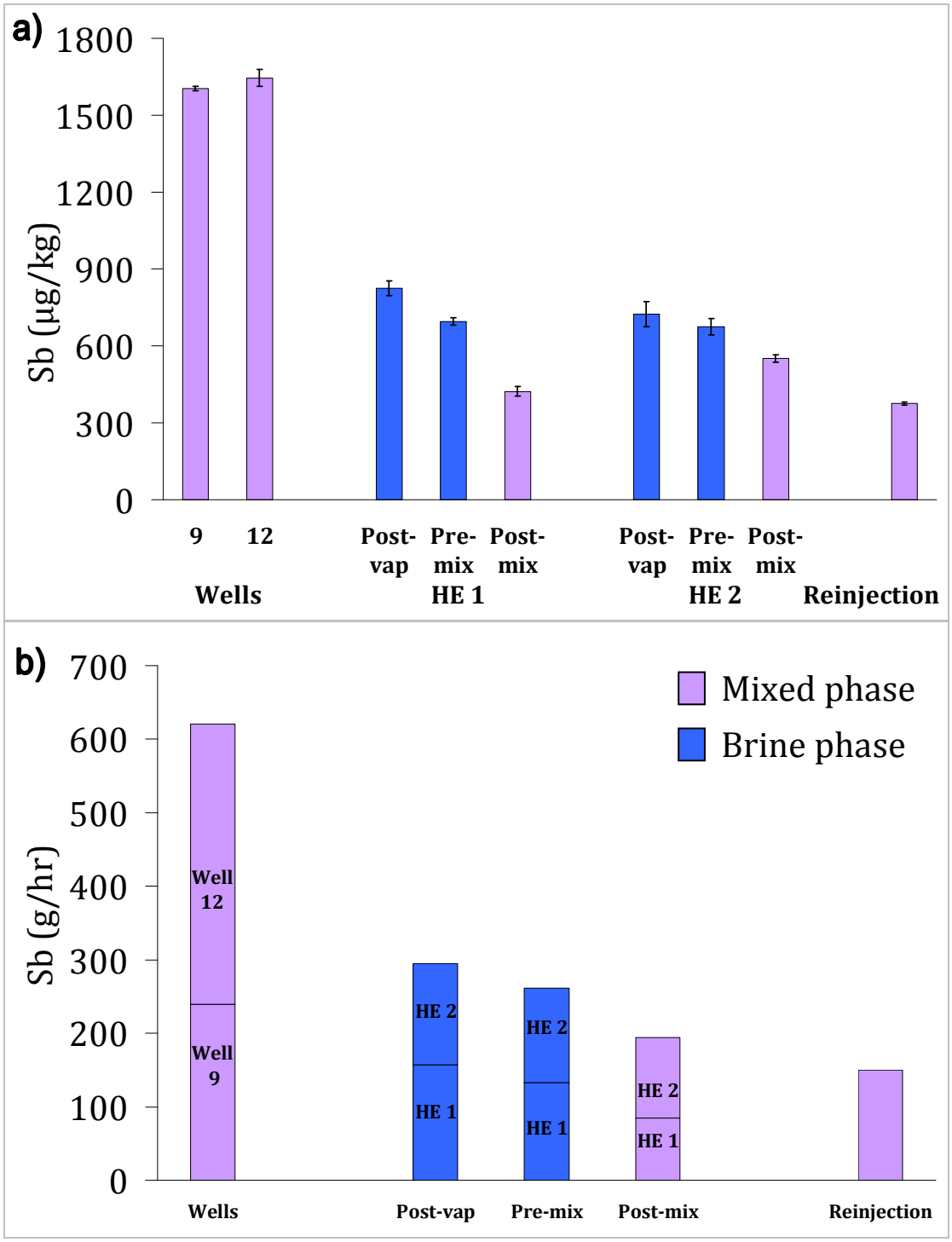

Figure 3.7 Results for the sampling sites at the Ngawha power station in terms of a) Sb concentrations, and b) Sb flux

3.5 THERMODYNAMIC MODELLING RESULTS

The purpose of modelling the fluid chemistry using SOLVEQ, CHILLER, and WATCH was to determine whether it was possible to predict the occurrence of Sb_2S_3 precipitation, and to identify factors controlling precipitation. Each power station system was modelled twice: once using measured Sb concentrations and once assuming that no Sb was removed from solution at any point within the power station. In the second scenario, it was assumed that changes in concentration were due only to dilution with condensed steam (a "no loss" scenario).

The modelling results, shown in Figure 3.8 for a) Rotokawa and b) Ngawha, are presented as saturation indices (SIs) for Sb_2S_3. The SI results are calculated as:

$$SI = log\ Q - log\ K \tag{3}$$

Where Q = activity product of the given solubility reaction and K = equilibrium solubility constant calculated from Equation 2. The results are presented in Figure 3.8 for both the original SOLTHERM data, and for the data calculated as above. If the thermodynamic data are accurate, and the system was at equilibrium at the sites sampled, then one would expect that: a) where Sb_2S_3 was not precipitating then $SI_{no\ loss} \approx SI_{measured}$, and b) where Sb was precipitating as Sb_2S_3, $SI_{no\ loss} > 0$, while $SI_{measured} = 0$. In all cases, SI values were higher for the updated Sb_2S_3 data than for the original data. That Sb_2S_3 precipitation is occurring at Rotokawa and Ngawha, but is not predicted using the original Sb_2S_3 solubility data, suggests the revised data is more accurate. Results using the original SOLTHERM data will not be further discussed.

3.5.1 ROTOKAWA MODEL

For the Rotokawa model, the initial "no-loss" Sb concentration was set at 955 μg kg^{-1}, which was the measured concentration of Sb in the post-accumulator brine line. For both the accumulator and OEC 1 input sites, SIs for measured and "no loss" modelled results (using the updated database) are in reasonable agreement. For the OEC 21 sites and the reinjection line, it appeared that the "no loss" data tend to favour Sb_2S_3 precipitation. The measured data were typically undersaturated with respect to Sb_2S_3 (at about -0.6 log units). Stibnite is known to be precipitating throughout the OEC 21 unit, suggesting Sb may have already been lost as Sb_2S_3 by the time the sample was taken. The most significant discrepancy is in the OEC 1 outlet, which further suggests there are unresolved sampling problems at this site (described earlier in this chapter).

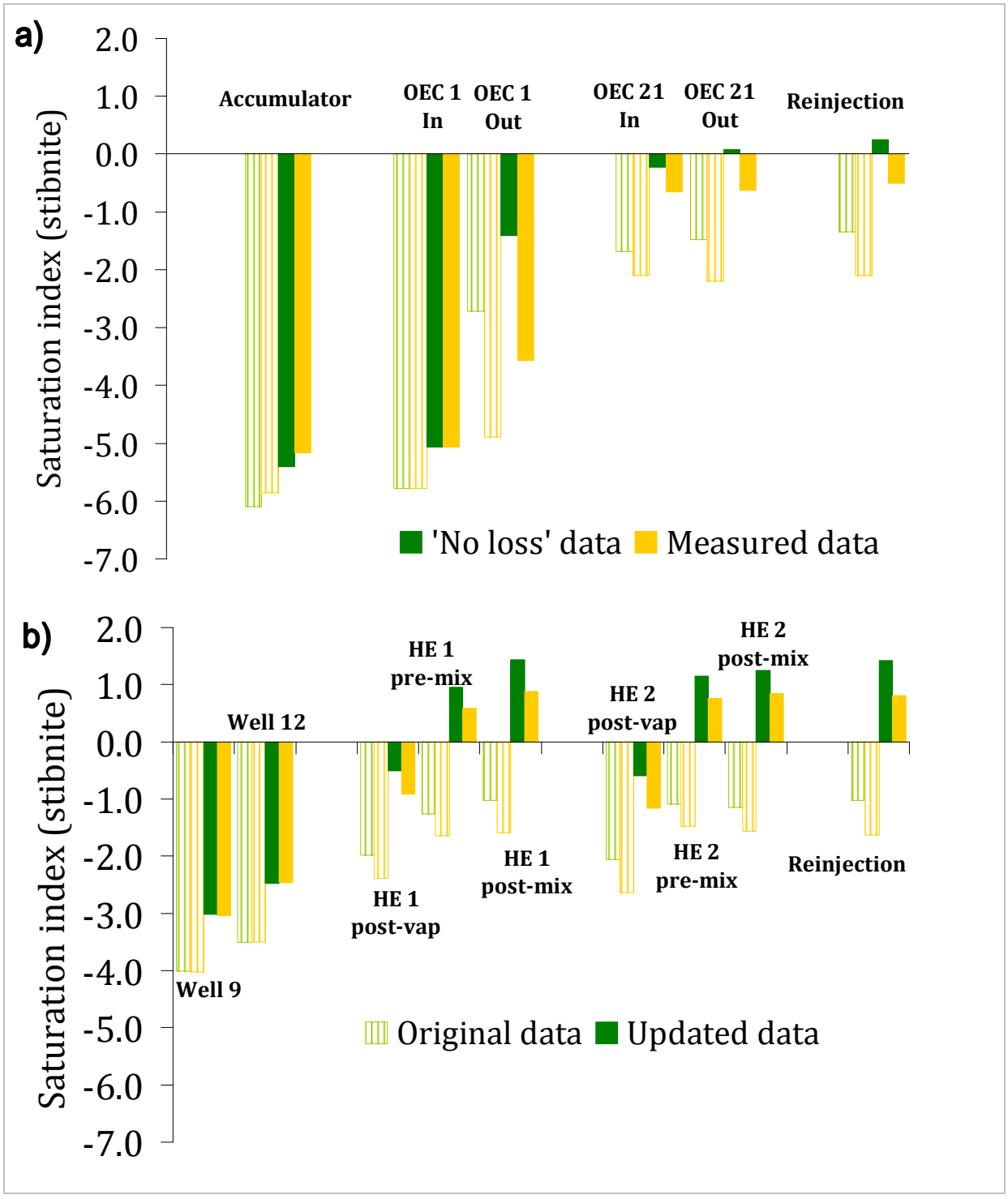

Figure 3.8 Stibnite saturation indices based on sampled Sb concentrations and a "no loss" model for a) Rotokawa and b) Ngawha. The dashed bars indicate data produced using the original SOLTHERM Sb_2S_3 data, the solid bars show the results using equation 2.

3.5.2 NGAWHA MODEL

For Ngawha, the initial "no-loss" value was set at 1630 μg kg^{-1}, the mean value of the NG 9 and NG 12 wells. It is clear from Figure 3.8b that precipitation of Sb_2S_3 is predicted to occur in the heat exchanger units, both before and after the brine and condensate are mixed, and also in the reinjection line. It had to be assumed for modelling purposes that the brines and condensates going through the separate HE units would have effectively identical chemical compositions, but as shown in Table 2, the pH, Sb and sulfide concentrations in HE 1 and HE 2 are different. Unusual fluid dynamics, which means that the mixing of these solutions is complex, is the most likely explanation (Franks K., Top Energy, Pers. Comm., 9 December 2005).

3.6 ANTIMONY TRANSPORT IN GEOTHERMAL POWER STATIONS

No Sb was detected in steam line samples at Rotokawa. That no Sb could be detected supports Dorrington and Brown's (2000) argument that carry-over of fluid droplets is responsible for any Sb_2S_3 scale found in the steam lines. It should also be noted that where Sb_2S_3 is observed to precipitate, as in OEC 21, the concentration of Sb in the scale is about 6-25 wt % (Ward, 2007), which is significantly higher than the 0.0023-0.017 wt % Sb concentration in vapour line scale as reported by Reyes et al (2002). It appears therefore that Sb is transported almost exclusively in the liquid phase of geothermal fluids, as proposed by Spycher and Reed (1989b).

There is evidence to suggest that the Rotokawa fluids achieve equilibrium relatively quickly. If the system was in disequilibrium, then SI would be consistently above zero where precipitation was occurring, describing a state in which the fluid was apparently oversaturated with respect to Sb_2S_3. Such oversaturation is predicted in the post-mix and reinjection samples at Ngawha, which are oversaturated with respect to Sb_2S_3, and precipitation may be expected further downstream. However, at Rotokawa, SI values in OEC 21 and the rejection line are ~ 0. Elsewhere (and at higher temperatures), it appears that the kinetics of Sb_2S_3 deposition from such fluids are not a significant limiting factor. The maximum error associated with these calculations, based on 5% analytical error and a fit error of 0.085 log units) is approximately ±0.18 units, which may mean than saturation conditions are reached at slightly higher temperatures and pH values. Nonetheless, the general conclusions are still valid.

3.6.1 FACTORS CONTROLLING STIBNITE PRECIPITATION

Figure 3.9 shows the degree of Sb_2S_3 saturation as a function of pH and temperature at both power stations. When temperature and pH decrease at Rotokawa, the likelihood of Sb_2S_3 precipitation increases, which is represented by the increased degree of saturation (Figure 3.9a). In the mildly acidic conditions within the mixed brine-condensate unit (pH ~5.7), saturation is predicted to occur at 154 ^oC. Under circum-neutral conditions (pH 6.5), saturation would not occur until temperatures had fallen to 145 ^oC. Therefore, the acidic condensate injected into OEC 21 is likely to be responsible for the Sb_2S_3 precipitation, and the overall drop in temperature from 224 ^oC at the accumulator to 151 ^oC at OEC 21 is not as important.

Because pH appears to be the principal control, chemical dosing at OEC 21 could be effective in preventing Sb_2S_3 scale, using an alkali reagent such as NaOH to raise the pH enough to keep Sb in solution. This is not necessarily an economically viable option though, and mechanical removal of the scale was the preferred option at this power station (Powell, T., Mighty River Power, 21 January, 2006). Ward (2007), proposed that only condensate should be used in the OEC 21 pre-heater unit, which would eliminate scale deposition because most of the required constituents are contained in the brine.

At Ngawha (Figure 3.9b), the change in temperature is more significant. By the time geothermal fluids have passed through the HE units, the temperature has decreased to < 100 ^oC, and the fluids are considerably oversaturated with respect to Sb_2S_3. At such temperature, even if the pH of the fluid could be increased to pH 8, precipitation of Sb_2S_3 is still predicted, and therefore chemical treatment may not be an effective option. This is especially the case given increasing the pH to such levels would encourage other scale minerals (such as calcite) to precipitate (Kristmannsdottir, 1989). This would eliminate one problem only to replace it with another. Altering the power station's operational conditions to minimise temperature decreases would mean that less electricity would be produced and the power station would not create as much revenue. At Ngawha, it appears that the current practise of chemically removing Sb_2S_3 with NaOH during station shutdowns remains the only practicable option.

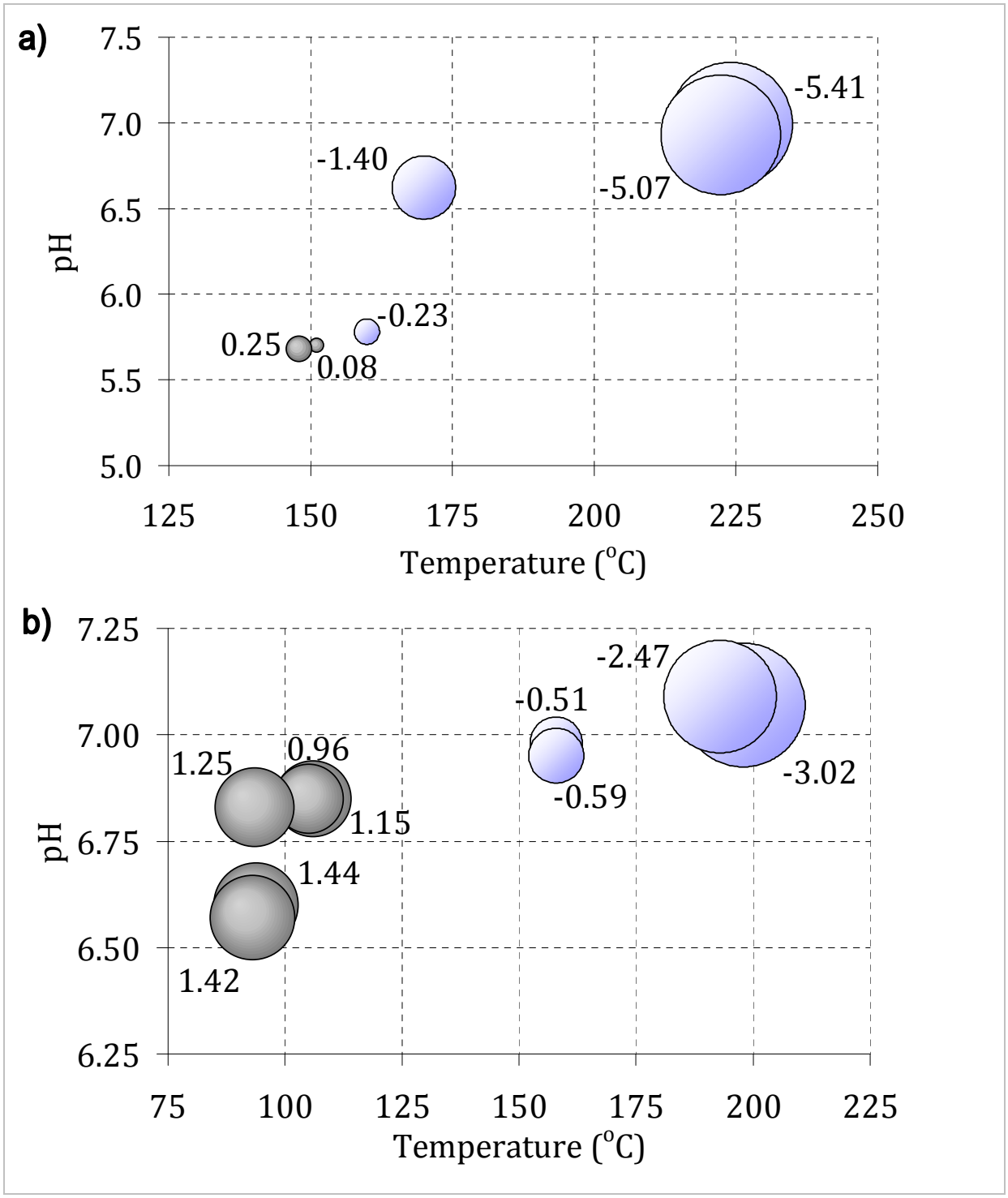

Figure 3.9 Saturation indices for specific pH and temperatures at a) Rotokawa and b) Ngawha. Saturation indices are given, with blue symbols indicating negative SI values and grey symbols indicating positive SI values.

Sulfide concentrations are another factor that affect Sb_2S_3 equilibria (Spycher and Reed, 1989a). However, as shown in Figure 3.10, while the addition of condensate leads to an increase in sulfide concentrations, the effect of such increases on saturation indices are insignificant. At Rotokawa (Figure 3.10a), pH appears to be more important, because under saturation of Sb_2S_3 is predicted even at higher H_2S concentrations if the pH is greater than 5.7. It should be stressed that Sb_2S_3 is never oversaturated at Rotokawa when H_2S concentrations are < 0.60 mmol/kg. For Ngawha (Figure 3.10b), temperature is still the most important factor and the amount of H_2S present in solution appears unimportant.

3.7 CONCLUSIONS AND POTENTIAL FURTHER RESEARCH

The behaviour of antimony in geothermal power station fluids is controlled by four factors: Antimony concentrations, temperature, pH, and, to a lesser extent, H_2S concentrations. According to the data presented, at Rotokawa the mixing of low pH condensate with near-neutral brines results in 750 kg of Sb_2S_3 precipitating every year in the mixed brine-condensate heat exchanger (OEC 21). While Sb_2S_3 precipitation was not predicted to occur using the original SOLTHERM database in the SOLVEQ model, the inclusion of more recent thermodynamic data for Sb_2S_3 solubility means that the system can be more accurately modelled.

At Ngawha, temperature is the principal driver for Sb_2S_3 precipitation, and 6 tonnes a year of Sb_2S_3 form, mostly in the two mixed brine-condensate heat exchanger units. Again, the use of more recent stibnite solubility data means that the scaling at Ngawha is now predicted to occur using the SOLVEQ model, when previously it was not.

No Sb (< 0.2 μg/kg) was detected in samples collected from the steam lines at Rotokawa. This means that there is no data to support the hypothesis that Sb is carried in both the aqueous and vapour phases, at least in relatively non-acidic conditions. At very low pH, gaseous SbH_3 may become more significant, but this was outside the scope of this research.

The use of the log K data for Sb_2S_3 solubility is somewhat limited by a lack of data below 473 K. Further research is therefore necessary regarding the solubility of Sb_2S_3 at relatively low temperatures, particularly between 363 and 473 K (90-200 ^{o}C), if better predictions of Sb_2S_3 scaling are to be made.

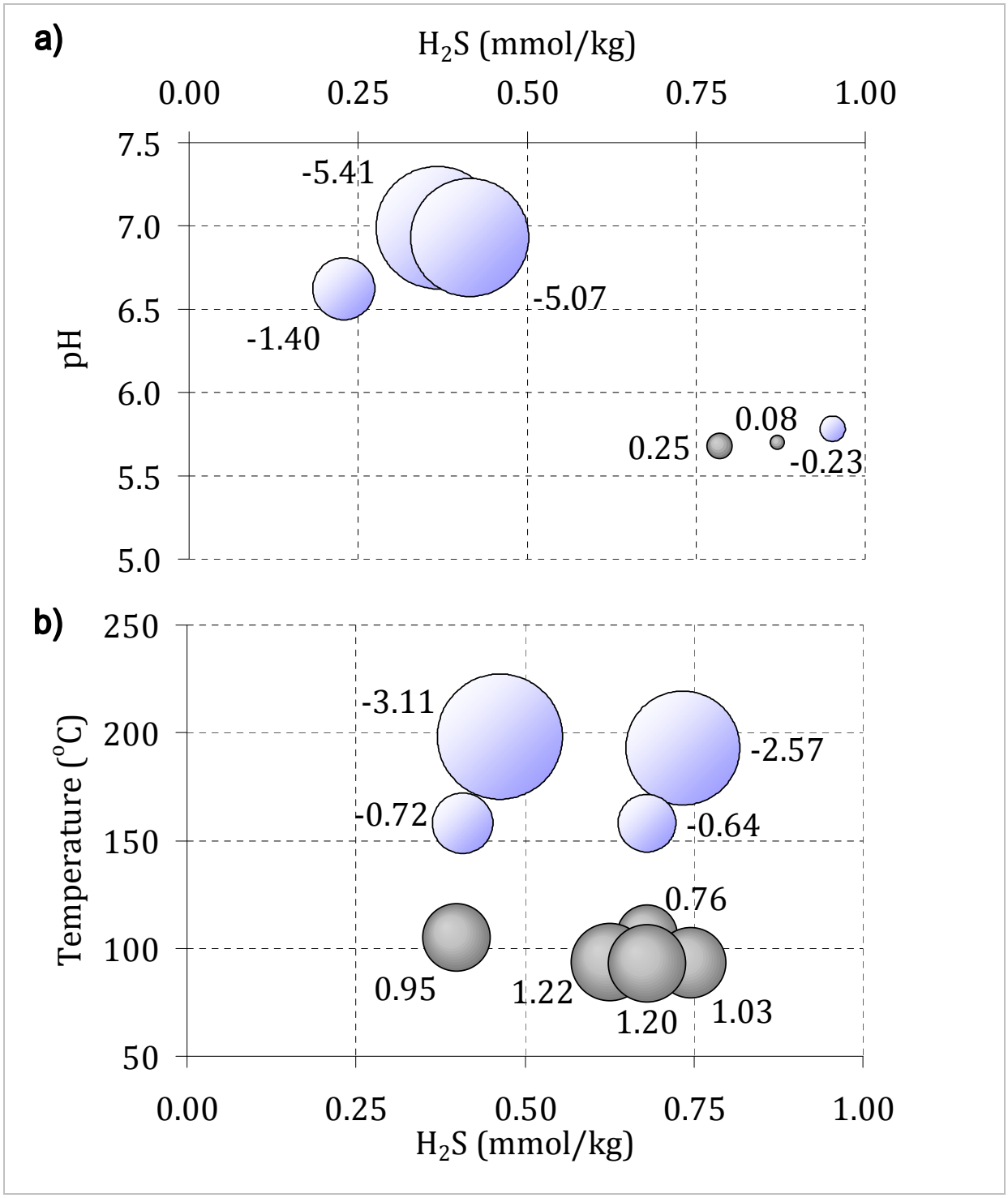

Figure 3.10 Stibnite saturation indices as a function of pH and H_2S concentrations at a) Rotokawa and b) Ngawha respectively. Saturation indices are given, with blue symbols indicating negative SI values and grey symbols indicating positive SI values.

CHAPTER FOUR

THE FATE OF ANTIMONY RELEASED FROM SURFACE GEOTHERMAL FEATURES

In this chapter, the behaviour of Sb in discharges from natural geothermal features will be investigated. While geothermal reservoir fluids in some of New Zealand's geothermal systems contain high (> 1000 μg/kg) concentrations of Sb, as listed in Table 1.2, the results presented in Chapter Three indicate that most of this Sb precipitates out when the fluids cool and/or the pH decreases. At Ngawha and Rotokawa, the Sb that has precipitated as Sb_2S_3 in the pipelines is physically or chemically removed, but what happens to the Sb that precipitates in the fluids of natural systems? Is Sb permanently precipitated as Sb_2S_3 as the fluids continue to cool at the surface, or are the precipitate minerals redissolved and remobilised? These are fundamental questions to be addressed in this chapter.

Data on the downstream remobilisation of Sb from geothermal features are limited, as was outlined in Chapter One. Of the few studies available, the most relevant to this research is that of Pope et al (2004), who discovered concentrations of Sb, along with As and Tl, exhibited diurnal variations downstream of Champagne Pool at the Wai-O-Tapu geothermal field. Metalloid concentrations reached maxima during the afternoon and minima during the night. Diurnal variations in trace element concentrations have been reported elsewhere, but such variation was caused by interaction with iron (e.g Fuller and Davis, 1989), or the remobilisation of elements in reducing conditions (e.g. Jones et al, 2003). At Wai-O-Tapu, Pope et al (2004) observed such diurnal variation in oxidising, low-Fe conditions.

Pope et al (2004) tentatively argued bacteria-catalysed oxidation of metalloid-sulfide minerals was the principal cause of the phenomenon. However, these results came from a single sampling event in winter, so it was not known whether such processes occurred year-round, nor whether it was a process unique to Wai-O-Tapu or ubiquitous across the Taupo Volcanic Zone. This chapter includes an attempt to resolve these issues.

4.1 BACKGROUND AND STUDY OBJECTIVES

The two geothermal fields used for this research, Wai-O-Tapu and Waimangu, are situated in the Taupo Volcanic Zone, and lie between Taupo and Rotorua, as shown in Figure 4.1. Both systems have "Protected Geothermal System" status under New Zealand law and cannot be exploited for geothermal power development (Hunt et al, 1994). Instead, Wai-O-Tapu and Waimangu are now major tourist attractions, and together with Orakei-Korako draw more than 270 000 visitors per annum, 70 % of whom are from overseas (Environment Waikato, 2002). The two systems were chosen for this study because both have major springs producing fluids with elevated levels of Sb (Ritchie, 1961).

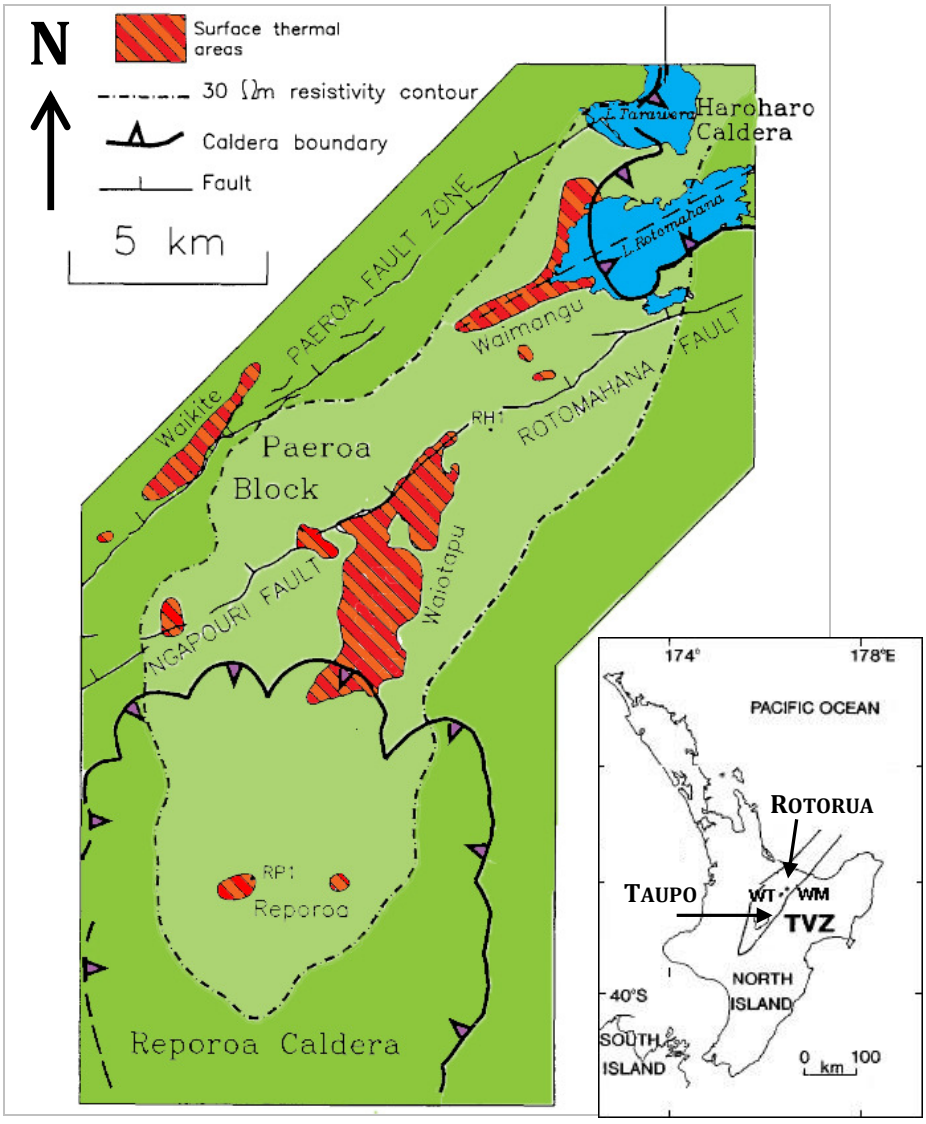

Figure 4.1 Geographic locations of the Waimangu and Wai-O-Tapu geothermal systems, adapted from Wood (1994). The lighter coloured area indicates the area where resistivity is < 30 Ωm. WT stands for the Waiotapu geothermal field, WM for the Waimangu geothermal field.

Wai-O-Tapu and Waimangu are geographically close, less than 20 km apart, but temporally disparate. Wai-O-Tapu is at least 15000 years old, although Champagne Pool is much younger (930 years old) (Hedenquist and Henley, 1985). Waimangu, in comparison, has the distinction of being the first geothermal system in the world to have its history documented from inception because the system formed after the Tarawera eruption of 1886. The eruption killed more than 150 people and destroyed Ō-tū-kapua-rangi and Te Tarata, the world-famous Pink and White Terraces, and Waimangu is the resultant crater-valley (Hunt et al, 1994). It has been claimed that entrained amorphous Sb-sulfides were the cause of the pink colour in the sinters that formed Ō-tū-kapua-rangi (Anheizen, 2003). Elsewhere it is argued that bacteria were responsible for the pigmentation (Mountain, 2007).

4.1.1 WAI-O-TAPU

The Wai-O-Tapu system is the ultimate product of eruptions 160 000 years ago and the subsequent seismic and hydrothermal activity (Hedenquist and Henley, 1985). The central feature of Wai-O-Tapu is Champagne Pool, a 70 m diameter and 60 m deep, slightly acidic (5.7 pH), chloride-sulfate spring, which is shown in Figure 4.2 (Lloyd, 1959). Hydrogen sulfide (H_2S) and carbon dioxide (CO_2) gases continually evolve from the 75 ^oC waters (mostly CO_2), and their tiny bubbles give the spring the champagne-like appearance for which the pool is named (Weissberg, 1969). The pool is rimmed with silica sinter, upon which an orange precipitate has formed. After silica and native sulfur, Sb and As sulfides are the next most abundant constituents of this precipitate, which also has elevated gold (Au), silver (Ag) and tellurium (Te) concentrations (Pope et al, 2005). There is no dissolved oxygen (DO) in Champagne Pool, so Sb in solution exists predominantly as Sb^{III}, and was considered by Krupp (1988) to occur as thioantimonite complexes ($H_{2-x}Sb_{2n}S_{3n+1}^{x-}$).

As the sub-surface waters cool, these complexes become oversaturated with respect to minerals such as Sb_2S_3 and therefore Sb precipitates (Hedenquist, 1986). Similar behaviour has been observed for As in Champagne Pool (Webster, 1990). The Sb/As-rich floc that coalesces to form the orange precipitate is visible in the near-surface of the pool and Sb abundance in the precipitate ranges from 2-40 wt % (Weissberg, 1969). Dissolved concentrations in the pool are typically in the order of 10 μg/kg, while dissolved arsenic concentrations can be up to 8 mg/kg (Pope, 2004). Similar precipitates historically occurred about the margin of the Ohāki Pool in the Broadlands geothermal field, also situated in the TVZ (Weissberg, 1969).

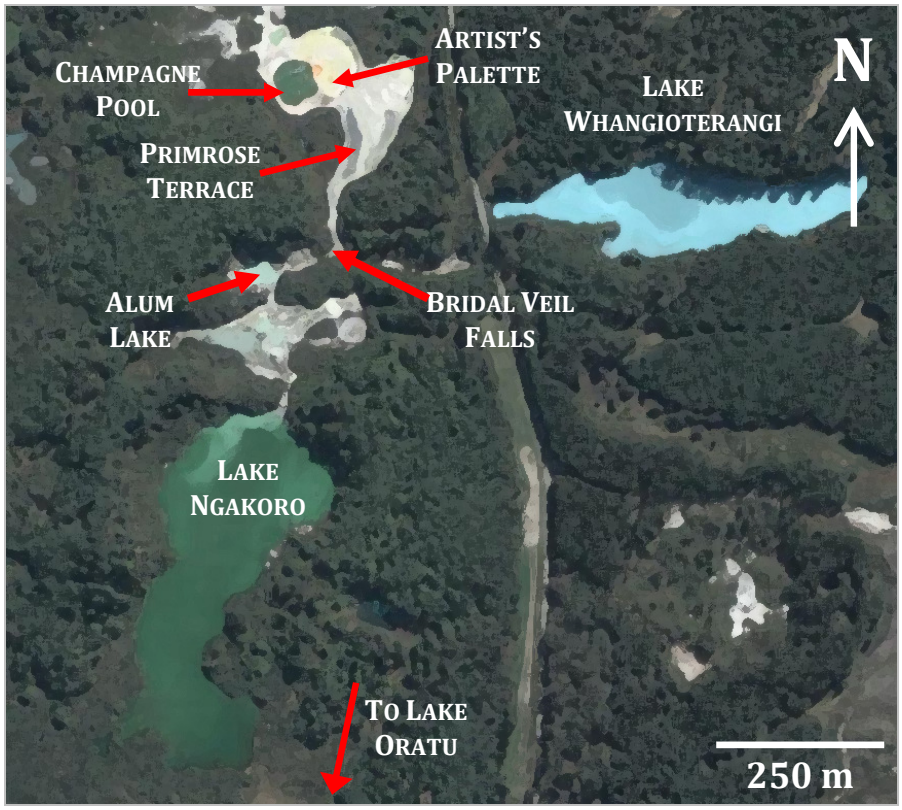

Figure 4.2 Map of the Wai-O-Tapu geothermal area showing locations of significance. Flow direction is north to south (map sourced from Google Earth™)

Copyright permission not granted

Figure 4.3 The formation of the orange-precipitate that surrounds Champagne Pool (adapted from Jones et al, 2001)

Alongside the abiotic Sb reaction processes, Phoenix et al (2005) have suggested that thioantimonite complexes attach to the amine groups (-NH_x) of bacteria within the pool. These bacteria are then trapped as silica uses the microbes for nucleation points (Jones et al, 2001). It is assumed that the direct bacterial transformation of Sb is not a significant process within Champagne Pool because methyl-antimonyl species constitute < 1 % of the dissolved Sb found in solution (Hirner et al, 1998).

The overflow from Champagne Pool has created a shallow pool upon the sinter terrace to the east, which is named Artist's Palette after the various and distinctly coloured sulfide precipitates (including As- and Sb-bearing minerals) that have formed as the previously warm hot-spring fluids cooled at the surface. While there may be some variation in the long term chemical composition of Champagne Pool (Jones et al, 2001), previous work by Pope et al (2004) showed that no significant short-term variation occurred when sampled over a 24 hour period in the winter of 2003. The discharge from Champagne Pool cools quickly once it has overflowed, and in this study it was observed that the waters would equilibrate with atmospheric temperatures (20-35 ^{o}C in summer, 5-10 ^{o}C in winter) within minutes. The continual discharge from Champagne Pool causes the pool on Artist's Palette to overflow south onto the silica-dominated Primrose Terrace (as shown in Figure 4.2).

At the bottom of Primrose Terrace, the overflow mixes with the discharge of Lake Whangioterangi, a relatively cold (20^{o} C) acid-sulfate lake, and then drains into Alum Lake, a yellow-green, water-filled crater containing elevated levels of H_2S and SO_4 (Hedenquist and Henley, 1985). Alum Lake overflows from its south-eastern corner, and drains towards Lakes Ngakoro and Oratu on the southern boundary of the Wai-o-tapu system (Figure 4.2). No surface discharges from these lakes appear on topographic or photographic maps of the area, but underground discharges may eventually reach Waiotapu Stream, a tributary of the Waikato River. The (potential) contribution of the Wai-O-Tapu geothermal field to the receiving environment will be discussed in Section 4.3.6. Photos of selected sites in this system are presented as Plates 4.1-4.3.

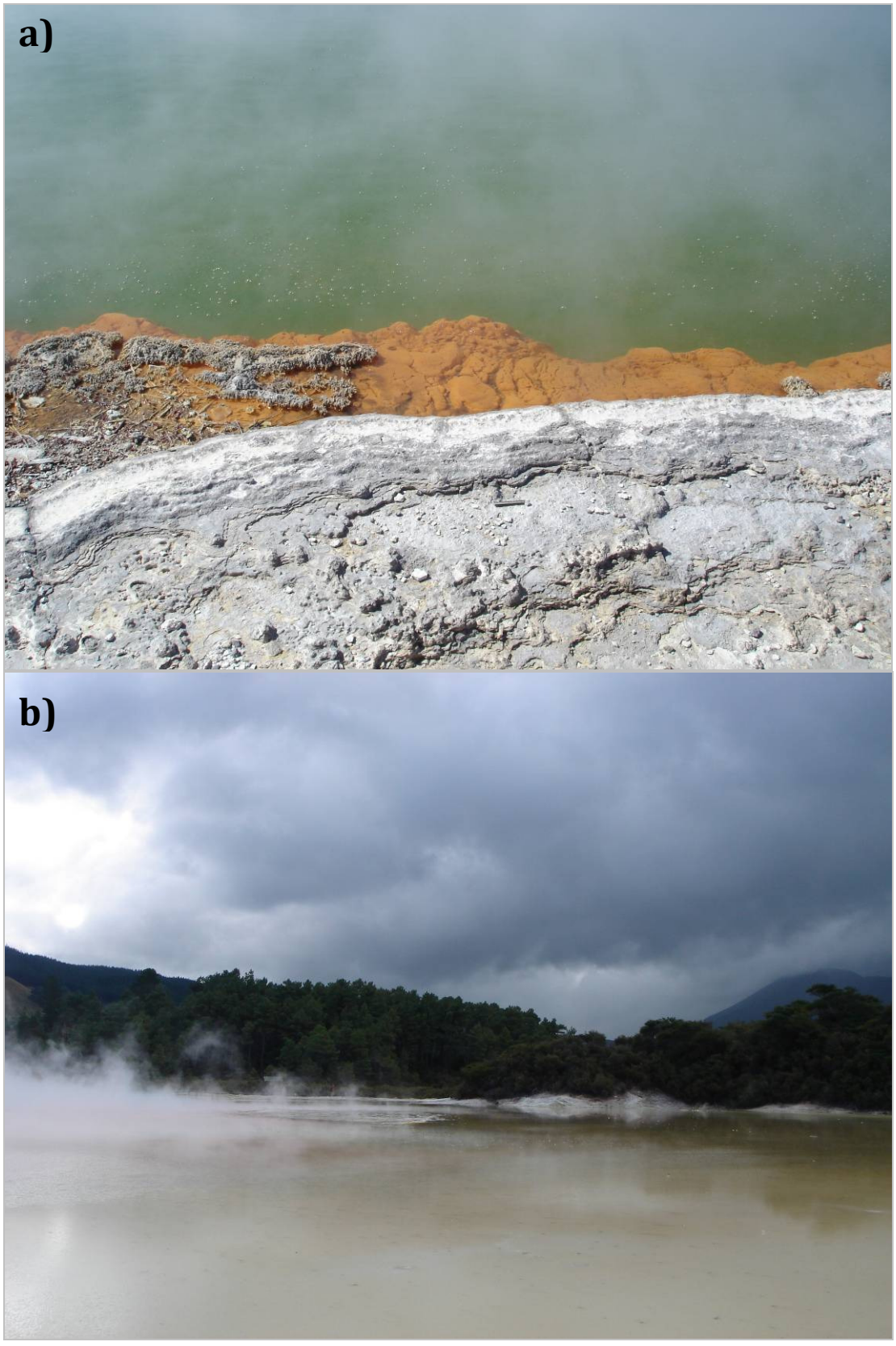

Plate 4.1 The precipitates at a) the margin of Champagne Pool and b) Artist's Palette

Plate 4.2 Downstream of Champagne Pool, a) Primrose Terrace and b) Bridal Veil Falls

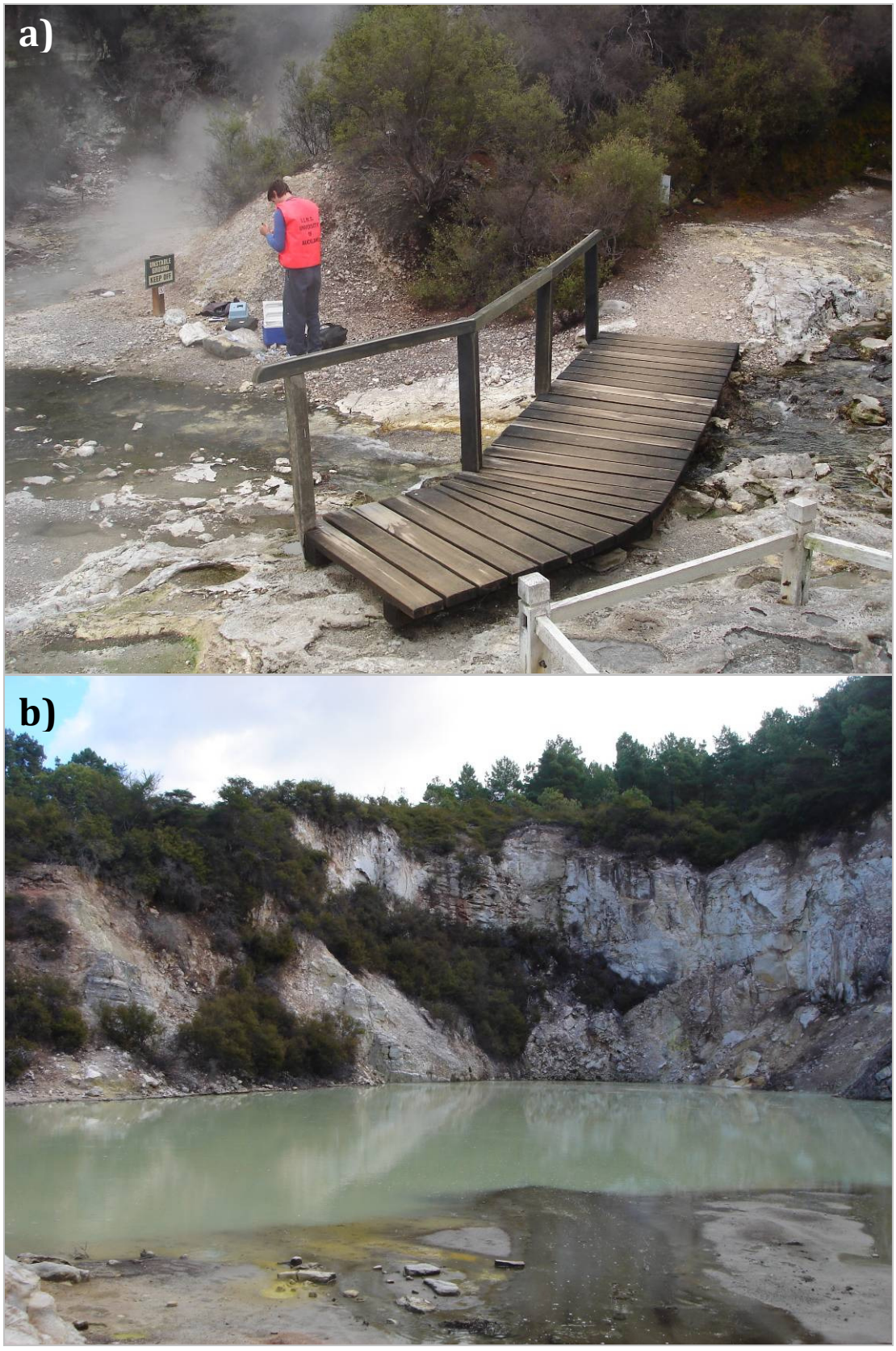

Plate 4.3 Sites below the confluence of the discharges from Champagne Pool and Lake Whangioterangi. a) Immediately downstream (Site WT 6) and b) Alum Lake

4.1.2 WAIMANGU

Waimangu is a younger system, forming after the Tarawera eruption in 1886, and shown in Figure 4.4 (Simmons et al, 1994). One of the central features of Waimangu is Frying Pan Lake (also known as Echo Lake), which formed as the result of hydrothermal eruptions in 1917 (Browne and Lawless, 2001). Ritchie (1961) reported similar levels of Sb in Frying Pan lake as found in Champagne Pool (~10 µg/L), and Sb- and As-sulfide minerals are present in Frying Pan Lake sediments (Seward and Sheppard, 1986). The lake is also characterised by the presence of large (up to 3 m long, 1.5 m wide) stromatolites (Jones et al, 2005). The lake covers 3.8 ha and discharges hot (50 °C) sulfate-chloride water from its northeast corner.

This discharge, called Hot Water Stream, is joined downstream first by the (inaccessible) Pareheru Stream, and then the discharge from Inferno Crater, an acid-sulfate spring, before mixing about 700 m downstream from Frying Pan Lake with Haumi Stream (the discharge waters of a non-geothermal crater lake). Inferno Crater and Frying Pan Lake are hydrologically linked, when levels rise in one spring, levels fall in the other (Glover et al, 1994).

The combined discharges drain into Lake Rotomahana, approximately 1.3 km further downstream. The only other significant addition is from a small stream that runs from the Warbrick Terrace. Photos of the system are presented as Plate 4.4-4.6

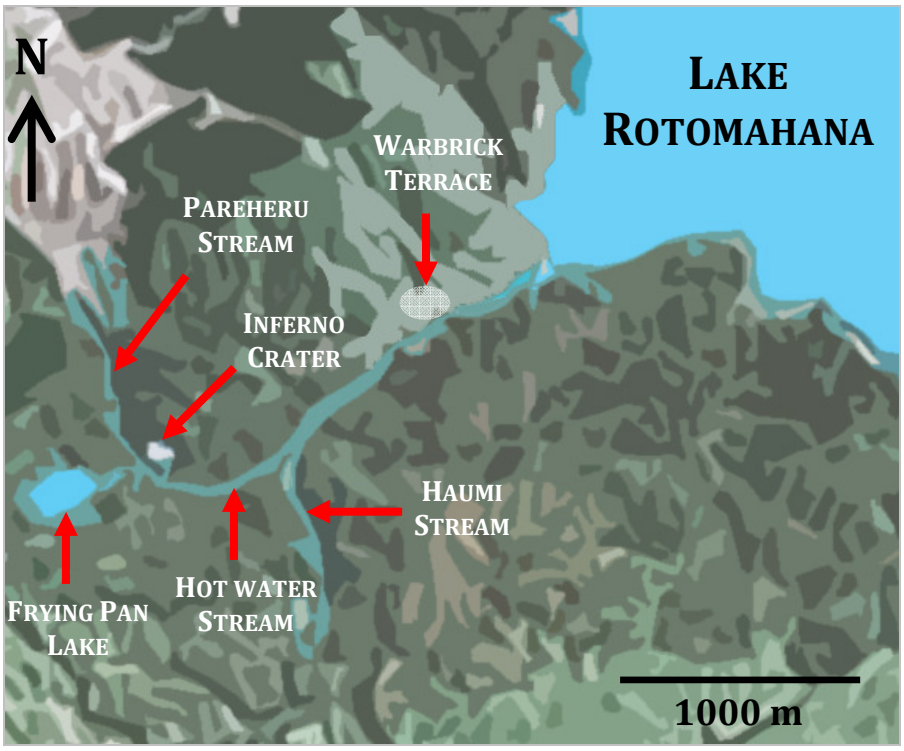

Figure 4.4 Map of the Waimangu geothermal area showing locations of significance. Flow direction is southwest to northeast (map sourced from Google Earth™)

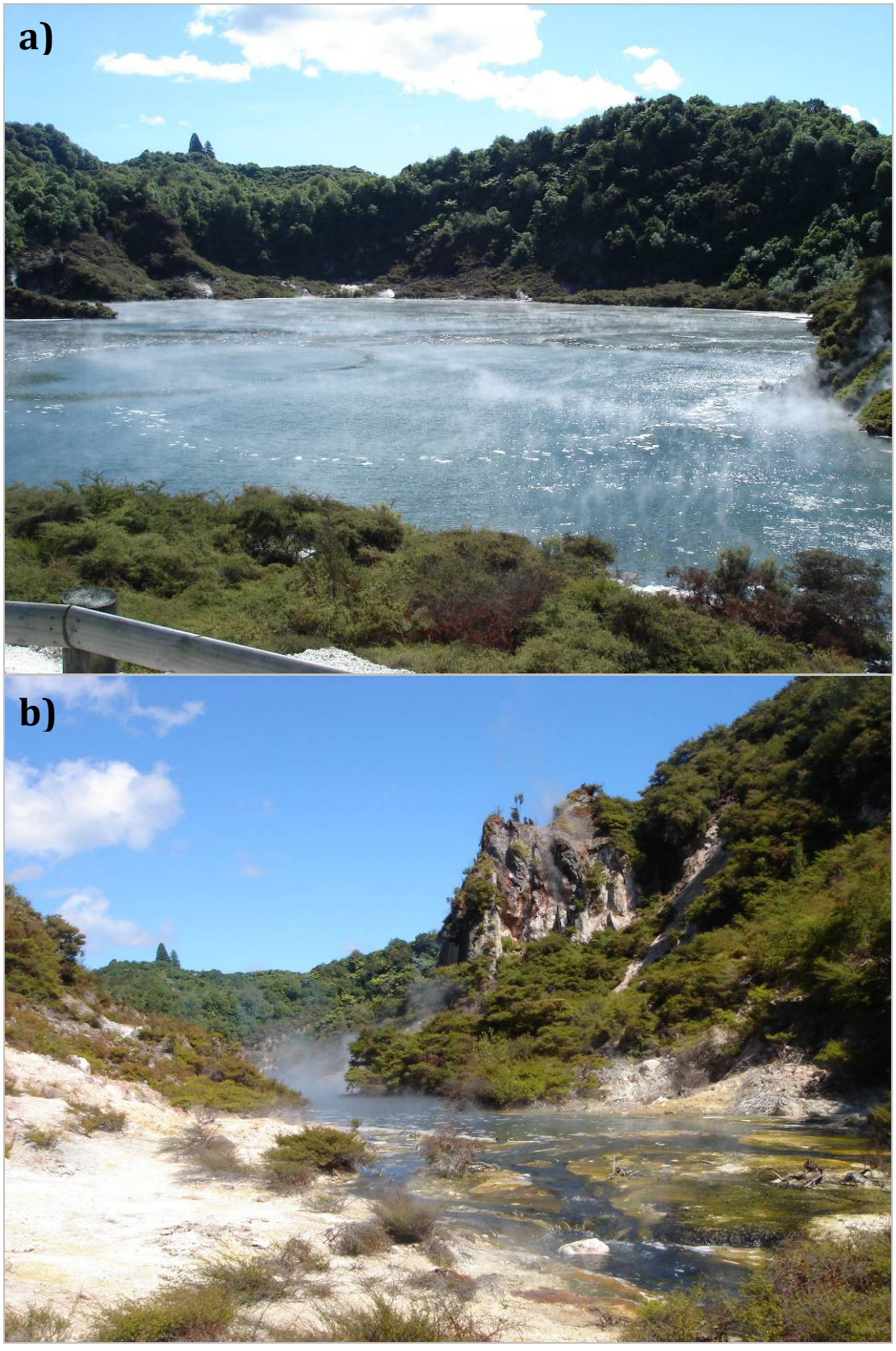

Plate 4.4 Photos of a) Frying Pan Lake, and b) the beginning of its discharge (Site WM 1)

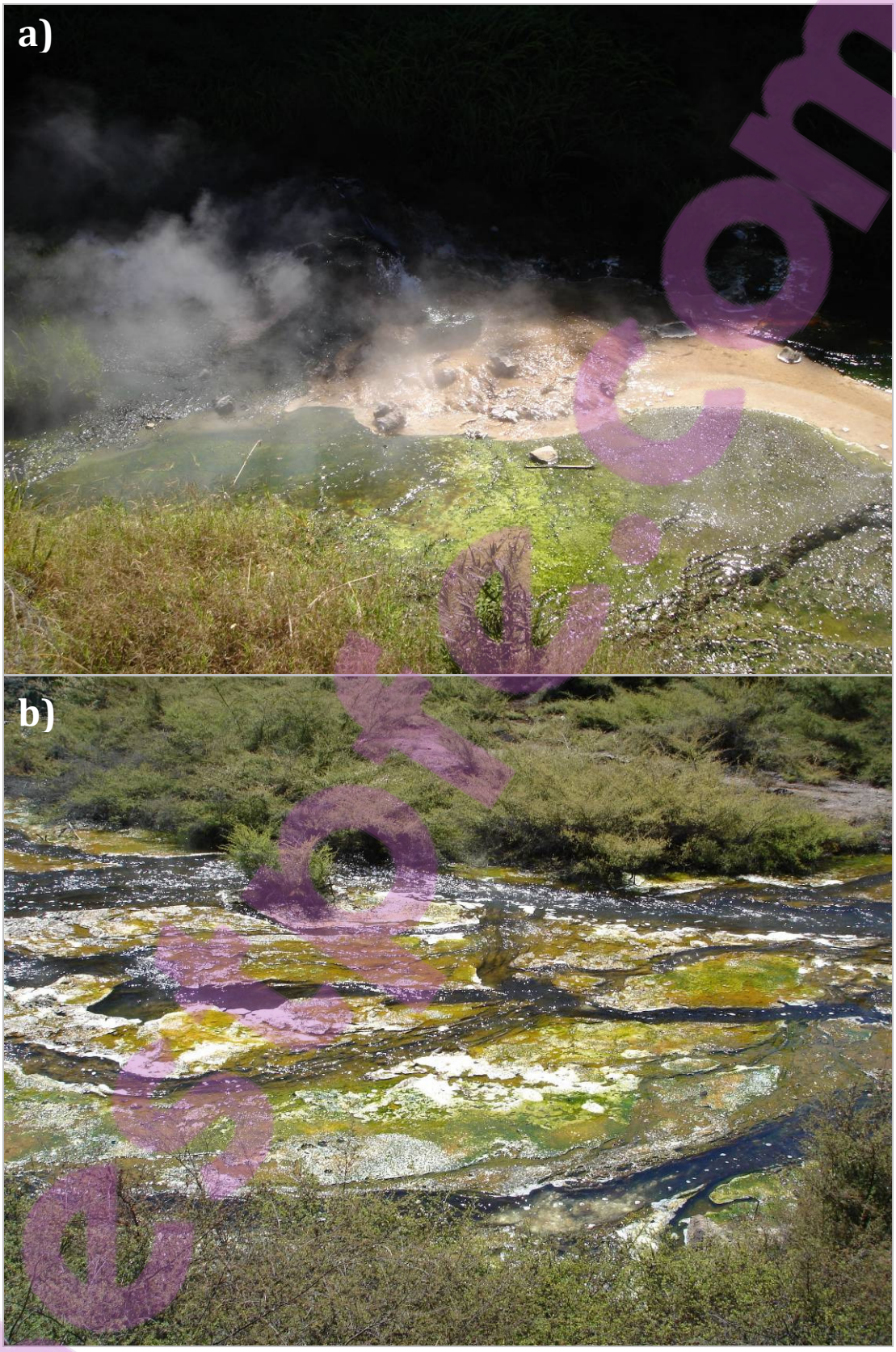

Plate 4.5 a) Hotwater stream, and b) algae growing within it

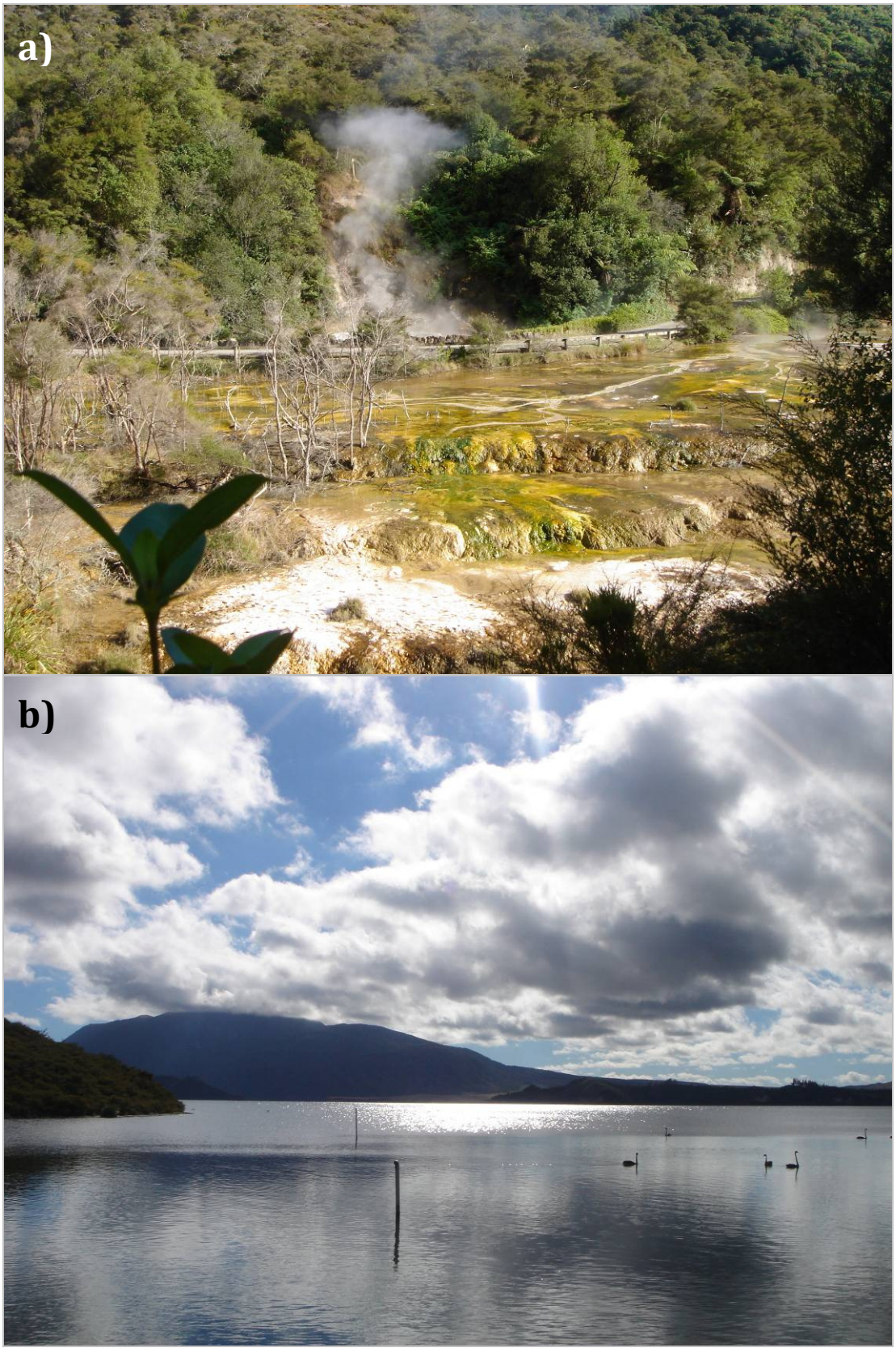

Plate 4.6 a) Terraces that lie alongside the lower reaches of Hotwater Stream (below the confluence with Haumi Stream), and b) Lake Rotomahana

4.2 SAMPLING PROTOCOLS

The Wai-O-Tapu and Waimangu geothermal fields are "Protected Geothermal Systems", which meant that a sampling permit was required from the Department of Conservation, and there were restrictions on the time of sampling and the type of sample that could be collected. Primarily for health and safety reasons, sampling could only be conducted between 8:30 a.m. and 4:30 p.m., so no sampling could occur overnight. Also, only aqueous samples and suspended particulate material in the water column (SPM) could be collected, which meant that bed sediment or precipitate samples could not be collected. However, because algae growing in the discharge were in the water column, algal samples from Waimangu were collected.

The time restrictions also meant that SPM collection was not always practical during the "all-day" collection events, because filtration was too time-consuming. Samples (500 mL) collected at both sites often took longer than an hour to filter because of the amount of suspended (and light-weight) material in solution. Consequently, SPM samples were only collected at Waimangu when single samples were collected from each site during later visits. However, the high algal content (based on visual estimates) in the summer SPM samples led to organic acids being produced during sample digestions, and this rendered the samples immeasurable for Sb or As by HG-AAS (as discussed in Chapter Two). Winter SPM from Waimangu contained fewer algae, and did not cause the same analytical problems.

Measurements of flow were not possible at either Wai-O-Tapu or Waimangu. At Wai-O-Tapu, access across the terraces was limited and the discharge was shallow (<0.4 m). At Waimangu, there was restricted access to Hotwater Stream, which was generally sampled from high (>2 m) bridges. Without flow data, it was not possible to calculate discharge fluxes.

4.2.1 SITES AND FREQUENCY

The Wai-O-Tapu system was sampled on January 6th and on June 28th, 2007. These dates were chosen as being as close as practicably possible to the longest and shortest days of the year (by daylight hours). In the summer survey, six sites from between Champagne Pool and the discharge from Alum Lake were each sampled five times over the course of the eight hours (sites are shown in Figure 4.5). During winter, the sites sampled were restricted to concentrate on the undiluted discharge above Bridal Veil Falls, and the discharge from Lake Whangioterangi (Site WT 9). The extra winter sites are shown in blue on Figure 4.5. Each site was sampled six times. A list of sites and a brief description of each is presented in Table 4.1.

Table 4.1 Site descriptions for Wai-O-Tapu sampling

Site Number	Description
WT 1	0.5 m above the bridge below Champagne Pool
WT 2	1.5 m below the bridge below Champagne Pool
WT 3	From the side-trench 80 m above Bridal Veil Falls
WT 4	At the bridge below Bridal Veil Falls
WT 5	10 m downstream of the bridge below Bridal Veil Falls
WT 6	40 m downstream Bridal Veil Falls, 1 m below the bridge
WT 7	5 m upstream of Alum Lake
WT 8	At the bridge across the Alum Lake discharge
WT 9	20 m upstream of the Whangioterangi stream confluence

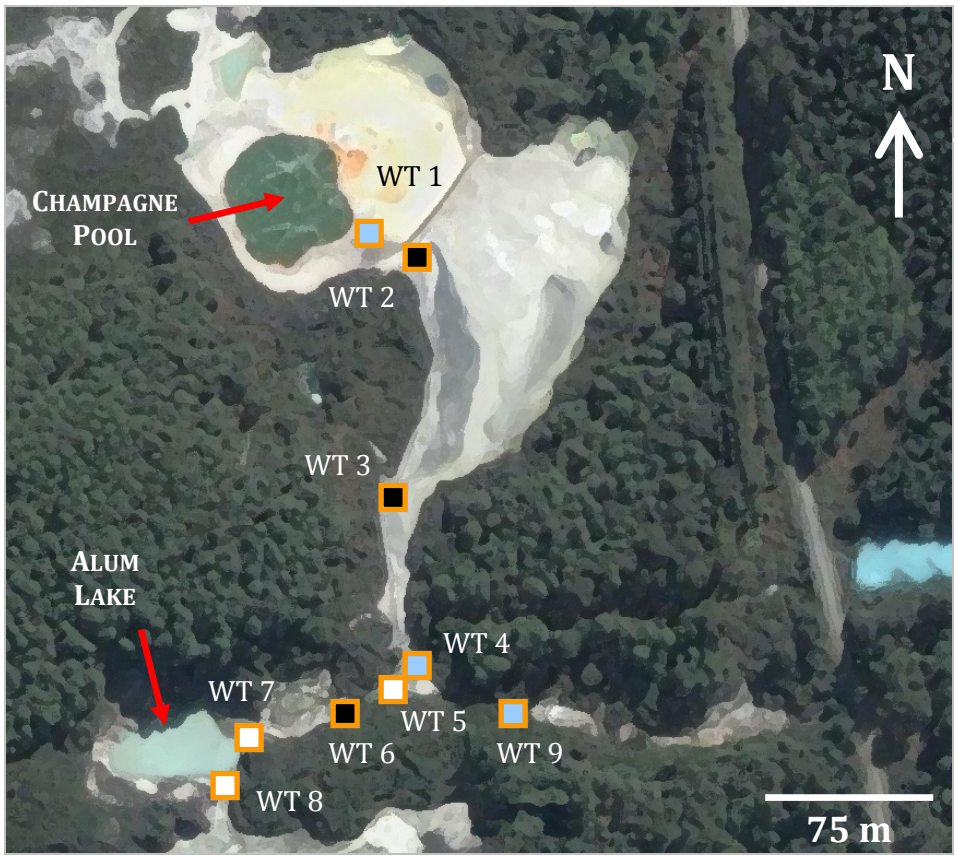

Figure 4.5 Wai-O-Tapu sampling sites. Summer only sites are marked as white boxes, winter only sites as blue boxes, sites used in both seasons as black boxes. Flow direction is north to south (map sourced from Google Earth™)

At Waimangu, sites WM 1 to 5 were sampled five times over 8 hours on January 7th, 2007 (sites shown in Figure 4.6). Because there was no evidence for diurnal variation at Waimangu during summer, the system was not resampled over a whole day in winter. Instead, single samples were collected from sites WM 5-9 and WB on February 27th, 2007 and from sites WM 1, WM 3, WM 5-9 and WB on August 31st, 2007.

Site descriptions for the Waimangu sampling are presented as Table 4.2. Samples of the algae, including *Phormidium fischerella* (as identified by Jones, 2005), were collected from sites WM 1, WM 3, and WM 5. Algal samples were collected using a polystyrene container fastened to the end of a telescopic pole.

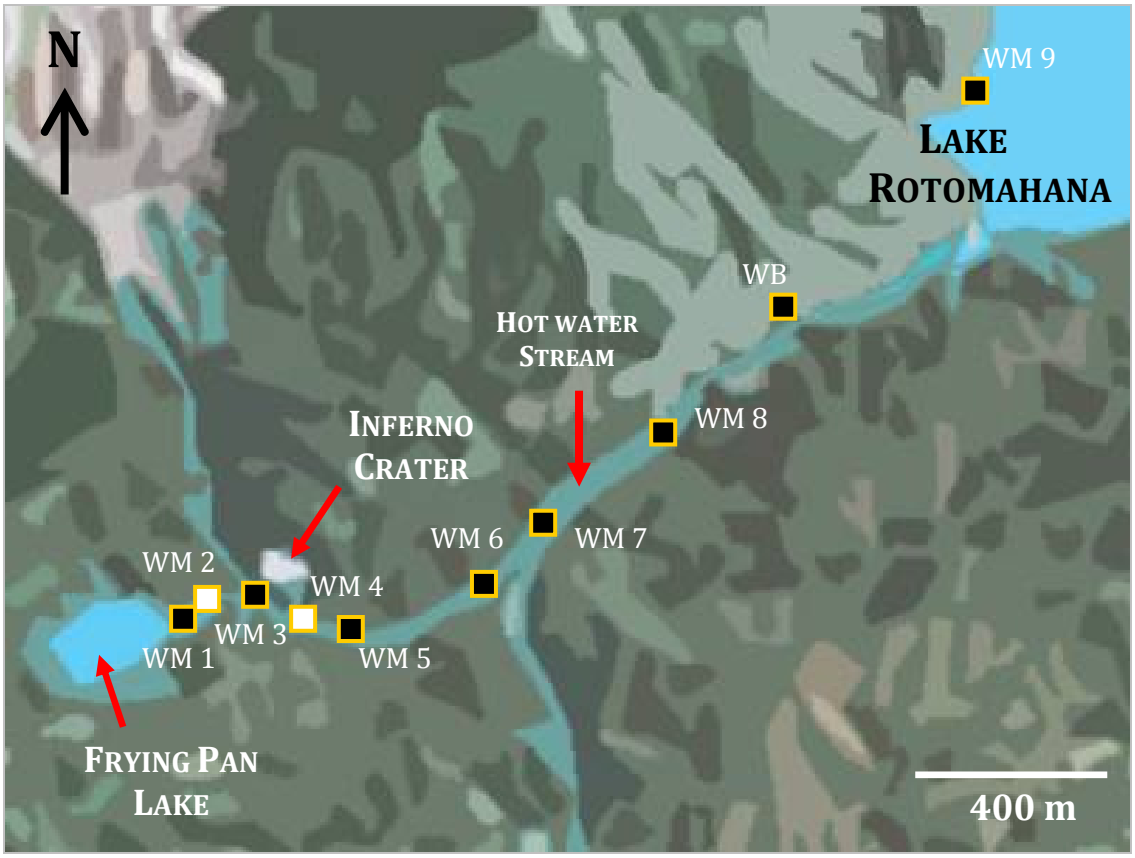

Figure 4.6 Waimangu sampling sites. Sites only used in summer are marked as white boxes, sites used in both seasons are marked as black boxes. Flow direction is southwest to northeast (map sourced from Google Earth™)

Table 4.2 Site descriptions for the Waimangu surveys

Site Number	Description
WM 1	Immediately downstream of Frying Pan Lake
WM 2	100 m downstream of Frying Pan Lake discharge
WM 3	At bridge 15 m above Inferno Crater discharge
WM 4	At bridge 3 m below Inferno Crater discharge
WM 5	At stream bank beside "Clamshell Spring" sign
WM 6	At bridge 10 m upstream of Haumi Stream confluence
WM 7	At bridge 180 m downstream of Haumi Stream confluence
WM 8	At bridge crossing Hot Water Stream
WM 9	At jetty on eastern shore of Lake Rotomahana
WB	At bridge 3m upstream of Warbrick Terrace confluence

4.3 THE BEHAVIOUR OF Sb AT WAI-O-TAPU

The data presented in this chapter were those judged to be the most relevant to the study aims. Not all the data collected during the research are presented in this chapter. Some data proved unreliable (such as flow measurements), while hourly measurements for light and some other parameters needed only to be described in general terms. A summary table of results from Wai-O-Tapu is presented as Tables 4.3 and 4.4, the complete data set for this chapter is given in Appendix II.

4.3.1 FIELD CONDITIONS AT WAI-O-TAPU

During summer sampling, the weather was fine (maximum brightness > 120 kLux) and the air temperatures warm (20-35 ^{o}C) throughout the day. In winter sampling, conditions were cold (air temperature 1-11 ^{o}C), with fog until 11:00 a.m., and overcast for the entire day (maximum brightness 26 kLux). Regardless of season, water temperatures peaked early afternoon (Figure 4.7a), typically later than the peaks in light intensity, which occurred about noon.

The pH of the discharge from Champagne Pool steadily declined with time during the day in both seasons (Figure 4.7b), and was circum-neutral (pH ~7) in summer and acidic (pH ~4) in winter. Below the confluence with the Whangioterangi discharge, pH over both seasons was ~ 2.5. Conductivity was higher in summer above Bridal Veil Falls, where measured conductivities approached 10 mS/cm (Figure 4.7c), while at all sites in winter, and downstream of Bridal Veil Falls in summer, conductivities were ~ 4 mS/cm.

Table 4.3 Summary table of selected analytical results from Wai-O-Tapu. Results are presented as medians with standard deviations (n =5 per site in summer, and n=6 per site in winter) in the discharge (light measurements were for ambient light). The full data set is presented in Appendix II

Site	Light (kLux)	Temp (^oC)	DO (mg/L)	pH	Cond (mS/cm)	Li (mg/kg)	H_2S (mg/kg)	SO_4 (mg/kg)	Cl (mg/kg)	As_{diss} (mg/kg)	Sb_{diss} (µg/kg)	Sb^{III} (µg/kg)
Summer												
WT 2	115 ± 22	32.0 ± 5.0	5.65 ± 0.81	6.84 ± 0.17	7.92 ± 2.07	10.4 ± 0.4	0.56 ± 0.31	162 ± 45	2220 ± 40	6.57 ± 0.43	83.1± 10.3	12.2 ± 3.4
WT 3	113 ± 45	31.2 ± 6.5	5.70 ± 1.19	7.15 ± 0.14	8.02 ± 1.13	10.5 ± 0.5	0.70 ± 0.34	161 ± 14	2270 ± 80	6.59 ± 0.36	160 ± 23.2	17.4 ± 8.6
WT 5	49.2 ± 40.3	30.4 ± 7.5	6.54 ± 0.83	3.99 ± 0.35	8.98 ± 1.63	11.0 ± 1.3	0.38 ± 0.28	256 ± 16	2650 ± 210	7.55 ± 0.96	63.9 ± 29.6	2.7 ± 0.7
WT 6	109 ± 40.8	29.9 ± 3.9	6.71 ± 0.41	2.51 ± 0.02	4.95 ± 0.37	4.42 ± 0.94	0.38 ± 0.18	358 ± 18	890 ± 113	2.20 ± 0.11	32.6 ± 11.3	1.5 ± 0.8
WT 7	111 ± 15	32.4 ± 4.1	5.56 ± 0.52	2.51 ± 0.02	5.00 ± 0.60	4.17 ± 0.37	0.79 ±0.08	367 ± 27	722 ± 82	2.07 ± 0.06	11.3 ± 6.0	< 0.2
WT 8	112 ± 11	34.5 ± 1.0	0.56 ± 0.26	2.45 ± 0.01	4.62 ± 0.10	2.85 ± 0.24	2.12 ±0.90	473 ± 6	631 ± 31	0.767 ± 0.344	< 0.2	< 0.2
Winter												
WT 1	12.0 ± 7.9	8.7 ± 2.1	6.90 ± 0.70	4.92 ± 0.97	4.88 ± 1.14	10.5 ± 0.7	0.13 ± 0.26	131 ± 41	2380 ± 60	5.79 ± 0.93	59.2 ± 49.2	18.9 ± 41.6
WT 2	13.0 ± 8.5	9.2 ± 1.4	8.47 ± 0.60	4.58 ± 0.51	4.91 ± 0.75	10.6 ± 0.7	0.19 ± 0.31	158 ± 43	2410 ± 40	6.10 ± 0.27	82.3 ± 44.7	43.9 ± 26.3
WT 3	10.9 ± 6.1	5.9 ± 1.3	9.13 ± 0.74	4.36 ± 0.76	4.77 ± 0.85	10.1 ± 0.7	< 0.05	180 ± 61	2350 ± 50	6.27 ± 0.23	143 ± 52	88.6 ± 32.1
WT 4	12.9 ± 5.5	4.7 ± 1.7	9.38 ± 0.88	3.60 ± 0.72	4.62 ± 0.91	10.1 ± 0.7	< 0.05	195 ± 38	2280 ± 10	6.17 ± 0.23	107 ± 37	53.6 ± 30.7
WT 6	13.0 ± 4.3	15.8 ± 0.6	7.40 ± 0.26	2.40 ± 0.01	3.00 ± 0.09	1.55 ± 0.14	< 0.05	487 ± 8	389 ± 7	0.235 ± 0.021	1.4 ± 0.5	0.4 ± 0.1
WT 9	1.39 ± 0.44	16.6 ± 0.6	5.76 ± 0.32	2.39 ± 0.07	2.94 ± 0.21	1.42 ± 0.08	< 0.05	486 ± 6	374 ± 1	0.219 ± 0.014	< 0.2	< 0.2

Table 4.4 Ranges for selected analytical results from Wai-O-Tapu. n =5 per site in summer, and n=6 per site in winter in the discharge (light measurements were for ambient light). The full data set is presented in Appendix II

Site	Light (kLux)	Temp (°C)	DO (mg/L)	pH	Cond (mS/cm)	Li (mg/kg)	H_2S (mg/kg)	SO_4 (mg/kg)	Cl (mg/kg)	As_{diss} (mg/kg)	Sb_{diss} (µg/kg)	Sb^{III} (µg/kg)
Summer												
WT 2	75.1 - 133	22.2 - 34.1	5.13 - 7.10	6.69 -7.13	3.34 - 8.21	9.5 - 10.6	< 0.05 - 1.0	146 - 254	2150 - 2250	5.69 - 6.79	71.8 - 98.7	6.3 – 14.0
WT 3	14.8 - 121	17.3 - 33.3	5.15 - 8.19	7.08 - 7.42	5.73 - 8.49	10.0 - 11.3	< 0.05 - 1.1	138 - 174	2090 - 2290	6.08 - 7.04	118 – 171	9.0 – 27.5
WT 5	37.6 – 125	15.4 - 33.3	5.78 - 7.93	3.80 - 4.68	5.88 - 9.71	10.8 - 13.6	< 0.05 - 0.9	223 - 264	2330 - 2820	6.15 - 8.38	37.0 – 111	2.1 – 3.6
WT 6	20.2 – 121	21.9 - 31.8	6.28 - 7.27	2.50 - 2.54	4.19 - 5.13	3.3 - 5.4	< 0.05 - 0.6	353 - 393	682 - 973	2.04 - 2.29	10.0 – 36.2	0.4 – 2.5
WT 7	94.6 – 126	24.1 - 34.0	5.36 - 6.60	2.48 - 2.53	3.74 - 5.17	3.6 - 4.5	0.7 - 0.8	350 - 419	632 - 820	2.00 - 2.17	3.8 – 17.9	< 0.2 – 1.7
WT 8	91.4 – 118	32.9 - 35.0	0.18 - 0.84	2.43 - 2.45	4.42 - 4.63	2.6 - 3.2	1.5 - 3.9	464 - 479	585 - 660	0.27 – 1.07	< 0.2	< 0.2
Winter												
WT 1	4.3 - 23.4	4.7 - 9.8	6.25 - 8.27	3.92 - 6.68	2.09 - 5.00	9.4 - 11.3	< 0.05 - 0.6	96 - 203	2360 - 2500	5.11 – 7.78	14.9 – 153	4.8 – 114
WT 2	5.6 - 26.4	6.7 - 10.1	8.04 - 9.71	4.17 - 5.41	3.05 - 4.96	9.3 - 11.4	< 0.05 - 0.7	118 - 209	2340 - 2440	5.81 – 6.54	44.7 – 154	14.6 – 93.6
WT 3	4.2 - 19.7	3.9 - 7.1	8.65 - 10.7	3.52 - 5.30	2.71 - 4.91	9.3 - 11.1	< 0.05 - 1.8	116 - 263	2300 - 2430	5.89 – 6.57	56.9 – 194	40.2 – 120
WT 4	4.8 - 19.3	2.2 - 6.3	8.47 - 10.8	3.24 - 5.08	2.45 - 4.81	9.1 - 10.7	< 0.05 - 0.8	150 - 245	2260 - 2300	5.78 – 6.33	37.8 – 119	2.7 – 75.6
WT 6	4.7 - 16.1	15.0 - 16.4	7.11 - 7.77	2.39 - 2.42	2.95 - 3.21	1.3 - 1.7	< 0.05	475 - 496	378 - 398	0.21 – 0.27	1.0 – 2.2	0.2 – 0.5
WT 9	1.0 - 2.2	16.0 - 17.3	5.19 - 6.04	2.30 - 2.51	2.85 - 3.43	1.3 - 1.6	< 0.05	472 - 488	373 - 377	0.20 – 0.25	< 0.2	< 0.2

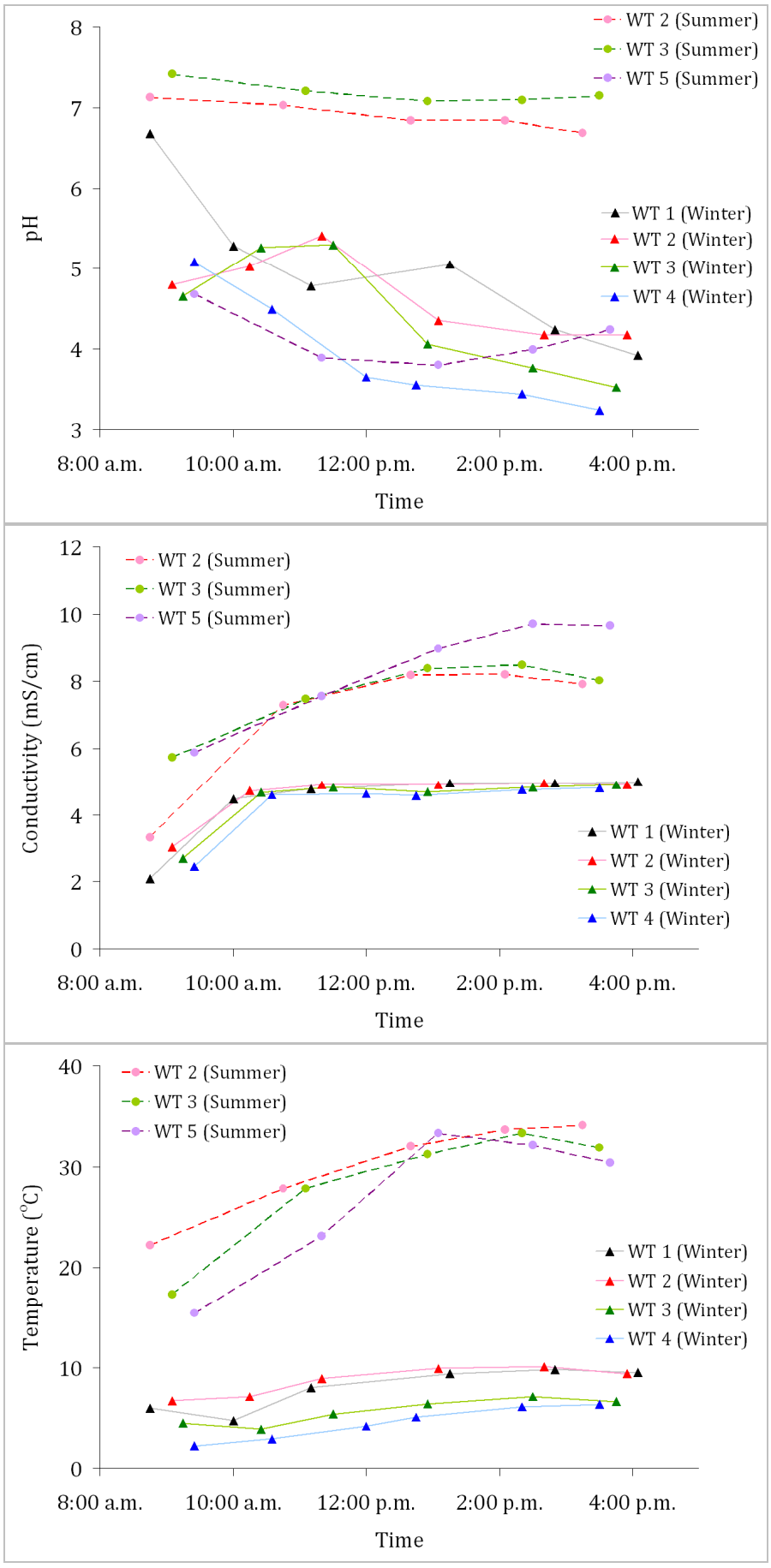

Figure 4.7 Changes in a) temperature, b) conductivity and c) pH in the first ~200 m of the discharge from Champagne Pool

Selected samples were sent to Hills Laboratories, an NZS/ISO/IEC 17025:2005 accredited laboratory, to be measured for a range of chemical elements by an ICP-MS screen. Overall, most element concentrations were higher in the discharge than those reported for Champagne Pool itself by Pope et al (2004), for example Na concentrations increase from 1044 mg/kg to 1300 mg/kg, which suggests that some evaporation of the discharge may occur across Artist's Palette. Downstream, concentrations of Cl and Li were stable (±10%), as shown in Table 4.3. Apart from As and Sb, the discharge also contains elevated levels of B and Li, both of which are also considered geothermal contaminants (Ellis and Mahon, 1977).

Results for As concentrations compared well with the data for this study produced by HG-AAS, but Sb concentration data produced by ICP-MS were higher (150-300 %) than the Sb concentration data presented elsewhere in this study (with the exception of the results from site WT 2 in winter, where Sb concentrations as produced by ICP-MS were 20 % lower than those produced by HG-AAS). However, the Sb concentration data produced using HG-AAS in this study compared well with Pope et al's (2004) data (Table 4.4). Because the ICP-MS data presented in Table 4.4 was only semi-quantitative, disparities were not investigated further.

Table 4.5 A comparison between dissolved element concentration data from Pope et al (2004) for Champagne Pool and semi-quantitative ICP-MS analyses of samples collected from Champagne Pool's discharge during this study. The units for all element concentrations are mg/kg.

Site	Pope et al (2004)	WT 2	WT 3	WT 2	WT 3	WT 3	WT 3
Season	Winter	Summer	Summer	Winter	Winter	Winter	Winter
Time	N/M	12:40 p.m.	12:55 p.m.	11:20 a.m.	9:15 a.m.	11:30 a.m.	2:30 p.m.
Al	0.079	0.16	0.14	0.14	0.21	0.22	0.27
Sb	0.0097	0.25	0.31	0.052	0.12	0.18	0.33
As	5.2	7.0	6.9	5.5	5.6	5.7	6.6
Ba	0.0067	0.017	0.016	0.011	0.01	0.011	0.013
B	36	29	28	25	25	25	29
Cs	1.4	1.6	1.7	1.4	1.3	1.4	1.7
Ca	44	42	42	39	37	38	41
Li	9.1	9.3	9.0	8.5	8.3	8.5	9.8
K	150	190	190	170	170	170	200
Rb	1.2	2.0	2.0	1.8	1.7	1.8	2.1
Na	1000	1300	1300	1200	1200	1200	1300
Th	0.000027	0.0028	0.0054	< 0.0010	< 0.0010	0.0026	0.0079

4.3.2 METALLOID CONCENTRATIONS BELOW CHAMPAGNE POOL

Figure 4.8 shows dissolved Sb concentrations downstream of Champagne Pool as a function of distance and time for summer and winter sampling events. Maxima were reached at site WT 3 (150 m), regardless of sampling date or sampling time. Below Bridal Veil Falls, dilution by the Lake Whangioterangi discharge is the main reason for the sharp decreases in Sb concentration at sites WT 4 – WT 7, while the continued decline at site WT 8 will be discussed in section 4.3.6. Dissolved Sb concentrations were below detection limits at all times at site WT9, the stream flowing out of Lake Whangioterangi.

The site of maximum Sb concentrations, site WT 3, was a trench on the western side of the sinter terraces, about half-way between Champagne Pool and Bridal Veil Falls. Between site WT 2 and WT 3 there were no visible Sb-mineral deposits, as such deposits appeared to be restricted to Artist's Palette.

Over the course of each day, both in summer and in winter, Sb concentrations increased from the first morning sample through until about 2:30 p.m. (mid-afternoon), after which time they began to decline. This phenomenon was also observed by Pope et al (2004) during their own work at Wai-O-Tapu.

The partitioning between dissolved and particulate Sb in the discharge from Champagne Pool also varied with distance and time, as shown in Figure 4.9. In the undiluted discharge of Champagne Pool (WT 1-4), dissolved Sb dominated, with the exception of the afternoon winter sample from site WT 1, which might have been contaminated with loose Sb-rich precipitates dislodged during sampling. Below Bridal Veil Falls, in the waters influenced by acid-sulfate discharges (WT 5-8), the relative proportion of dissolved Sb declined with distance. In samples from the discharge of Alum Lake, only particulate Sb (> 0.45 μm) was detected.

The speciation of Sb, specifically the proportions of Sb^{III} and Sb^{V}, was also determined. In summer, most of the dissolved Sb was present as Sb^{V}. Sb^{III} species were typically < 20% of the total dissolved Sb concentrations (Figure 4.10). However, in winter, Sb^{III} species appeared to be more stable, which may reflect slower oxidation kinetics in the colder waters. Assuming that Sb^{III} was the dominant species in Champagne Pool itself, it appears the the most significant geographic oxidation zone was across Artist's Palette, because Sb^{V} concentrations were ~50 % at site WT 1. The proportion of Sb^{III} was typically higher in samples from above Bridal Veil Falls than downstream of the confluence with the Lake Whangioterangi discharge. Oxidative catalysis by Mn or Fe solid phases may be the cause of downstream oxidation (Belzile et al, 2001), but the process was not investigated.

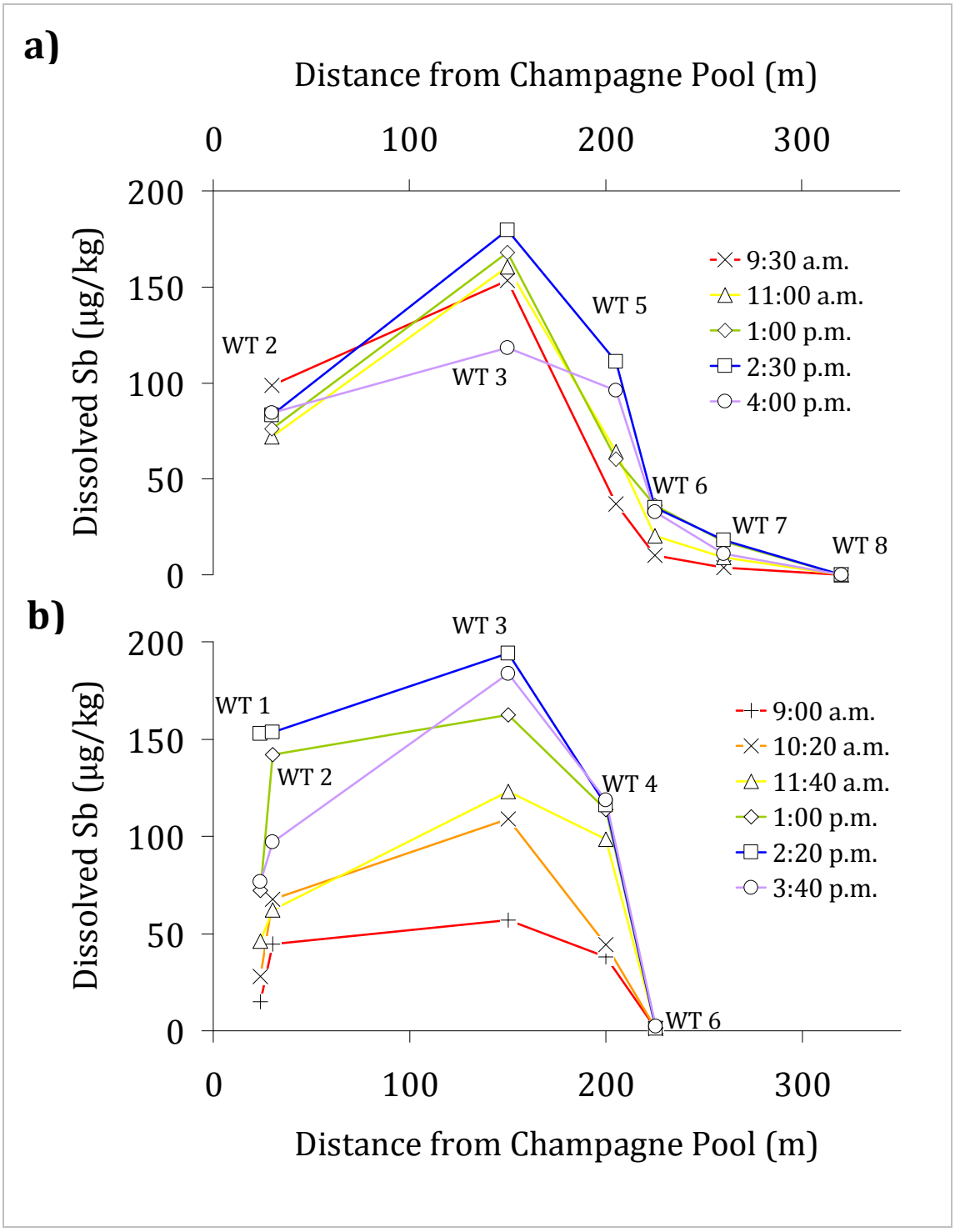

Figure 4.8 Antimony concentrations at Wai-O-Tapu as a function of time and distance downstream from Champagne Pool, showing a) the results for summer, and b) the results for winter.

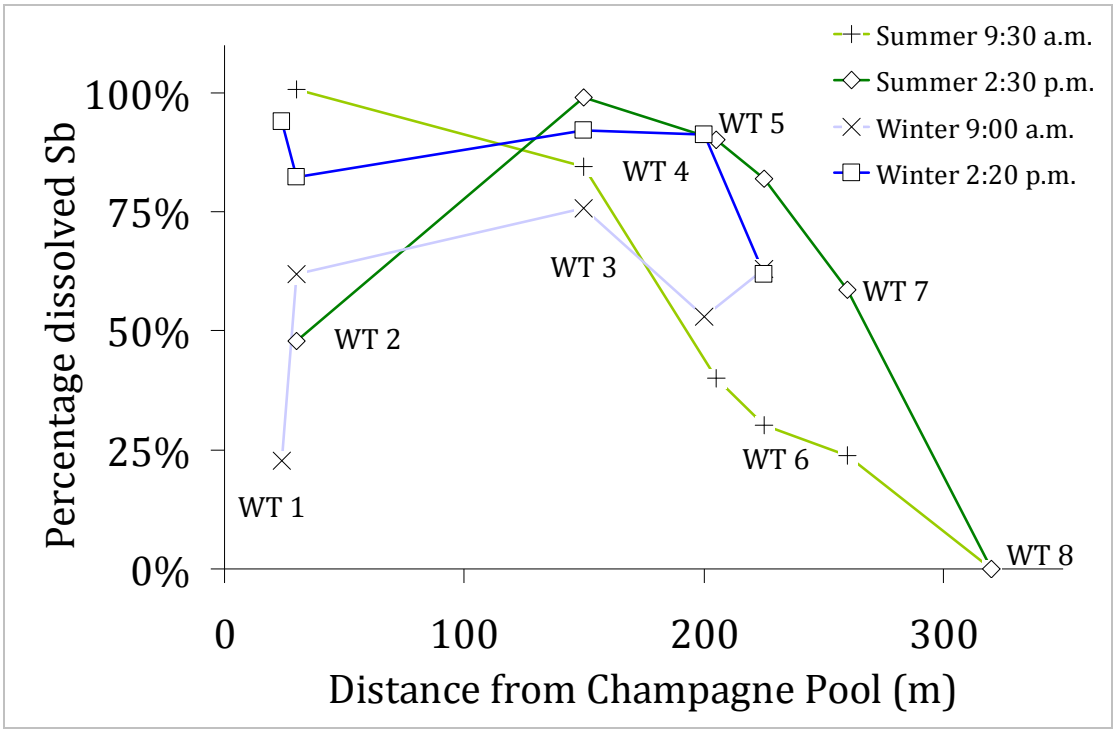

Figure 4.9 Changes in Sb partitioning in the discharge from Champagne Pool

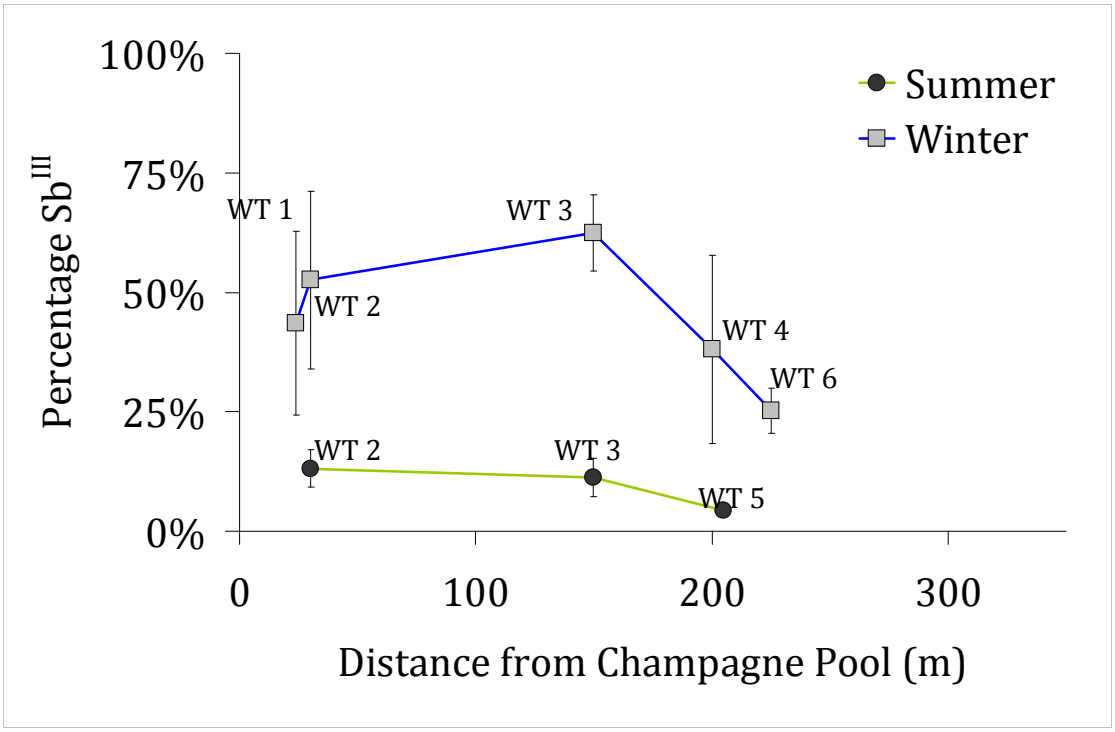

Figure 4.10 Sb^{III} proportions at the Wai-O-Tapu study sites, presented as average values across all times sampled (n=5 in summer, n=6 in winter). Results are not presented for sites where dissolved Sb concentrations were below detection limit (< 0.3 µg/kg).

ARSENIC

Arsenic concentrations are orders of magnitude higher than Sb concentrations in the discharge from Champagne Pool. Compared to Sb, similar diurnal patterns were observed, as shown in Figure 4.11, but the changes were proportionally smaller. Unlike Sb, As concentrations did not peak at site WT 3. In summer, As concentrations peaked at site WT 5, below Bridal Veil Falls, in waters influenced by the input from Lake Whangioterangi. In winter, the highest recorded As concentrations occurred at site WT 1. WT 5 was not sampled in winter, but concentrations of As at site WT 4 were not notably different from those of upstream sites, and downstream As concentrations decreased sharply as the waters became diluted.

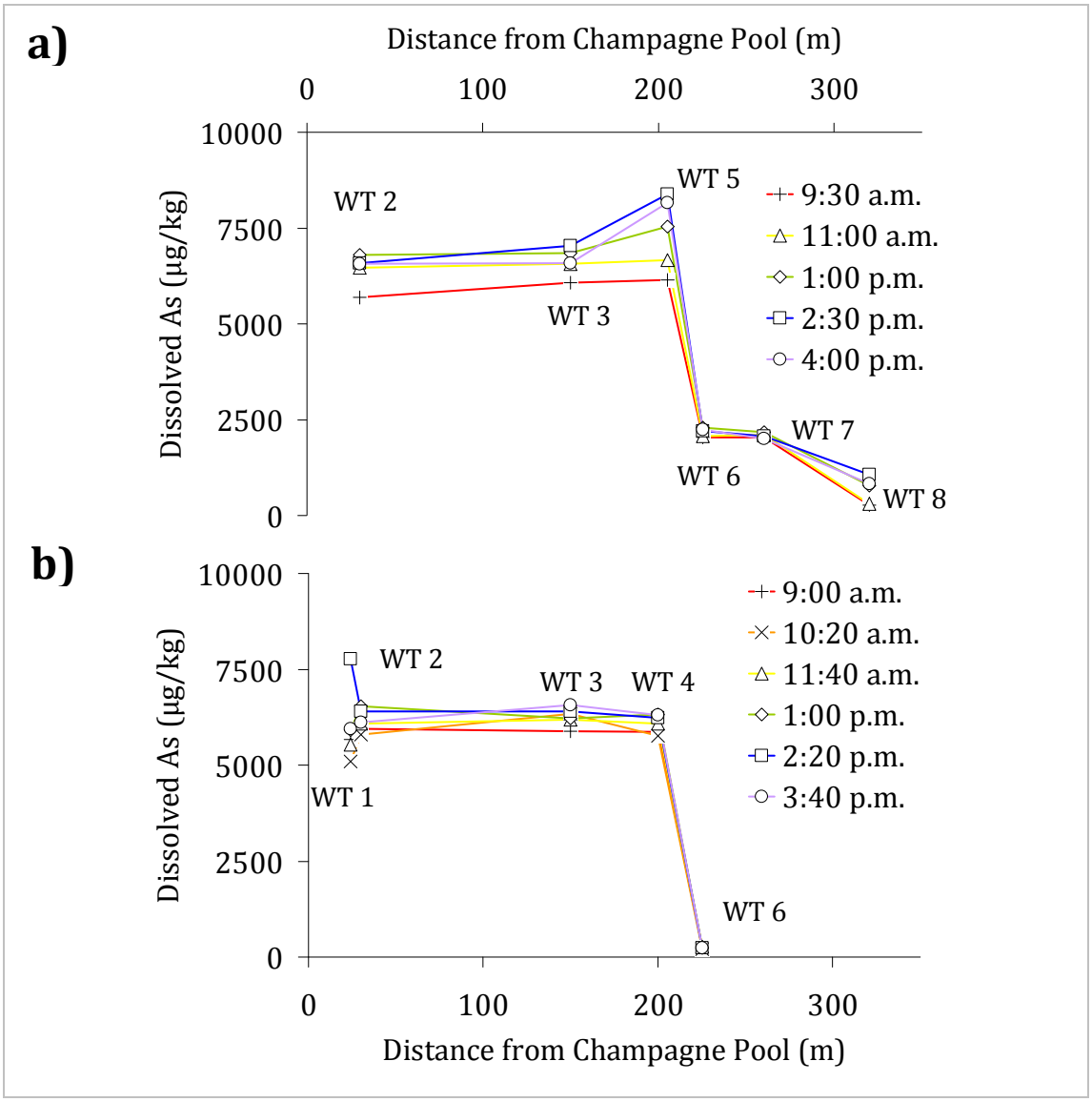

Figure 4.11 Arsenic concentrations at Wai-O-Tapu as a function of time and distance downstream from Champagne Pool, showing a) the results for summer, and b) the results for winter.

4.3.3 CORRELATIONS BETWEEN VARIABLES AT WAI-O-TAPU

Different variables from the Wai-O-Tapu data set were compared to determine any links between those variables as they were measured between Champagne Pool and Bridal Veil Falls (sites WT 1-4), and the results shown in Figure 4.12. The purpose of these comparisons was to learn about how Sb behaves (e.g. how mobile geothermally derived Sb is, relative to As), and to compare dissolved Sb with other ions used as conservative geochemical tracers such as Li and Cl (Schemel et al, 2006; Tate et al, 1996). Because Sb is a chalcophile, Sb concentrations were also compared to dissolved sulfur-species (particularly H_2S and SO_4) as well as to more general parameters (DO, conductivity, light and temperature).

ARSENIC, SULFIDES AND SULFATE

The strongest correlations between Sb and any other measured parameter occurred within the winter dataset, where Sb concentrations correlated slightly with As (R^2 = 0.55, Figure 4.12a) and reasonably well with SO_4 concentrations (R^2 0.73, Figure 4.12b). For As, the R^2 value for the correlation is relatively low, but this in part can be explained by the problems inherent in comparing values of such different magnitudes. The correlation between As and SO_4 concentrations for the winter data set was weaker (R^2 = 0.40, not shown).

No correlation was observed between Sb concentrations and H_2S concentrations during either season, as shown in Figure 4.12c. This comparison was somewhat limited because in winter H_2S concentrations were often below the detection limit (< 0.05 mg/kg).

CONSERVATIVE ELEMENTS

Figure 4.12d (Sb:Li) and Figure 4.12e (Sb:Cl) show that there were no correlations between Sb and either of the conservative elements measured in the discharge of Champagne Pool. Concentrations of both Cl and Li fluctuated during the sampling, but this variation was not systematic, and relatively minor at most sites (< 10 % for Li at all sites except WT 6 in summer, where variation was 20 %, and < 4 % at all sites for Cl). Comparisons between Sb concentrations and conservative element concentrations over time showed the diurnal pattern observed for Sb concentrations over time also occurred with respect to Sb:Li or Sb:Cl ratios, an example of which is shown in Figure 4.13.

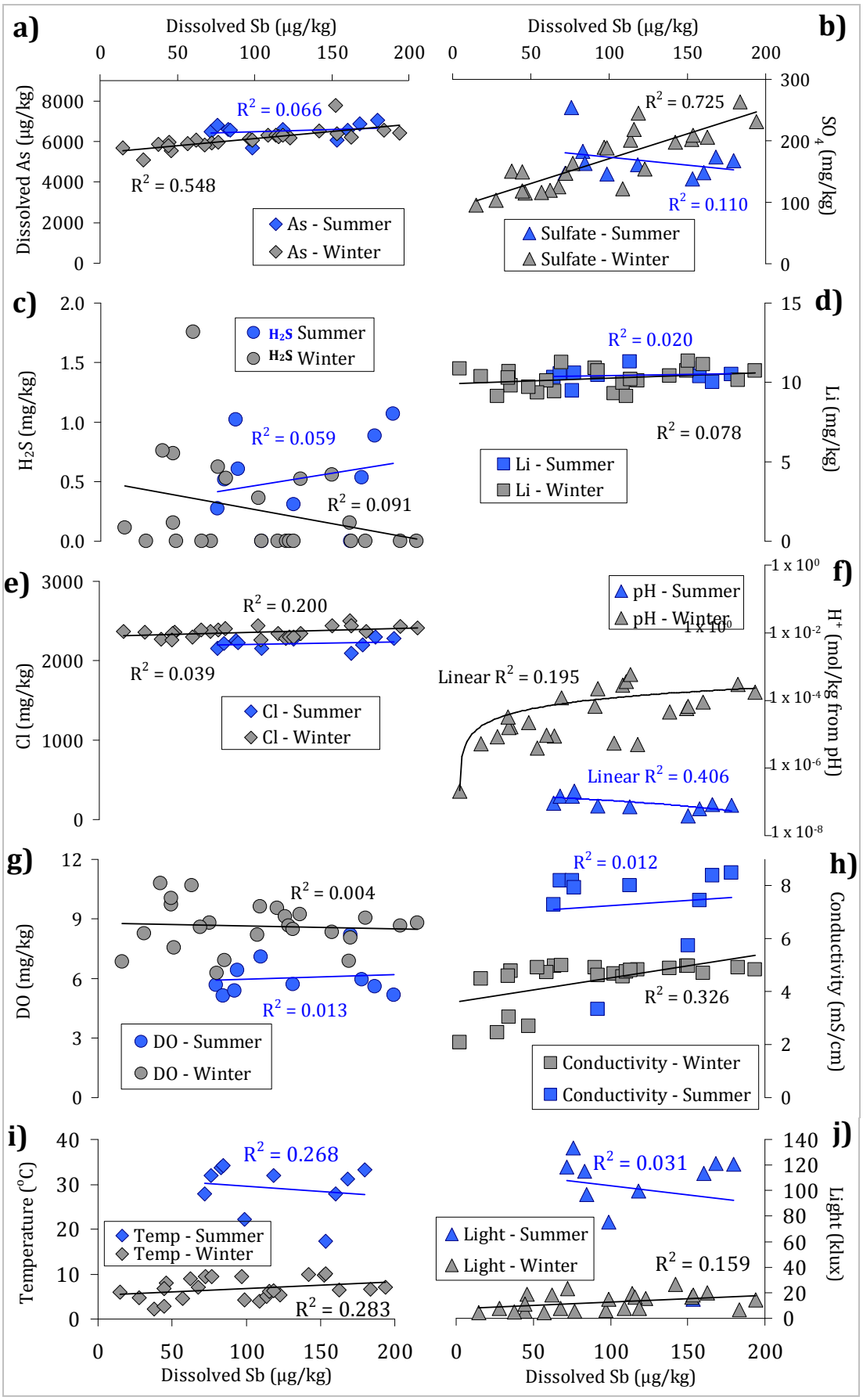

Figure 4.12 Linear correlations between Sb concentrations and a) As, b) Li, c) Cl, d) Conductivity, e) H_2S, f) SO_4, g) DO, h) pH (plotted as $[H^+]$), i) Temperature, j) Light. Values below detection limit have been plotted as o

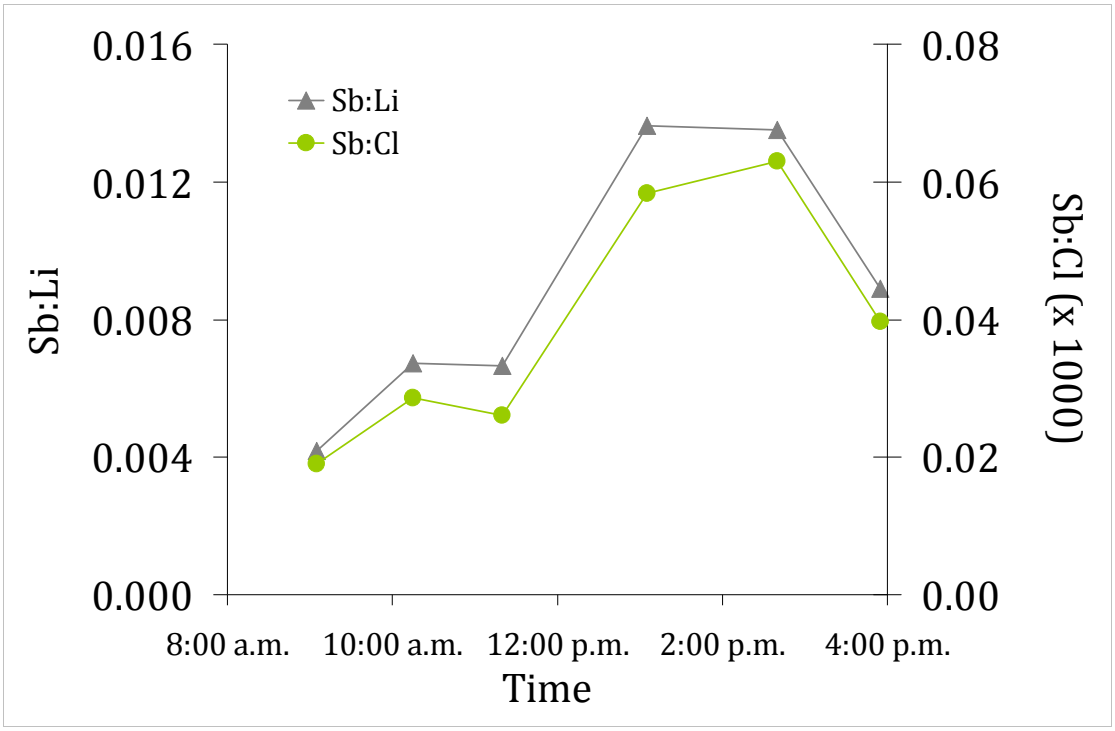

Figure 4.13 Changes in Sb:Li and Sb:Cl ratios with respect to time at site WT 2 in winter

OTHER PARAMETERS

A very weak correlation (R^2 = 0.41) is apparent between Sb concentrations and pH during winter, as shown in Figure 4.12f. In summer, where the correlation is poorer (R^2 = 0.19), Sb concentrations increase with increasing pH, but in winter Sb concentrations appeared to increase with decreasing pH. There was no evidence of any relationship between Sb and DO (Figure 4.12g). In winter, a very weak correlation (R^2 = 0.33) was observed between Sb concentrations and conductivity, where Sb concentrations appeared to increase with increasing conductivity (Figure 4.12h). In summer, this correlation was non-existent (R^2 = 0.01)

In summer and winter, no correlations were observed between Sb concentrations and either light (R^2 = 0.28, Figure 4.12i) or temperature (R^2 = 0.16, Figure 4.12j). The results from summer are skewed by low light and temperature results for site WT 3 at 9:00 a.m., during which time the site was under shade. When changes in Sb concentrations with time were compared to changes in light and temperature with time (examples shown in Figure 4.14), it was further evident that changes in either light or temperature were not clearly reflected by changes in Sb concentration. However, despite the overall lack of correlation, changes in Sb concentrations over time were more similar to changes in temperature, than to changes in light conditions.

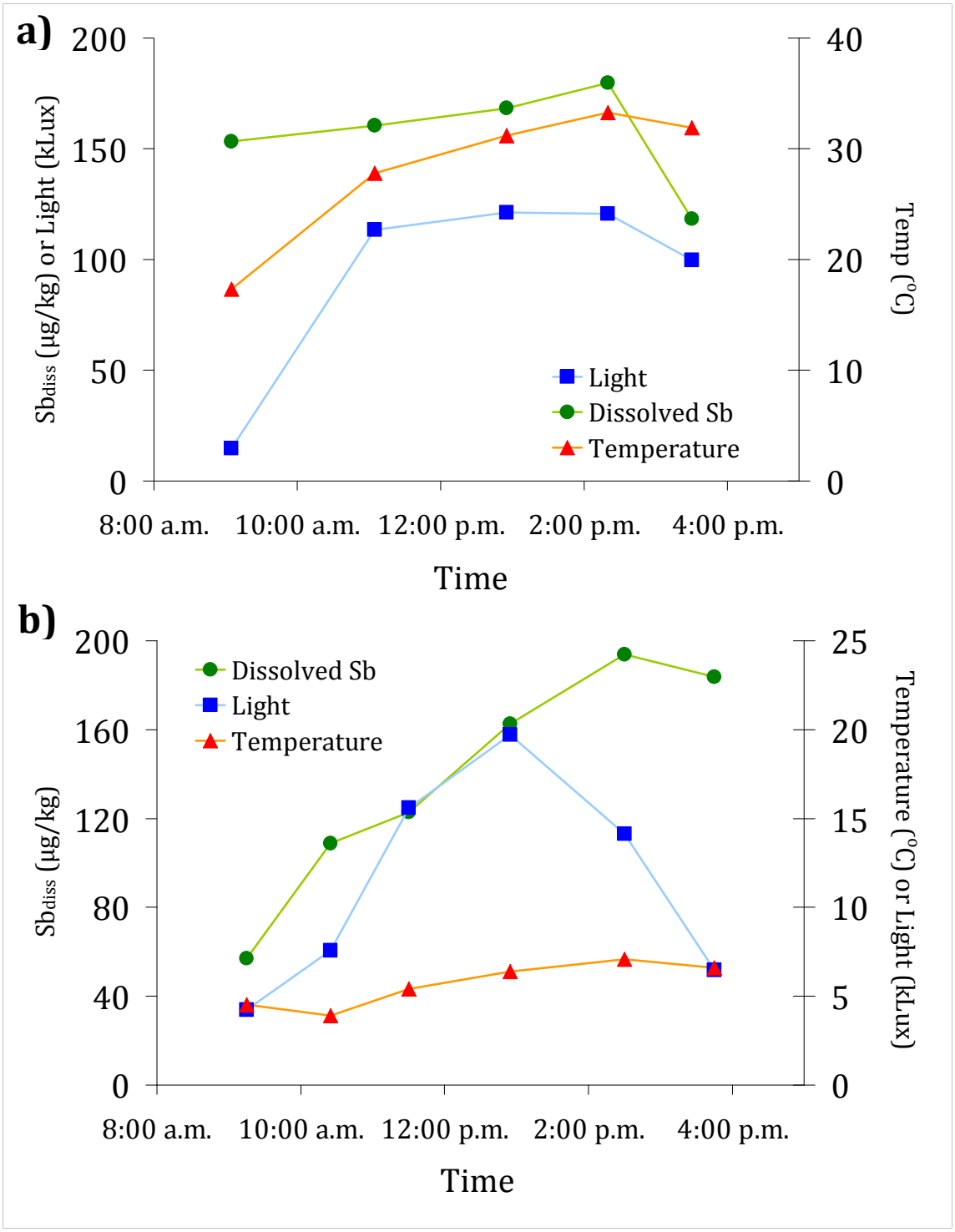

Figure 4.14 Direct comparisons between dissolved Sb concentrations, time and light at site WT 3 during a) summer and b) winter.

4.3.4 ANALYSIS OF SUSPENDED MATERIAL FROM WAI-O-TAPU

Images captured using Scanning Electron Microscopy (SEM) of the 0.45 μm filter membranes collecting during the winter sampling show that the algal/bacterial communities found within Champagne Pool are morphologically distinct from those in the discharge downstream (Plate 4.7 for Champagne Pool, Plate 4.8 for the discharge). Stibnite could not be identified in the SEM photo taken of the solids collected onto a filter membrane after disturbing the Champagne Pool rind, but Sb is present in the fine (< 1 μm) matrix. Downstream, microbiota are more common. The dominant species appear to be the diatom *Pinnularia sp.*, identified from the description of Cooper (1996), but a filamentous algae is also present, probably *Chlorothix sp.* (also identified from the description of Cooper, 1996).

4.3.5 DIURNAL FLUCTUATIONS IN Sb CONCENTRATIONS

Both Li and Cl are conservative elements, and are therefore not usually removed by precipitation processes in geothermal environments. The fact that there was no correlation between Sb concentrations and either Li or Cl suggests that changes in Sb concentrations are not simply caused by changes in geothermal fluid flows. While wind direction and speed may change the flow of fluids across the sinter terrace, such effects only affect the flux of remobilised material, and should not influence the concentrations.

Evaporation can also be eliminated, because any concentrating process should increase the concentrations of all conservative elements and therefore the ratios of, for example, Sb:Li or Sb:Cl should remain constant. If physical processes are not the principal cause, then chemical and/or biogeochemical processes need to be investigated.

The chemical dissolution of Sb_2S_3 proceeds as shown in Equation 4.1a or 4.1b:

$$Sb_2S_{3(s)} + 6H_2O_{(l)} \leftrightarrows 2\ H_3SbO_{3(aq)} + 3\ H_2S_{(aq)} \qquad (4.1a)$$

$$\text{Or} \qquad Sb_2S_{3(s)} + 6\ H_2O_{(l)} \leftrightarrows 2\ H_3SbO_{3(aq)} + 3\ HS^-_{(aq)} + 3\ H^+_{(aq)} \qquad (4.1b)$$

The oxidation of antimonite to antimonate proceeds as shown in Equation 4.2:

$$H_3SbO_{3(aq)} + 2\ H_2O_{(l)} + \tfrac{1}{2}\ O_{2(aq)} \leftrightarrows H_6SbO_6^-{}_{(aq)} + H^+_{(aq)} \qquad (4.2)$$

Assuming thermodynamic equilibrium conditions, in the absence of oxygen (reducing conditions), Sb^{III} should dominate. In the presence of oxygen (oxidising conditions), and the absence of H_2S, the Sb^{III} released from dissolving Sb_2S_3 should oxidise to Sb^{V}, especially given likely presence of Sb-oxidising bacteria.

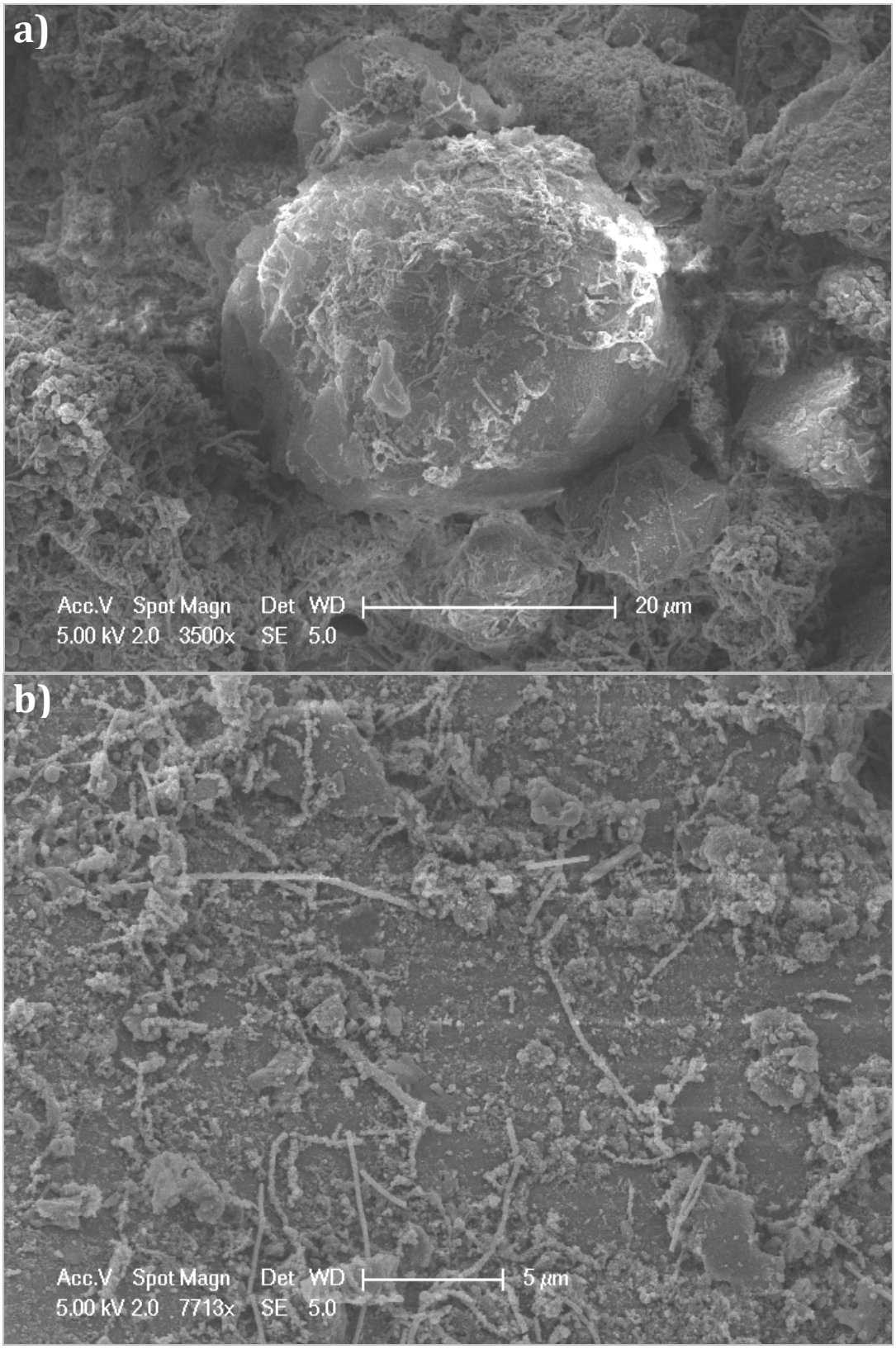

Plate 4.7 The rind from Champagne pool is a mixture of a) larger ball-shaped silicates in b) a finer grained matrix, which is a composite of filamentous algae and amorphous Si-rich material (5 % Sb)

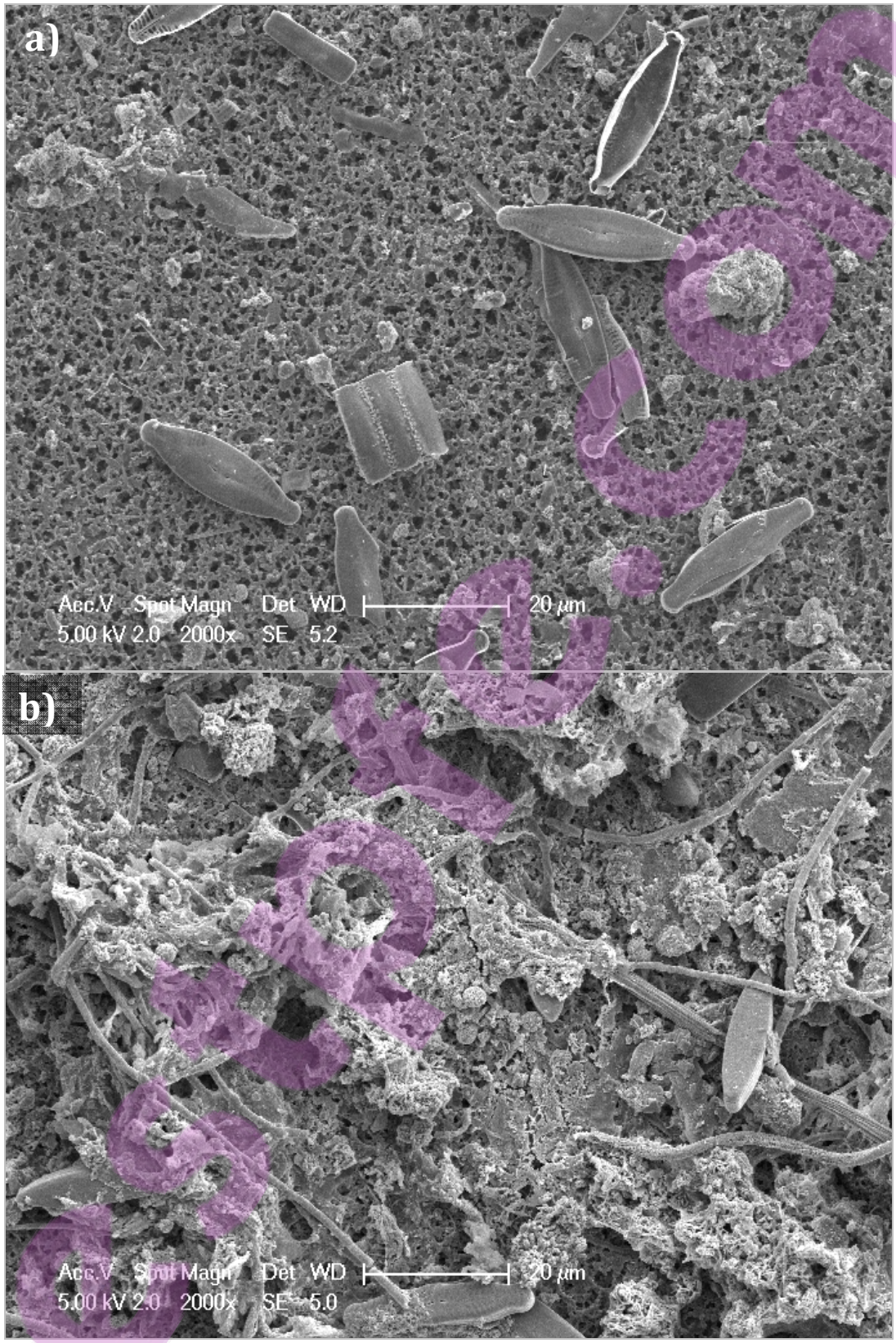

Plate 4.8 Downstream from Champagne Pool, SEM photos show that a) diatoms dominate at WT 2, but b) further downstream along Primrose terrace Si fragments are more common, and filamentous algae, larger than that observed in Champagne Pool, are increasingly present.

DIRECT BIOGEOCHEMICAL CONTROLS ON Sb SOLUBILITY

If the fluids discharged from Champagne Pool were subject only to chemical processes and were at thermodynamic equilibrium, two predictions could be made: that the concentrations of Sb would be lower in winter than in summer, reflecting the lower pH of the system, and that, given the presence of oxygen in the system, all Sb present in solution should be Sb^{V}. However, while morning Sb concentrations were lower in winter than in summer, the maximum amounts measured were similar, and the Sb in solution was not exclusively Sb^{V}. The system is therefore not at equilibrium, and biogeochemical processes, such as bacterial catalysis may also be occurring.

Pope et al (2004) argued that the diurnal changes in Sb and As concentrations were caused by the bacterially-catalysed destabilisation of sulfide minerals, in the presence of oxygen, on the basis that organisms such as *Thiobacillus sp*. have been shown to catalyse the oxidation of Sb and As sulfides, and have been documented in the Champagne Pool system. Work published by Torma and Gabra (1977) suggested that the optimal conditions for bacterial oxidation (at least for Sb_2S_3) are pH 1.75 and 35 ^{o}C. In the discharge from Champagne Pool, the fluids are either warm (in summer), or acidic (in winter), but not both.

In acidic conditions, the bio-mediated oxidation of Sb_2S_3 could also result in the formation of an insoluble antimony-oxide-sulfate, as shown in equations 4.3 and 4.4 (Torma and Gabra, 1977):

$$Sb_2S_{3(s)} + 6O_{2(aq)} \xrightarrow{\text{Thiobacillus oxidans}} Sb_2(SO_4)_{3(aq)} \qquad (4.3)$$

$$Sb_2(SO_4)_{3(aq)} + 2\,H_2O_{(l)} \leftrightarrows (SbO)_2SO_{4(s)} + SO_4^{2-}{}_{(aq)} + 2H^+{}_{(aq)} \qquad (4.4)$$

The stability of $(SbO)_2SO_4$ at low pH is questionable though, because when H^+ (or H_3O^+) ions are available, the reaction should proceed in reverse (i.e. the $Sb_2(SO_4)_3$ complex would be favoured), and the bio-oxidation process should result in higher dissolved Sb concentrations. In waters with higher pH, such as those measured in summer, the formation of insoluble $(SbO)_2SO_4$ could mean that the remobilisation of Sb from dissolved sulfide-minerals is somewhat mitigated. However, near-maxima Sb concentrations were reached earlier in summer than in winter, so if the process described by Torma and Gabra were occurring, its influence was minor.

Bacterial leaching of Sb from Sb_2S_3 can also be ruled out. Leaching by *Thiobaccilus oxidans* typically involves a proton attack, as shown in equation 4.5 (Schippers and Sand, 1999). This is unlikely to affect Sb_2S_3, which is less soluble under acidic conditions (Wilson et al, 2007).

$$MS_{(s)} + 2H^+_{(aq)} \leftrightarrows M^{2+}_{(aq)} + H_2S_{(aq)} \quad (4.5)$$

where M is a metal. A further problem with any explanation that requires a biological entity as the principal agent, is that disparate seasonal temperatures, pH and available light produced similar maximum dissolved Sb concentrations. If photosynthetic organisms were directly responsible, the observed changes should be more significant in summer conditions (warmer and more light) when microbiotic activity should be higher (assuming the biota are not psychrophiles) (Todar, 2008).

INDIRECT BIOGEOCHEMICAL CONTROLS ON Sb SOLUBILITY

There is are alternative hypothese for the diurnal fluctuations of metalloids such as Sb in the waters downstream of Champagne Pool. One such alternative hypothesis is that such changes may be the by-product of changes in $H_2S \leftrightarrows HS^- \leftrightarrows SO_4^{2-}$ equilibria (equations 4.6 and 4.7).

$$H_2S_{(aq)} \leftrightarrows HS^-_{(aq)} + H^+_{(aq)} \quad (4.6)$$

$$HS^-_{(aq)} + 2\ O_{2(aq)} \leftrightarrows SO_4^{2-}{}_{(aq)} + H^+_{(aq)} \quad (4.7)$$

The fluid in Champagne Pool degasses as it cools, and so while H_2S concentrations are approximately 10 mg/kg within the hot pool itself, concentrations in the overflow fluids that create Artist's Palette are more than an order of magnitude lower (Pope et al, 2004). In daylight hours, photosynthetic bacteria living in the cooler downstream waters produce abundant oxygen, and therefore any residual H_2S is oxidised into SO_4^{2-}, a reaction that is also catalysed by bacteria (Eckert, 1987). This shift in equilibrium causes sulfide precipitates to redissolve; in the case of Sb, this occurs via equation 4.1. The mechanism can explain why there is no correlation between dissolved oxygen and Sb concentrations, because photosynthetic processes will not influence stibnite solubility unless the system is oxygen-limited.

Antimony concentrations better correlate instead with sulfate, as shown in Figure 4.12. Sulfate is a correlating factor because the aqueous sulfides produced by the dissolution reaction are ultimately oxidised into SO_4^{2-}, sometimes via intermediate metastable sulfur species such as $S_2O_3^{2-}$ or SO_3^{2-} (Xu et al, 1998). While these thiosulfate species are usually metastable, heterotrophic such species can be oxidised by bacteria such as *Thermos scotoductus*, converting the thiosulfates into sulfate (Skirnisdottir et al, 2001).

Changes in light affect temperature and changes in temperature affect the kinetics of these processes. The similarity in patterns between Sb and As concentrations above Bridal Veil Falls (Figures 4.7 and 4.10 respectively) suggests that the processes affecting As are similar to those for Sb.

In winter, the lower temperatures and pH mean that $H_2S_{(aq)}$ is favoured over $HS^-_{(aq)}$. This inhibits the conversion of HS^- into SO_4^{2-} and therefore the dissolution of Sb_2S_3, already suppressed because of the system's lower pH, is further retarded. The proportional changes in temperature are greater in winter, and this may mean the shift in Sb_2S_3 equilibria is more dramatic once the bacterially catalysed changes in H_2S-HS^--SO_4 equilibria begin.

If shifts in sulfide-sulfate equilibria are the driver for the observed diurnal patterns, the likely reason that Sb concentration maxima are similar in both winter and summer is that the processes outlined previously cause an "on-off" effect, rather than reflecting a true diurnal process where Sb concentrations are directly related to daytime fluctuations in light and temperature. Pope et al (2004) showed that, at night, DO concentrations in the discharge from Champagne Pool were below detection limit (< 0.1 mg/kg), and this coincides with minima in Sb concentrations. The DO in the discharge from Champagne Pool must therefore be mainly produced by photosynthetic bacteria. However, the conversion of HS^- to SO_4^{-2}, which requires oxygen to proceed, is also bacterially catalysed, and it may be that the bacteria responsible for HS^- oxidation do not activate until a certain temperature (or light level) is reached. Once these bacteria become active, there should be a significant shift in Sb_2S_3 solubility equilibrium, which may take time to re-equilibrate, and further changes in conditions may only cause minor fluctuations until the sun sets, the system becomes anoxic and the conditions begin to favour Sb_2S_3 (and As_2S_3) precipitation again.

The enrichment of Sb in the margins of a sulfide deposit in the Juan De Fuca Ridge in the Pacific Ocean, described by Houghton et al (2004), may be an abiotic analogue of this process. Within the ridge, Sb_2S_3, along with certain other metal-sulfides (Pb, Cd and Ag), contained within the centre of hydrothermal sulfide mounds are thought to be remobilised following seawater infiltration, which shifts the redox conditions from reducing (H_2S-rich fluids) to oxidising (SO_4-rich fluids). The remobilised elements are subsequently reprecipitated on the outside of the mounds as cooling temperatures affect the various mineral-solubilities. At Wai-O-Tapu, photosynthetic bacteria may be affecting the system in a similar way to the seawater in the Juan De Fuca Ridge.

Such an explanation can also explain why similar Sb concentration maxima occur in disparate ambient chemical conditions. The "on-off" process would result in approximately the same amount of Sb being dissolved on any day that the phenomenon occurred. The only variable between days would be the time it took for the system to re-equilibrate, which would depend on light and temperature (generally occurring faster in summer than in winter).

The current data set is insufficient to test this theory, and therefore this hypothesis remains untested. Ideally, the discharge from Champagne Pool would need to be sampled intensively, perhaps at just a single site, in order to study the transition from an anoxic to an oxygen-rich system. The presence or absence of thio-Sb species could also be investigated, as could the implications of Sb speciation changes downstream from Champagne Pool, as both may play a role in the observed diurnal changes.

The robustness of the proposed explanation may also be enhanced if more was known about the Champagne Pool discharge's bacterial community and the community's sulfur-oxidising bacteria in particular. Hetzer et al (2007) have recently described three novel bacterial species within Champagne Pool itself, but the downstream ecology is not well documented. Further research avenues will be discussed in more depth in Chapter Six.

4.3.6 THE FATE OF Sb PRODUCED FROM CHAMPAGNE POOL

In Alum Lake, dissolved Sb concentrations were below detection limit (< 0.2 μg/kg), which suggests that, given Sb concentrations were above detection limit in the incoming stream, Alum Lake may be acting as a sink for Sb. Determining whether Alum Lake is in fact a sink for Sb can be normally undertaken by examining the ratio of Sb to a conservative ion such as Li. However, the pond has additional subsurface inputs, and therefore the amount of Li in the outflow (WT 8) is lower than that in the inflow (WT 7), as shown in Table 4.3.

If an assumption is made that the sub-surface inputs are similar in nature to the acid-sulfate discharge from Lake Whangioterangi and that the relative contributions to Alum Lake are 30 % surface inflow and 70 % sub-surface inflows, 100 % of the Li and SO_4^{2-} can be accounted for, as can 80 % of the Cl. From this assumption, the calculated Sb:Li ratios suggest that dissolved Sb concentrations should range between 1 and 4 μg/kg, depending on the time of day, if Sb was not being removed from solution (The Sb:Li ratios in the inflow were 0.003 ± 0.001, the outgoing should have been 0.0004 - 0.0018). Given that dissolved Sb concentrations were < 0.2 μg/kg (Sb:Li < 0.0001), it appears that Alum Lake is indeed acting as a sink for the metalloid.

The As:Li ratio is 0.5 in the inflow, but in the discharge from Alum Lake the ratio varies from 0.097 to 0.340 mid-afternoon. Using the assumed mix of surface and sub-surface inputs, the As:Li ratio should be ~0.27, suggesting that Alum Lake is acting as a sink for As at certain times (such as in the morning of the summer sampling), but as a source at other times (such as mid-afternoon during the summer sampling).

Such a conclusion assumes that the subsurface flows contain similar concentrations of As to those measured in the Lake Whangioterangi discharge. If the subsurface flows contain elevated concentrations of As relative to those measured in the Whangioterangi discharge, the ratio calculations for the metalloid are invalid and that Alum Lake is a sink, rather than a source of As no matter what the time of day.

Given the acidic and reducing nature of Alum Lake (pH 2.45, DO < 0.5 mg/kg and H_2S > 2 mg/kg as shown in Table 4.3) stibnite precipitation might be expected. Thermodynamic modelling of the Alum Lake system using the MINTEQ database and PHREEQCi predicted that these conditions do favour Sb_2S_3 precipitation and therefore it is possible that the Sb remobilised within the Artist's Palette area reprecipitates in Alum Lake, rather than being transported out of the system.

As well as the precipitation processes, adsorption onto sediments in Alum Lake may also remove Sb from solution. As discussed in Chapter Five, Sb^V adsorbs on to SPM derived from the Waikato River at low (< 4) pH. Therefore, Alum Lake, at pH ~2.4, would provide suitable conditions for Sb^V adsorption, and the limited flow out of the lake means that there is enough time for much of the SPM to settle and deposit, rather than be carried through the lake system. Such mechanisms cannot be properly tested without the analysis of bottom sediments, which could not be collected during the study (because of restrictions under the sampling permit), but may warrant further investigation.

In conclusion, Sb and As exhibit similar behaviour in the discharge from Champagne Pool, despite concentrations of As being several orders of magnitude higher than those of Sb. Both metalloids can be remobilised during daylight hours from the precipitates that form within Champagne Pool, a process that is influenced by the activity of photosynthetic bacteria, which increase dissolved oxygen concentrations, and in turn cause changes in sulfide-sulfate equilibrium. However, the acidic and reducing nature of Alum Lake means that little of the Sb remobilised downstream of Champagne Pool is transported out of the Wai-O-Tapu system and into the receiving environment.

4.4 THE BEHAVIOUR OF Sb AT WAIMANGU

The lack of diurnal variation in the discharge from Waimangu (which will be presented and discussed later in this section) meant that the study approach used at Wai-O-Tapu had to be altered somewhat. The focus changed from attempting to understand the processes occurring immediately downstream of the central feature (Frying Pan Lake) to investigating what happens to Sb as the element is transported along the drainage from a natural geothermal system into a receiving environment (Lake Rotomahana).

4.4.1 FIELD CONDITIONS AT WAIMANGU

A summary table of data collected from Waimangu is presented as Table 4.6. Light measurements were only recorded during the January sampling. Similar to Wai-O-Tapu, the weather produced clear skies and bright sunshine (> 120 kLux at its peak). In February the weather was similar, but in winter conditions were overcast.

Water temperatures differed from Wai-O-Tapu in that the discharge from Frying Pan Lake remains warm at least until its dilution with Haumi Stream (up to 50 ^{o}C in summer, 44 ^{o}C in winter). Downstream of the confluence with Haumi Stream, temperatures are about 10 ^{o}C cooler than upstream, but still warmer than Lake Rotomahana (which was 22 ^{o}C in summer and 14 ^{o}C in winter).

At Waimangu there were only minor differences in other physico-chemical parameters between January (mid summer), February (late summer) and August (late winter) sampling events. Summer samples contained slightly less oxygen, most likely because of reduced capacity for O_2 uptake with the higher temperatures (Stumm and Morgan, 1996), while conductivities were 20-30 % lower in the August samples. Concentrations of H_2S were below detection limit for all samples collected from Waimangu (< 0.050 mg/L).

4.4.2 METALLOID DISTRIBUTION DOWNSTREAM OF FRYING PAN LAKE

In the first 500 m downstream of Frying Pan Lake, Sb concentrations were relatively stable during the all-day January sampling, as shown in Figure 4.15a. Reduced (Sb^{III}) species made up about 10 % of dissolved Sb at all sites, at most times. Arsenic concentrations (Figure 4.15b) were somewhat more variable during the course of the day, except perhaps at WM 1. However, there was no evidence for any systematic (or at least diurnal) variation at WM 1. Pareheru Stream, which joins Hot Water Stream between sites WM 2 and WM 3, appears to dilute the concentrations of both metalloids, which were highest at WM 2.

Table 4.6 Summary table of selected analytical results from sampling at Waimangu. Results for January are presented as medians with standard deviations (n = 5), "n/m" means not measured. The full data set is presented in Appendix II

Site	Light (kLux)	Temp (°C)	DO (mg/L)	pH	Cond (mS/cm)	Li (mg/kg)	SO_4 (mg/kg)	Cl (mg/kg)	As_{diss} (mg/kg)	Sb_{diss} (µg/kg)	Sb^{III} (µg/kg)
January											
WM 1	102 ± 39	47.0 ± 1.3	4.76 ± 0.33	5.99 ± 0.05	4.09 ± 0.02	3.31 ± 0.21	233 ± 7	675 ± 3	694 ±49	13.1 ± 0.8	1.5 ± 0.1
WM 2	123 ± 36	44.8 ± 5.4	5.32 ± 0.59	6.17 ± 0.06	4.08 ± 0.03	3.41 ± 0.23	241 ± 8	674 ± 8	697 ± 73	15.4 ± 0.6	1.5 ± 0.1
WM 3	8.61 ± 52.8	47.5 ± 1.8	5.29 ± 0.39	6.56 ± 0.11	3.99 ± 0.05	3.26 ± 0.22	228 ± 12	650 ± 13	641 ± 30	13.1 ± 0.3	1.2 ± 0.3
WM 4	11.4 ± 47.8	47.5 ± 0.7	5.22 ± 0.33	6.61 ± 1.58	3.93 ± 0.46	3.40 ± 0.67	228 ± 33	630 ± 52	683 ± 111	14.1 ± 1.8	1.2 ± 0.4
WM 5	117 ± 47.3	48.3 ± 1.1	5.64 ± 0.41	6.77 ± 0.31	4.00 ± 0.10	3.35 ± 0.31	229 ± 9	653 ± 27	619 ± 64	14.9 ± 0.6	1.3 ± 0.1
February											
WM-5	n/m	52.6	7.10	6.47	4.14	3570	218	623	648	16.0	n/m
WM-6	n/m	46.7	4.01	7.70	3.73	3450	221	615	560	15.9	n/m
WM-7	n/m	34.8	5.34	7.80	1.81	2020	150	301	331	8.8	n/m
WM-8	n/m	36.9	5.16	7.54	1.92	1900	159	345	376	9.9	n/m
WM-9	n/m	21.9	5.94	7.06	1.30	1700	131	266	232	2.7	n/m
WB	n/m	21.0	6.07	6.53	0.57	343	139	64.5	67.3	3.5	n/m
August											
WM-1	n/m	44.0	10.2	6.00	3.52	2750	262	721	761	21.5	n/m
WM-3	n/m	43.2	9.49	6.69	3.26	2530	241	657	691	19.9	n/m
WM-5	n/m	43.9	7.20	6.92	3.27	2250	236	657	677	19.1	n/m
WM-6	n/m	40.6	7.46	7.89	3.11	2420	233	637	680	18.8	n/m
WM-7	n/m	28.0	8.57	7.67	1.21	1480	138	263	294	9.3	n/m
WM-8	n/m	29.4	7.90	7.69	1.28	1410	135	270	310	10.6	n/m
WM-9	n/m	13.6	7.78	7.07	1.06	1600	123	281	211	4.4	n/m
WB	n/m	18.6	9.46	6.94	0.49	232	145	49.8	63.2	3.8	n/m

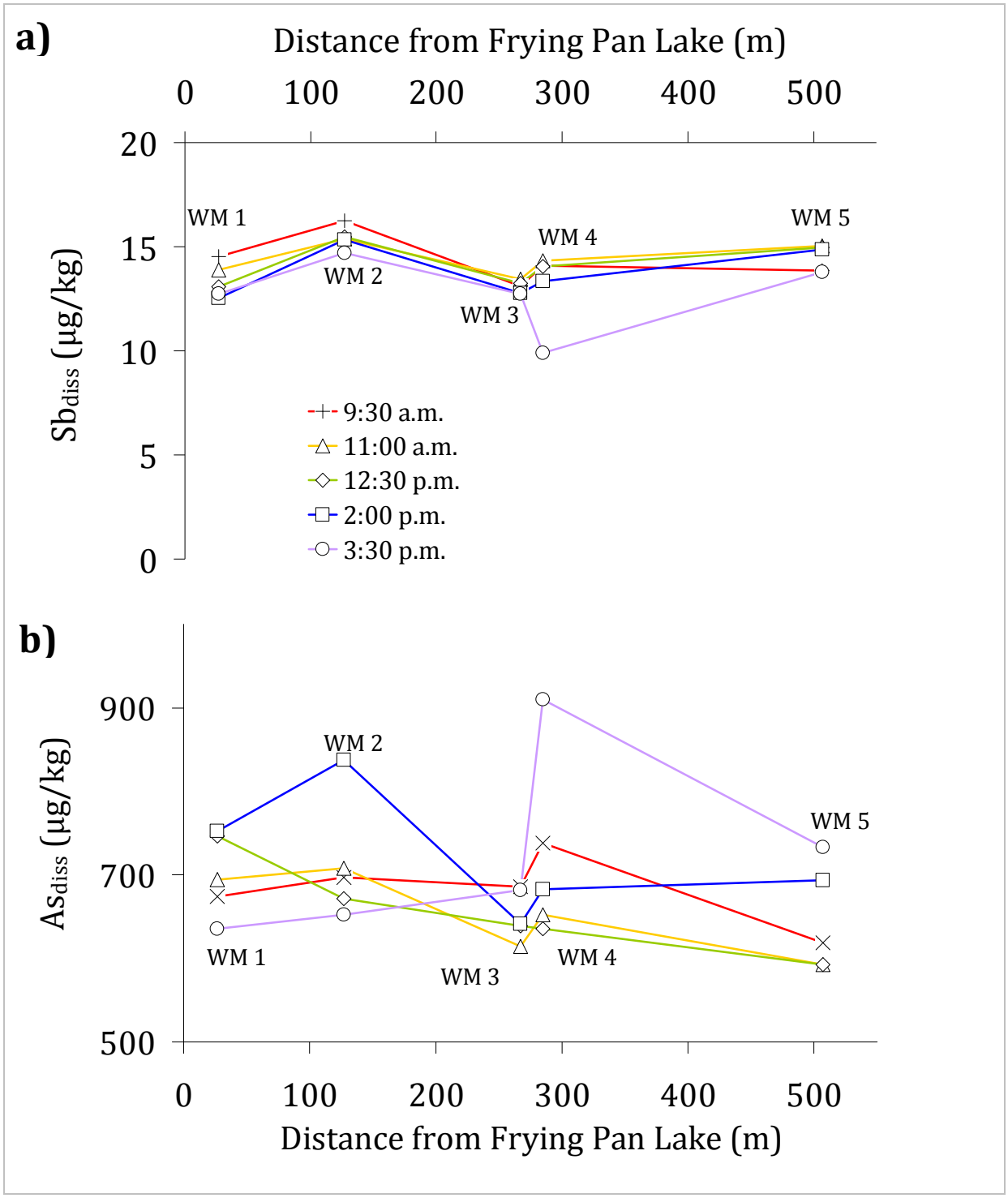

Figure 4.15 Concentrations of a) Sb and b) As in the first 500 m downstream of Frying Pan Lake over time in January 2007

The only significant change throughout the day was a sudden decrease in dissolved Sb in the late afternoon at site WM 4. This reduction in Sb concentration coincided with an increase in As concentration and a sudden decrease in pH (from 6.5 to 3.1). Using back-calculations based on this collected data, and on data for pH, Li, Cl and SO_4 from Simmons et al (1994), these changes can be attributed to a temporary increase in flow from Inferno Crater. The dissolved Sb^{III} minima for sites WM 3-5 (Table 4.5) are likely to be because there was proportionately lower dissolved Sb^{III} in the Inferno Crater than there is dissolved Sb^{III} in the Frying Pan lake discharge. The low values for total dissolved Sb and Sb^{III} upstream at site WM 3 may have been caused by the increased flow from Inferno Crater being forced slightly upstream where the two water bodies converge.

Figure 4.16 presents Sb concentration data for the entire drainage system, and shows that the confluence with Haumi Stream (between sites WM 6 and WM 7) causes further dilution of dissolved Sb concentrations. Concentrations of Sb and As were lower in Lake Rotomahana than in Hot Water Stream, and concentrations of both metalloids were also lower in the discharge from Warbrick Terrace (WB).

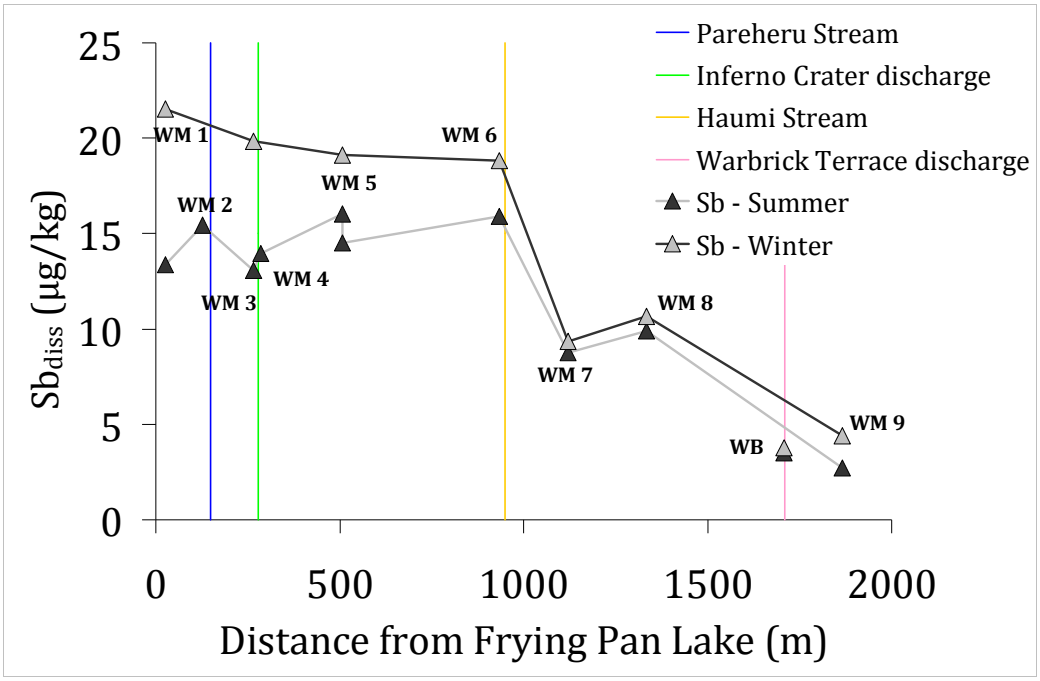

Figure 4.16 Dissolved antimony concentrations in the discharge from Frying Pan Lake through to Rotomahana, January data has been averaged (n=5) and included with the February data for summer

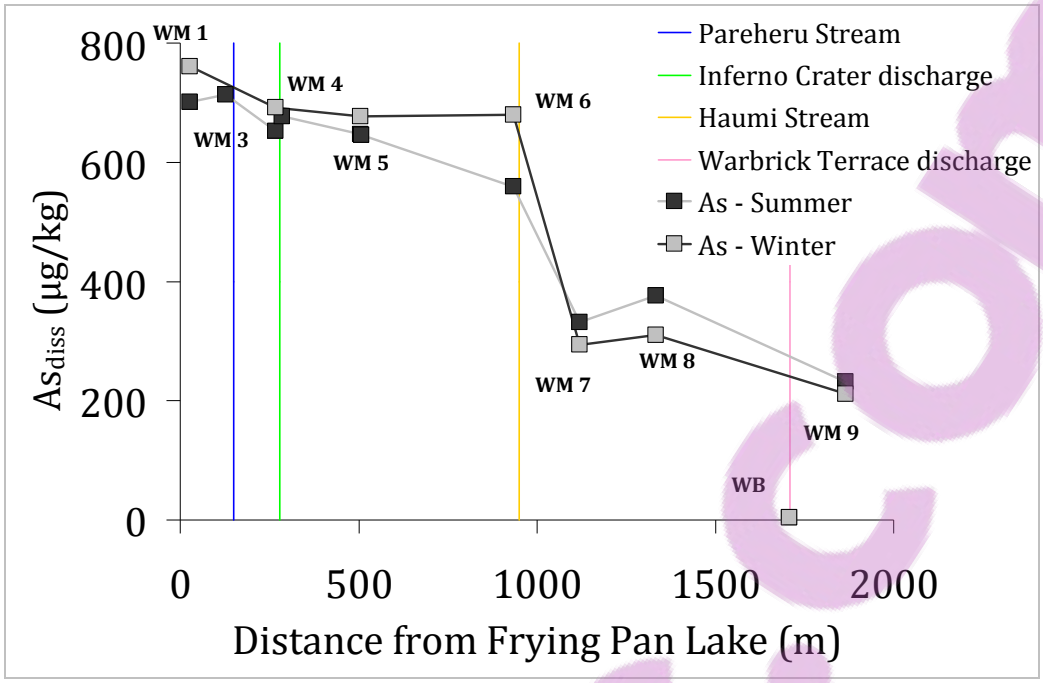

Figure 4.17 Arsenic concentrations in Hot Water Stream through to Rotomahana, January data has been averaged (n=5), and included with the February data for summer

Most of the Sb present in solution was dissolved at all sites, and any portioning between dissolved and particulate Sb appeared to occur independently of pH, as shown in Figure 4.17. Similarly, the As in solution was predominantly in the dissolved phase (Figure 4.17).

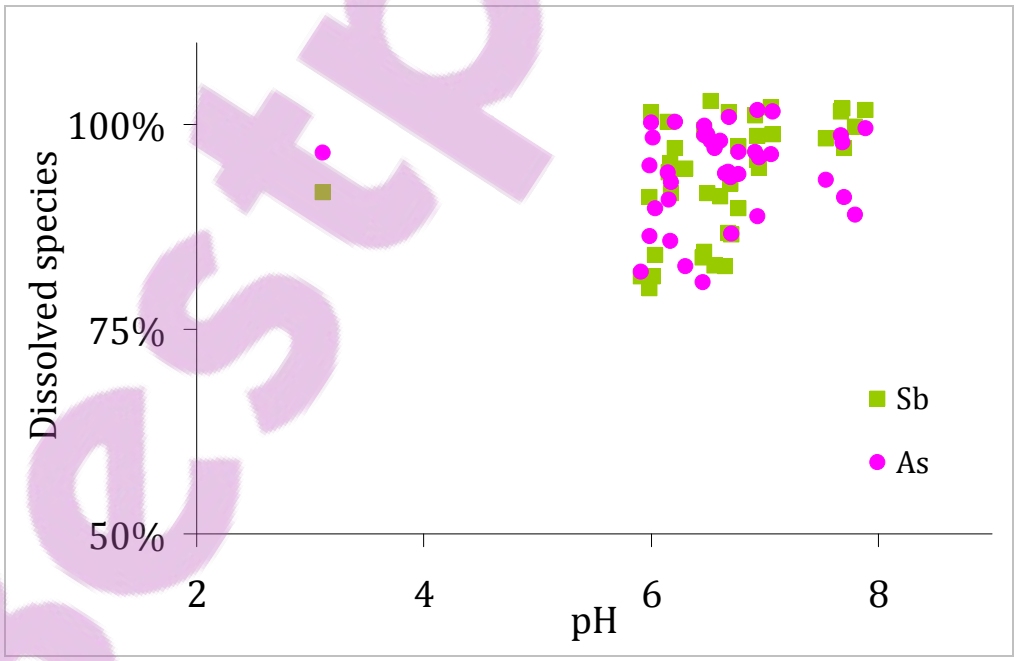

Figure 4.18 Proportion of dissolved Sb and As, relative to pH in Hot Water Stream

4.4.3 AQUEOUS RELATIONSHIPS AT WAIMANGU

In the first 500 m downstream of Frying Pan Lake, As concentrations increased when Sb concentrations decreased, and vice versa, as shown in Figure 4.19. This is best illustrated by the differences in the site immediately below Inferno Crater (WM 4) at 3 p.m. following the sudden input from the crater spring. The most likely explanation is the concentrations of Sb and As differ in the different fluid sources.

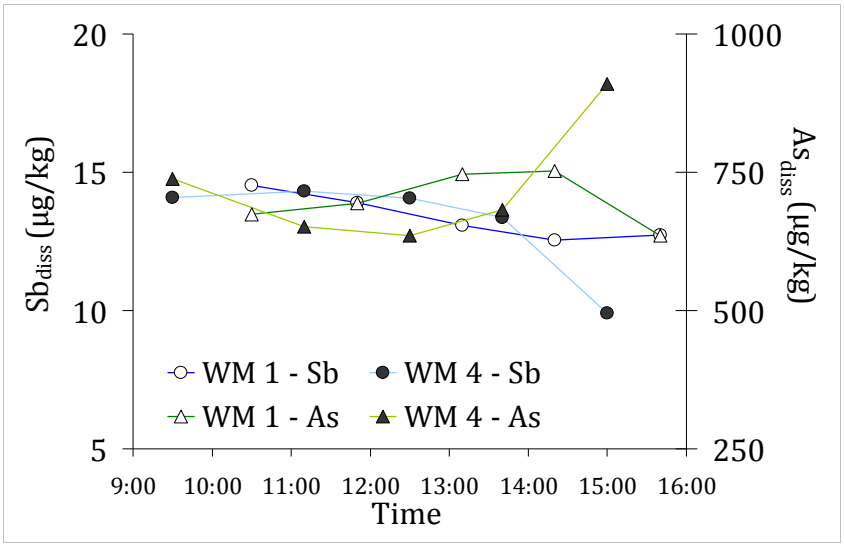

Figure 4.19 Changes in dissolved Sb and As concentrations with time in the first 500 m downstream of Frying Pan Lake (sites WM 1 and WM 4)

While the concentrations of Sb and As may vary in the source fluids of Frying Pan Lake and Inferno Crater, downstream there appears to be a strong positive correlation between the two, as shown in Figure 4.20a. It is likely therefore, that any metalloid removal processes operating in Hot Water Stream affect both elements.

The correlation between Sb and Li was not strong (Figure 4.20a). Lithium is conservative, so the weaker correlation could have suggested that Sb is being preferentially removed from solution, either close to the source or as it is transported downstream. However, this is unlikely given the strong correlation between Sb and Cl (Figure 4.20b), which is also a conservative ion.

A more plausible explanation is that there are additional inputs of geothermal fluids containing elevated Li concentrations, but not Sb (or As). Despite this, ratios of Sb:Li were relatively stable with distance (< 10 % variation), as shown in Figure 4.20c, until Lake Rotomahana. In Lake Rotomahana, ratios were only 30 % of those ratios calculated upstream, regardless of season.

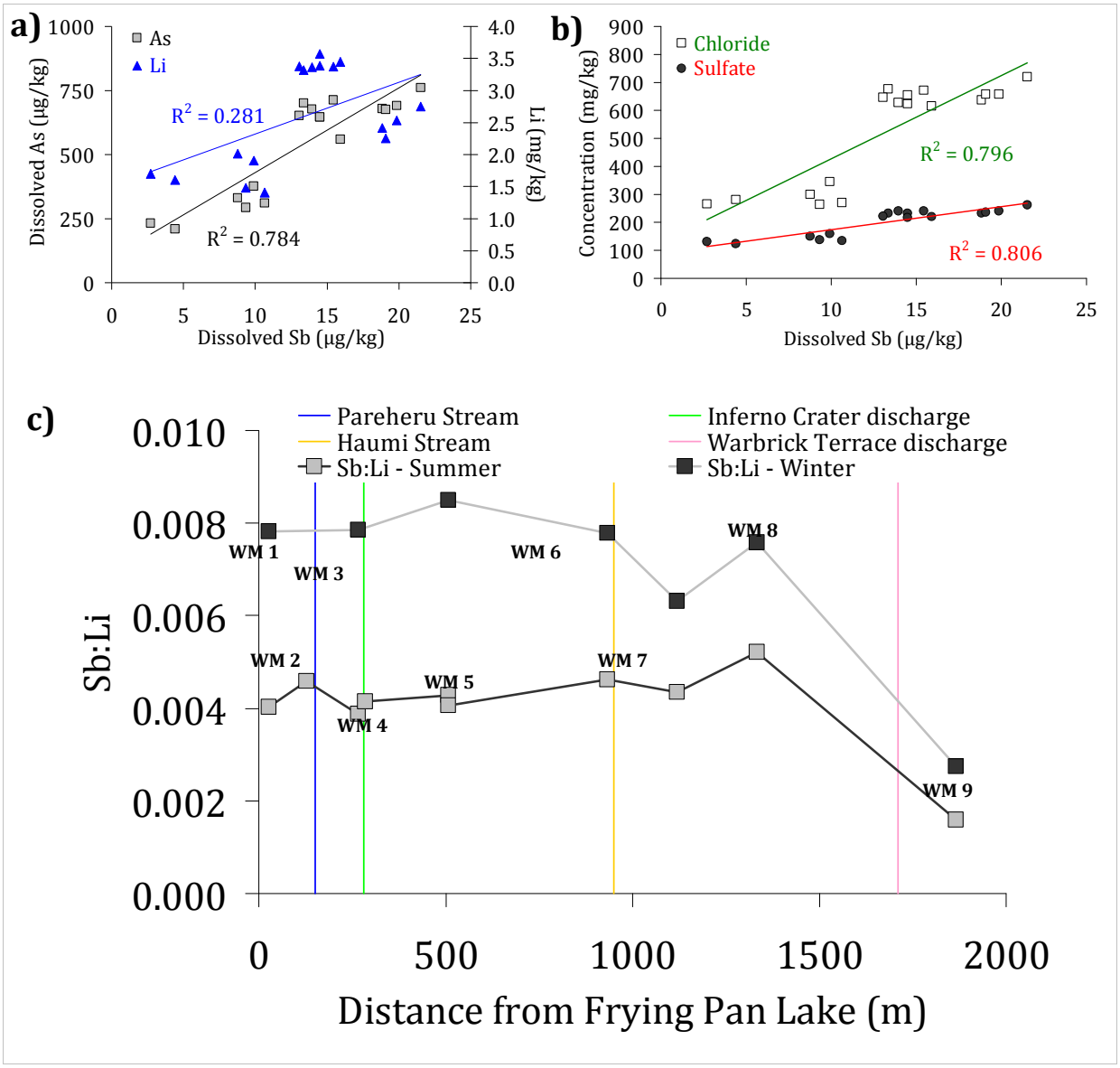

Figure 4.20 The relationship between Sb concentrations and a) As concentrations and b) Li concentrations at Waimangu. Figure 4.18c shows Sb:Li ratios with distance. Data from the all day sampling in January has been averaged (n=5, except for site WM 4, where n=4). The data affected by the increased Inferno Crater flow (at WM 4) have been omitted, as have data from the Warbrick Terrace discharge (WB).

According to the data presented in Figure 4.20b, Sb correlates well with Cl and SO_4, suggesting all three elements are derived from the same fluids. That Sb concentrations correlate relatively well with Cl suggests any Sb removal processes occurring in the drainage must be relatively minor, at least until the fluids reach Lake Rotomahana. Because Sb and As concentrations in the drainage also correlate well, it appears As is not removed either. Sediment and algal analyses were undertaken to confirm this.

4.4.4 SUSPENDED SEDIMENTS AND ALGAE

SEDIMENT

During summer, SPM concentrations were very low in the drainage and insufficient sample could be collected to study metalloid concentrations in the SPM. However, metalloid concentrations from the winter SPM samples are presented in Figure 4.21a. The concentrations of both Sb and As in the SPM fluctuated over the distance between Frying Pan Lake and Lake Rotomahana, but no obvious trend or pattern was evident for either. However, this type of data analysis does not take into account the dilutive effects of Paraheru and Haumi Streams (or any minor geothermal inputs).

Distribution coefficients (k_d) are useful for mitigating the effects of independent changes in SPM and dissolved element concentrations, and have been calculated as:

$$k_d = \frac{[M_{SPM}]}{[M_d]}$$

where $[M_{SPM}]$ is the concentration of a given element in the SPM and $[M_d]$ is the dissolved concentration of the element. Presented in Figure 4.21b, k_d values for As and Sb suggest that the degree of adsorption to SPM of both Sb and As may be greater downstream of the Haumi Stream confluence (i.e. at sites WM 7 and WM 8).

ALGAE

The algae collected from in the first 500 m of Hot Water Stream were predominantly *Phormidium sp.,* identified from the description of Jones et al (2005). The results of the analysis of the algae suggest that uptake is a significant process for As, but not for Sb, as is shown in Figure 4.20c. The concentrations of As range from 500 mg/kg to over 2000 mg/kg dry weight, well above concentrations found in SPM, and suggest the algae are accumulating As. The algal concentrations of Sb were much lower, ranging from 12 mg/kg to 30 mg/kg dry weight. Such concentrations are similar in magnitude to that found in the SPM, and trapped SPM particles within the algae may be the source of the Sb measured.

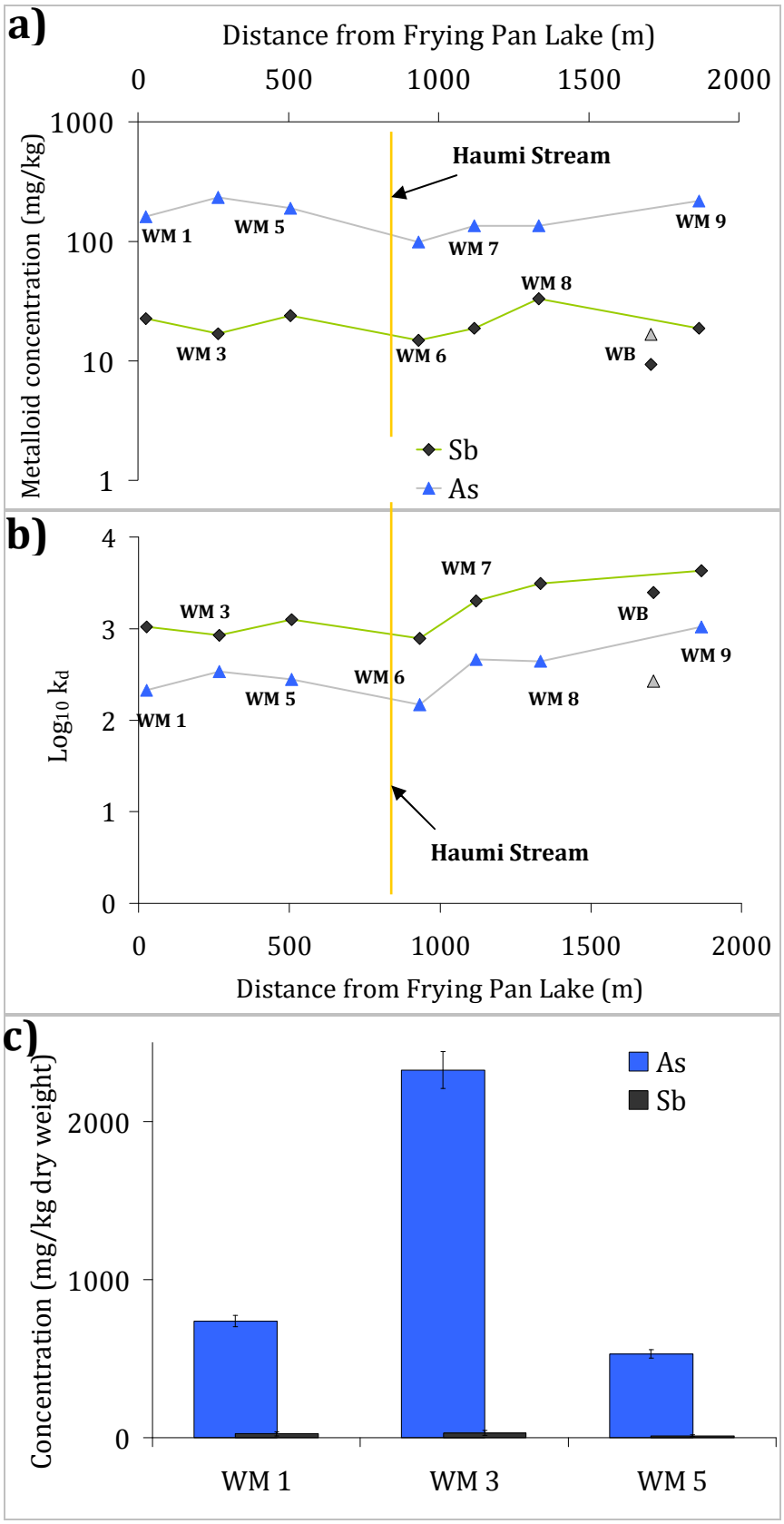

Figure 4.21 Arsenic and Sb concentrations in a) SPM b) $\log_{10}$ distribution coefficients (k_d), and c) algae. In 4.20a and 4.20b, data for the Warbrick Terrace discharge (WB) are left separate because they come from a tributary, rather than from Hot Water Stream.

4.4.5 THE FATE OF Sb PRODUCED FROM FRYING PAN LAKE

The explanation offered to explain the role of sulfide-sulfate equilibria in daytime variations of Sb and As concentrations at Wai-O-Tapu may also explain why similar diurnal phenomena were not observed at Waimangu. The waters produced from Frying Pan Lake are chemically stable and consistently warm, and therefore there are no chemical changes occurring that might change the sulfide-sulfate equilibrium, and H_2S concentrations are universally low. At Waimangu, physical processes, such as changes in geothermal flow inputs, appear to be a more important control on dissolved metalloid concentrations. Within Hot Water Stream, Sb behaviour is therefore essentially conservative, apart from perhaps some minor adsorption onto SPM below the Haumi Stream confluence. However, As may be removed when the algae in the upper reaches of the stream take up As. The evidence suggests the algae do not take up Sb. Although As is removed by algae, this must be only a small proportion of the As available in solution because As:Li and Sb:As ratios do not change significantly downstream.

The lower Sb:Li ratios in Lake Rotomahana suggest the lake serves as a sink for the metalloid. However, because the 902 Ha lake has numerous other geothermal inputs apart from the discharge from Frying Pan Lake, and no surface outflows, it was not possible to determine the eventual fate of Sb from Waimangu in the Rotomahana system. If Lake Rotomahana is acting as a sink for Sb, the processes removing dissolved Sb would differ somewhat from that observed at Alum Lake. Whereas Alum Lake is a reducing, acidic environment, inducing both Sb_2S_3 precipitation and adsorption of Sb onto sediment, Lake Rotomahana is oxidising and neutral (pH 7), which suggests precipitation of Sb as Sb_2S_3 will not occur. However, Sb adsorption is still possible. The loss of CO_2 from Frying Pan Lake and the resultant increase in pH means that Fe-oxyhydroxides are precipitated downstream of this feature (Scott, 1994; Seward and Sheppard, 1986). It is reasonable to speculate that other geothermal inputs to the neutral Lake Rotomahana may also produce Fe-hydroxides as well. Haumi Stream is also a source of Fe- and Mn-hydroxides, as is evident in the increased Fe and Mn concentrations in SPM collected below confluence of Haumi Stream with the Hot Water Stream, as shown in Table 4.6.

Fresh iron-hydroxides will readily adsorb Sb even at neutral pH (Tighe et al, 2005b), and therefore the minor adsorption processes witnessed along the lower reaches of Hot Water Stream may become major processes within the Lake. Further investigation of the fate of Sb and As in Lake Rotomahana is warranted, but would need to include quantification of other geothermal inputs, as well as analysis of lake-bottom sediment.

Table 4.7 Antimony, Fe and Mn concentrations in SPM collected from the Waimangu system in August, 2008.

Site	Sb (mg/kg)	Fe (wt %)	Mn (wt %)
WM 1	22.6	1.43%	<0.10%
WM 3	16.8	1.85%	<0.10%
WM 5	23.9	1.88%	<0.10%
WM 6	14.8	1.66%	<0.10%
WM 7	18.8	4.66%	0.10%
WM 8	33.3	4.92%	0.13%
WM 9	18.8	3.41%	0.47%
WB	9.3	1.79%	<0.10%

4.5 CONCLUSIONS

The diurnal variations observed in Sb concentrations downstream of Champagne Pool were attributed to changes in sulfide-sulfate equilibrium, which is in turn controlled by photosynthetic processes. Such conditions do not exist at Waimangu, and therefore similar diurnal variations are not observed there. Although the Sb concentration changes observed at Champagne Pool are significant, downstream afternoon increases in Sb concentrations are mitigated during passage through the acidic, reducing Alum Lake, which acts as a sink for the metalloid. At Waimangu, no such sink exists, and the antimony discharged from Frying Pan Lake eventually makes its way to Lake Rotomahana, ~2 km downstream. In Lake Rotomahana, the presence of oxygen, the absence of H_2S, and the neutral pH waters, means the only potential removal mechanism for geothermally-derived Sb appears to be adsorption onto sediments. How much Sb is removed by this mechanism is still unclear.

Overall, the processes that affected dissolved Sb also affected dissolved As. However, the reverse was not true, as there was evidence for As accumulation by *Phormidium sp.*, the stromatolite-forming algae at Waimangu, which was not similarly evident for Sb.

Although the diurnal variations observed at the Wai-O-Tapu geothermal system were not found to have any significant effect on Sb concentrations in the downstream receiving environment, these diurnal variations remain intriguing. Sustained (12 or 24 hour) sampling of sites downstream of natural geothermal features has rarely been undertaken. Given the small data-set, it is not yet clear whether such variability is the norm or the exception. Furthermore, although diurnal variability in individual spring chemistry may not cause any noticeable changes in downstream chemistry, if the overall contributions of geothermal systems to their receiving environments can vary depending on the time of day, the implications for the management of such resources are significant.

CHAPTER FIVE
THE BEHAVIOUR OF GEOTHERMAL ANTIMONY IN RECEIVING ENVIRONMENTS

This chapter focuses on how Sb behaves in oxygen-rich freshwater environments, larger bodies of water that are chemically more stable (Giller and Malmqvist, 1998) than those examined in the previous two chapters. While they are the least dynamic of the systems investigated in this thesis, the processes that control Sb removal in Waiotapu Stream and the Waikato River are probably the most important from an environmental management perspective. In geothermal systems, it is likely that any species living in the environment will have adapted to living with elevated Sb concentrations. In receiving environments, the likelihood is significantly reduced.

5.1 BACKGROUND AND STUDY OBJECTIVES

When this research was originally conceived, it was envisaged that Sb behaviour in the Waikato River could be compared with how Sb behaves in the Waitangi River, a Northland river that may receive inputs from the Ngawha geothermal area. However, Sb concentrations were below detection limit (< 0.2 μg/kg) at all sites investigated in the Waitangi catchment (including surface waters in the Ngawha geothermal field itself). The choice was made to focus on the Waikato River and Waiotapu Stream instead.

The Waikato River (Figure 5.1) is the longest river in New Zealand, and more than 300 000 people live within its catchment (Bilinska, 2005; McLaren and Kim, 1995). The river originates from Lake Taupo, which lies in the southern half of the Taupo Volcanic Zone, and the upper reaches of the river receive a number of geothermal inputs. Lake Taupo itself is the product of a series of rhyolitic eruptions, and pumice characterises the geology of the upper reaches of the Waikato River (Reid, 1983). Downstream from Ohakuri, tephra deposits become more common, and from about Arapuni north unconsolidated sediments dominate (McDowall, 1996).

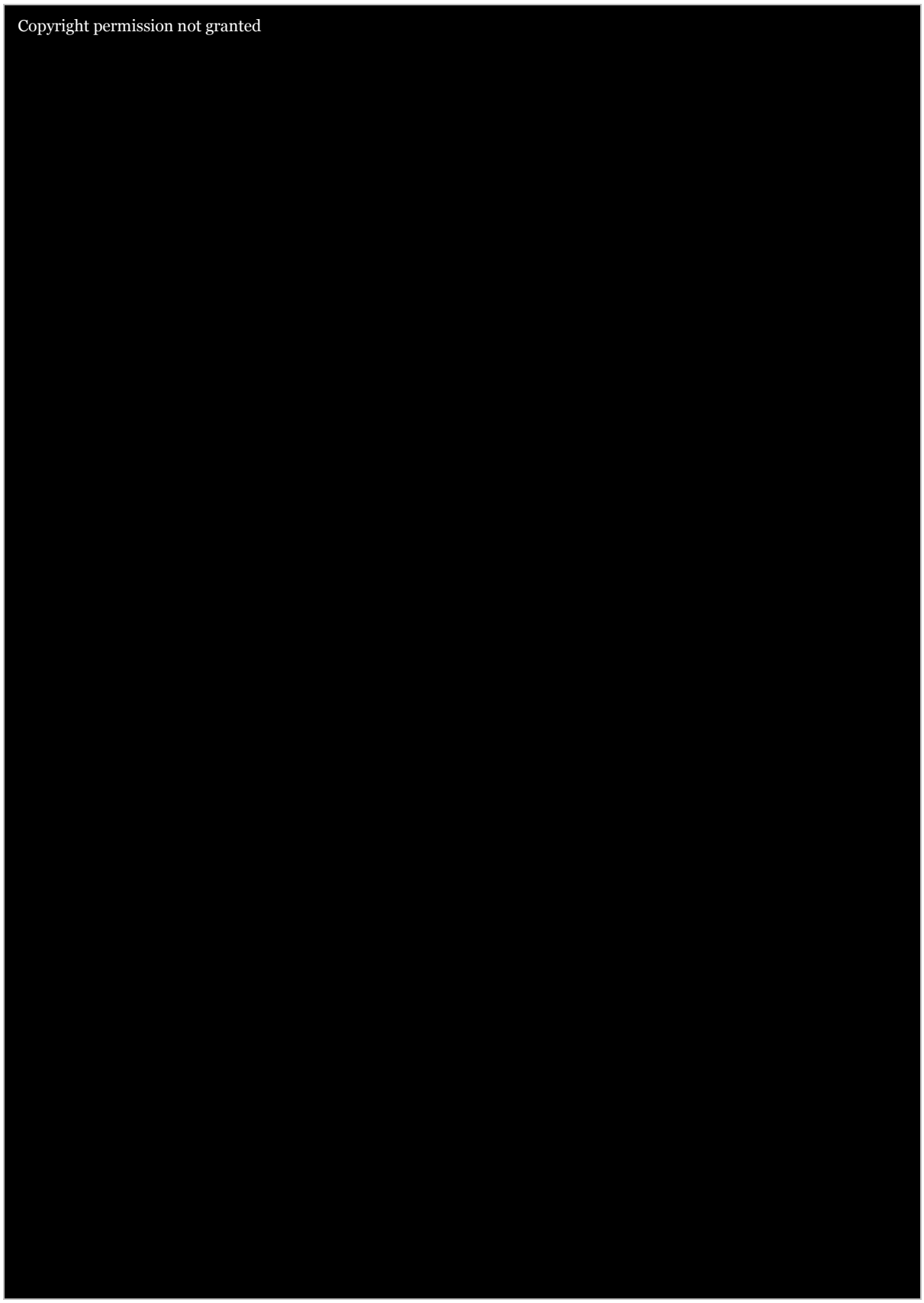

Figure 5.1 Map of the upper-middle North Island, highlighting the Waikato River, and the major settlements within the region (adapted from Mighty River Power, 2001).

Lake Taupo is oligotrophic (containing low nutrient levels), but the Waikato River has been heavily modified and has a wide range of anthropogenic impacts (Chapman, 1996). More than a dozen sewage treatment plants discharge into the river, along with a number of major industrial discharges, and intensive dairying is extensive along the entire length (Bilinska, 2005). Eight major hydroelectric dams, marked on Figure 5.1, have been built along the Waikato River, creating a series of lakes, and a thermal power station is built on the banks of the river at Huntly. The river is also a source of drinking water for more than 30 communities, including Hamilton, a city in excess of 120 000 people (McLaren and Kim, 1995).

Two geothermal power stations also lie on the Waikato River (Wairakei and Ohāki), and the Wairakei power station discharges geothermal waste fluids directly into the river (McLaren and Kim, 1995). The geothermal inputs into the Waikato River, both natural and anthropogenic, contain elevated concentrations of elements such as B, Li and As, and some of the geothermal inputs contain elevated Sb concentrations as well. The most significant input of geothermal fluid into the Waikato River is the discharge from the Wairakei Power Station, which historically contributed about 45 % of the river's Cl, Li, As and B (Timperley and Huser, 1996). Under current consent conditions, Contact Energy, the power station owners, discharge 60 000 tonnes/day untreated waste fluids into the Waikato, contributing 30 % of the dissolved As found downstream (Contact Energy, 2007; Webster and Nordstrom, 2003).

The presence of geothermal contaminants in the Waikato River, particularly As, has encouraged multidisciplinary research on aspects such as the uptake of As by both plants (Robinson et al, 2003) and fish (Robinson et al, 1995b), dissolved As behaviour in stratified lakes (Aggett and Kriegman, 1988), and the overall fate of aqueous As in the Waikato River system (Webster-Brown et al, 2000). Of particular interest is the seasonal variation in dissolved As concentrations, which are typically lower in winter than in summer, even when factors such as dilution have been taken into account (McLaren and Kim, 1995). Various explanations have been offered for the seasonal changes, the most compelling is that winter As concentration minima are caused by the dilution of geothermal fluids during the wetter winter months, in combination with increased adsorption of As onto Fe-oxide-rich SPM, which is more prevalent in winter (Webster-Brown and Lane, 2005a).

In comparison, there is a dearth of information for Sb in the Waikato River. Only one set of published data regarding Sb concentrations in the Waikato River could be found in the scientific literature: McLaren and Kim (1995), who reported that Sb concentrations were less than 2 μg/kg at the Hamilton City water intake, but there is also a limited amount of Sb concentration data in Pope's (2004) doctoral thesis for several sites either side of the confluence of Waiotapu Stream, a geothermally fed tributary. In a recent survey, Environment Waikato presented Sb concentration data for 4 sites along the river, but there was no commentary on the results, presumably because the Sb concentrations were low (compared to elements such as As) (Smith, 2006). There is no publicly available data for Sb concentrations in the Wairakei Power Station discharge, but a single sample from the discharge, collected by the author, suggested that Sb concentrations could be as high as 40 μg/kg. This thesis is sponsored in part by Mighty River Power (a direct competitor of Contact Energy) so, in the interests of commercial sensitivity, no additional samples were collected.

The next most significant surface input of geothermal fluids into the Waikato River is Waiotapu Stream, which is formed from the confluence of the geothermally fed Hakereteke (Kerosene) Creek, and the meteoric Waikokomuka Stream. As shown in Figure 5.2, Waiotapu Stream flows to the southwest, passing through the Wai-O-Tapu geothermal area (Timperley and Huser, 1996). Pope (2004), in the only previous study to have investigated Sb distribution in this stream, presented data showing that Sb concentrations in the stream range from less than 0.6 μg/kg above the Wai-O-Tapu geothermal area, to more than 20 μg/kg downstream following inputs from the western side of the field. Pope (2004) also measured Sb concentrations in the Waikato River either side of the confluence with Waiotapu Stream, but reported no difference in the concentration of Sb (1.29 μg/kg) between upstream and downstream, although this might be because the sampling sites were too close to the stream itself and therefore not in well-mixed zones. Given that the stream contains measurable (>0.2 μg/kg) Sb concentrations, and that it links the Wai-O-Tapu geothermal field with the Waikato River, Waiotapu Stream should present a transitional link between natural and receiving geothermal environments.

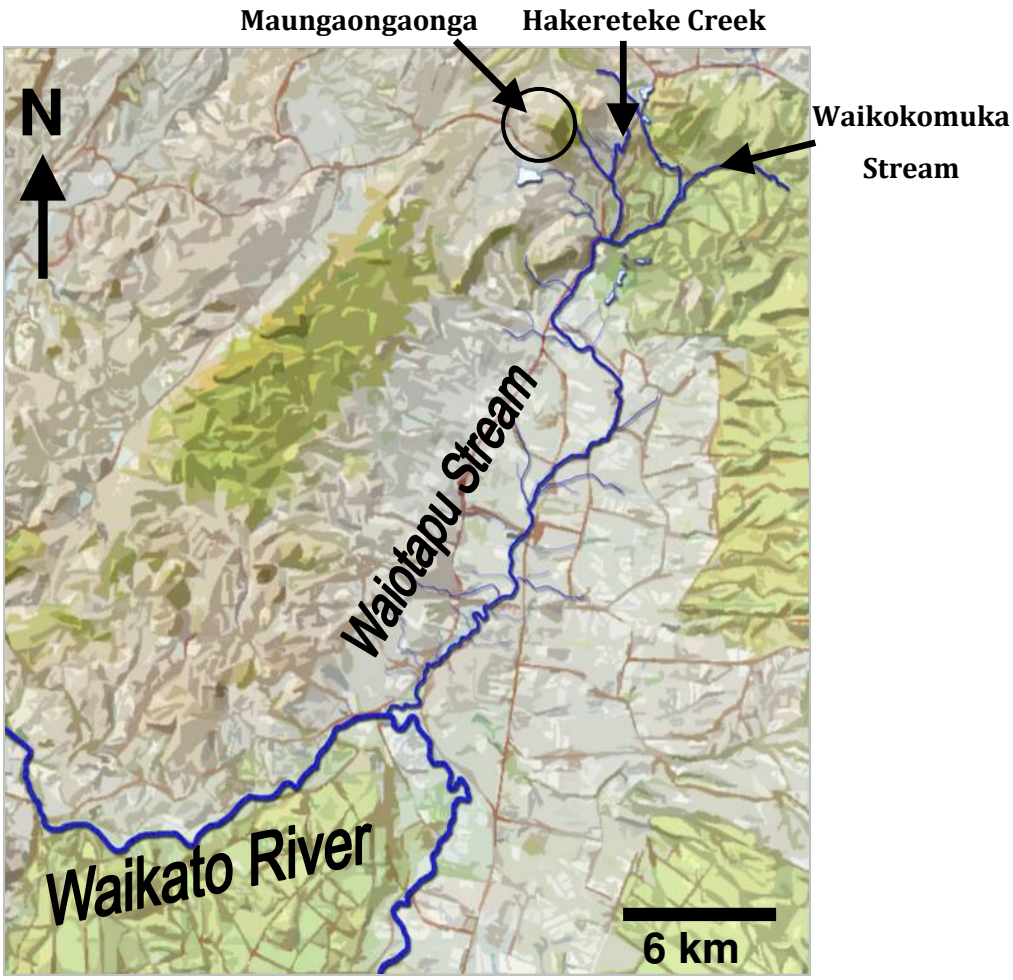

Figure 5.2 Map of the Waiotapu Stream catchment (adapted from the NZ 260 1:50 000 map series)

5.1.1 STUDY GOALS

There are two hypotheses to be tested in this chapter:

1. In receiving environments, Sb behaves similarly to As, and therefore is subject to similar removal processes
2. In receiving environments, the behaviour of Sb is essentially conservative, and therefore, in the absence of aqueous sulfides, the element is not subject to any significant removal processes

In order to investigate these hypotheses, two drainage systems were investigated:

- Waiotapu Stream
- The Waikato River, including:
    - Trends along the length of the river
    - Monthly sampling at Tuakau
    - The hydro-electric lakes in the Waikato River
    - The estuarine mouth of the Waikato River

5.2 WAIOTAPU STREAM

Waiotapu Stream was sampled twice in 2007, once in summer (February) and once in winter (August), and all sampling points used are shown in Figure 5.3. When the summer sampling was conducted, the focus of the study centred on the relationship between the Wai-O-Tapu features described in Chapter Four and Waiotapu Stream. It was assumed that, based on the topography, Sb produced from features such as Champagne Pool should drain southwest into Waiotapu Stream, somewhere below the site marked as WS 2. Therefore, in summer, sites WS 2-5 and the inflow from features on or around Maungaongaonga were sampled (MG), with the Mangaharakeke Stream (MH) used as a background (i.e. non-geothermal) site, as marked on Figure 5.3.

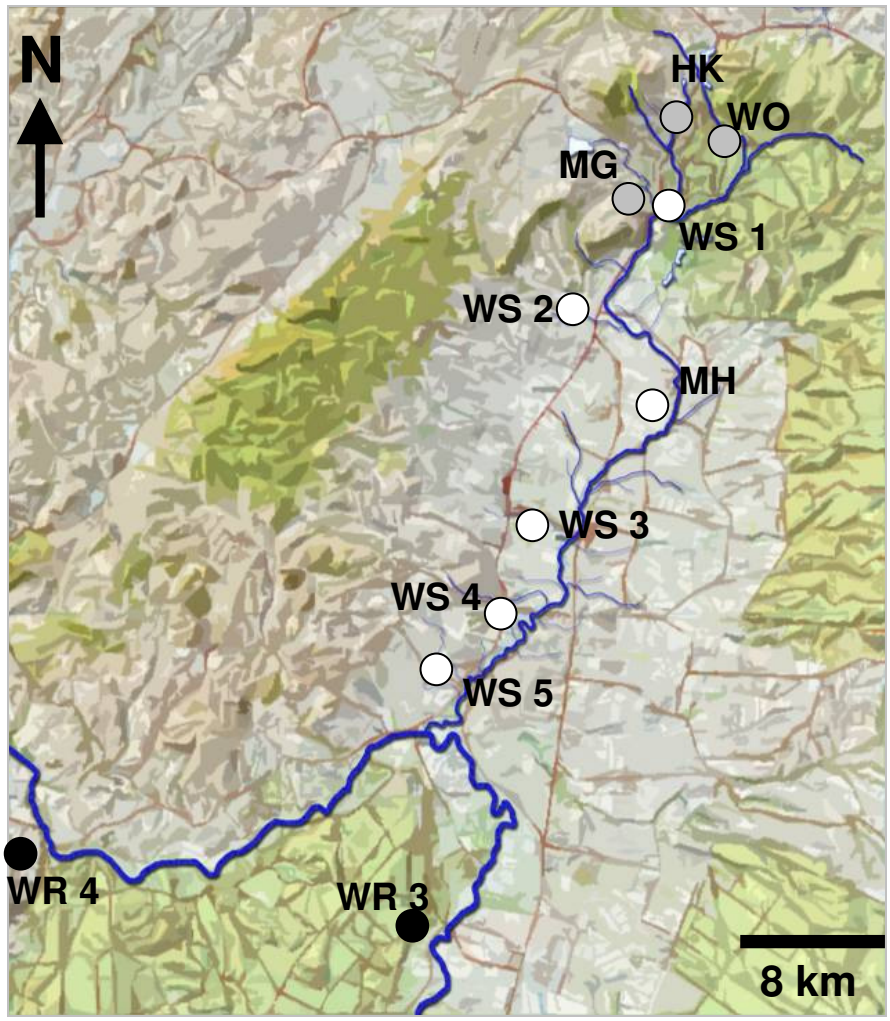

Figure 5.3 Waiotapu Stream catchment sampling points. White circles indicate Waiotapu Stream sites, grey circles indicate tributary sites, and black circles indicate Waikato River sites. Results for the Waikato River are discussed in section 5.3 (adapted from NZ 260 1:50 000 map series)

As the research evolved, it became apparent that the behaviour of aqueous Sb within Waiotapu Stream was also significant, and that more sites were required. Being a system that is acidic at the headwaters and neutral at its discharge into the Waikato River, it meant it was possible to investigate the effects of pH upon aqueous Sb by sampling all along the Waiotapu Stream.

Therefore, to develop a better understanding of this system in winter, sites WS 1 and 6 along Waiotapu Stream were added, as were sites on the upstream tributaries, Hakereteke Creek (site HK) and Waikokomuka Stream (site WO). Waikokomuka Stream, having meteoric origins rather than geothermal, was used as a control site and the Mangaharakeke Stream was not re-sampled. Descriptions of all sites used in the study are presented as Table 5.1. In August, bed sediment samples were collected where possible. Because of the hard-bottomed nature of the stream at sites WS 1 and HK, bed sediment could not be collected from either site, nor was sediment collected from Mangaharakeke Stream.

Table 5.1 Site descriptions for the Waiotapu Stream catchment. Distance is in km upstream from the confluence with the Waikato River

Site	Name	Distance (km)	Description
HK	Hakereteke Creek	24	Immediately downstream of bridge along forestry road
WO	Waikokomuka Stream	24	Immediately upstream of bridge on Waikaremoana Rd
MG	From Maungaongaonga	20	Bridge on Waiotapu Loop Rd
WS 1	Wai-O-Tapu	21	Footbridge in Wai-O-Tapu geothermal park
WS 2	Campbell Rd	18	Bridge
WS 3	Settlers Rd	12	Bridge
WS 4	Reporoa Rd	9	Bridge
WS 5	Homestead Rd	6	Bridge
WS 6	Golden Springs	3	Left bank of reserve
MH	Mangaharakeke Stream	N/A	Bridge

5.2.1 RESULTS

Selected results from the summer survey are presented in Table 5.2. The complete set of data for both seasons is provided in Appendix III.

According to these results, the acid-sulfate inflow from features about Maungaongaonga, described by Lloyd (1959), represented a significant input of aqueous Sb into Waiotapu Stream. However, in summer this inflow's relative contribution to Waiotapu Stream could not be determined, because no sites upstream of the Wai-O-Tapu geothermal park were included in the survey. If any geothermal drainage southwest from the Wai-O-Tapu geothermal park was entering Waiotapu Stream, it did not appear to contain elevated concentrations of Sb, because Sb concentrations decreased downstream and Sb:Li ratios were relatively constant (Table 5.2).

Table 5.2 Results from the analysis of aqueous samples collected from the Waiotapu Stream catchment in summer, 2008.

Site	Temp °C	pH	Cond µS/cm	DO mg/L	Cl mg/kg	SO_4 mg/kg	Li µg/kg	Sb_{diss} µg/kg	As_{diss} µg/kg	Sb:Li
MG	43.1	4.64	1860	5.56	322	129	2150	34.5	774	0.016
WS 2	30.0	5.49	802	7.17	142	98	884	8.0	39	0.009
MH	15.6	6.32	76	8.97	7	3	13	< 0.2	3	N/A
WS 3	24.1	6.37	567	8.54	106	68	626	5.0	44	0.008
WS 4	23.7	6.41	541	8.55	108	67	589	4.6	61	0.008
WS 5	21.9	6.12	464	6.51	86	54	603	3.9	52	0.006

Selected results for winter aqueous samples are presented in Table 5.3. Concentrations for some parameters were slightly lower than had been measured in summer.

Table 5.3 Results from the analysis of aqueous samples collected from the Waiotapu Stream catchment in winter, 2008 (N/A = non applicable)

Site	Temp °C	pH	Cond µS/cm	DO mg/L	Cl mg/kg	SO_4 mg/kg	Li µg/kg	Sb_{diss} µg/kg	As_{diss} µg/kg	Sb:Li
HK	32.0	3.10	910	7.50	95	150	697	5.3	96	0.008
WO	13.0	6.23	96	9.35	8	16	29	< 0.2	2	N/A
WS 1	26.3	3.33	785	8.01	132	116	615	7.3	204	0.012
MG	39.0	3.76	1576	6.48	302	117	4635	38.9	631	0.008
WS 2	24.6	5.35	652	7.47	140	100	852	9.7	53	0.011
WS 3	19.2	6.22	500	7.74	106	71	591	6.2	31	0.010
WS 4	17.9	6.51	350	7.50	93	64	445	5.2	40	0.012
WS 5	16.1	6.66	351	7.28	74	53	336	4.1	39	0.012
WS 6	15.1	6.70	341	7.15	68	50	350	4.4	40	0.013

Differences were most apparent in the discharge from the Maungaongaonga area. Antimony and Li concentrations were higher in winter, but all other parameters, including As concentrations, were lower. These results coincided with increased flows (based on visual estimates).

The concentrations of all parameters, except DO, Sb and As, in Table 5.2 and 5.3 are in relatively good agreement (± 30 %) with those reported in the winters of 2000/01 by Pope (2004) in his thesis. However, Pope's (2004) reported DO concentrations (measured by the Winkler titration method) are higher. More importantly, Sb and As concentrations are also significantly higher at most sites in Pope's (2004) thesis, up to three times higher for Sb, and as much as twenty times higher for As. Pope's (2004) results, when presented as fluxes, are also much higher than flux data published by Timperley and Huser (1996), which was explained by Pope (2004) as being a combination of poor flow estimates (by Timperley and Huser, 1996) and differing hydrological conditions. The focus of Pope's thesis was a broad range of trace elements, all analysed by ICP-MS. The analysis of As by ICP-MS is notoriously difficult (Sheppard et al, 1990), and it may be that Pope's high results were a function of non-specific calibrations, or that the chemistry of the samples caused interferences in Sb and As analysis that were not detected by Pope (2004).

Analyses for Sb^{III} and As^{III} concentrations for all sites in the winter survey are presented as Table 5.4. Sb^{III} concentrations could only be detected at three sites (WS 1, WS 2 and MG) and was only significant (> 10 %) at WS 1, where Sb^{III} accounted for 22 % of the dissolved Sb species. Given the rapid oxidation rate of Sb^{III}, as discussed in Chapter Four, these results suggest that the site was in close proximity to a sub-surface geothermal flow.

Table 5.4 Sb^{III} and As^{III} concentrations (and % of total dissolved concentrations) in the Waiotapu Stream catchment (N/A = non-applicable)

Site	Sb^{III} (µg/kg)	% Sb^{III}	As^{III} (µg/kg)	% As^{III}
HK	< 0.3	N/A	15.6	16 %
WO	< 0.3	N/A	< 0.5	N/A
WS 1	1.6	22.6 %	13.9	7 %
MG	3.3	8.5 %	41.6	7 %
WS 2	0.3	3.5 %	13.1	25 %
WS 3	< 0.3	N/A	7.7	25 %
WS 4	< 0.3	N/A	6.9	17 %
WS 5	< 0.3	N/A	6.7	17 %
WS 6	< 0.3	N/A	3.4	8 %

The results for As^{III} concentrations, which were also measured, are quite different. Apart from the meteorically derived Waikokomuka Stream, As^{III} concentrations were detectable at all sites, and produced a somewhat different trend to that observed for Sb^{III} concentrations, reaching a maximum at WS 2, and gradually declining downstream. That the maximum percentages of Sb^{III} and As^{III} (of total dissolved concentrations) are reached at different sites suggests that geothermal inputs into Waiotapu Stream vary in chemical composition.

5.2.2 ANALYSIS AND DISCUSSION OF SB IN THE WAIOTAPU STREAM

Figure 5.4 shows dissolved Sb concentrations with respect to distance along Waiotapu Stream. Two things are clear. First, most of the Sb present in solution is in the dissolved phase, confirming the results of Pope (2004), despite the differences in overall concentrations. Secondly, the drainage from Maungaongaonga is a significant contributor of aqueous Sb into the system. However, it is not easy to quantify the contribution of the Maungaongaonga feature(s), because there are a number of small geothermal (potentially containing Sb) and non-geothermal (containing negligible amounts of Sb) inputs that occur between the confluence of the Maungaongaonga discharge and site WS 2 at Campbell Rd.

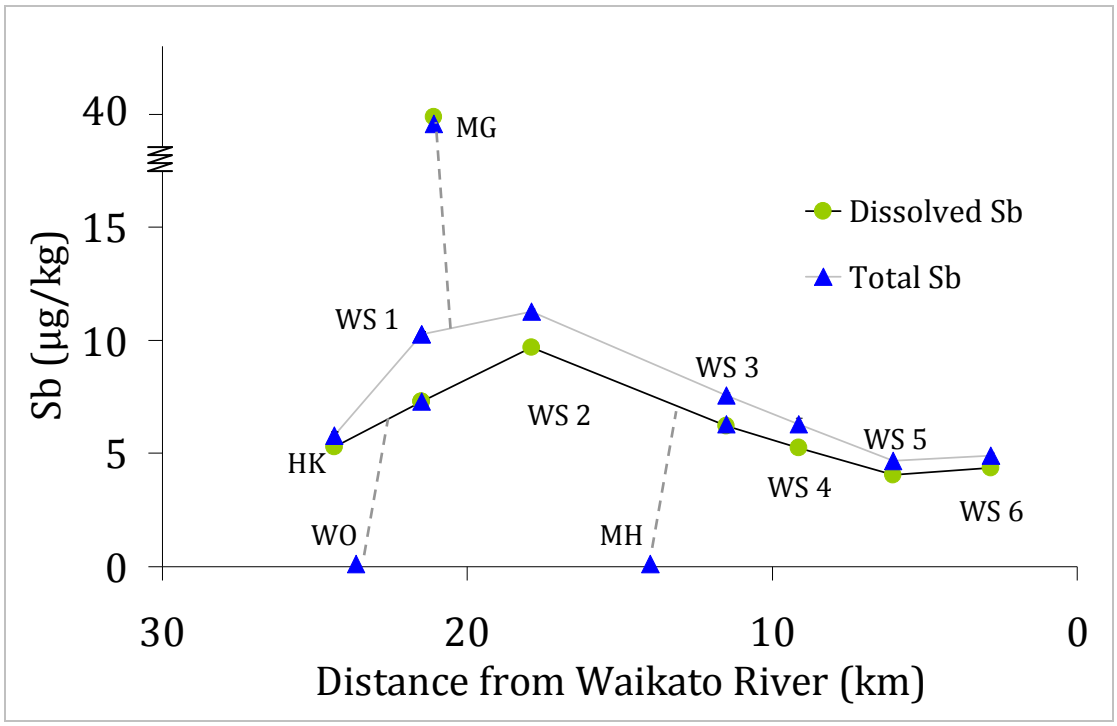

Figure 5.4 Antimony concentrations measured in the Waiotapu Stream catchment during winter.

No flow data was available upstream of WS 2, but based on a visual estimate, the flow from Maungaongaonga was about half that of Waiotapu Stream at site WS 1, and by the time the stream reached site WS 2 at Campbell Rd, it had approximately doubled in volume. A 7:3:5:5 combination of Waiotapu Stream, the Maungaongaonga inflow, meteoric inputs (similar to site WO) and geothermal inputs (similar in content to site HK) would match this visual estimate (Table 5.5). Using this ratio yields results similar to those measured at site WS 2 for temperature, conductivity, DO, Cl, SO_4, Sb (dissolved and total) and total As (± 20 %). The use of such a ratio means that Li concentration is overestimated (by 30 %), but this is minor compared to the dissolved As concentration, which is overestimated by 400 % (191 µg/kg instead of the measured 52.5 µg/kg). The ratio calculation is certainly not precise, but it definitely implies that dissolved As is behaving in a different manner to dissolved Sb in the stream.

Table 5.5 End member chemistry for Waiotapu Stream calculations

Site	Temp °C	DO mg/L	Cond µS/cm	Cl mg/kg	SO_4 mg/kg	Li mg/kg	Sb_d mg/kg	Sb_t mg/kg	As_d mg/kg	As_t mg/kg
WS 1	26.3	8.01	785	132	116	615	7.3	10.3	204	253
MG	39.0	6.48	1580	302	117	4640	38.9	38.3	631	718
WO	13.0	9.35	96.4	7.9	16.4	29.4	< 0.2	< 0.2	2.4	2.5
HK	32.0	7.50	910	94.9	150	697	5.3	5.8	96.0	131
WS 2	24.6	7.47	652	140	99.6	852	9.7	11.2	52.5	210
Estimate	**26.3**	**7.99**	**762**	**117**	**99.6**	**1090**	**9.7**	**10.8**	**191**	**230**

METALLOIDS IN WAIOTAPU STREAM SEDIMENTS

There are also differences between Sb and As concentrations in the sediment, as shown in Figure 5.5. The amount of Sb in both sediments decreases with distance, and overall the differences between Sb bound to either SPM or bed sediments are negligible. For As, the distribution pattern differs in two key aspects. First, the As concentrations in the SPM and bed sediment from Maungaongaonga is lower than that found downstream. Furthermore, As concentrations in the SPM are about an order of magnitude higher than that found in the sediment. This means that, unlike Sb, where the $SPM_{Sb} \approx Bed_{Sb}$, As may be actively being bound to SPM.

The differences between Sb and As are also evident in distribution coefficient calculations (k_d) for Waiotapu Stream (Figure 5.6). Apart from at sites WS 1 (winter) and WS 4 (summer), k_d values for Sb are relatively stable. At WS 1, it can be assumed that there is an active input of geothermally-derived Sb, and thus k_d is lower. At WS 4, the higher k_d may indicate an upstream tributary is a source of SPM rich in Fe (or Mn) oxides.

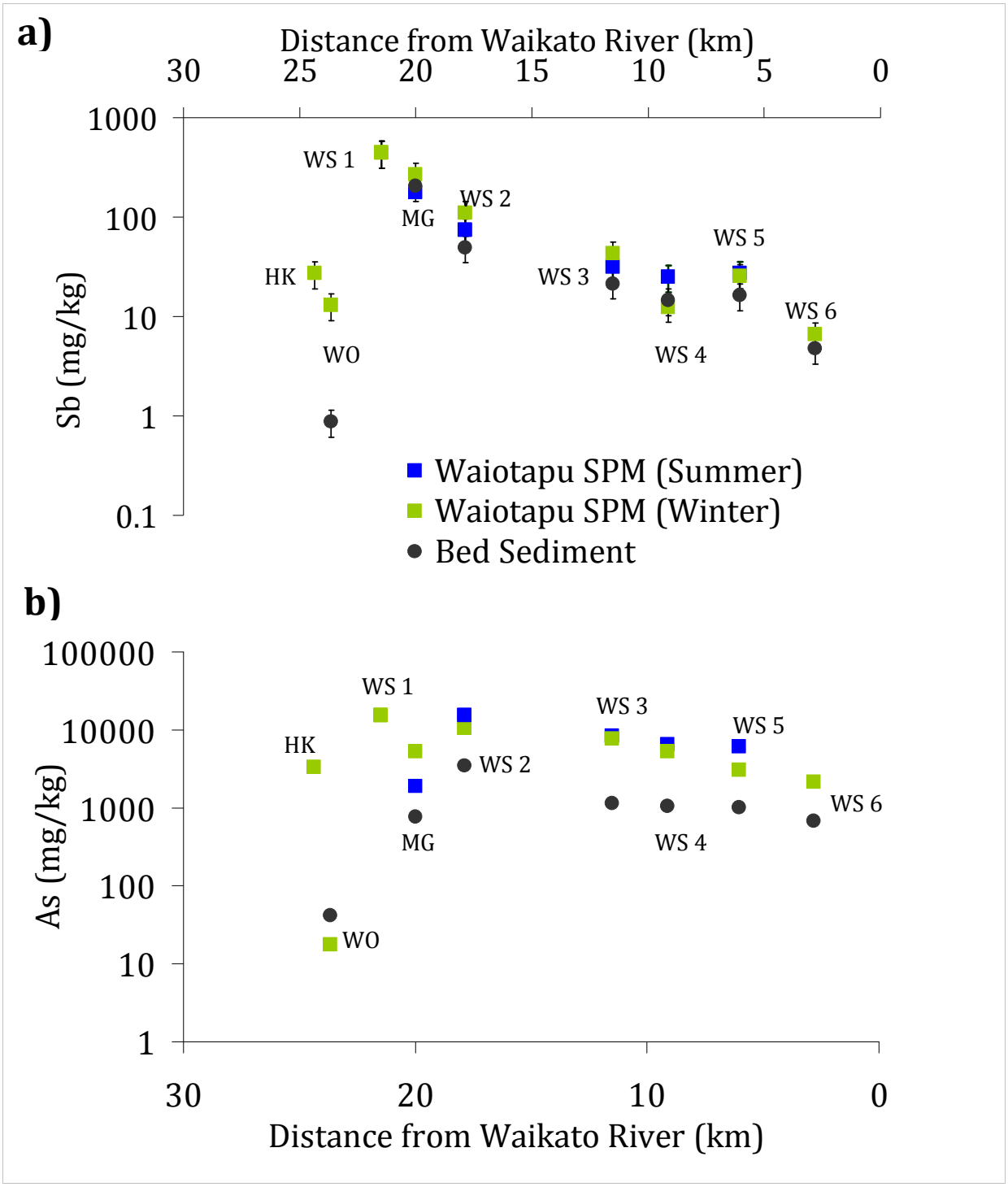

Figure 5.5 Results for SPM and bed sediment (< 0.63 µm fraction) analyses for a) Sb and b) As at Waiotapu Stream

For As, log k_d values are lower above site WS 2 than they are downstream. This coincides with an increase in pH and higher particulate As concentrations. Similar to Sb, k_d values for As are high at WS 4, further evidence of an upstream source of adsorptive material, and such inputs may also lie between WS 5 and WS 6. The generally higher As k_d values suggest As is more readily adsorbed onto SPM than Sb.

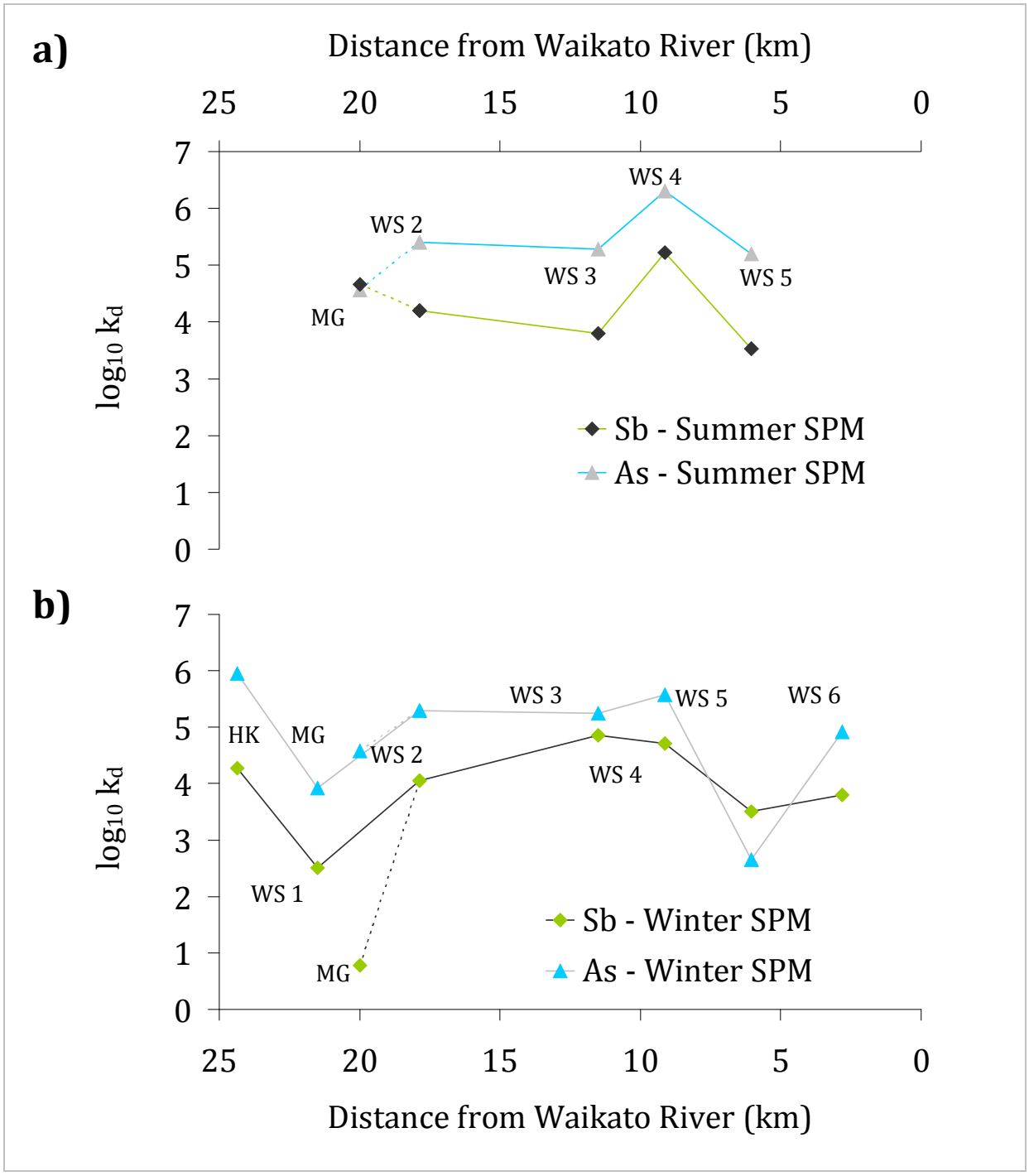

Figure 5.6 $\log_{10}$ K_d values for Sb and As in Waiotapu Stream during a) summer and b) winter

Further evidence of the more conservative behaviour of Sb, relative to As, can be seen in Figure 5.7, a plot of the relative proportion of dissolved concentrations of Sb and As against pH in the Waiotapu system. Antimony is predominantly in the dissolved (< 0.45 µm) phase, irrespective of pH, although the proportion of particulate Sb may increase slightly at pH <4. For As, there is a significant increase in the proportion of particulate As in solution, especially below pH 4.5.

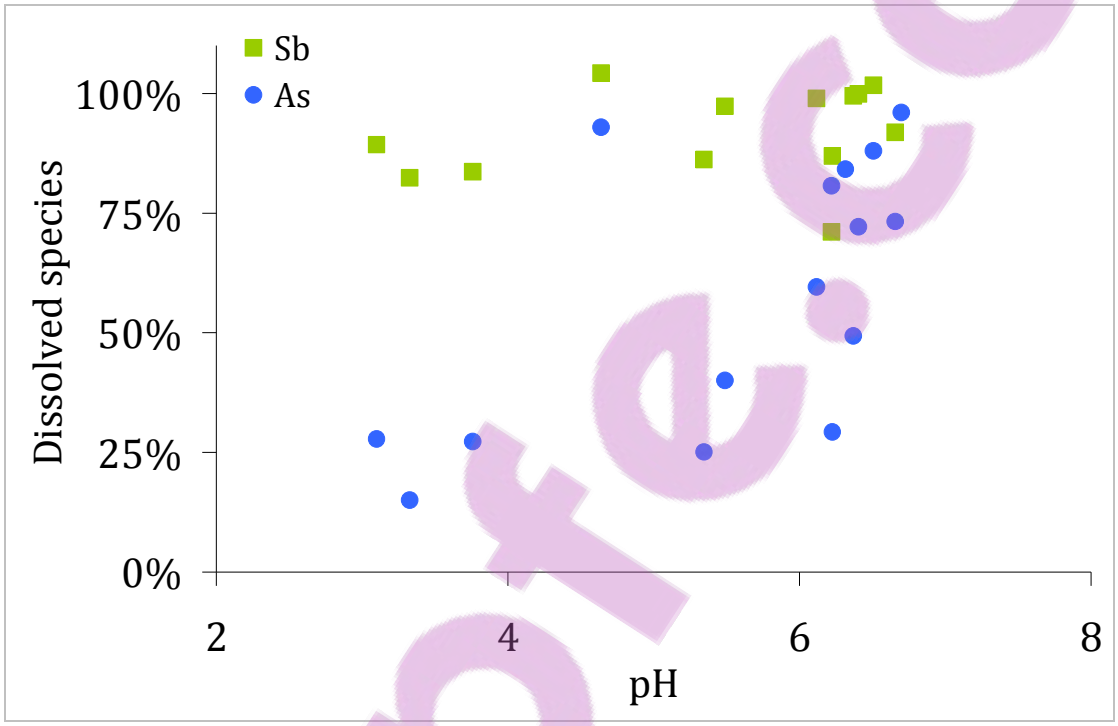

Figure 5.7 Proportion of dissolved Sb and As in Waiotapu Stream with respect to pH

Pope (2004) also observed similar As behaviour in 2000/01, and suggested that the adsorption of As to Fe and Al precipitates was the principle cause. In low pH waters (pH <3), Fe, Al and Mn oxides are dissolved and therefore adsorption onto the metal-oxide surfaces cannot occur. In less acidic waters, such as Waiotapu Stream itself, the metal-oxyhydroxides precipitate, and the negatively charged As oxyanions such as $H_2AsO_4^-$ bind onto the positively charged surface layers (Dzombak and Morel, 1990). Pope (2004) also concluded that aqueous Sb behaved conservatively in Waiotapu Stream, which is supported by the sediment data presented here. However, the first cluster of data in Figure 5.7 suggests Sb behaviour is not as simple as it first appears, because partitioning of Sb onto SPM does occur at pH < 4. Comparisons with other conservative elements were used to clarify the issue.

THE BEHAVIOUR OF SB COMPARED TO CONSERVATIVE ELEMENTS

If dissolved Sb concentrations measured at Waiotapu Stream are plotted against Li concentrations, the correlation is positive, but relatively weak (R^2 =0.63). However, when the data from each season are treated separately, the resulting correlations, shown in Figure 5.8, are strong (R^2 =0.95 in summer and R^2 =0.98 in winter). The correlation between Sb concentrations and Cl concentrations across both seasons was also strong (R^2 =0.8). That dissolved Sb correlates well with Li and Cl concentrations suggests that dissolved Sb is behaving conservatively within the stream.

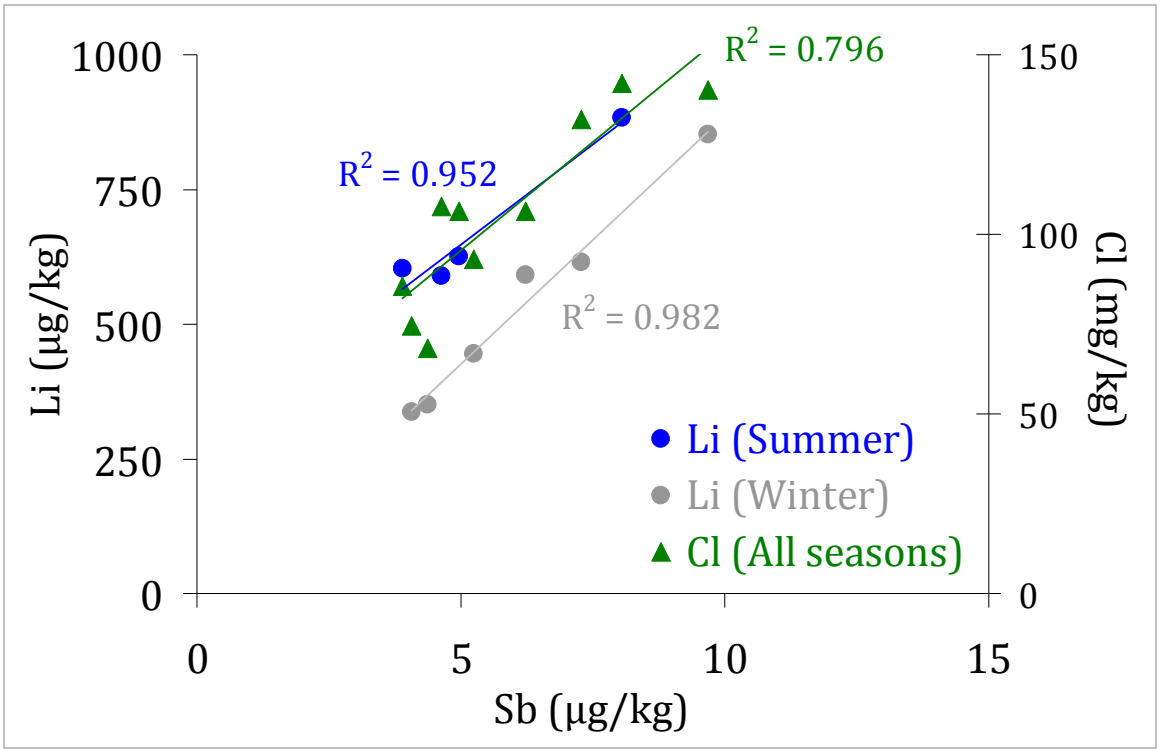

Figure 5.8 Correlations between Sb concentrations and Cl and Li concentrations at Waiotapu Stream sites (WS 1 – WS 6).

WAIOTAPU STREAM CONCLUSIONS

The results presented in this chapter thus far confirm the general findings of Pope (2004), that, generally, Sb behaves conservatively in Waiotapu Stream, especially compared to As. While there is evidence for the potential removal of As by way of adsorption onto the metal-oxide surfaces of SPM, Sb adsorption onto such surfaces is not a significant removal process within the system.

5.3 THE WAIKATO RIVER

Environment Waikato (EW), the regional authority for the Waikato region, monitors sites along the entirety of the Waikato River at regular intervals, and most research upon the river has used EW's sampling sites. This has allowed ease of comparison between data sets, and a long and rich data-history has developed (Aggett and Aspell, 1977; McLaren and Kim, 1995; Webster-Brown and Webster, 2000; Vant and Smith, 2004; or Smith, 2006).

In keeping with tradition, when developing the current study the existing EW sites were used, where they coincided with the proposed sampling point. In February 2006, at the height of New Zealand's summer, 9 of the 15 sites shown in Figure 5.9 (and listed in Table 5.6) were selected along the length of the river (WR 1-6,WR 8, WR 10, WR 12), and aqueous samples were collected and analysed for Sb, As, DO, conductivity and pH from each.

Table 5.6 Site names and descriptions. Distance refers to the distance in km from Lake Taupo, which is the source of the Waikato River

Site	Name	Distance (km)	Sampled in Feb 2006	Description
WR 1	Taupo	1	Yes	Control gates bridge
WR 2	Aratiatia	13	Yes	Jetty close to dam
WR 3	Ohāki	40	Yes	Bridge
WR 4	Mihi	49	Yes	Jetty upstream of bridge
WR 4a	Tutukau	62	No	Ramp upstream of bridge
WR 5	Ohakuri	79	Yes	Dam – Central flow
WR 6	Whakamaru	105	Yes	Dam – Central flow
WR 7	Waipapa	130	No	Dam – Central flow
WR 8	Arapuni	155	Yes	Arapuni Landing at shore
WR 9	Karapiro	180	No	Dam – Central flow
WR 10	Hamilton	205	Yes	Narrows jetty
WR 11	Horotiu	225	No	Bridge
WR 12	Huntly	250	Yes	Bridge
WR 13	Mercer	288	No	Bridge
WR 14	Tuakau	300	N/A	Ramp downstream of bridge
WR 15	Port Waikato	325	N/A	Multiple points from shore

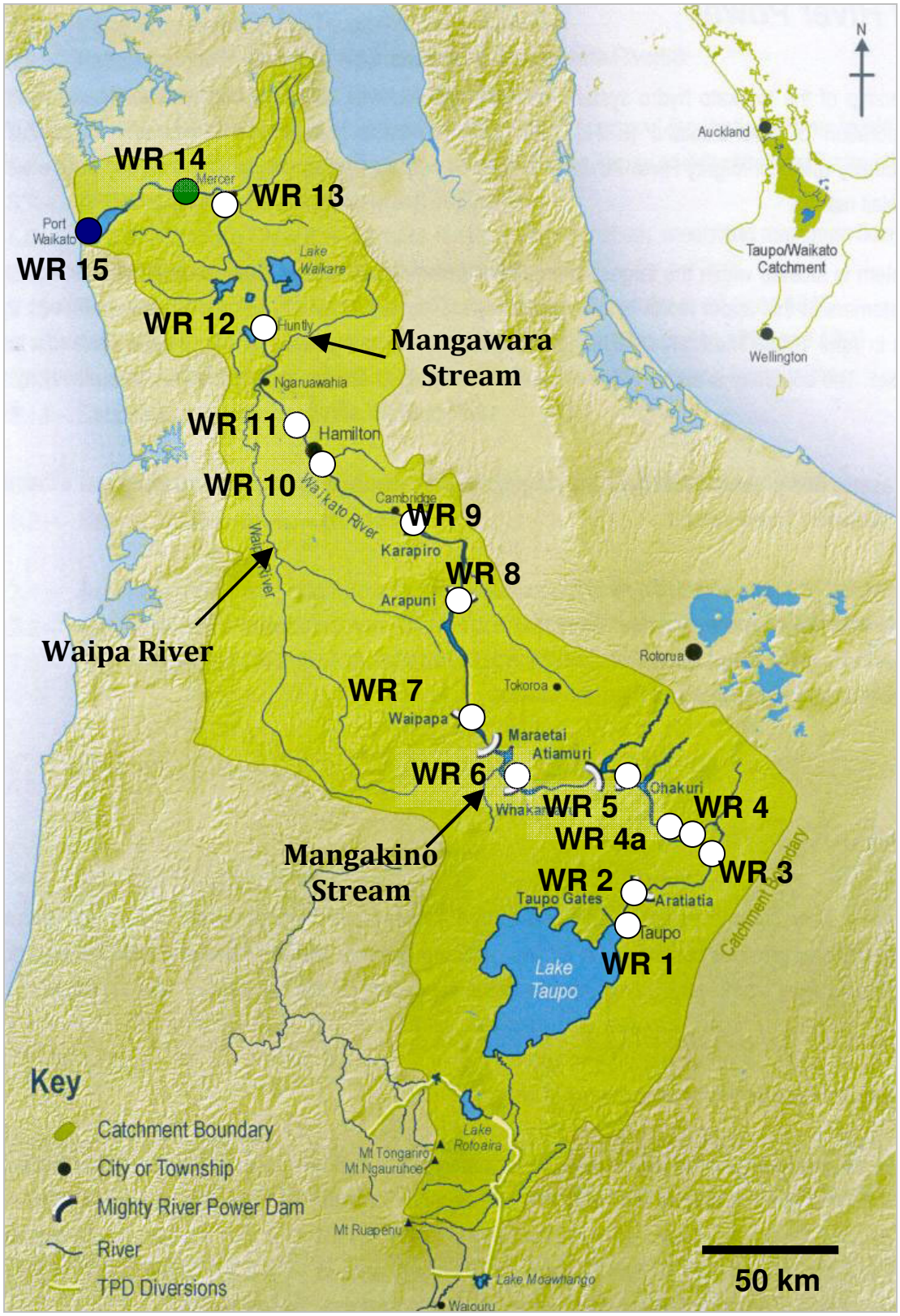

Figure 5.9 Map of the study sites used along the Waikato River, marked as WR 1-15. WR 1-13 constitute the sites discussed in this section, results from WR-14 and WR-15 will be discussed in sections 5.4 and 5.7 respectively. Map adapted from Mighty River Power (2001).

The Waikato River was sampled along its lengths four times, summer 2006 (February), winter 2006 (August), summer 2007 (February) and a second winter sample in August 2007. Extra sites were also added (WR 7, WR 9, WR 11 and WR 13). Suspended particulate material samples were collected during both sampling events in 2007 and bed sediment was collected from all sites as well. A decision was also made to collect samples from one site monthly for two full years (24 months). For ease of sampling, the site at Tuakau (WR 14), which was the closest site to Auckland, was chosen. As the research developed, specific attention was centred on the behaviour of Sb in the hydro-electric lakes along the river, and in the Port Waikato estuary (WR 15), but both these aspects will be discussed separately later in this chapter. The complete data set for all of the Waikato River results are included in Appendix III

5.3.1 ANTIMONY ALONG THE LENGTH OF THE WAIKATO RIVER

Antimony concentrations for the Waikato River sites are shown in Figure 5.10a. The results from Tuakau, which were collected separately at the beginning of each month, are not included, and will be discussed in Section 5.4. The original sampling point at WR 4, 49 km downstream from Lake Taupo, was moved because the sample from summer 2006 was not reflective of well mixed waters, and instead had undue influence from Waiotapu stream, which is why the point is not connected in Figure 5.10. The As concentration measured at WR 4 was not similarly elevated, and therefore Sb contamination of the sample could not be eliminated, but the site was moved regardless. Neither the original site, nor its replacement 13 km further downstream at the Tutukau Bridge (WR 4a), are EW sites.

Overall, Sb concentrations were higher along the length of the river in summer and lower in winter. The results from the first 50 km of the river in the winter of 2007 were the only exception. The overall trends for As are similar (Figure 5.10b), being higher in summer and lower in winter except for in the first 50 km of the river in the winter of 2007. The most likely reason for the elevated concentrations of both Sb and As at that time was that the Wairakei Power station may have been discharging more spent geothermal fluids into the Waikato River than normal. Whether such a discharge occurred could not be confirmed.

Overall, Sb concentrations were in agreement with results published by EW for 2005 (Smith, 2006), as shown in Figure 5.10. The one exception was a high result reported by EW in May 2005 for Lake Ohakuri (WR 5). However, similarly high concentrations in this lake were recorded in March 2007 during the lake survey, discussed in Section 5.6.

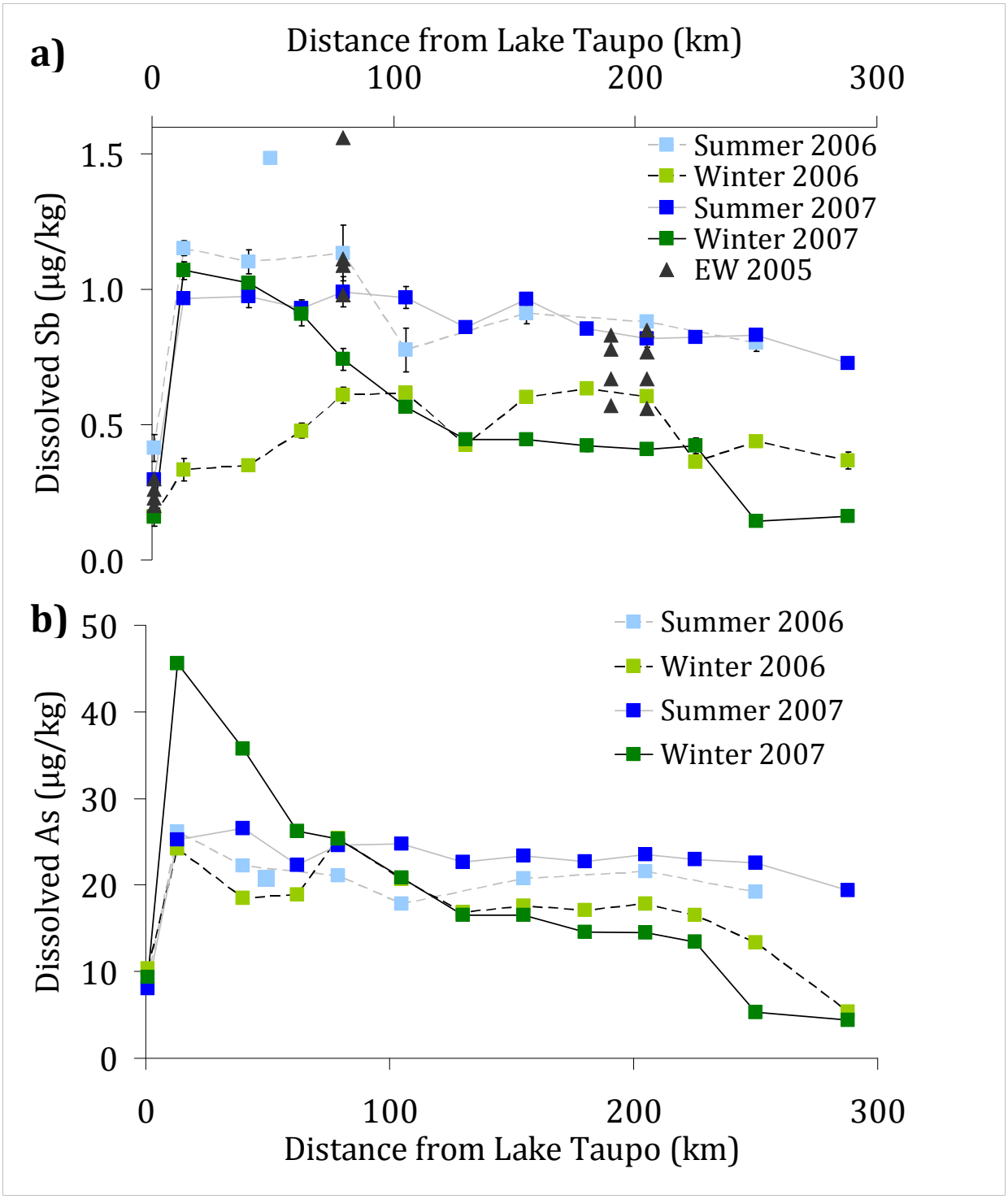

Figure 5.10 Dissolved concentrations of a) Sb and b) As along the Waikato River. The results from Environment Waikato for 2005 are from Smith (2006)

The Sb concentrations are at a maximum immediately downstream of the discharge from Wairakei Power station (WR 2) and indicate that, as for As concentrations, the station's discharge is the most significant source of Sb to the river. The decline in concentrations with distance in both seasons (Figure 5.10) is almost certainly related to dilution, particularly in the lower reaches, where the Waikato River is joined first by the Waipa River and then by the sediment laden Mangawara Stream between the site at Horotiu (WR 11, 200 km downstream of Lake Taupo) and that at Huntly (WR 12, 240 km downstream). Flows in the Waikato River upstream of Cambridge (approximately 165 km downstream from Lake Taupo) are relatively constant all year round because of the series of hydro-electric power station dams built from Ohakuri (WR 5, 79 km downstream,) to Karapiro (WR 9, 160 km downstream). In 2007, mean flow for this stretch of the river was 252 ± 16 m^3/s (Beard, 2008). Further downstream, the influence of tributaries such as the Waipa River varies with catchment rainfall, and, in 2007, the mean flow from Huntly (WR 12) to Mercer (WR 13) was 365 ± 70 m^3/s (Beard, 2008). In summer, flows are lower, and therefore the decline in Sb concentrations with distance is less. In the wetter winters, swollen tributaries mean more significant dilution of Sb and As concentrations.

Occasional filtered samples were analysed for Sb^{III} concentrations, but Sb^{III} concentrations were always below detection limit (0.3 µg/kg). This may be in part because Sb concentrations were low enough that even significant (> 20 %) concentrations of Sb^{III} could exist, but still be below detection limit. Such a situation is unlikely though, given the absence of Sb^{III} in samples from Waiotapu Stream, where dissolved Sb concentrations were significantly higher.

PARTITIONING OF Sb IN THE WAIKATO RIVER

Similar to Waiotapu Stream, most of the aqueous Sb in the Waikato River is present in the dissolved phase, as shown in Figure 5.11. The poor results for WR 1 are most likely because Sb concentrations were at detection limits, and so even minor differences appear significant. The erroneous result from Lake Waipapa (WR 7) in the winter of 2006 is not as easily explained, but is perhaps the result of sample contamination. As was observed for Waiotapu Stream, there were only minor differences between Sb concentrations in the SPM and Sb concentrations in bed sediment, especially between summer SPM results and bed sediment results for the river (Figure 5.12). However, despite the large errors inherent in the method used to analyse Sb in sediment, there was evidence to suggest that Sb concentrations in SPM were higher in winter than in summer between sites WR 3 (Ohāki) and WR 8 (Lake Arapuni).

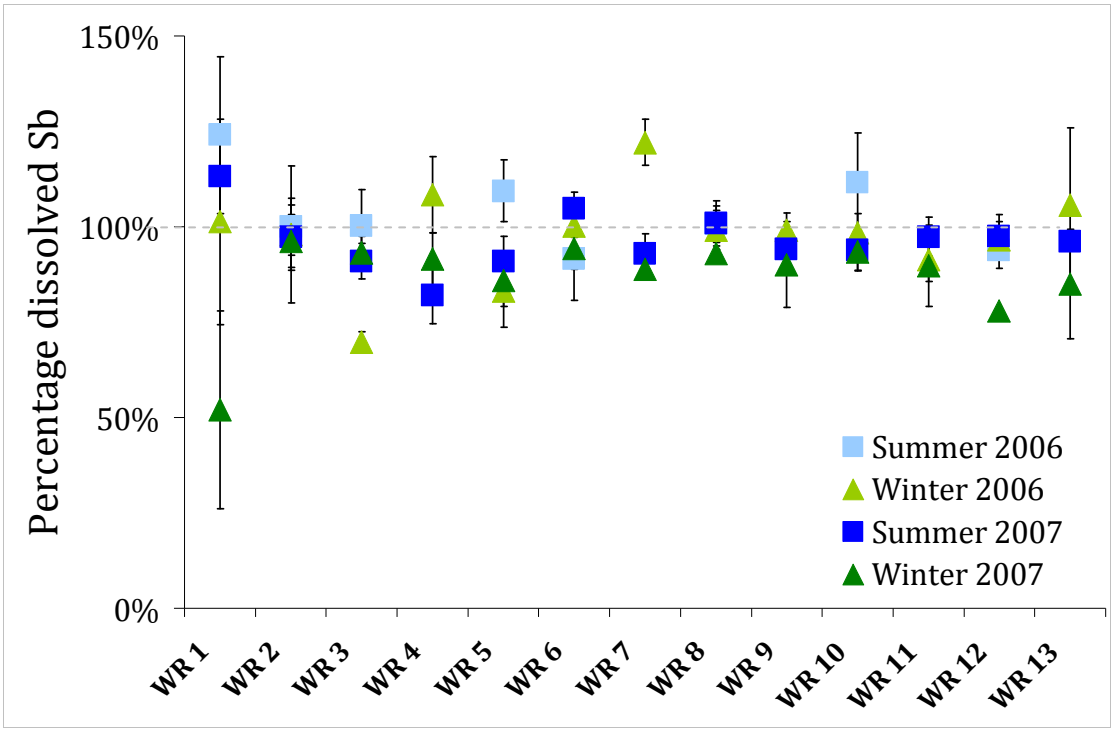

Figure 5.11 The proportion of Sb in the dissolved phase in results from the Waikato River

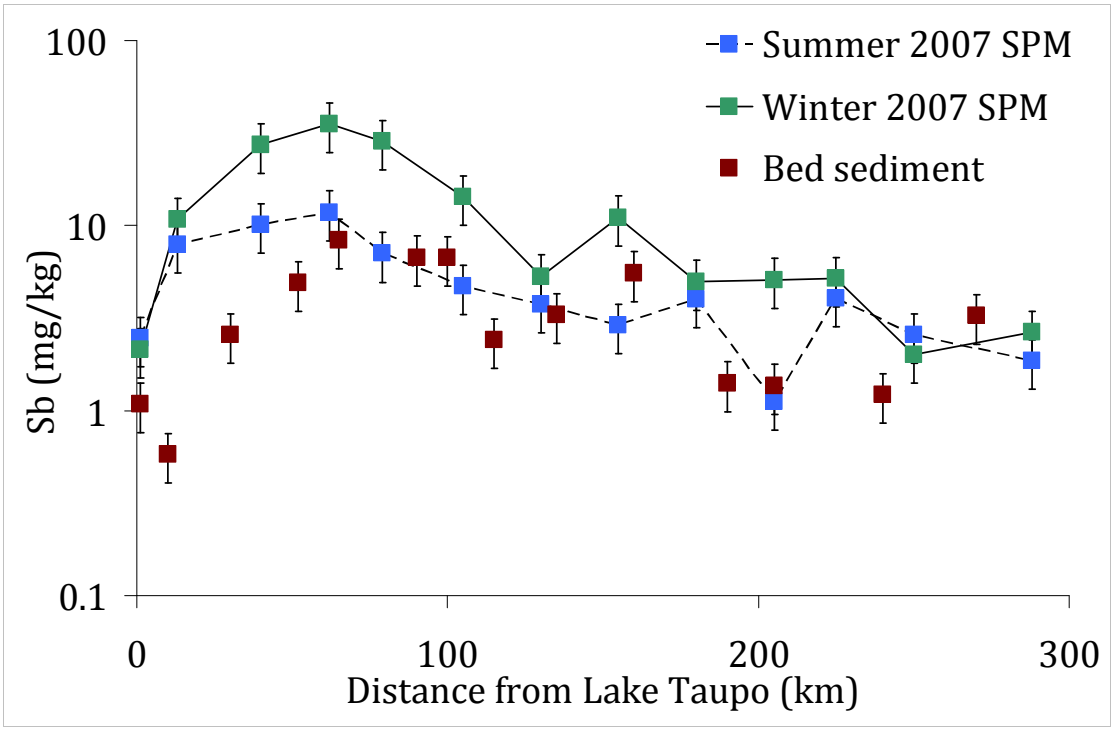

Figure 5.12 Antimony concentrations in SPM and bed sediment along the Waikato River

Distribution coefficient values (k_d) values, presented as log_{10} values in Figure 5.13, also show a difference in the equilibria between dissolved and particulate Sb between summer and winter, with winter values higher and relatively constant, while summer values decrease with distance.

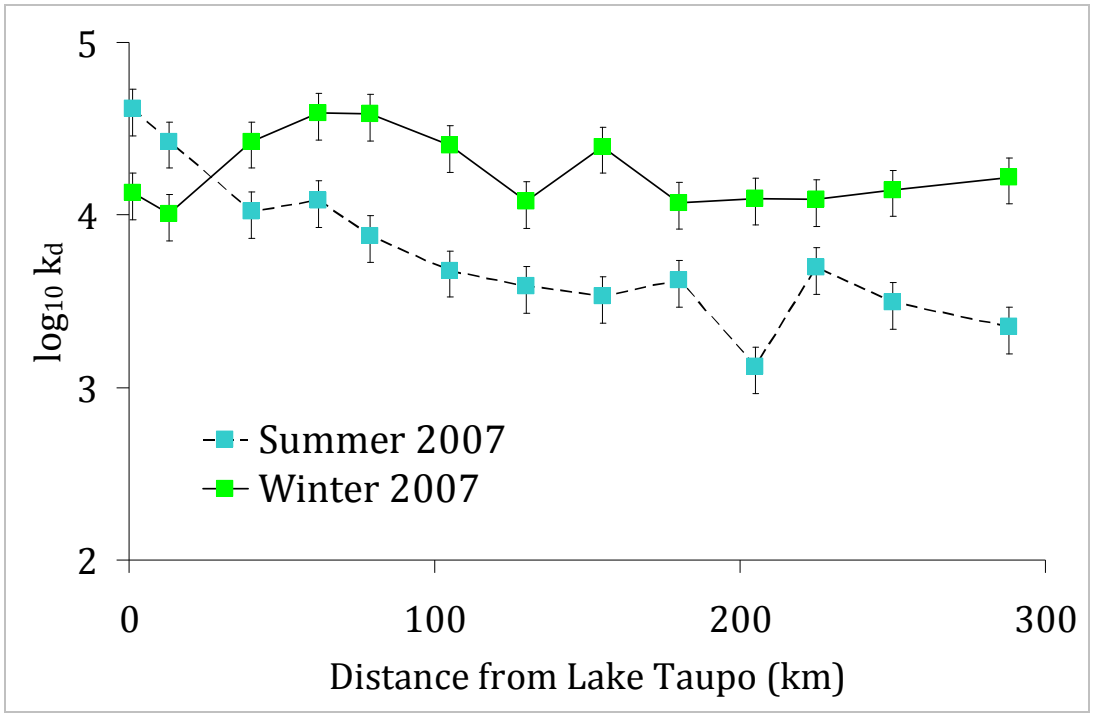

Figure 5.13: K_d values for Sb from the Waikato River

When k_d values for Sb in the Waikato River are compared to Fe concentrations in the SPM, as shown in Figure 5.14a, with the exception of two summer results (for sites WR 1 and WR 2), it appears that k_d values for Sb in the Waikato River are related to SPM Fe concentrations. Particle concentration effects have not been considered, because the SPM concentrations in the Waikato River are relatively low (<100 mg/kg)

A similar pattern can also be observed for for As (Figure 5.14b). The single exception is for results from site WR 2 (Lake Aratiatia) in winter, but the reasons why are unclear. Overall, these results are in agreement with those of Webster and Lane (Webster-Brown and Lane, 2005a). This suggests that, while the degree of Sb adsorption onto Waikato River SPM is typically close to an order of magnitude lower than that observed for As, the general conclusion that Fe content is a significant influence upon adsorption to Waikato River SPM holds for Sb as well.

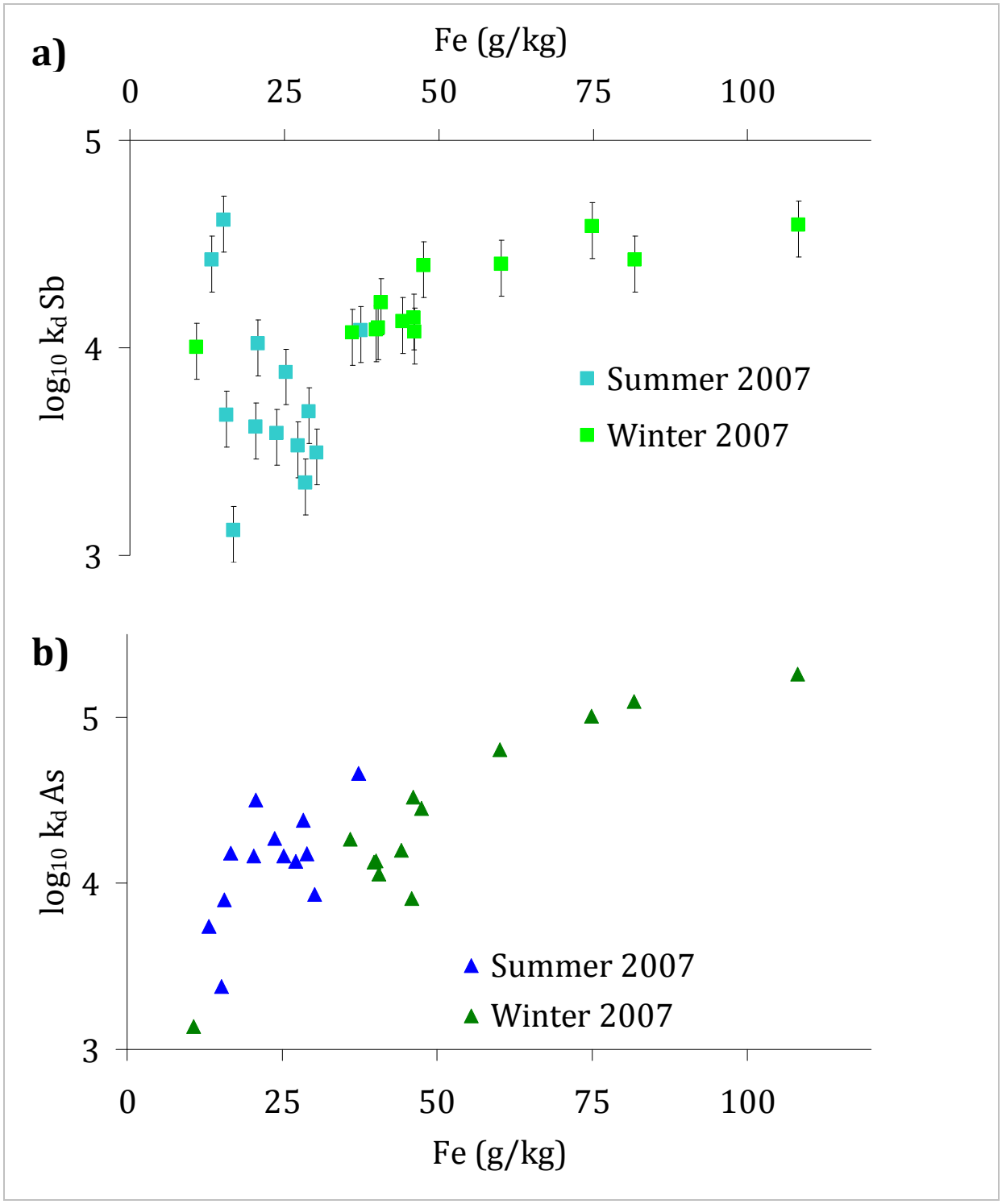

Figure 5.14 Comparisons between k_d values for a) Sb and b) As with SPM Fe concentrations in the Waikato River

COMPARISONS WITH OTHER ELEMENTS

In winter, there is a positive correlation between dissolved Sb and dissolved As in the Waikato River, as shown in Figure 5.15a, further evidence that increased Fe concentrations in winter SPM are a significant influence upon the behaviour of both metalloids. In summer, there is little evidence of a correlation between Sb and As concentrations. This suggests that some process is occurring in summer that affects one of the metalloids, but not the other.

A comparison of dissolved Sb with Li suggests that, while seasonal differences in SPM Fe concentrations affect Sb behaviour, the overall impact is relatively minor (Figure 5.15b). This is because the differences between Sb concentrations with respect to Li in winter compared to summer are relatively small, and even when the data for dissolved Sb and Li along the length of the Waikato River is compared, regardless of season, there is still a strong correlation (R^2 = 0.76, not shown)

The positive correlations between Sb and Li, regardless of season, suggest that the behaviour of Sb is mainly conservative, whereas some further process must be influencing As behaviour in summer that does not similarly affect Sb. Results of a more frequent sampling programme in the lower reaches of the Waikato River may provide further insights.

5.4 SEASONAL PROFILING IN THE WAIKATO RIVER: TUAKAU

Samples from Tuakau (WR 14) were collected monthly from 31 January, 2006 (considered, for this study a February sample), until the first week of January 2007, creating a data set spanning 24 months and 24 sampling occasions. Originally, it had been assumed that nitric acid digests of SPM samples, being prepared at the same time for a separate research project on the Waikato River (Dee, 2007) could be used for Sb analyses as well, but for the reasons explained in Chapter Two, such samples were unsuitable. Suspended particulate material samples were collected for aqua regia digestion from August 2006 onwards (18 samples in total). Environment Waikato provided the flow data, which was collected upstream at the closest point unaffected by tidal influence, at Mercer Bridge (WR 13). A summary table of data is presented as Table 5.7, the complete set of data is included in Appendix III.

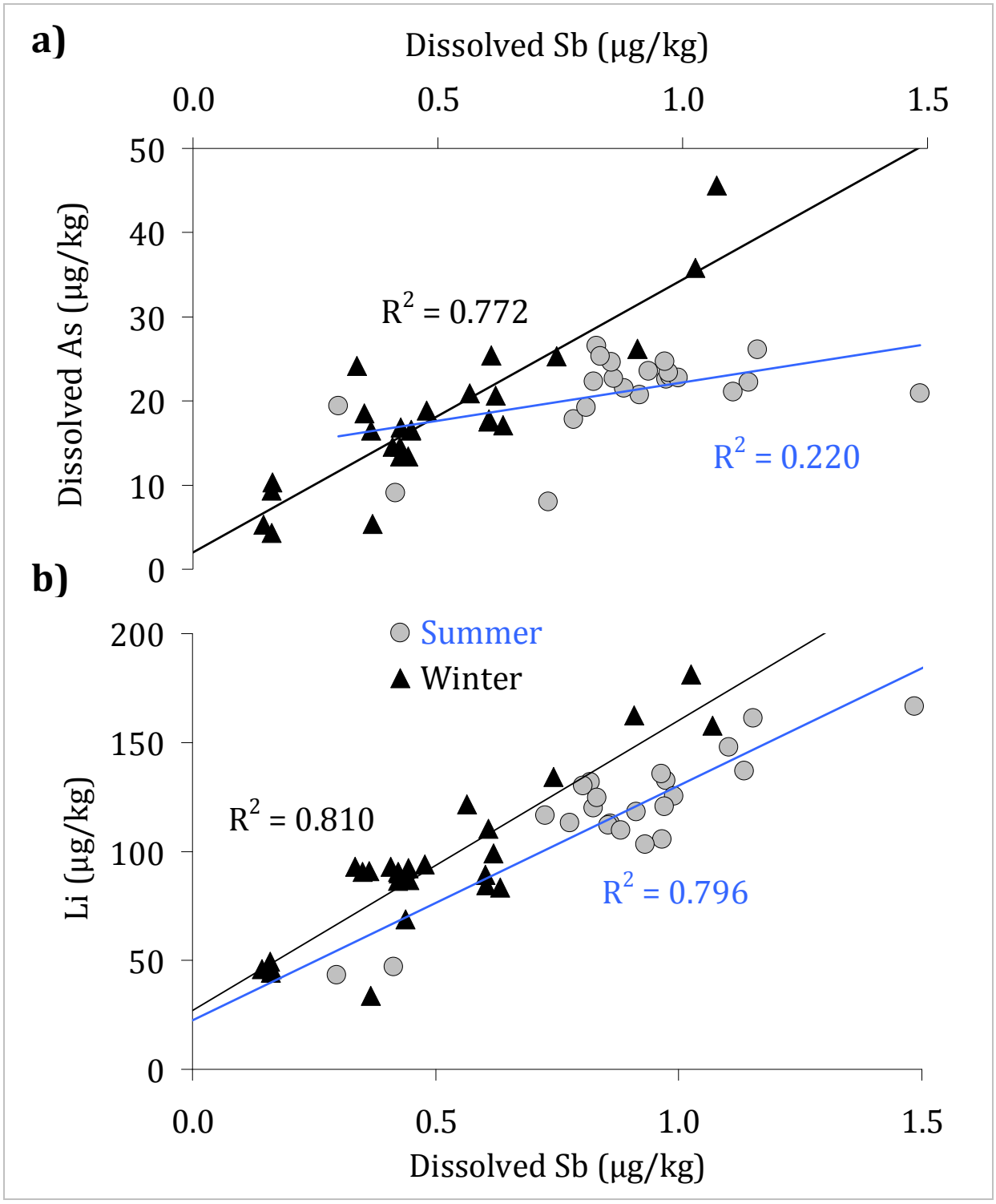

Figure 5.15: Comparisons between Sb concentrations and a) As and b) Li for sites along the length of the Waikato River

Table 5.7 Summary table of data from monthly sampling at Tuakau. Flow data was provided by Environment Waikato. An instrument problem meant that no temperature or pH data was recorded in January 2008, n/m= not measured.

Month	Temp °C	pH	Flow m^3/s	SPM mg/L	Sb_{diss} µg/kg	As_{diss} µg/kg	Sb (SPM) mg/kg	Fe (SPM) g/kg
Feb-06	24.7	7.30	367	n/m	0.4	14.9	n/m	n/m
Mar-06	20.9	8.48	293	n/m	0.3	21.5	n/m	n/m
Apr-06	21.7	7.74	269	n/m	0.5	18.0	n/m	n/m
May-06	18.8	7.02	624	n/m	0.6	12.8	n/m	n/m
Jun-06	12.8	7.00	575	n/m	0.2	9.0	n/m	n/m
Jul-06	14.7	7.12	472	n/m	0.3	12.9	n/m	n/m
Aug-06	13.0	7.11	524	7	0.3	13.7	2.0	45.1
Sep-06	14.8	7.31	477	17	0.3	9.3	1.4	33.9
Oct-06	16.3	7.14	496	19	0.3	11.3	1.2	45.6
Nov-06	18.0	7.59	426	10	0.4	18.4	1.8	49.0
Dec-06	18.7	7.41	453	16	0.3	17.4	1.8	33.6
Jan-07	18.7	6.64	262	29	0.4	19.5	1.0	17.9
Feb-07	22.7	7.18	284	52	0.5	22.3	1.0	6.8
Mar-07	23.5	7.90	290	14	0.6	24.6	2.6	23.2
Apr-07	20.5	7.40	247	17	0.8	17.8	1.3	26.5
May-07	17.3	7.08	246	6	0.5	19.0	2.6	38.9
Jun-07	14.9	5.72	284	15	0.9	25.9	2.1	20.1
Jul-07	11.7	5.51	469	17	0.6	16.1	2.8	41.9
Aug-07	11.5	6.23	817	14	0.2	5.1	1.4	42.0
Sep-07	13.7	6.29	375	14	0.4	10.9	1.1	44.8
Oct-07	15.9	7.32	403	17	0.5	13.5	2.1	37.2
Nov-07	16.1	7.03	489	34	0.4	11.2	1.3	43.8
Dec-07	20.5	7.60	253	25	0.6	24.4	1.6	45.0
Jan-08			170	15	0.8	28.5	1.2	16.4

5.4.1 SEASONAL TRENDS IN Sb CONCENTRATIONS AT TUAKAU

Antimony concentrations over the 24 month survey are presented in Figure 5.16, and were higher in 2007 than they were in 2006. Overall the average concentration at Tuakau was 0.46 (± 0.08) µg/kg, for both dissolved and total Sb, again indicating that aqueous Sb exists almost exclusively in the dissolved phase in the circum-neutral pH oxic conditions of the Waikato River.

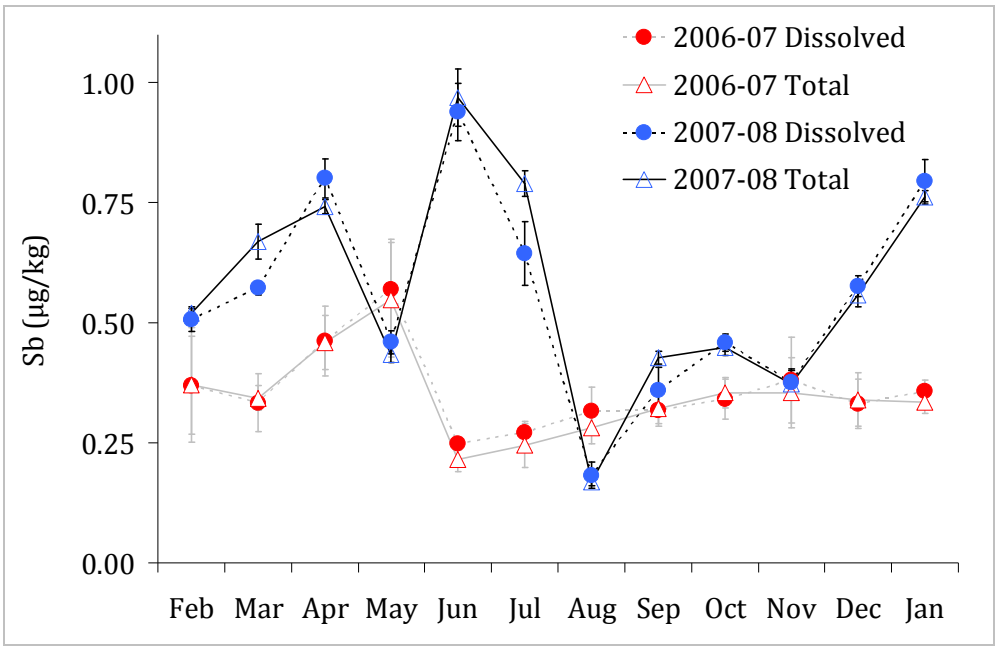

Figure 5.16: Monthly Sb concentrations at Tuakau

Peaks in May 2006 and in June-July 2007, disrupted the general pattern for Sb concentrations, which overall suggested concentrations of Sb were highest in summer and lowest in winter, similar to results for the Waikato River as a whole. For aqueous As, shown in Figure 5.17, the general pattern is more evident, even though similar peaks occurred in June/July 2007 to those observed for Sb.

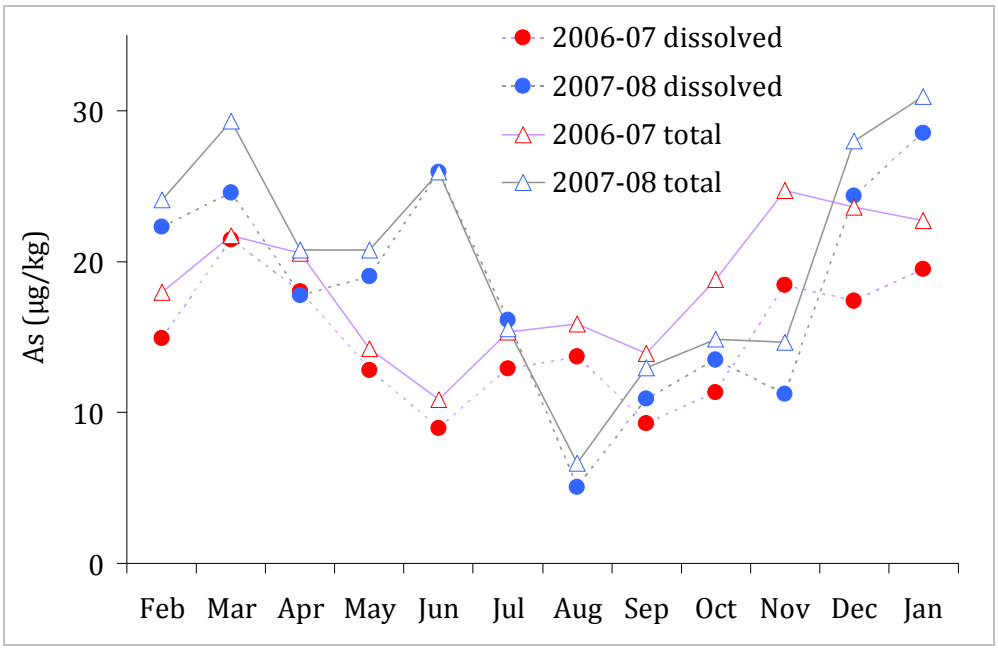

Figure 5.17 Monthly As concentrations at Tuakau

The data collected for As is remarkably consistent with data collected by Webster-Brown and Webster (2000) in 1998/1999. Arsenic concentrations are highest in summer, and lowest in winter, which agrees with previously reported findings (McLaren and Kim, 1995; Webster-Brown and Lane, 2005a).

FLUX CALCULATIONS FOR TUAKAU DATA

At a site such as Tuakau, for which river flow is influenced by rainfall in the large upstream catchment, flux data can prove useful. The flux calculations, derived from concentration data (µg/kg) and flow data (m^3/s), are shown in Figure 5.18 for Sb and Figure 5.19 for As.

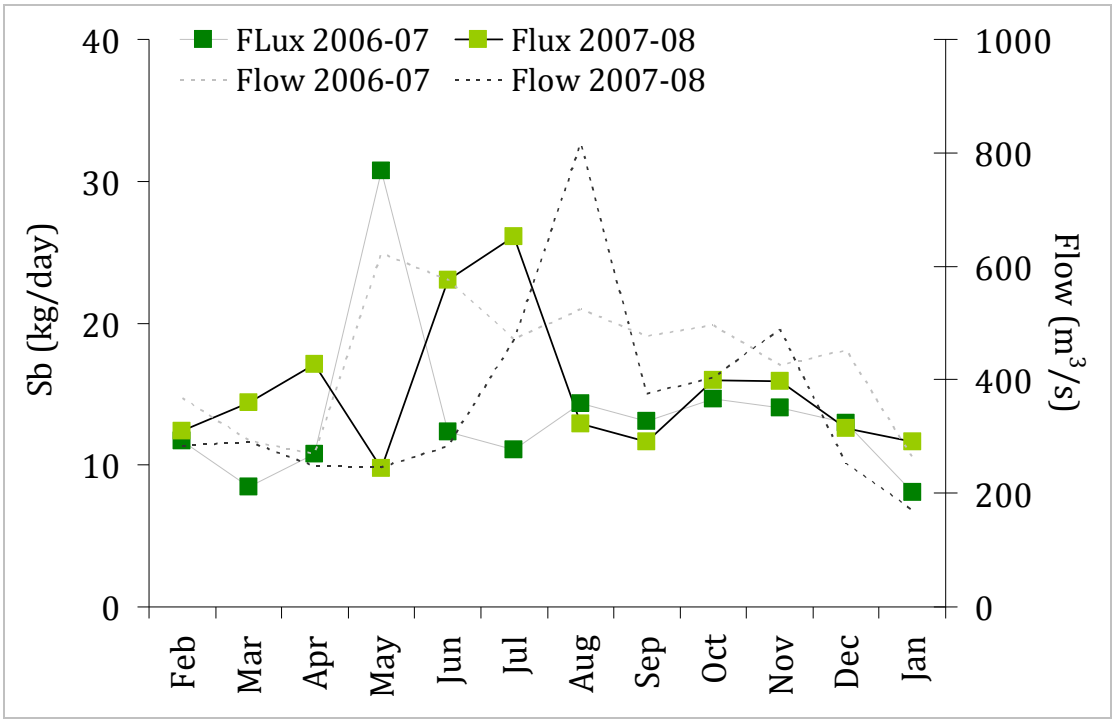

Figure 5.18 Flux and flow data for dissolved Sb at Tuakau

When flux data for for Tuakau are examined, the peak in May 2006, co-inciding with peak flow for 2006, becomes more evident for both Sb and As. In fact, for Sb (Figure 5.18a), apart from a second peak over June and July of 2007, Sb flux at Tuakau was relatively constant, despite quite variable flow. This suggests that, rather than the changes in Sb-adsorption onto Fe-oxides in SPM, changing river flow (i.e. dilution) is the principal control upon Sb concentrations in the Waikato River. This is further evidence that, in terms of seasonal variability, Sb exhibits generally conservative behaviour.

Flux data for As is more variable (Figure 5.19). If the May 2006, and the June/July 2007 peaks were excluded, it could be argued that the increased adsorption of As onto SPM richer in Fe during winter meant that less As reached Tuakau during winter than in summer. The removal of As from the water column presumably occurs as SPM settles out in the hydro-electric lakes upstream.

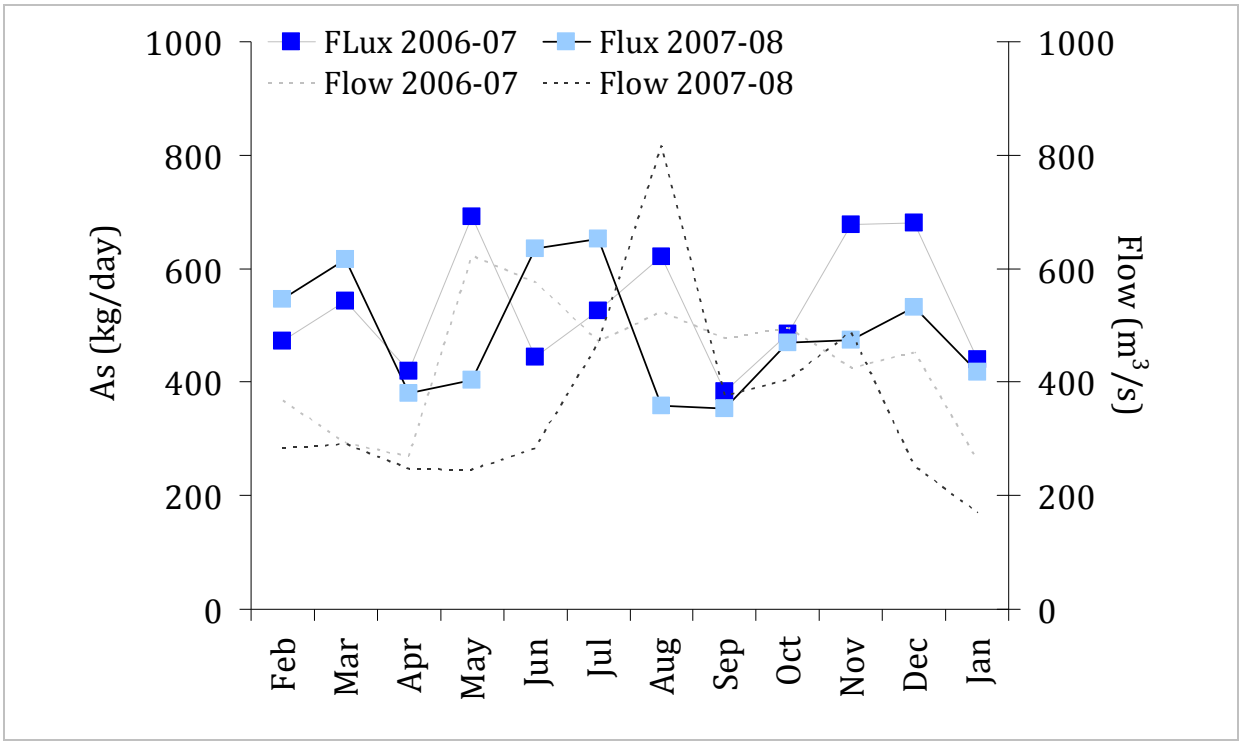

Figure 5.19 Flux data and flow data for dissolved As at Tuakau

5.4.2 SEASONAL CHANGES IN Sb PARTITIONING AT TUAKAU

The peaks in Sb and As flux do not appear to be correlate to similar changes in SPM composition. There is no clear pattern for concentrations of either metalloid SPM, based on the results presented in Figure 5.20, although these data are somewhat compromised by the lack of data for the peak in May 2006, and a large amount of analytical error for the Sb data. There is a peak in SPM concentrations of both Sb and As in July 2007, but metalloids SPM concentrations were lower in June than they were in May. The peak for As in November 2006 coincided with the maximum concentration of SPM-Fe (4.9 g/kg).

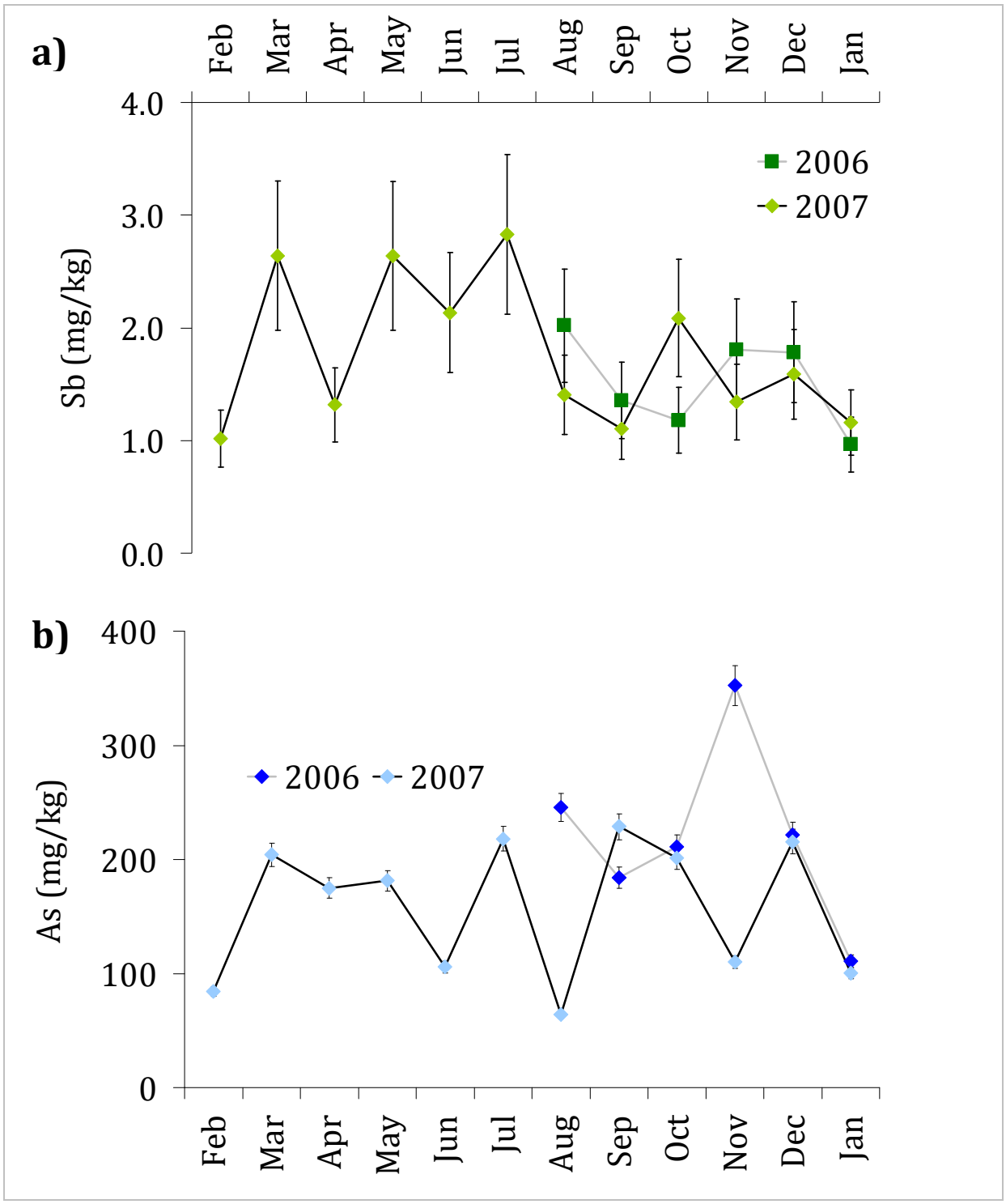

Figure 5.20 Concentrations of a) Sb and b) As in SPM collected from Tuakau

Calculated k_d values, presented as $\log_{10}$ values in Figure 5.21, provide further evidence for increased adsorption of both metalloids during winter. The pattern over time for Sb is somewhat unclear (Figure 5.21a), in part because of the large inherent errors associated with the Sb-SPM analyses. Competition with other elements may also be a factor. For As (Figure 5.21b), increases in k_d during winter months are more obvious, as are the subsequent decrease in k_d over summer, in keeping with the findings of Webster-Brown and Lane (2005a). When $\log_{10}$ k_d values for both metalloids are plotted against SPM Fe concentrations (Figure 5.21c), the results, similar to those presented in Section 5.3, show that there is a general pattern of increasing k_d values with increasing concentrations of Fe within river SPM. There was no relationship between dissolved As concentrations and SPM Fe concentrations, also in agreement with Webster-Brown and Lane (2005a). It is again evident that As is the more readily adsorbed metalloid, because the changes in k_d with Fe-SPM content for As are significantly greater than those for Sb.

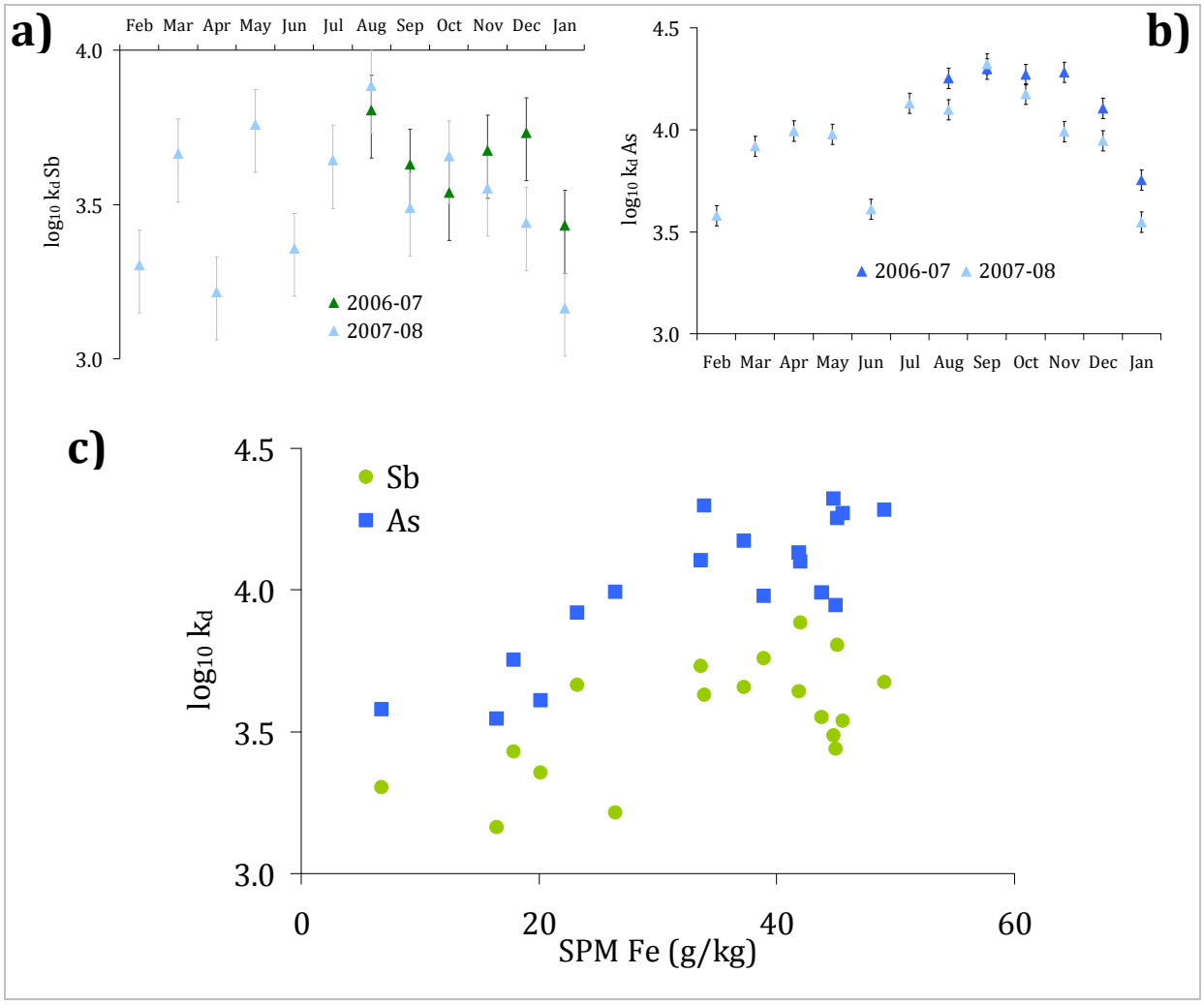

Figure 5.21: $\log_{10}$ k_d values plotted against time for a) Sb and b) As, and c) plotted against SPM-Fe concentrations for both metalloids.

COMPARISONS BETWEEN Sb, AS AND Li AT TUAKAU

In the previous section, the linear relationship between Sb and Li along the length of the Waikato River, indicated the behaviour of Sb in the river was predominantly conservative behaviour. The flux data presented in Figure 5.18 provided further evidence for conservative behaviour, but the source of the peaks in Sb (and As) flux do not appear to be related to changes in SPM content. Analysis of Li data can be used to determine if the observed peaks were instead the result of increased inputs of upstream geothermal fluids.

The data presented in Figure 5.22a, shows dissolved Sb concentrations plotted against Li concentrations, the results can be split into two distinct clusters, with the three Sb flux peak values of May 2006 and June/July 2007 separate from the main set along with two other outliers. The data in this splinter group are characterised as having elevated Sb concentrations relative to Li, and suggest a specific release of Sb somewhere upstream. The other two outliers were for April 2007 and January 2008, during which time Sb concentrations were relatively high, but Sb fluxes were unexceptional.

For As, as shown in Figure 5.22b, a relatively strong correlation between all dissolved As concentrations and the Li concentrations was observed at Tuakau (R^2=0.81). The As flux peak data (black circles) are effectively indistinguishable from the rest of the results, and this implies that increased geothermal inputs cannot be ruled out as an explanation for the peaks observed in As flux.

It appears that, while Sb exhibits predominantly conservative behaviour in the Waikato River, that there are occasions when the amount of Sb in the river increases independent of changes in geothermal input contributions. Of the conceivable mechanisms for such contributions, two seemed more likely that the rest. Antimony could be released from dying macrophytes (aquatic plants), either during dam clear-outs or because of cold conditions, or Sb in lake sediments is being remobilised. Both scenarios will be discussed later in this chapter.

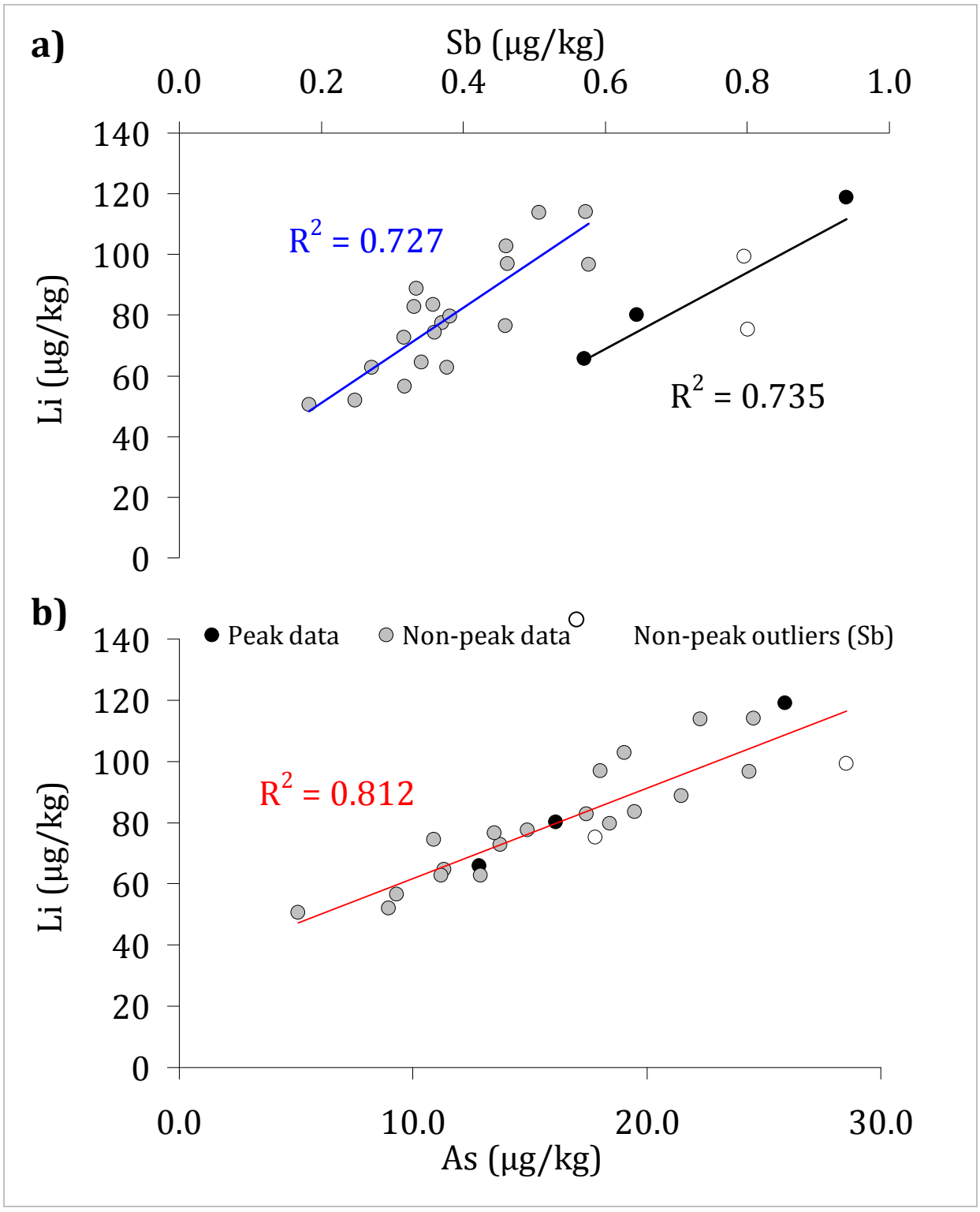

Figure 5.22: Correlations between a) dissolved Sb concentrations and b) dissolved As concentration and Li concentrations at Tuakau

5.5 ADSORPTION PROCESSES IN THE WAIKATO RIVER

Before the behaviour of Sb in lakes and lake plants is discussed, it should be acknowledged that there are gaps in the scientific literature regarding how dissolved Sb species react with solid sediment phases, as discussed in Chapter One (Filella et al, 2002b). One aspect for which no data is currently available is for the adsorption of dissolved Sb onto natural SPM. The published work so far has focussed on Sb adsorption onto bed sediments (Li et al, 1984) or flood-plain soils (Tighe et al, 2005b), but there is no information for dissolved Sb interactions with the solid phase it is most likely to encounter in the aquatic environment. In order to address this imbalance, Sb adsorption experiments were conducted using Tuakau SPM.

Samples of Tuakau SPM were collected in August 2003 (winter) by Vincent Lane and in November 2006 (spring), by the author, by filtering 20-40 L of collected water, air-drying and then freeze-drying the sediment. The general characteristics of the 2006-2008 Tuakau SPM and the winter 2003 SPM are shown in Table 5.8. The results show that the 2003 winter SPM contained concentrations of Sb and As comparable to that measured in 2006-08, and was therefore valid for use in the experiments. Because there was more winter SPM collected than spring SPM, the winter SPM was also selected for a sequential extraction, in order to characterise how naturally adsorbed Sb was bound to the material.

Table 5.8 Typical characteristics of Tuakau SPM (n=18). There was insufficient sample to measure Fe and Mn in winter SPM, n/m = not measured

	Sb (mg/kg)	As (mg/kg)	Fe (wt %)	Mn (wt %)
Mean	1.7 ± 0.8	180 ± 30	3.4 ± 0.5	0.23 ± 0.04
Maximum	2.8	350	4.9	0.38
Minimum	1.0	64	1.35	0.13
Spring SPM	1.3	110	4.40	0.13
Winter SPM	1.0	190	n/m	n/m

5.5.1 SEDIMENT CHARACTERISATION

The results of the sequential extraction and single organic/sulfide extraction of winter SPM are presented as Figure 5.23. The Sb bound to the easily exchangeable fraction (specific and non-specific sorption) was minor, accounting for just 2 % of the total Sb bound, and only a further 7 % was bound to organic or sulfide binding sites.

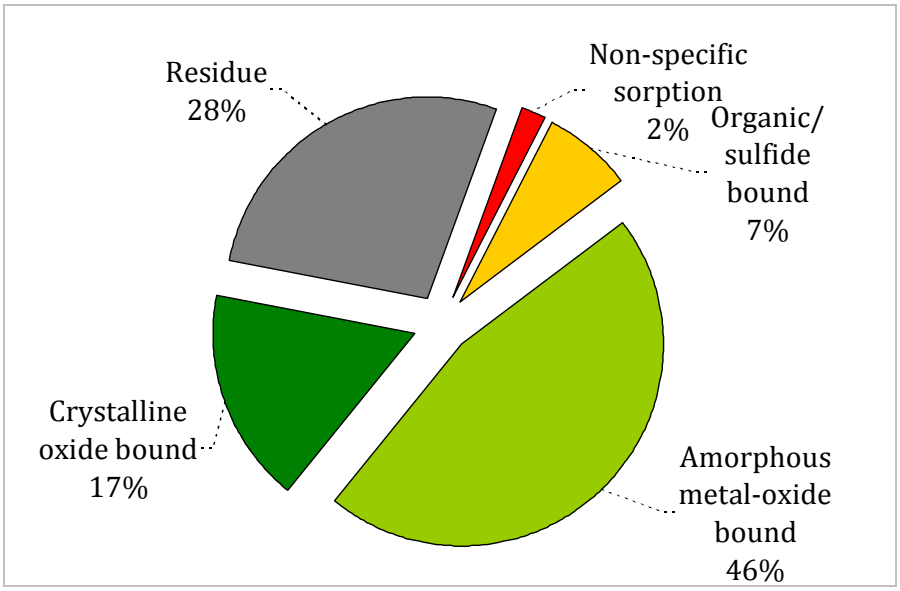

Figure 5.23 Sequential extraction of winter SPM collected at Tuakau

Most of the Sb in the winter SPM is bound to metal (predominantly Fe and Mn) oxide sites, similar to results found for estuarine and anaerobic bed sediments in the United States (Brannon and Patrick, 1985; Crecelius et al, 1975), and river sediments in Europe (Leleyter and Probst, 1999). The origin of the bound Sb (geothermally derived or otherwise) appears to have little effect on how aqueous Sb is eventually bound onto solids, and therefore it is likely that the adsorption edges developed for Waikato River SPM collected at Tuakau should be able to be applied elsewhere.

5.5.2 ADSORPTION ONTO TUAKAU SPM

The first set of adsorption edges were measured over a 24-hour period, using the method described in Chapter Two. The results are shown in Figure 5.24.

The first thing to note is that Sb^{III} adsorption onto Waikato River SPM, which is in agreement with the results for Sb^{III} adsorption onto metal-oxyhydroxides reported by Thanabalasingam and Pickering (1990), is much higher than Sb^{V} adsorption onto similar SPM. It is reasonable to assume then most of any dissolved Sb^{III} that reaches the Waikato River will adsorb to SPM and eventually be removed from the water column. However, given that Sb^{III} is typically a minor constituent of the total Sb in oxic waters, and that Fe- and Mn-oxyhydroxides have been shown to oxidise Sb^{III} species to Sb^{V} species (Belzile et al, 2001), such a removal process is unlikely to ever be that significant in natural oxic waters (Filella et al, 2002a).

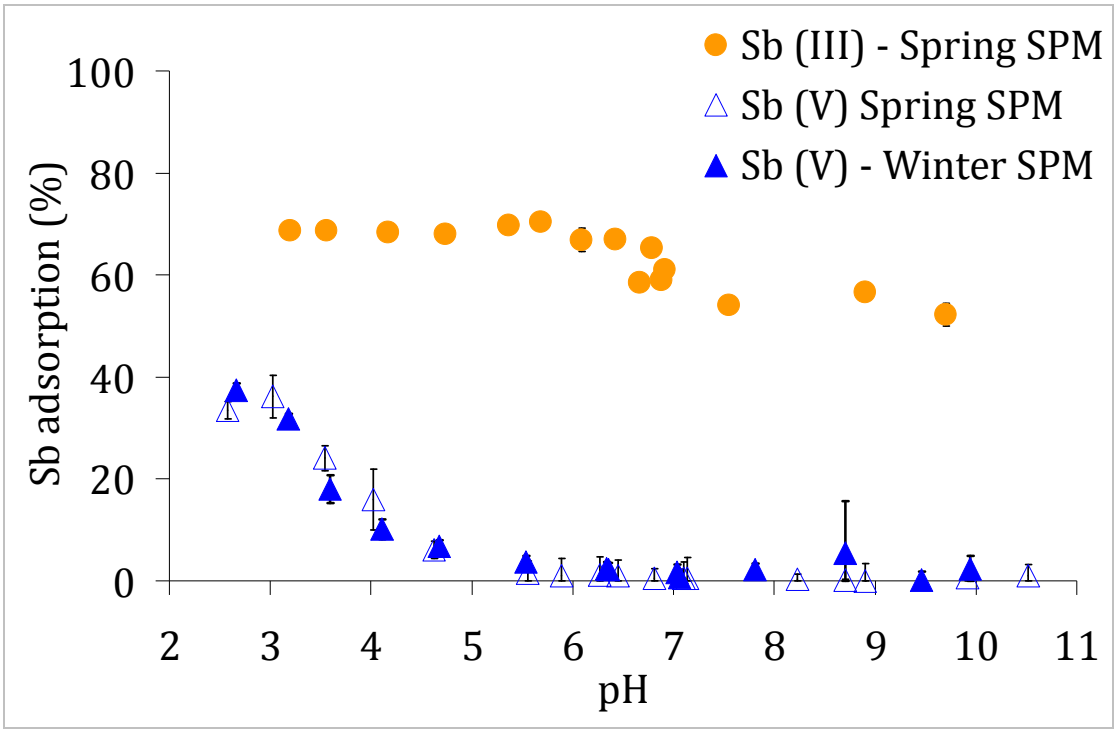

Figure 5.24: Adsorption of Sb onto Tuakau SPM. Error bars represent analytical error.

Secondly, for Sb^V there were no significant differences between results for winter SPM and spring SPM nor was there evidence for any adsorption of Sb^V above pH 5. This may explain, in part, why aqueous Sb behaves conservatively in natural waters, because conditions in freshwaters such as the Waikato River (pH 6-8) simply do not favour adsorption onto Fe or Mn oxide surfaces in the SPM. The results of the adsorption experiment also explain why there were significant levels of particulate Sb in the upper reaches of Waiotapu Stream, where pH < 5. McComb et al (2007) investigated the adsorption of Sb^V onto amorphous iron oxide and found that maximum adsorption occurred at pH ≤ 3, so it is likely that the adsorption observed for Tuakau SPM is also onto amorphous Fe hydroxides.

A scenario that also needed to be considered was whether Sb adsorption to SPM might be a slow process, and that 24 hours may not be enough time for the system to reach equilibrium. Such a question was valid, given the lack of information available for Sb despite McComb et al (2007) reporting Sb adsorption reaching a maximum in less than two hours (using amorphous iron oxide at pH 3). The scenario was also important because the results of the 24 hour experiment were not consistent with findings in the previous sections, where winter k_d values were higher than in other seasons.

In order to measure the rate of adsorption, two 10 day experiments were set up. In the first experiment, the pH of samples was fixed at ~3, where maximum adsorption had been shown to occur. In the second, the pH of samples was fixed at ~7, where no adsorption had been observed, and which represented conditions more typical of the Waikato River.

The results of the timed experiment, shown in Figure 5.25, indicate that Sb adsorption onto Waikato River SPM reaches equilibria at pH 3 in about 5 days (120 hours), much slower than for synthetic iron oxide adsorption surfaces (McComb et al, 2007). At pH 7, if adsorption onto natural SPM was occurring, it took at least 7 days (168 hours) to occur, and that the degree of adsorption (< 10 %) may explain why the differences in k_d between summer and winter reported in the previous sections are slight. Unfortunately, a lack of SPM meant that the experiment could not be re-run, but overall the results do appear to confirm that Sb adsorption at neutral pH is not a significant process. Additional adsorption after 24 hours was minor, but given the residence time of water in the Waikato River is in the order of 4-6 weeks (Lam, 1981), the results of the experiments can be reconciled with the results for Sb distribution coefficients (k_d) presented elsewhere in this chapter.

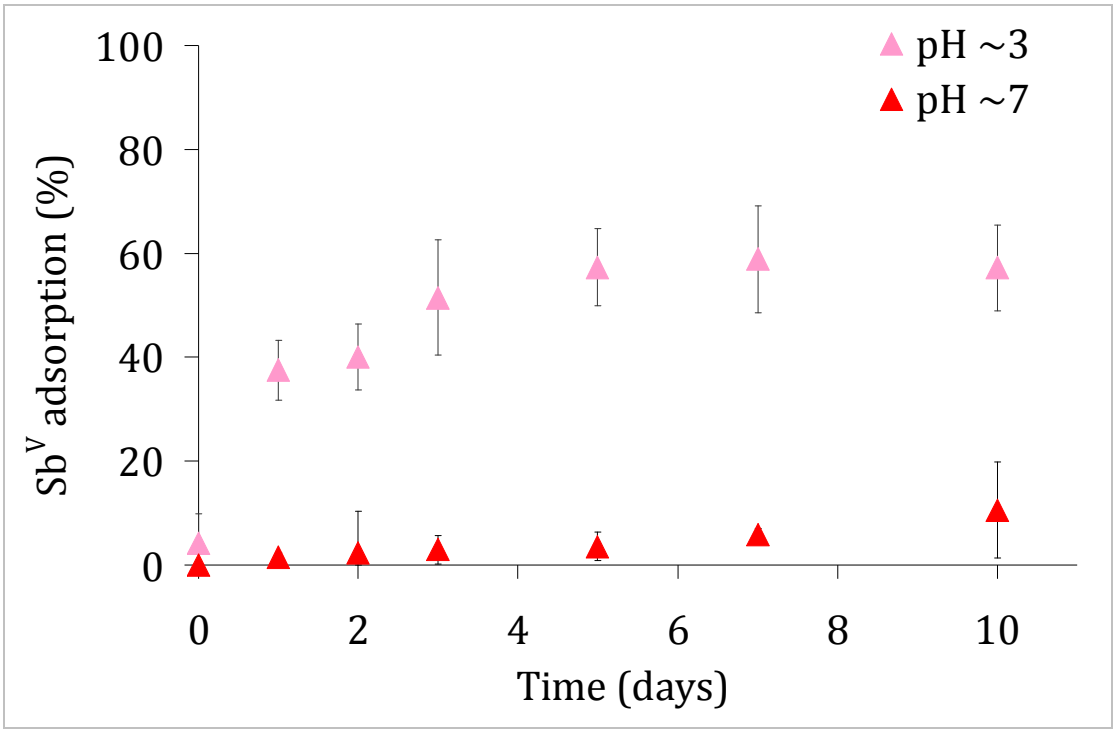

Figure 5.25: Adsorption of Sb^V with time using Tuakau SPM

Above pH 2.7, antimonate dissociates from H_7SbO_6 to form $H_6SbO_6^-$ (Jain and Banerjee, 1961), and because the antimonite molecule carries a negative charge, adsorption to positively charged surfaces would be expected. However, Leuz et al (2006) argue that $H_6SbO_6^-$ may form ion pairs with alkali metals[6], and this could explain why adsorption decreases above pH 5, well before the surface charge on amorphous Fe oxide changes from –ve to +ve, ~pH 7-8 (Dzombak and Morel, 1990). There is no data in the MINTEQ or SOLTHERM databases for Sb ion pairs.

Adsorption of Sb^V to goethite decreases from pH 6-7 upwards (depending on ionic strength), and Sb^V adsorption to amorphous iron oxide decreases with pH, at pH > 3 (Leuz et al, 2006; McComb et al, 2007). It is therefore conceivable then that even weak ion pairing in more complex systems (such as freshwaters) is sufficient to prevent Sb^V adsorption to SPM.

The results of this study do not entirely agree with those shown for the adsorption of dissolved Sb onto humic acids, Fe-oxyhydroxides, or mine-derived flood plain soils presented by Tighe et al (2005b), for which selected results are shown in Figure 5.26. However, Tighe et al (2005b) used much higher concentrations than those ever likely to be present in a system like the Waikato River (28 – 11300 μg/kg Sb in solutions with suspended solid concentrations between 400 and 50 000 mg/kg), and do present a pattern of decreasing adsorption with decreasing Sb(V) concentrations.

Buschmann and Sigg (2004) showed that dissolved Sb^{III} will adsorb to humic acids at pH > 6 in laboratory conditions. However, it has been shown elsewhere that binding of dissolved Sb^{III} to humic acids is only significant if Sb^{III} concentrations are greater than 10 μM, the equivalent of ~1.2 mg/kg Sb (Oelkers et al, 1998), orders of magnitude higher than the observed Sb concentrations in freshwaters studied in this research.

Arsenic, in comparison, exhibits different degrees of adsorption to Tuakau SPM depending upon the season (Hegan, 2005), and a comparison between Sb and As adsorption is shown in Figure 5.27. Apart from the affects of increasing Fe contents in the SPM, as described in this chapter and elsewhere by Webster-Brown and Lane (2005a), the relative abundance of the species *Asterionella formosa* appears to also play a part in how As adsorption occurs in the Waikato River (Hegan, 2005).

[6] Leuz et al (2006) used $KClO_4$ to control ionic strength, so reported ion pairs with K^+. In the case of the Tuakau experiments, the ion pair would presumably form with Na^+.

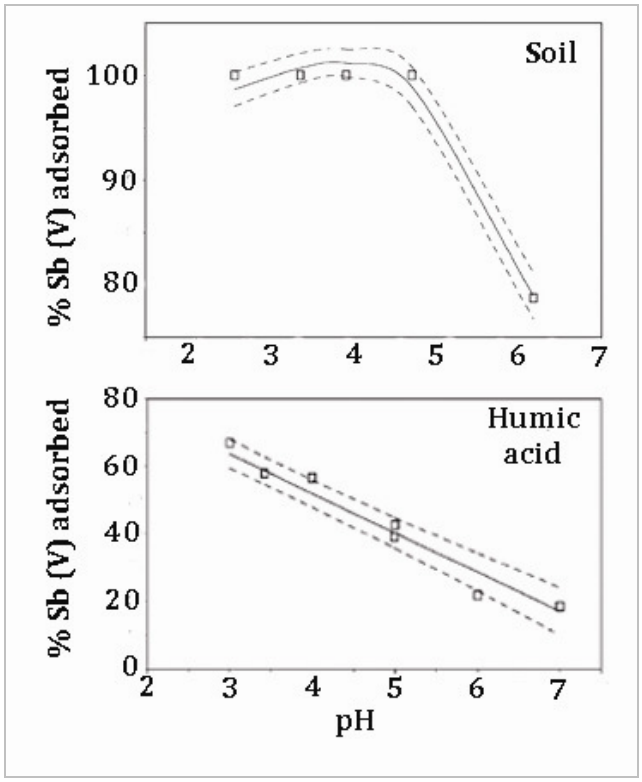

Figure 5.26 Results of Sb (V) adsorption experiments (Sb concentration 28.25 µg/kg), adapted from Tighe et al (2005)

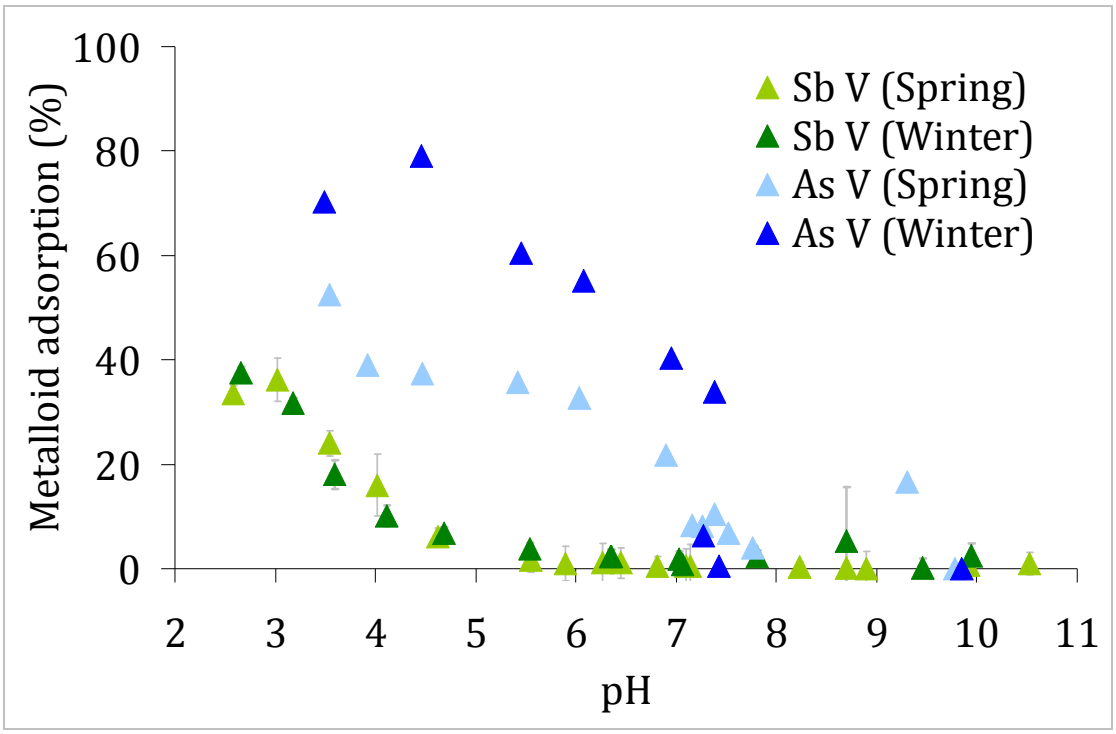

Figure 5.27 Comparisons between dissolved Sb^V and As^V adsorption to Waikato River SPM. Results for As adsorption from Hegan (2005)

5.6 LAKES ALONG THE WAIKATO

The series of hydro-electric dams along the Waikato River, marked on Figure 5.28, has not only affected the aesthetic character of the river, it has also changed the sediment loading and water chemistry (Coulter et al, 1983). The changes in water chemistry occur particularly in late summer when, if conditions are suitable (high temperatures, low rainfall and low wind), the lakes begin to stratify (Bilinska, 2005). The deepest lakes along the Waikato, and therefore the lakes most likely to stratify, are Maraetai (68 m), Arapuni (49 m) and Ohakuri (40 m). Of these, Lake Ohakuri is the only lake with a documented history regarding its stratification, stretching back at least as far as 1970 (Magadza, 1979).

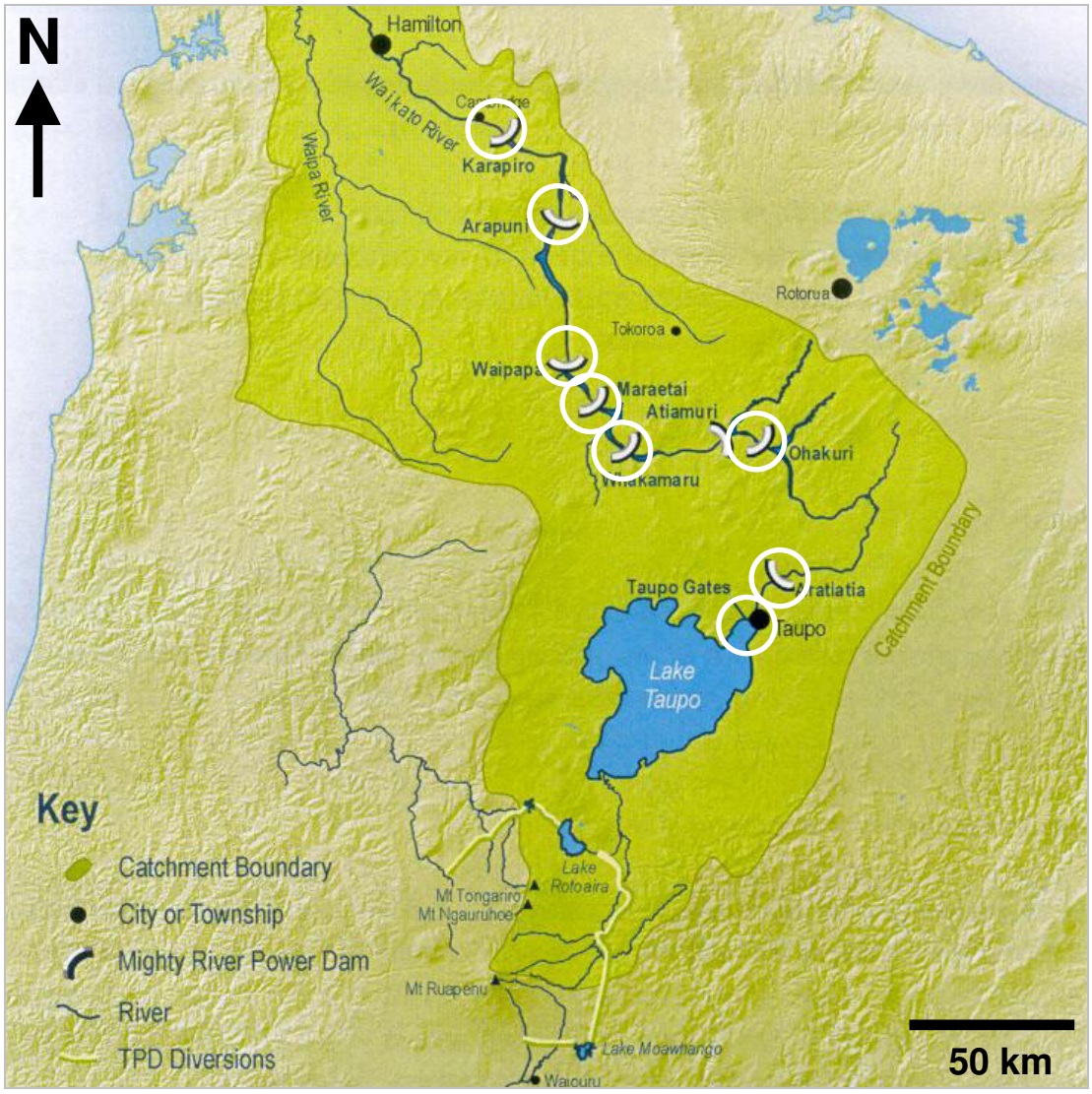

Figure 5.28 Map of the Waikato River, with the eight lakes used in this study circled in white. Map adapted from Mighty River Power (2001).

One of the more interesting phenomena produced by lake stratification is the development of an oxygen depleted, chemically-reducing layer at the bottom (Aggett and O'Brien, 1985). The change in conditions in, for example Lake Ohakuri (shown in Figure 5.29), results in the release of Fe and Mn from the sediments, and any elements previously entrained with them (such as As) are released at the same time (Aggett and Roberts, 1986). The consequence of this should be that when the lakes turn over there is a "pulse" of water downstream with elevated concentrations of such elements. However, the turnover process occurs over a matter of days at most, and therefore predicting turnover is not trivial. Such a pulse may have been responsible for the increased As concentrations in the Waikato River reported in April 1998 by Webster-Brown and Lane (2005b).

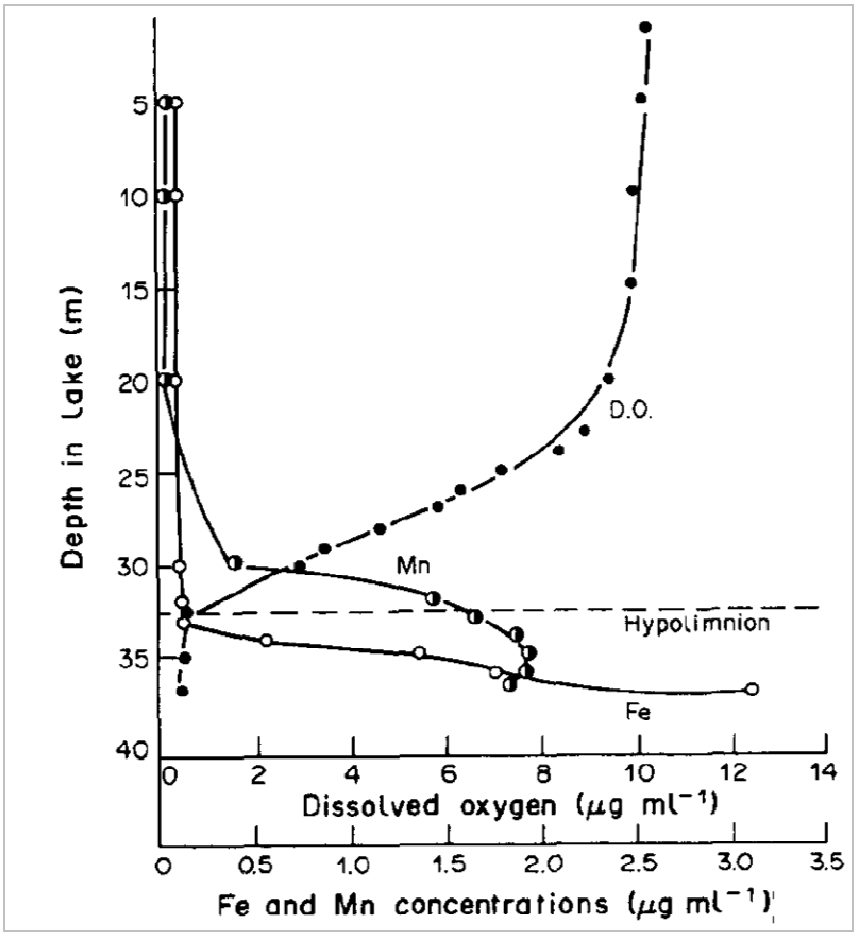

Figure 5.29 The effects of lake stratification upon DO, Fe, and Mn concentrations (from Aggett and Kriegman, 1988)

The "pulse" hypothesis could explain the observed flux peaks for Sb in late autumn (May 2006) at Tuakau. The possibility of lake turnover causeingthe Sb flux peak in June/July 2007 is less likely, given that lake turnover usually occurs in mid-late autumn (Bilinska, 2005), and would require an unusual set of climatic conditions.

In order to examine this theory, Lake Ohakuri, along with Lakes Maraetai and Arapuni, were sampled in March 2007. The three lakes were chosen because they were the three lakes most likely to stratify, being the three deepest lakes, and the lakes with the longest retention times (Bilinska, 2005). At the same time, bed sediment and macrophyte (aquatic plant) samples were collected from all the lakes except for Atiamuri, because Lake Atiamuri is essentially the overflow dam for Lake Ohakuri.

5.6.1 DEPTH PROFILES AT OHAKURI, MARAETAI AND ARAPUNI

Lakes Ohakuri, Maraetai and Arapuni were sampled at sites are close as possible to points of maximum lake depth. Accurate bathymetry data for the three lakes could not be acquired (topographic maps are included in Appendix V). The three lakes were initially sampled at three depths, (surface, 20 m and 40 m), with additional DO readings at depths between 20 and 40 m if there was any evidence for chemical stratification. Stratification was only apparent at Lake Ohakuri, as shown in Figure 5.30. Lake temperatures were warmer at the surface than they were at 40 m, but the difference was only 2 ^{o}C for Lake Ohakuri and just 0.5 ^{o}C within Lakes Maraetai and Arapuni.

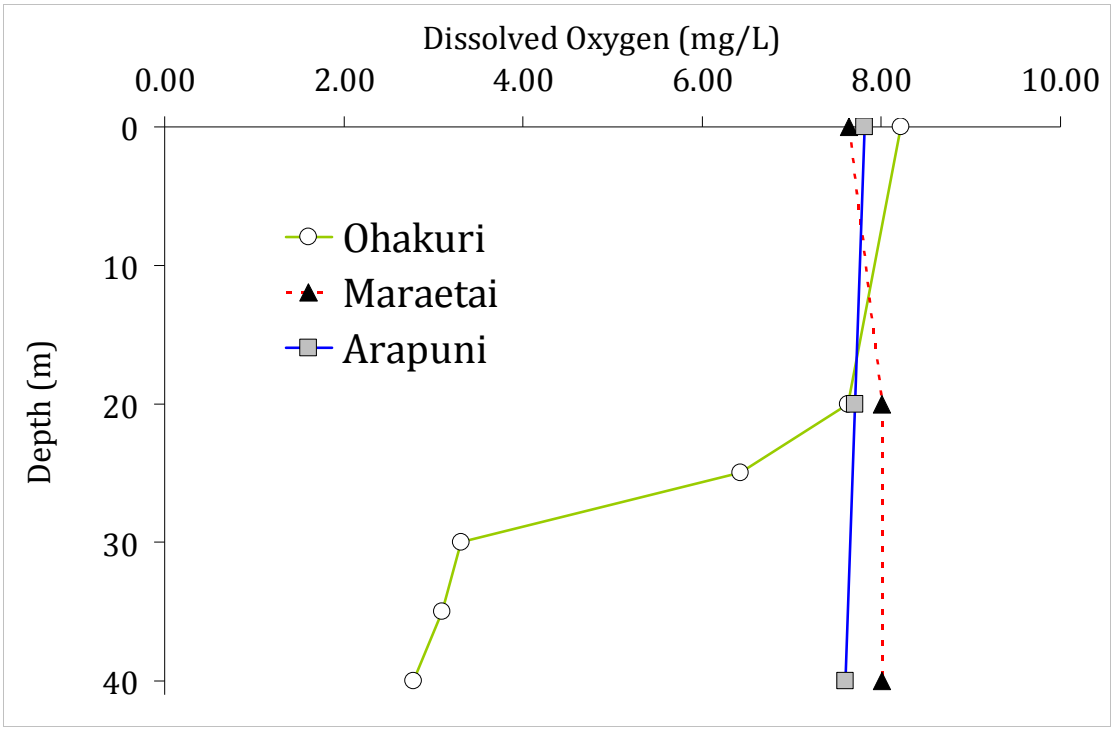

Figure 5.30 DO concentrations with depth at the three lakes studied on the Waikato River

Having established that Lake Ohakuri might be stratified (and that the other two were not), it had been expected that at the bottom of Lake Ohakuri there might be an increase in Sb concentrations. The results shown in Figure 5.31 suggest otherwise, with Sb concentrations decreasing below 20 m not just in Lake Ohakuri, but in Lake Maraetai as well.

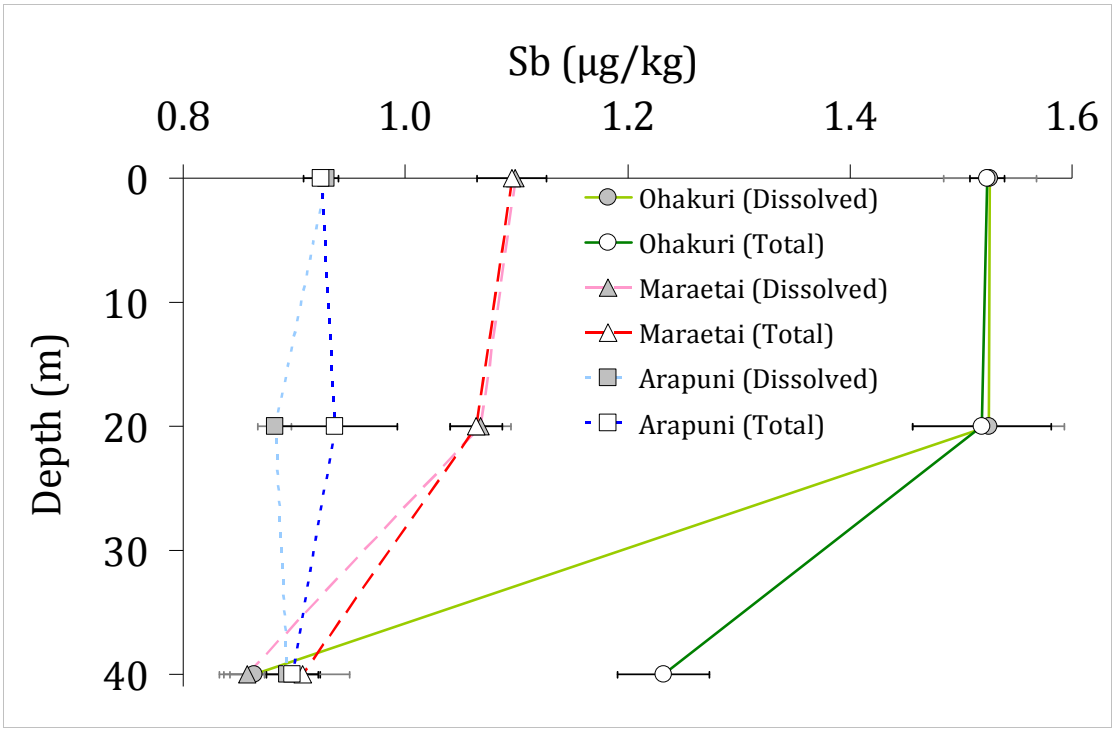

Figure 5.31 Sb concentrations with depth in the three Waikato lakes.

Dissolved Sb concentrations can be compared with the depth-profile concentrations of other elements (As, Fe and Mn), as shown in Figure 5.32. It is clear that the behaviour of Sb is different to these elements: Fe and Mn are being released from Fe- and Mn-rich sediments in Lake Ohakuri, and also perhaps in Lake Maraetai. There is also evidence of a slight increase in As concentrations at the bottom of Lake Ohakuri. Rather than being released from sediments into oxygen-depleted lake waters, it appears that Sb is removed from solution instead.

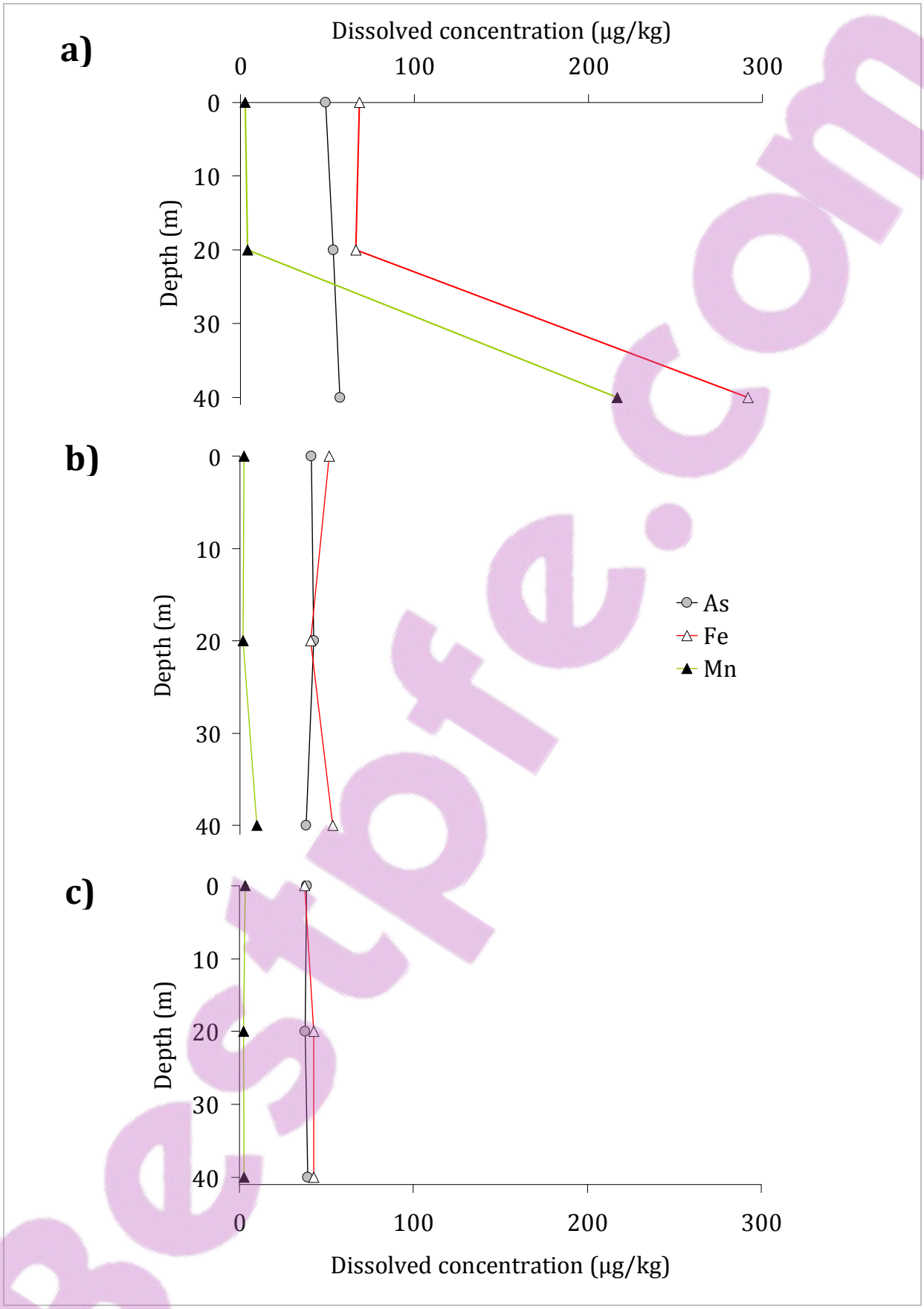

Figure 5.32 Dissolved element concentrations measured at a) Lake Ohakuri, b) Lake Maraetai and c) Lake Arapuni

ANTIMONY REMOVAL PROCESSES IN LAKE WATERS

Adsorption of Sb^{III} is a mechanism that would explain this phenomenon. The results from Section 5.5 show that Sb^{III} will adsorb to Waikato SPM even at neutral pH, and the chemically reducing conditions of an oxygen-depleted environment may mean that Sb^{III} species could become dominant. Unfortunately, logistical problems caused by a laboratory relocation at the University of Auckland meant it took two months before filtered samples of lake water could be analysed, and by then no Sb^{III} was detectable. However, modelling of the system using PHREEQCi and the MINTEQ v.4 database (updated with the Sb_2S_3 data discussed in Chapter Three) predicts that dissolved Sb at the bottom of Lake Ohakuri should be present as Sb^{III}; the S^{-2}/S^{+6} redox couple was used to estimate redox conditions.

However, what would the Sb^{III} be adsorbing onto, if Fe oxides in the bottom sediment were dissolving in the anoxic conditions? While enough oxide material may have been dissolved to cause significant increases in the dissolved concentrations of Fe and Mn, concentrations of Fe in bottom sediment may still remain high, and removal of the surface layer of the oxides may expose oxide layers underneath with more potential binding sites. Furthermore, while particulate Mn only made up 20 % of the total Mn at the bottom of Lake Ohakuri, 80 % of the Fe in the water column was particulate (1.4 mg/kg), and with plenty of suspended material available for Sb^{III} to adsorb onto, the nature of the bed sediment may not be as critical as it might first appear.

A second removal mechanism may be the precipitation of Sb as Sb_2S_3. Trace amounts (24 µg/kg) of sulfide species (as H_2S) were also detected at the bottom of Lake Ohakuri[7]. Even this low concentration is sufficient for PHREEQci to predict an approach to Sb_2S_3 saturation conditions ($\log_{10}SI$ = -0.24 using surface water Sb concentrations, and -0.47 using Sb concentrations from 40 m deep). Whether such precipitation was actually occurring could not be tested, as the amount of Sb_2S_3 produced would be too small (ng/g or pg/g total sediment) to measure, or view using SEM. However, the reduction of dissolved Sb^{V} to Sb^{III}, leading to Sb^{III} adsorption to suspended Fe-oxyhydroxides or the formation of Sb_2S_3 if H_2S is present, appears to be a viable mechanism to explain the observed decline in dissolved Sb concentrations.

[7] Samples for H2S analysis were preserved using Zn-acetate, and then pre-concentrated by allowing the samples to settle and accurately removing the supernatant. The detection limit for lake H_2S samples was 0.02 mg/kg.

While a combined process mechanism can be used to explain the situation occurring at Lake Ohakuri, it does not in any way explain the decrease observed at Lake Maraetai, where there is no other evidence for stratification except for minor increases in dissolved Mn and Fe concentration at 40 m deep (Figure 5.32b). The variation at Lake Maraetai, rather than being related to chemical processes, may instead reflect the input of the Mangakino Stream, because the waters of Mangakino Stream do not have the same geothermal inputs as the Waikato River. If the stream were slightly colder than the main body of water, then it may flow into the bottom of the lake, and what was sampled from 40 m deep in Lake Maraetai was possibly Mangakino Stream water, rather than potentially stratified Waikato River water.

A plot of Sb:Li can be used to confirm this. If the Mangakino Stream had fewer geothermal influences (but increased inputs of Fe and Mn), and Lake Maraetai was not subject to any stratification processes, then a plot of Sb and/or As concentrations against Li concentrations for the lake should be linear. The results from Figure 5.33 show that such a linear relationship exists, and thus a colder input can explain the apparently low Sb concentration at 40 m deep in Lake Maraetai. Furthermore, the only points that plot off the linear line of best fit (for both elements) are the ones from 40 m deep at Lake Ohakuri, providing further evidence for Sb removal processes occurring there that are not occurring in the other lakes.

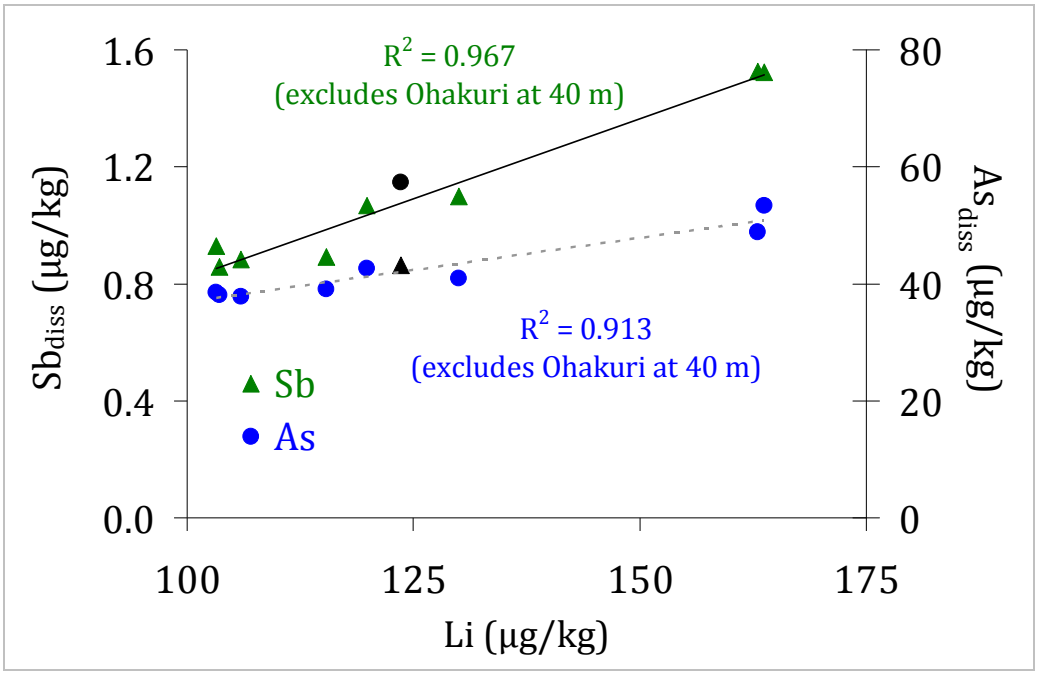

Figure 5.33 Dissolved Sb and As vs Li for Lakes Ohakuri, Maraetai and Arapuni (at all three depths). The results from the bottom of Ohakuri are marked in black.

Therefore, to conclude, a chemical removal mechanism for Sb seems likely in the stratified basal waters of Lake Ohakuri. It is conceivable that, following the re-establishment of an oxygen rich environment at the bottom of Lake Ohakuri after lake turnover, the adsorbed (and/or precipitated) Sb could remobilise and ultimately cause the peaks in Sb flux observed at Tuakau in May 2006, and perhaps June/July as well. The downstream transport of Sb-enriched SPM from Lake Ohakuri may also contribute to the flux peaks.

5.6.2 PLANT UPTAKE IN THE WAIKATO RIVER

The alternative explanation for the Sb flux peaks was the potential uptake and release from aquatic plants. Bed sediment from the Waikato River, and a sample of the most common species of macrophyte at each site were collected from the eight lakes surveyed. From Taupo to Ohakuri, *Egeria densa* (Figure 5.34a) dominated, further downstream *Ceratophyllum demersum* (Figure 5.34b) was more prevalent. Macrophytic uptake of As in the Waikato is well established (see Robinson et al (2003) or Gibbs and Costley (2000)), and the results in Figure 5.35a, which show As concentrations in the macrophyte samples collected as part of this study, are in good agreement with previous studies. Similar to the results for algae collected at Waimangu, macrophyte concentrations of Sb (Figure 5.35b) were too low to suggest that macrophyte uptake of Sb was a significant removal process.

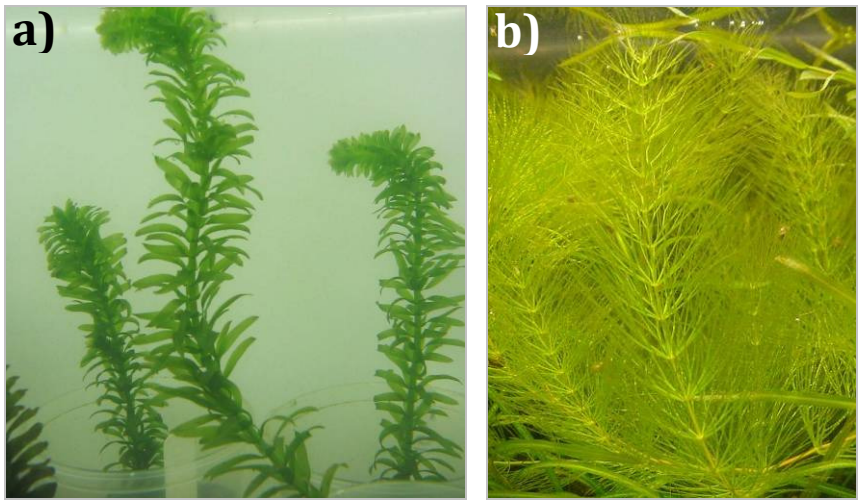

Figure 5.34 The two macrophyte species collected during the eight-lake survey: a) *Egeria densa* (photo from www.clr.pdx.edu/projects/plants/egeria.php) and b) *Ceratophyllum demersum* (photo from naturalaquariums.com/plants/ceratophyllum.html)

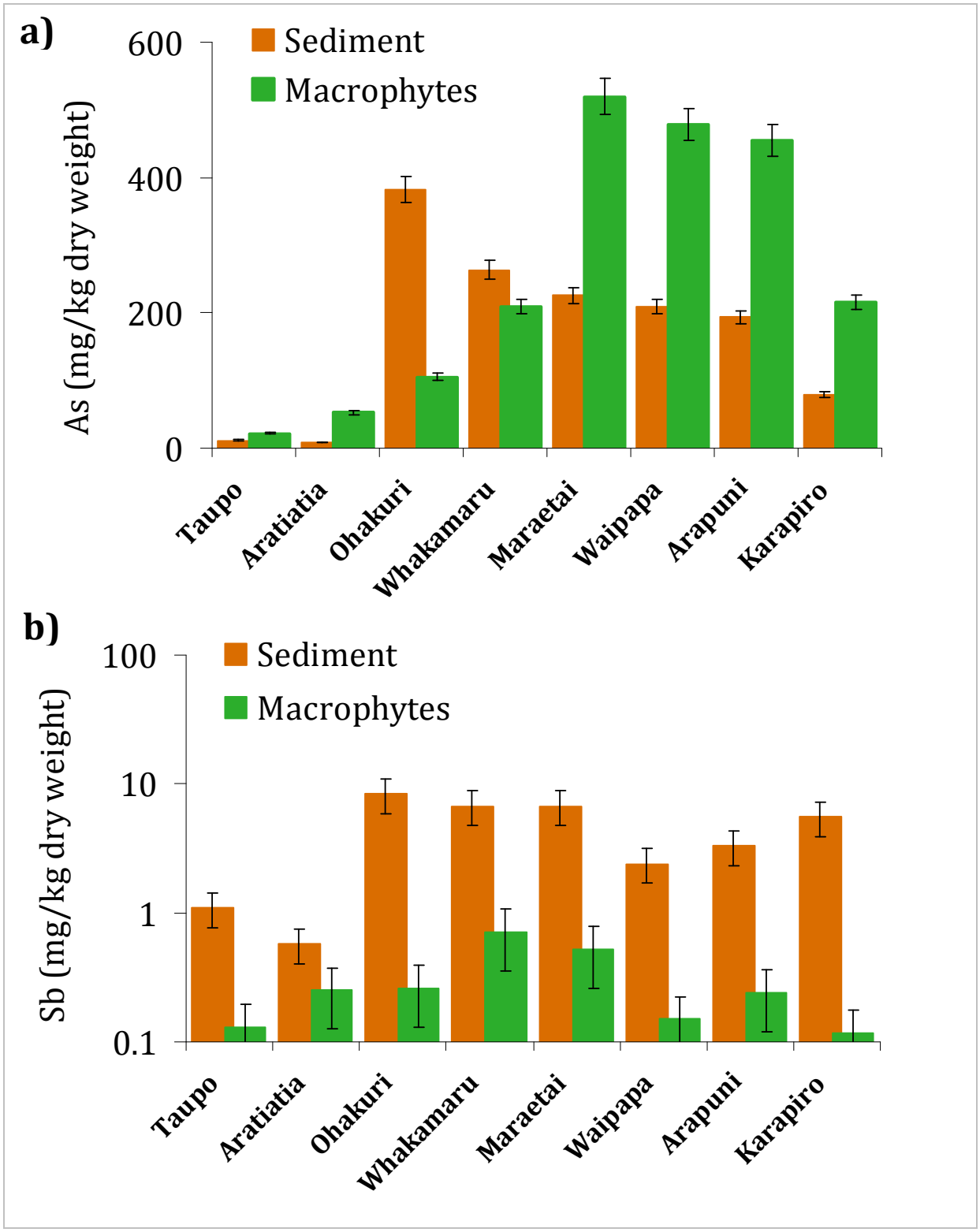

Figure 5.35 Bed sediment and macrophyte concentrations for a) As and b) Sb for the eight lakes sampled along the Waikato River

The overall bio-enrichment of Sb compared to As were calculated using the equation:

$$\frac{[M]_{macrophyte}}{[M]_{sediment}}$$

where M is either Sb or As. The results of these calculations for selected sites are presented in Figure 5.36, and show that the enrichment of As in macrophytes is significantly high than for Sb.

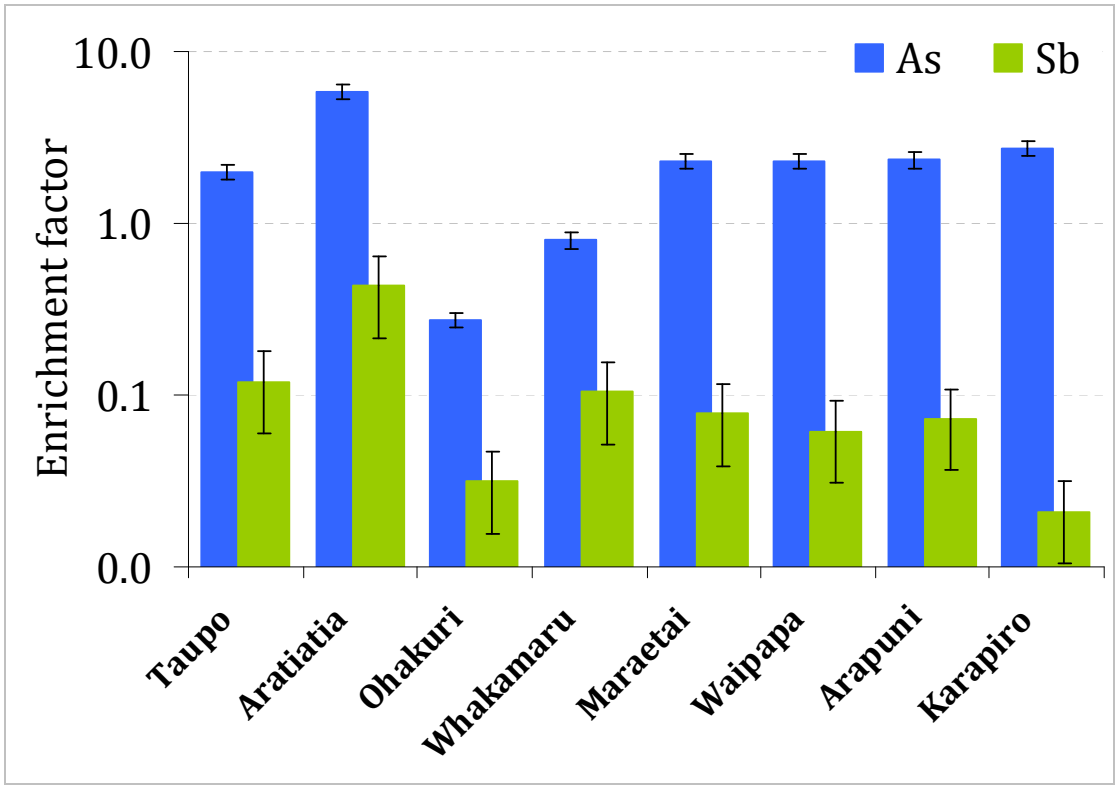

Figure 5.36 Enrichment factors for As and Sb in the Waikato River.

Therefore, based on the evidence so far, lake-turnover following stratification, releasing a pulse of Sb-rich water into the river, appears to be the most likely explanation for the Sb flux peaks observed at Tuakau, and may also contribute to the As flux peaks observed as well. Antimony adsorption onto SPM is unlikely to be significant in the main flow of the Waikato River because the buffering capacity of the Waikato River is too high for such a process to occur anywhere except immediately downstream of a (very) low-pH point source. Neither is there any evidence for removal of Sb by sediments or plants.

5.7 THE PORT WAIKATO ESTUARY

The final aspect of Sb behaviour in receiving environments to be investigated was Sb behaviour in the estuary at the mouth of the Waikato River. If Sb behaves conservatively in an estuarine setting as well, it must be concluded that the Tasman Sea is the eventual sink for virtually all of the aqueous Sb produced from geothermal systems that drain into the Waikato River. There are few published studies for the behaviour of Sb in estuaries, and the consensus appears to be the element's behaviour depends upon the nature of the estuary (Filella et al, 2002a).

The first step in investigating how Sb might behave in the Port Waikato estuary was to conduct a laboratory mixing experiment. The experiment was modelled on a similar experiment for As (Webster-Brown et al, 2000). Aliquots of unfiltered Waikato River water (140 μS/cm) collected from Tuakau were spiked with $KSb(OH)_6$, and mixed with increasing amounts of unfiltered seawater (46 mS/cm) collected from the beach ~ 500 m south of site WR 15 to create a series of samples ranging from 0% - 100 % seawater. These samples were then shaken for 30 minutes, and then unfiltered, 0.45 μm filtered and 0.1 μm filtered aliquots were extracted for analysis. The results of the mixing experiment are presented as Figure 5.37a.

In the study by Webster et al (2000), it was shown that, overall, As exhibited conservative behaviour. The laboratory mixing experiment for Sb similarly suggested that dissolved Sb would behave conservatively in the Port Waikato estuary, because all the data fell on a linear mixing curve. When the estuary itself was sampled in January 2008 (the results of which are presented as Figure 5.37b), the results again plotted on a linear mixing curve. While the behaviour of Sb may be different in other estuaries, in Port Waikato dissolved Sb, similar to As, behaves conservatively.

Bed sediment and SPM data was collected for Port Waikato, on the basis that perhaps the behaviour of Sb might change according to estuarine conditions, and therefore the sediment might be enriched in Sb despite the aqueous results. At 0.8 mg/kg, Sb concentrations in Port Waikato SPM was lower than recorded at Tuakau, and while the Sb concentration of bed sediment was higher in Port Waikato (1.9 μg/g) than at Tuakau (0.8 mg/kg), Sb concentrations in bed sediment further upstream at Mercer were higher (3.3 mg/kg), so the case for Sb enrichment of estuarine sediment is a relatively weak one. A bed sediment transect from the mouth of the Waikato upstream towards Tuakau may clarify the matter, but this was not considered a high priority for this research.

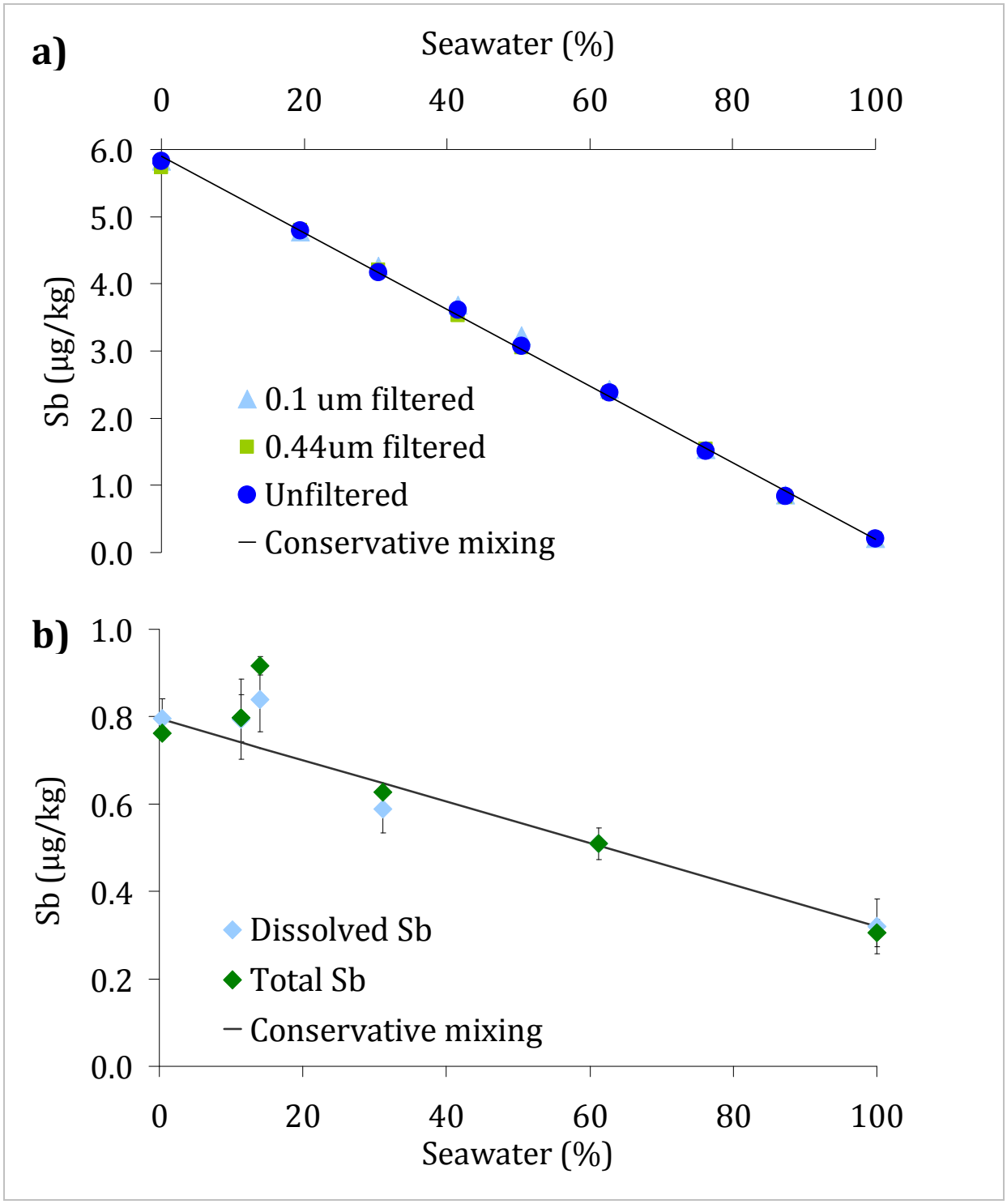

Figure 5.37: Dissolved Sb behaviour in estuarine conditions, a) the results from a laboratory mixing experiment, b) the results of sampling from Port Waikato.

5.8 OVERALL CONCLUSIONS

The two hypotheses to be tested in this chapter were:

1. In receiving environments, Sb behaves similarly to As, and therefore is subject to similar removal processes
2. In receiving environments, the behaviour of Sb is essentially conservative, and therefore, in the absence of aqueous sulfides, the element is not subject to any significant removal processes

The first hypothesis can be rejected. It is true that aqueous As and Sb behave similarly at times, and the metalloids' respective behaviour within the Port Waikato estuary is a classic example. In general terms, Sb in Waiotapu Stream and the Waikato River essentially behaves like As, but significantly more conservatively. This is best reflected in the seasonal differences in k_d values observed for both metalloids, where the degree to which k_d changed was much greater for As than it was for Sb. However, at the bottom of a stratified Ohakuri, and in their interactions with macrophytes, the behaviour of Sb and As is different.

The second hypothesis cannot be rejected outright. For the most part aqueous Sb does behave conservatively, and there is, on most occasions, a strong correlation between Sb and Li. However, the potential exists for Sb adsorption on to Fe-oxide surfaces in SPM or bed sediment, and there are seasonal peaks in Sb flux, possibly caused by lake turnover events. Therefore Sb should be considered to exhibit predominantly conservative behaviour on a drainage system scale, but accumulation of Sb onto sediment at a local scale should not be precluded.

While detectable levels of dissolved Sb in the Waikato River effectively classify the river as being Sb-impacted, from an environmental management point of view, Sb concentrations should not be a cause for concern. Antimony concentrations in the river are below even the most stringent of water quality guidelines, the Japanese drinking water limit of 2 μg/L (Shotyk and Krachler, 2007), and therefore present no known risk to human health, agriculture or ecosystems. When compared to As, which reaches concentrations in excess of 40 μg/kg, Sb is only a minor contaminant in the Waikato River.

CHAPTER SIX
SYNTHESIS AND CONCLUSIONS

> *No other Principles of Antimony have hitherto been shewn besides a metallic Regulus, and a common Sulphur. True it is, the Opinions of Authors on this Head are various and in Part ridiculous; and being but bare Opinions must certainly go for such. I own myself a professed Enemy to all abstracted Speculations in the practical Sciences, as such easily may, and commonly do, lead Men astray from the Truth and Simplicity of Nature...*[1]

6.1 INSIGHTS INTO GEOTHERMAL Sb BEHAVIOUR

In Chapter One, a series of objectives were listed. In this, the concluding chapter, each objective will be restated, and the overall findings for each will be discussed.

MODELLING STIBNITE SOLUBILITY

Objective:

- To determine factors controlling Sb_2S_3 precipitation at two New Zealand geothermal power stations, using field measurements and geochemically modelled predictions of Sb solubility.

Chapter Three focussed on the thermodynamic behaviour of Sb, and of Sb_2S_3 in particular. It was clear that the thermodynamic data for Sb_2S_3 in the databases developed by Spycher and Reed (1989b) for SOLVEQ overestimated the solubility of the metalloid. The precipitation of Sb_2S_3 in the OEC units of the Rotokawa and Ngawha geothermal power stations had been unexpected, so no-one had calculated theoretical solubility. Even if they had, it is likely that the precipitation of Sb_2S_3 would not have been predicted using this dataset.

The inherent errors in SI calculations, when combined with the assumption of equilibrium conditions that are required for modelling purposes, mean that it may always be difficult to always predict the behaviour of Sb in cooling geothermal fluids. Nonetheless, the more recent data for stibnite solubility provided by Zotov et al (2003), when converted for use in the SOLTHERM database, provided predictions for Sb_2S_3 precipitation that were more consistent with observed Sb behaviour in the Rotokawa and Ngawha geothermal power stations.

[1] Shaw, P., (1747) A Philosophical and Chymical Analysis of Antimony: Giving a Rational Account of the Nature, Principles and Properties of that Celebrated Drug. Published by Joseph Davidson, London, 90 pp, page 9.

The chemistry of geothermal fluids can be diverse, being influenced by reservoir temperature and geology. This means it should never be assumed that the behaviour of Sb in fluids used for power generation at one geothermal power station will be the same as for another on a different geothermal field. At Ngawha for example, the mixing of acidic condensate with separated brine is relatively inconsequential, because temperature change is the driving force for Sb_2S_3 precipitation. At Rotokawa, the mixing of condensate and brine plays a much more important role because the condensate is condensed at high pressure, and therefore contains high H_2S and has low pH.

A useful outcome of this work is that the new data for Sb_2S_3 equilibria (Zotov et al 2003) provides a better fit with actively occurring phenomena, and has been successfully tested against field observations. Therefore, these data from Zotov et al (2003) should be incorporated into the databases used by thermodynamic modelling software such as SOLVEQ or PHREEQ to allow more reliable prediction of Sb2S3 scaling in geothermal power station pipelines.

REMOBILISATION OF Sb IN SURFACE GEOTHERMAL ENVIRONMENTS

Objective:

- To investigate whether Sb that has precipitated in surface geothermal features at Wai-O-Tapu and Waimangu can be remobilised, and, if so, to determine the mechanisms and the conditions required for mobility.

Pope et al (2004) reported diurnal fluctuations in Sb concentrations in the drainage from Champagne Pool in the Wai-O-Tapu geothermal field during a single winter sampling event. This was intriguing, but it was unknown how widespread or frequent such variability might be. In Chapter Four, the evidence presented showed that these apparent daytime fluctuations in Sb (and As) concentrations in the discharge from Champagne Pool occurred in winter and summer. It also confirmed that this phenomenon may not occur downstream of all Sb-rich geothermal springs, as daytime variations in Sb concentrations did not occur downstream of Frying Pan lake in the Waimangu geothermal field.

A hypothesis was proposed to explain the phenomenon observed in the discharge from Champagne Pool. This hypothesis, as yet untested, proposed that sulfide-sulfate equilibria controls the amount of Sb remobilised from stibnite, with sulfide-sulfate equilibria partly controlled by biotic processes.

According to the hypothesis, when there is enough solar radiation and it is warm enough, algae and bacteria photosynthesise, producing oxygen, and other bacteria catalyse the oxidation of HS^- into SO_4^{2-}. This would mean that previously over-saturated sulfide-minerals, such as Sb_2S_3, redissolve as the concentration of HS- decreases and elements such as Sb are released into the discharge fluids.

The proposed process would not be not instant, instead Sb would be gradually released into solution until the middle of the afternoon. In darkness, when oxygen production ceases, and the system becomes more reducing and HS^- rich, the rate of release of Sb from Sb_2S_3 slows.

The daytime Sb concentration changes observed at Wai-O-Tapu do not occur in the discharge from Frying Pan Lake at the Waimangu geothermal field. In the Frying Pan Lake discharge, the water temperatures are constantly warm and dissolved oxygen concentrations are relatively high. This means the sulfide-sulfate equilibrium does not vary in the same way.

In summary, changes sulfide-sulfate equilibria are likely to be a significant factor determining how much Sb is remobilised from precipitated Sb_2S_3 in any given surface geothermal feature. The role of algae and bacteria in the remobilisation of Sb (and other metalloids) may be an indirect one, mainly influencing Sb_2S_3 solubility through changing DO concentrations and catalysing aqueous sulfide oxidation processes.

THE FATE OF Sb FROM GEOTHERMAL SPRINGS IN RECEIVING ENVIRONMENTS

Objective:

- To assess the significance of geothermal Sb contributions to receiving (non-geothermal) environments downstream of Wai-O-Tapu and Waimangu and to determine what, if any, natural processes exist to remove geothermally-derived dissolved Sb.

The discharges from both Champagne Pool and Frying Pan Lake contain elevated levels of Sb. However the nature of the downstream environment is critical when determining how much aqueous Sb is transported away from there. At the Wai-O-Tapu geothermal field, the acidic and anoxic Alum Lake appears to remove nearly all of the Sb remobilised from the Champagne Pool discharge, and therefore Sb contributions from Champagne Pool to the greater receiving environment are minor. At Waimangu, minor adsorption of the element occurs in the lower reaches of Hot Water Stream, but most of the aqueous Sb produced from Frying Pan Lake reaches Lake Rotomahana, after which the element's eventual fate is not known. There is no evidence to suggest that the algae growing in the discharge from Frying Pan Lake take up Sb to any significant degree.

In the downstream receiving environments of Waiotapu Stream and later the Waikato River, there are few processes operating to remove dissolved Sb. The relatively low pH waters of some geothermal tributaries are likely to enhance the degree of Sb adsorption onto SPM. Similarly, the anoxic bottom layers of stratified lakes on the Waikato River may convert the generally conservative Sb^{V} into more readily adsorbed Sb^{III}. There is also evidence that Sb adsorbtion onto natural SPM in the river is controlled, in part, by the Fe content of the adsorptive material. However, in neutral pH, oxic waters, such as the main flow of the Waikato River, adsorption is likely to be a minor process.

There is no evidence for any bio-accumulation of Sb in the macrophytes that grow within the Waikato River hydroelectric-dams, nor is there evidence of any accumulation of Sb in the bed sediments. Dissolved Sb appears to behave conservatively in the Port Waikato estuary, so it may therefore be concluded that any dissolved Sb discharged into the Waikato River will be eventually transported to the ocean.

Overall, the significance of geothermally-derived aqueous Sb contributions to the wider receiving environment is once again dependant on the pH of the receiving waters and their redox state. Dissolved Sb from geothermal discharges will be removed from low pH and reducing environments, but in neutral pH and oxic receiving environments, geothermally-derived Sb exhibits generally conservative behaviour.

ANTIMONY AND ARSENIC: A COMPARISON OF BEHAVIOUR

Objective:

- To compare the behaviour of geothermal Sb to that observed for geothermal As, and to determine under what circumstances the two metalloids might behave distinctly differently, and when the two might behave in a similar manner.

Geothermal Sb and As are derived from similar geothermal sources, and the diurnal remobilisation of Sb observed in the discharge from Champagne Pool was also observed for As. However, in the wider receiving environment, As is more readily adsorbed metalloid. Partitioning of As between the dissolved and particulate phases was more pronounced (more likely to be in the particulate phase) in most aqueous environments although As, like Sb, behaves conservatively in the Port Waikato estuary. Arsenic, unlike Sb, appears to be bioaccumulated in macrophytes and algae. This is because arsenate chemically resembles the phosphate ion, an important plant nutrient, whereas antimonate with its octahedral, rather than tetrahedral, co-ordination does not.

It is likely that strategies used to manage aqueous Sb contamination of aquatic systems will also prove successful for As, but the reverse does not apply. Antimony behaves more conservatively than As in natural waters, and furthermore Sb^{III} adsorption to SPM is greater than Sb^{V} adsorption to SPM, whereas the reverse holds for As (Webster and Nordstrom, 2003). Therefore processes designed to remove As from solution may not necessarily remove Sb at the same time.

6.2 SYNTHESIS

Concentrations of Sb in high temperature geothermal fluids can be greater than 1000 µg/kg, but as the fluids cool, most of the Sb in solution will precipitate as Sb2S3. In the Ngawha and Rotokawa powerstations, 75 % of the Sb has been removed from solution by the time the geothermal fluids have cooled to 100 °C. Therefore, it is likely that most of the Sb dissolved in underground geothermal fluids is removed before those fluids reach the surface. At the surface, where Sb concentrations vary from 10-200 µg/kg, Sb may be remobilised, but this remobilisation appears to be localised. In the Waikato River, a river which receives geothermal inputs, dilution with freshwaters means concentrations of Sb are rarely greater than 1 µg/kg. A conceptual model of these changes in Sb concentrations with changing environments is presented in Figure 6.1.

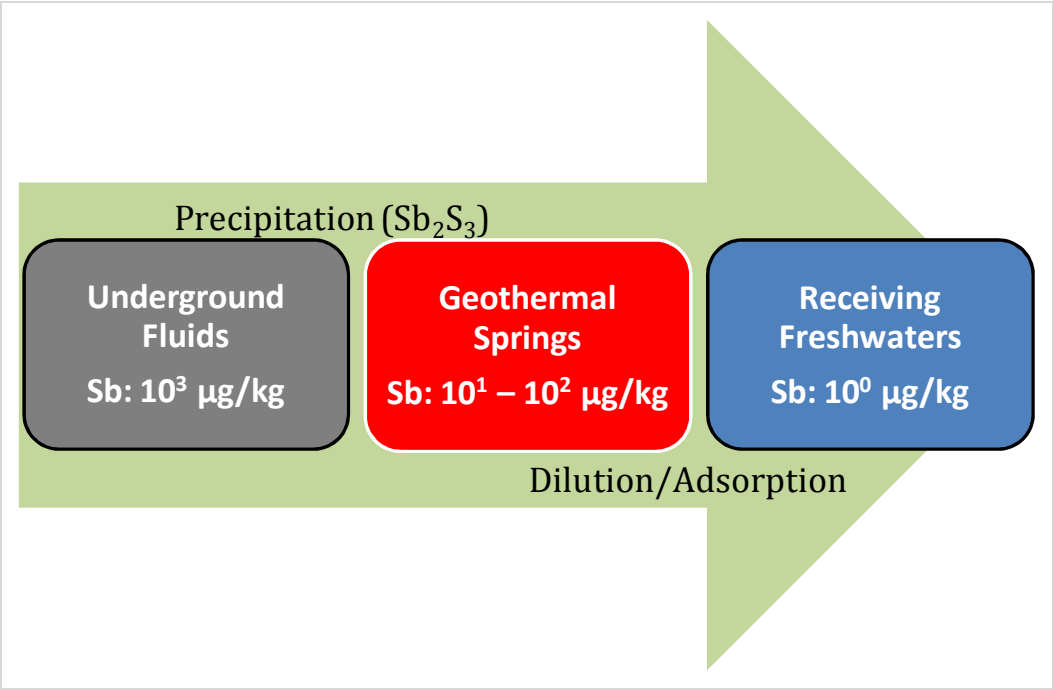

Figure 6.1 Progressive changes in Sb concentrations through the environments studied in this thesis. Major controls affecting concentration are also shown.

Figure 6.2 is a conceptual model summarising the research presented in this thesis. Two removal mechanisms were identified: precipitation (at low pH in the presence of H_2S) and adsorption (especially at relatively low pH and in reducing conditions). Oxidising conditions mobilise Sb, especially in circumneutral pH waters. Biological processes may indirectly enhance the mobilisation of Sb discharged from geothermal springs, but there was no evidence for bio-accumulation of Sb by algae growing in Hotwater Stream, nor by macrophytes growing in the Waikato River.

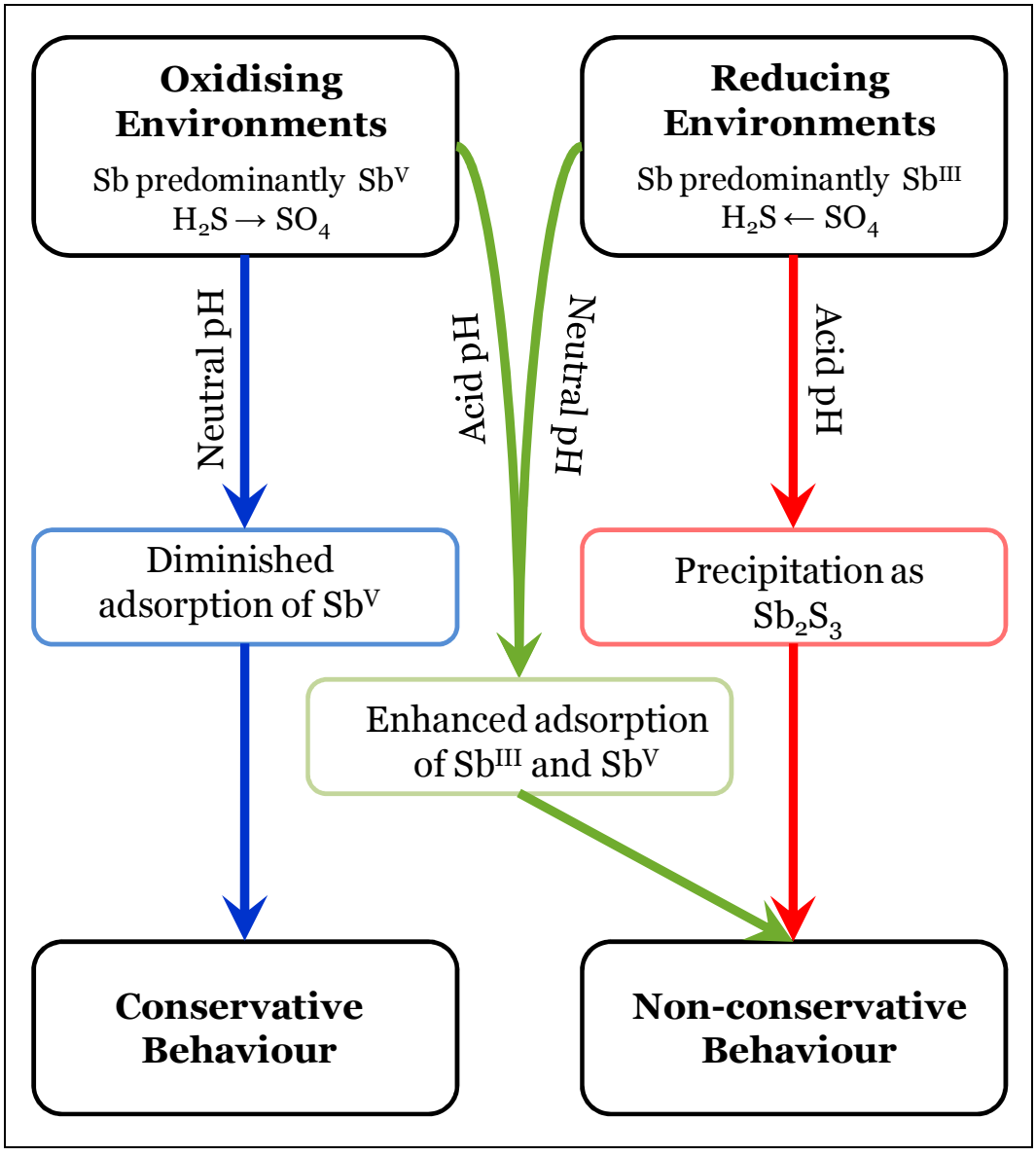

Figure 6.2 Conceptual model summarising the behaviour of Sb in aqueous environments

6.3 LIMITATIONS

There are some caveats that need to be applied to this research. The most significant of these were the restrictions put in place by the Department of Conservation for sampling of Wai-O-Tapu and Waimangu, but methodological problems that could not be avoided should be re-iterated as well.

The parks in the Wai-O-Tapu and Waimangu geothermal fields are aesthetically beautiful areas, and it is understandable that they should be kept as pristine as is practicably possible. Sediment sampling of Alum Lake, let alone Artist's Palette and Primrose Terrace may cause more damage than can be scientifically justified. The only way to overcome this problem would be to find a system similar to Wai-O-Tapu or Waimangu, but was not as aesthetically, commercially, or ecologically sensitive.

In hindsight, Lake Rotomahana could have been more thoroughly sampled. Data for Sb in bottom sediments, as well as aqueous samples from different geographic locations (such as the lake centre) and at various depths may have added a great deal of depth to the understanding the fate of aqueous Sb produced from Frying Pan Lake. It was the nature of this research that the benefits of additional study only became clear at the end of the project, but the logistics involved in this sampling would have always been demanding.

The lack of a truly effective and reliable method for the analysis of Sb in sediment and plant material was a source of significant frustration, particularly because concentrations of Sb in the collected material were too low for analysis by HG-AAS following microwave digestion. The cost of processing the required samples at outside laboratories using methods with lower detection limits (allowing the dilution of concentrated acid-digests) was prohibitive, and there was no guarantee that the results of such analyses would have been any better than the data presented in this thesis. It is accepted that more accurate solid phase Sb data could lead to somewhat different interpretations of the metalloid's behaviour in the Waikato River.

6.4 FUTURE RESEARCH

There are a number of different research paths that could lead on from this thesis.

6.4.1 THERMODYNAMICS

Perhaps the most important requirement for any future investigations of geothermal Sb behaviour is the generation of more thermodynamic data for the solubility of Sb_2S_3 (and other Sb-minerals for that matter) at temperatures below 300 ^oC. These data are critical for the development of accurate models of Sb_2S_3 formation in geothermal power stations, and in geothermal systems more generally. Ideally, the development of these thermodynamic species should consider the role of thio-Sb species as well as Sb-hydroxide and Sb-oxyanion species, because the available data for the thio-Sb set of species is even more sparse than the limited dataset available for the latter. Such research would, for example, allow more accurate predictions of Sb chemistry in Champagne Pool discharge.

6.4.2 SPECIATION

It would be of great interest to know if the behaviour of Sb produced from the surface features investigated at the Wai-O-Tapu or Waimangu geothermal fields, is similar to that of Sb in other natural geothermal systems. Indeed, it would be interesting to know if there is any such thing as a "typical geothermal system" with respect to the behaviour of Sb.

The role and distribution of thio-Sb species in the discharges from geothermal springs is not yet well understood. Consequently, the role of thio-antimonite and thio–antimonate species could not be considered in this research, in part because there was no available instrumental technique for measuring such species. However, there is a possibility that methods recently developed for the determination of thio-As species in geothermal samples, as described by Planer-Friedrich et al (2007), could be adapted to measure thio-Sb species. Methods for analysing thio-Sb species in environmental samples would mean that the behaviour and importance of thio-Sb species in geothermal environments could be studied. The development of such techniques would also mean that any new thermodynamic data produced for thio-Sb species could be tested against Sb measured in an environment, in a similar way to how thermodynamic data for stibnite was tested in Chapter Three.

6.4.3 BACTERIA AND KINETICS

Interactions between Sb and bacteria, whether these are direct or indirect are another research avenue yet to be explored. Researchers such as Oremland et al (2003) are developing a detailed understanding of the complex relationships between As, S and bacteria. Places such as Wai-O-Tapu and Waimangu provide ideal sites to begin similar studies focussed on Sb and its relationship with the biosphere.

A better understanding of how bacteria interact with Sb may advance our understanding of Sb oxidation and reduction kinetics. At present, the rate of oxidation and reduction of Sb species in aqueous environments is not understood at all, as reflected in the ongoing debate on how best to preserve samples (discussed in Chapter Two). Reaction kinetics are often overlooked in environmental research, and were not considered in any depth in the research presented in this thesis. Future research regarding Sb in aqueous environments could only benefit from a better understanding of this field.

6.4.4 ADSORPTION AND REDOX CHEMISTRY

The results of adsorption edge experiments presented in Chapter Five were deliberately simple, and were designed to examine the adsorption of Sb onto SPM at various pH in a solution with a specific ionic strength. Further insights could be gleened by investigating the adsorption of Sb onto SPM at different concentrations and/or ratios of Sb and SPM, at various ionic strengths, and in more complex solutions, such as natural river waters. The effects of competition with other elements, such as As, may also prove informative.

Changes in Sb chemistry in response to stratification in Lake Ohakuri (and potentially other lakes along the Waikato River) could also be further investigated. The accessibility of the Waikato hydro-electric dams, combined with their elevated concentrations of geothermal elements, provide an opportunity to investigate how Sb will react to changes in redox conditions in a natural environment.

6.4.5 SITES AND SAMPLING

There were no surface connections between the discharge from Champagne Pool and Waiotapu Stream. If a geothermal system actively discharging fluids with elevated Sb concentrations directly into a large stream or river system could be found, perhaps one of the features near Maungaongaonga, it would be possible to more reliably document the behaviour of aqueous geothermal Sb after discharge into a cold water environment. Further study of Lake Rotomahana would also be useful in this regard.

If it were possible to collect a range of samples, including bed sediment, from apparent Sb-sinks such as Alum Lake at Wai-O-Tapu or Lake Rotomahana, it would be also possible to develop a much better understanding of the eventual fate of Sb produced from geothermal springs.

Finally, it might be possible to investigate whether diurnal changes in metalloid concentrations at natural geothermal surface features are reflected in receiving environments. For example, even if most of the dissolved Sb remobilised from the Champagne Pool discharge settles in Alum Lake, some particulate material may make it through the lake to be discharged downstream. Therefore there is a chance that the overall input to Waiotapu Stream may change over a 24 hour period, something that may impact on how the water quality of the stream is monitored. It would be of interest to know what, or if, there are temporal variations in Sb and/or As concentrations in Lake Rotomahana, Waiotapu Stream, and perhaps even the Waikato River. Such studies could be conducted over a 24-hour period, to determine the effects of any diurnal processes.

If any diurnal variations were detected, week- or month-long daily surveys could provide further insight, as would an extended period of sampling at a site such as Wai-O-Tapu. Day to day variations in parameters such as pH, temperature and light may help determine the relative influence of these parameters have on metalloid concentrations, and therefore help identify the exact process that drives thevarious phenomena described in this thesis.

6.5 FINAL CONCLUSIONS

The overall fate of geothermal Sb is intimately linked to the presence or absence of sulfide ions. In the high temperature sulfide-rich fluids of the underground reservoir that are used for geothermal power generation, the behaviour of aqueous Sb is dependant upon a number of factors, with temperature and pH being the most important. In fluids exposed at the surface, the oxidation of sulfides to sulfate species mean that the behaviour of Sb changes. By the time Sb reaches the oxidised, neutral pH waters of the Waikato River, the metalloid's behaviour is mainly conservative, affected only by minor adsorption to sediment, particularly under low pH and/or low oxygen conditions.

"Are there any fundamental differences between geothermally produced Sb and Sb produced from mining or other such contaminated environments?" was one of the principal questions to be answered in this thesis. It seems likely that Sb precipitation and adsorption processes identified in this research are universal, and therefore lessons learnt from the study of Sb from geothermal environments are applicable in other environmental contexts as well.

REFERENCES

Aggett, J. & Aspell, A. 1977. Release of Arsenic into Waikato River from Geothermal Sources. *New Zealand Medical Journal*, **86** (594), 203-203.

Aggett, J. & Kriegman, M. R. 1987. Preservation of Arsenic(III) and Arsenic(V) in Samples of Sediment Interstitial Water. *Analyst*, **112** (2), 153-157.

Aggett, J. & Kriegman, M. R. 1988. The Extent of Formation of Arsenic(III) in Sediment Interstitial Waters and Its Release to Hypolimnetic Waters in Lake Ohakuri. *Water Research*, **22** (4), 407-411.

Aggett, J. & O'Brien, G. A. 1985. Detailed Model for the Mobility of Arsenic in Lacustrine Sediments Based on Measurements in Lake Ohakuri. *Environmental Science & Technology*, **19** (3), 231-238.

Aggett, J. & Roberts, L. S. 1986. Insight into the Mechanism of Accumulation of Arsenate and Phosphate in Hydro Lake Sediments by Measuring the Rate of Dissolution with Ethylenediaminetetraacetic Acid. *Environmental Science & Technology*, **20** 183-186.

Ainsworth, N., Cooke, J. A., & Johnson, M. S. 1990a. Distribution of Antimony in Contaminated Grassland: 1-- Vegetation and Soils. *Environmental Pollution*, **65** (1), 65-77.

Ainsworth, N., Cooke, J. A., & Johnson, M. S. 1990b. Distribution of Antimony in Contaminated Grassland: 2-- Small Mammals and Invertebrates. *Environmental Pollution*, **65** (1), 79-87.

Akinfiev, N. N., Zotov, A. V., & Shikina, N. D. 1993. Experimental Investigation and Thermodynamic Correlation in the Sb(III)-S(II)-O-H System. *Geokhimiya*, (12), 1709-1723.

Al-Ashban, R. M., Aslam, M., & Shah, A. H. 2004. Kohl (Surma): A Toxic Traditional Eye Cosmetic Study in Saudi Arabia. *Public Health*, **118** (4), 292-298.

Almela, C., Jesus Clemente, M., Velez, D., & Montoro, R. 2006. Total Arsenic, Inorganic Arsenic, Lead and Cadmium Contents in Edible Seaweed Sold in Spain. *Food and Chemical Toxicology*, **44** (11), 1901-1908.

Andreae, M. O., Asmode, J. F., Foster, P., & Vantdack, L. 1981. Determination of Antimony(III), Antimony(V), and Methylantimony Species in Natural-Waters by Atomic-Absorption Spectrometry with Hydride Generation. *Analytical Chemistry*, **53** (12), 1766-1771.

Andrewes, P., Kitchin, K. T., & Wallace, K. 2004. Plasmid DNA Damage Caused by Stibine and Trimethylstibine. *Toxicology and Applied Pharmacology*, **194** (1), 41-48.

Anheizen. *Pink Terraces*. The Story of Tarawera, The Landscape Renovator. 2003, Accessed: 28 March, 2008, http://www.anheizen.com/terraces/index.php?content=pink.php

Australian and New Zealand Environment and Conservation Council. 2000. *Australian and New Zealand Guidelines for Fresh and Marine Water Quality*. ANZECC, Canberra, pp.

APHA. 1998. *Standard Methods for the Examination of Water and Wastewater*, 20th Edition. Washington D.C., APHA, 1200 pp.

Ariza, J. L. G., Morales, E., Sanchez-Rodas, D., & Giraldez, I. 2000. Stability of Chemical Species in Environmental Matrices. *Trac-Trends in Analytical Chemistry*, **19** (2-3), 200-209.

Arnorsson, S., Sigurdsson, S., & Svavarsson, H. 1982. The Chemistry of Geothermal Waters in Iceland. I. Calculation of Aqueous Speciation from 0 to 370 ^{O}C. *Geochimica et Cosmochimica Acta*, **46** (9), 1513-1532.

Ashley, P. M., Craw, D., Graham, B. P., & Chappell, D. A. 2003. Environmental Mobility of Antimony around Mesothermal Stibnite Deposits, New South Wales, Australia and Southern New Zealand. *Journal of Geochemical Exploration*, **77** (1), 1-14.

Ashley, P. M., Craw, D., Tighe, M. K., & Wilson, N. J. 2006. Magnitudes, Spatial Scales and Processes of Environmental Antimony Mobility from Orogenic Gold-Antimony Mineral Deposits, Australasia. *Environmental Geology*, **51** (4), 499-507.

Ashley, P. M., Graham, B. P., Tighe, M. K., & Wolfenden, B. J. 2007. Antimony and Arsenic Dispersion in the Macleay River Catchment, New South Wales: A Study of the Environmental Geochemical Consequences. *Australian Journal of Earth Sciences*, **54** (1), 83-103.

Auer, C. *Stibnite, Antimony Mine, Stadtschlaining, Oberwart, Burgenland, Austria*. 1980, Accessed: http://www.mindat.org/photos/006128200120137718 9.jpg

Azaroual, M., Kervevan, C., Durance, M. N., & Durst, P. 2004. Scale2000: Reaction-Transport Software Dedicated to Thermokinetic Prediction and Quantification of Scales Applicability to Desalination Problems. *Desalination*, **165** 409-419.

Baes, C. F. & Mesmer, R. E. 1976. *The Hydrolysis of Cations*, New York, Wiley, 489 pp.

Baroni, F., Boscagli, A., Protano, G., & Riccobono, F. 2000. Antimony Accumulation in Achillea Ageratum, Plantago Lanceolata and Silene Vulgaris Growing in an Old Sb-Mining Area. *Environmental Pollution*, **109** (2), 347-352.

Beard, S. 2008. *Waikato River Water Quality Monitoring Programme: Data Report 2007*. Environment Waikato, Technical Report 2008/20. 53 pp.

Bednar, A. J., Garbarino, J. R., Ranville, J. F., & Wildeman, T. R. 2002. Preserving the Distribution of Inorganic Arsenic Species in Groundwater and Acid Mine Drainage Samples. *Environmental Science & Technology*, **36** (10), 2213-2218.

Belzile, N., Chen, Y. W., & Wang, Z. J. 2001. Oxidation of Antimony (III) by Amorphous Iron and Manganese Oxyhydroxides. *Chemical Geology*, **174** (4), 379-387.

Bentley, R. & Chasteen, T. G. 2002. Microbial Methylation of Metalloids: Arsenic, Antimony, and Bismuth. *Microbiology and Molecular Biology Reviews*, **66** (2), 250.

Bertani, R. 2005. World Geothermal Power Generation in the Period 2001-2005. *Geothermics*, **34** (6), 651-690.

Bibby, H. M., Caldwell, T. G., Davey, F. J., & Webb, T. H. 1995. Geophysical Evidence on the Structure of the Taupo Volcanic Zone and Its Hydrothermal Circulation. *Journal of Volcanology and Geothermal Research*, **68** (1-3), 29-58.

Bibby, R. L. & Webster-Brown, J. G. 2006. Trace Metal Adsorption onto Urban Stream Suspended Particulate Matter (Auckland Region, New Zealand). *Applied Geochemistry*, **21** (7), 1135-1151.

Bilinska, K. 2005. *Thermal Stratification in the Waikato Hydro Lakes*, Centre for Water Research, Unpublished Honours Dissertation, University of Western Australia, Perth.

Bingqiu, Z., Jinmao, Z., Lixin, Z., & Yaxin, Z. 1986. Mercury, Arsenic, Antimony, Bismuth and Boron as Geochemical Indicators for Geothermal Areas. *Journal of Geochemical Exploration*, **25** (3), 379-388.

Bornhorst, J. A., Hunt, J. W., Urry, F. M., & McMillin, G. A. 2005. Comparison of Sample Preservation Methods for Clinical Trace Element Analysis by Inductively Coupled Plasma Mass Spectrometry. *American Journal of Clinical Pathology*, **123** (4), 578-583.

Braman, R. S., Foreback, C. C., & Justen, L. L. 1972. Direct Volatilization Spectral Emission Type Detection System for Nanogram Amounts of Arsenic and Antimony. *Analytical Chemistry*, **44** (13), 2195.

Brannon, J. M. & Patrick, W. H. 1985. Fixation and Mobilization of Antimony in Sediments. *Environmental Pollution Series B, Chemical and Physical*, **9** (2), 107-126.

Brown, K. L. 2003. *Pipeline Deposits at Rotokawa Geothermal Field*. GEOKEM, Report for Mighty River Power, Final Report. 45 pp.

Brown, K. L. & Simmons, S. F. 2003. Precious Metals in High-Temperature Geothermal Systems in New Zealand. *Geothermics*, **32** (4-6), 619-625.

Browne, P. R. L. & Lawless, J. V. 2001. Characteristics of Hydrothermal Eruptions, with Examples from New Zealand and Elsewhere. *Earth-Science Reviews*, **52** (4), 299-331.

Buschmann, J. & Sigg, L. 2004. Antimony(III) Binding to Humic Substances: Influence of pH and Type of Humic Acid. *Environmental Science & Technology*, **38** (17), 4535-4541.

Byrd, J. T. 1990. Comparative Geochemistries of Arsenic and Antimony in Rivers and Estuaries. *Science of the Total Environment*, **97-8** 301-314.

Cabon, J. Y. & Louis Madec, C. 2004. Determination of Major Antimony Species in Seawater by Continuous Flow Injection Hydride Generation Atomic Absorption Spectrometry. *Analytica Chimica Acta*, **504** (2), 209-215.

Cappetti, G., D'Olimpio, P., Sabatelli, F., & Tarquini, B. 1995. *Inhibition of Antimony Sulphide Scale by Chemical Additives: Laboratory and Field Test Results*. 1995, World Geothermal Congress, Florence, Italy.

Casiot, C., Ujevic, M., Munoz, M., Seidel, J. L., & Elbaz-Poulichet, F. 2007. Antimony and Arsenic Mobility in a Creek Draining an Antimony Mine Abandoned 85 Years Ago (Upper Orb Basin, France). *Applied Geochemistry*, **22** (4), 788-798.

Chapman, M. A. 1996. Human Impacts on the Waikato River System, New Zealand. *GeoJournal*, **40** (1), 85-99.

Claypool, G. E. & Kaplan, I. R. 1974. *The Origin and Distribution of Methane in Marine Sediments*. In I. R. Kaplan, Natural Gases in Marine Sediments, Plenum Press, 99-140.

Cloy, J. M., Farmer, J. G., Graham, M. C., MacKenzie, A. B., & Cook, G. T. 2005. A Comparison of Antimony and Lead Profiles over the Past 2500 Years in Flanders Moss Ombrotrophic Peat Bog, Scotland. *Journal of Environmental Monitoring*, **7** (12), 1137-1147.

Contact Energy. 2007. *Contact Energy Sustainability Report 2007*. Contact Energy Limited, 38 pp.

Cooper, V. C. 1996. *Microalgae: Microscopic Marvels*, Hamilton, New Zealand., Riverside Books, 164 pp.

Coulter, G. W., Davies, J., & Pickmere, S. 1983. Seasonal Limnological Change and Phytoplankton Production in Ohakuri, a Hydro-Electric Lake on the Waikato River. *New Zealand Journal of Marine and Freshwater Research*, **17** 169-183.

Craw, D., Rufaut, C., Haffert, L., & Paterson, L. 2007. Plant Colonization and Arsenic Uptake on High Arsenic Mine Wastes, New Zealand. *Water Air and Soil Pollution*, **179** (1-4), 351-364.

Craw, D., Wilson, N. J., & Ashley, P. 2004. Geochemical Controls on the Environmental Mobility of Sb and as at Mesothermal Antimony and Gold Deposits. *Transactions of the Institution of Mining and Metallurgy. Section B, Applied earth science*, **113** B3-B10.

Crecelius, E. A., Bothner, M. H., & Carpenter, R. 1975. Geochemistries of Arsenic, Antimony, Mercury, and Related Elements in Sediments of Puget Sound. *Environmental Science & Technology*, **9** (4), 325-333.

Cutter, G. A. & Cutter, L. S. 2006. Biogeochemistry of Arsenic and Antimony in the North Pacific Ocean. *Geochemistry Geophysics Geosystems*, **7**

Cutter, G. A., Cutter, L. S., Featherstone, A. M., & Lohrenz, S. E. 2001. Antimony and Arsenic Biogeochemistry in the Western Atlantic Ocean. *Deep-Sea Research Part II-Topical Studies in Oceanography*, **48** (13), 2895-2915.

De Gregori, I., Quiroz, W., Pinochet, H., Pannier, F., & Potin-Gautier, M. 2007. Speciation Analysis of Antimony in Marine Biota by HPLS-(UV)-HG-AFS: Extraction Procedures and Stability of Antimony Species. *Talanta*, **73** (3), 458-465.

de la Calle-Guntinas, M. B., Madrid, Y., & Camara, C. 1992. Stability Study of Total Antimony, Sb(III) and Sb(V) at the Trace Level. *Fresenius Journal of Analytical Chemistry*, **344** (1-2), 27-29.

Dee, T. 2007. *A Study of the Relationship between SPM and Trace Metals in the Lower Waikato River*, Department of Chemistry, Unpublished M. Sc. thesis, University of Auckland, Auckland.

DiPippo, R. 2005. *Geothermal Power Plants: Principles, Applications and Case Studies*, Oxford, Elsevier Advanced Technology, 450 pp.

Dodd, M., Grundy, S. L., Reimer, K. J., & Cullen, W. R. 1992. Methylated Antimony(V) Compounds - Synthesis, Hydride Generation Properties and Implications for Aquatic Speciation. *Applied Organometallic Chemistry*, **6** (2), 207-211.

Dodd, M., Pergantis, S. A., Cullen, W. R., Li, H., Eigendorf, G. K., & Reimer, K. J. 1996. Antimony Speciation in Freshwater Plant Extracts by Using Hydride Generation Gas Chromatography Mass Spectrometry. *Analyst*, **121** (2), 223-228.

Dopp, E., Hartmann, L. M., Florea, A. M., Rettenmeier, A. W., & Hirner, A. V. 2004. Environmental Distribution, Analysis, and Toxicity of Organometal(Loid) Compounds. *Critical Reviews in Toxicology*, **34** (3), 301-333.

Dorrington, P. & Brown, K. L. 2000. *Management of Stibnite Deposition at Ngawha*. 2000, 22nd New Zealand Geothermal Workshop, Auckland.

Dzombak, D. A. & Morel, F. M. M. 1990. *Surface Complexation Modelling*, New York, Wiley, 393 pp.

Eckert, W. 1987. Electrochemical Identification of Microbially Mediated Hydrogen Sulfide Oxidation. *Biogeochemistry*, **4** (1), 15-26.

Ellis, A. J. & Mahon, W. A. J. 1966. Geochemistry of Ngawha Hydrothermal Area. *New Zealand Journal of Science*, **9** (2), 440-456.

Ellis, A. J. & Mahon, W. A. J. 1967. Natural Hydrothermal Systems and Experimental Hot Water/Rock Interactions (Part 2). *Geochimica Et Cosmochimica Acta*, **31** (4), 519.

Ellis, A. J. & Mahon, W. A. J. 1977. *Chemistry and Geothermal Systems*, New York, Academic Press, 392 pp.

Ellwood, M. J. & Maher, W. A. 2002. Arsenic and Antimony Species in Surface Transects and Depth Profiles across a Frontal Zone: The Chatham Rise, New Zealand. *Deep-Sea Research Part I-Oceanographic Research Papers*, **49** (11), 1971-1981.

Environment Waikato. 2002. *Numbers of Visitors to Geothermal Attractions in the Waikato Region*. Environment Waikato, Technical Series 2002/05. 22 pp.

Ettler, V., Mihaljevic, M., Sebek, O., & Nechutny, Z. 2007. Antimony Availability in Highly Polluted Soils and Sediments - a Comparison of Single Extractions. *Chemosphere*, **68** (3), 455-463.

Evans, J. 1634. *The Vniversall Medicine: Or the Vertues of the Antimoniall Cup*, London, John Haviland, 16 pp.

Filella, M., Belzile, N., & Chen, Y. W. 2002a. Antimony in the Environment: A Review Focused on Natural Waters I. Occurrence. *Earth-Science Reviews*, **57** (1-2), 125-176.

Filella, M., Belzile, N., & Chen, Y. W. 2002b. Antimony in the Environment: A Review Focused on Natural Waters II. Relevant Solution Chemistry. *Earth-Science Reviews*, **59** (1-4), 265-285.

Filella, M., Belzile, N., & Lett, M.-C. 2007. Antimony in the Environment: A Review Focused on Natural Waters. III. Microbiota Relevant Interactions. *Earth-Science Reviews*, **80** (3-4), 195-217.

Fjallborg, B. & Dave, G. 2004. Toxicity of Sb and Cu in Sewage Sludge to Terrestrial Plants (Lettuce, Oat, Radish), and of Sludge Elutriate to Aquatic Organisms (Daphnia and Lemna) and Its Interaction. *Water Air and Soil Pollution*, **155** (1-4), 3-20.

Fleming, C. A. 1945. Hydrothermal Activity at Ngawha, North Auckland. *New Zealand Journal of Science and Technology*, **26B** 255-276.

Flores, E. M. D., da Silva, L. L. C., Barin, J. S., Saidelles, A. P. F., Zanella, R., Dressler, V. L., & Paniz, J. N. G. 2001. Minimization of Volatile Nitrogen Oxides Interference in the Determination of Arsenic by Hydride Generation Atomic Absorption Spectrometry. *Spectrochimica Acta Part B-Atomic Spectroscopy*, **56** (10), 1883-1891.

Flores, E. M. D., Paula, F. R., da Silva, F. E. B., de Moraes, D. P., Paniz, J. N. G., dos Santos, E. P., Dressler, V. L., & Bittencourt, C. F. 2003. Selective Determination of Sb(III) in Drugs by Flow Injection Hydride Generation AAS. *Atomic Spectroscopy*, **24** (1), 15-21.

Flynn, H. C., Meharg, A. A., Bowyer, P. K., & Paton, G. I. 2003. Antimony Bioavailability in Mine Soils. *Environmental Pollution*, **124** (1), 93-100.

Fuller, C. C., & Davis, J. A. 1989. Influence of Coupling of Sorption and Photosynthetic Processes on Trace-element Cycles in Natural-waters. *Nature* **340** (6228), 52-54.

Gal, J., Hursthouse, A., & Cuthbert, S. 2007. Bioavailability of Arsenic and Antimony in Soils from an Abandoned Mining Area, Glendinning (Sw Scotland). *Journal of Environmental Science and Health Part a-Toxic/Hazardous Substances & Environmental Engineering*, **42** (9), 1263-1274.

Gál, J., Hursthouse, A., & Cuthbert, S. 2006. Chemical Availability of Arsenic and Antimony in Industrial Soils. *Environmental Chemistry Letters*, **3** (4), 149-153.

Gayer, K. H. & Garrett, A. B. 1952. The Equilibria of Antimonous Oxide (Rhombic) in Dilute Solutions of Hydrochloric Acid and Sodium Hydroxide at 25 ^{o}C. *Journal of the American Chemical Society*, **74** (9), 2353-2354.

Gebel, T. 1997. Arsenic and Antimony: Comparative Approach on Mechanistic Toxicology. *Chemico-Biological Interactions*, **107** (3), 131-144.

Gebel, T., Christensen, S., & Dunkelberg, H. 1997. Comparative and Environmental Genotoxicity of Antimony and Arsenic. *Anticancer Research*, **17** (4A), 2603-2607.

Gianella, V. P. & White, D. E. 1947. Minerals of Steamboat Springs, Nevada. *American Mineralogist*, **32** (3-4), 200-201.

Gibbs, B. M., Thompson, D., & Argent, B. B. 2008. Mobilisation of Trace Elements from as-Supplied and Additionally Cleaned Coal: Predictions for Ba, Be, Cd, Co, Mo, Nb, Sb, V and W. *Fuel*, **87** (7), 1217-1229.

Gibbs, M. & Costley, K. 2000. *Heavy Metals in Waikato Hydro Power Station Weed-Dump Sites*. NIWA, Report number MRP01231. 23 pp.

Giggenbach, W. F. 1992. Isotopic Shifts in Waters from Geothermal and Volcanic Systems Along Convergent Plate Boundaries and Their Origin. *Earth and Planetary Science Letters*, **113** (4), 495-510.

Giggenbach, W. F. 1995. Variations in the Chemical and Isotopic Composition of Fluids Discharged from the Taupo Volcanic Zone, New Zealand. *Journal of Volcanology and Geothermal Research*, **68** (1-3), 89-116.

Giller, P. S. & Malmqvist, B. 1998. *The Biology of Streams and Rivers*, Oxford, Oxford University Press, 304 pp.

Gillis, G. & Varhaug, M. *Oilfield Glossary*. Schlumberger Limited. 2008, Accessed: 26 May, 2008, http://www.glossary.oilfield.slb.com/Display.cfm?Term=kerogen

Glover, R. B., Stewart, M. K., Crump, M. E., Klyen, L. E., & Simmons, S. F. 1994. The Relationship of Chemical Parameters to the Cyclic Behaviour of Inferno Crater Lake, Waimangu, New Zealand. *Geothermics*, **23** (5-6), 583-597.

Gomez, D. R., Gine, M. F., Bellato, A. C. S., & Smichowski, P. 2005. Antimony: A Traffic-Related Element in the Atmosphere of Buenos Aires, Argentina. *Journal of Environmental Monitoring*, **7** (12), 1162-1168.

Greenwood, N. N. & Earnshaw, A. 1984. *Chemistry of the Elements*, Oxford, Pergamon Press, 1542 pp.

Gunnarsson, I. & Arnorsson, S. 2005. Impact of Silica Scaling on the Efficiency of Heat Extraction from High-Temperature Geothermal Fluids. *Geothermics*, **34** (3), 320-329.

Hammel, W., Steubing, L., & Debus, R. 1998. Assessment of the Ecotoxic Potential of Soil Contaminants by Using a Soil-Algae Test. *Ecotoxicology and Environmental Safety*, **40** (1-2), 173-176.

Hayes, R. B. 1997. The Carcinogenicity of Metals in Humans. *Cancer Causes & Control*, **8** (3), 371-385.

He, M. C. & Yang, J. R. 1999. Effects of Different Forms of Antimony on Rice During the Period of Germination and Growth and Antimony Concentration in Rice Tissue. *Science of the Total Environment*, **244** 149-155.

Hedenquist, J. W. & Henley, R. W. 1985. Hydrothermal Eruptions in the Waiotapu Geothermal System, New Zealand: Their Origin, Associated Breccias, and Relation to Precious Metal Mineralization. *Economic Geology*, **80** (6), 1640-1668.

Hedenquist, J. W. 1986. *Waiotapu Geothermal Field*. In R. W. Henley & J. W. Hedenquist & P. J. Roberts, Guide to the Active Epithermal (Geothermal) Sysytems and Precious Metal Deposits of New Zealand, Monograph Series on Mineral Deposits, Volume 26, Gebruder Borntraeger, Berlin, Stuttgart. 65-79.

Hegan, A. F. 2005. *A Preliminary Investigation into the Role of Diatoms in the Binding of Copper and Arsenic onto SPM*, School of Geography and Environmental Science, Unpublished M. Sc. thesis, University of Auckland, Auckland.

Henley, R. W. & Ellis, A. J. 1983. Geothermal Systems Ancient and Modern: A Geochemical Review. *Earth-Science Reviews*, **19** (1), 1-50.

Hetzer, A., Morgan, H., McDonald, I., & Daughney, C. 2007. Microbial Life in Champagne Pool, a Geothermal Spring in Waiotapu, New Zealand. *Extremophiles*, **11** (4), 605-614.

Hindmarsh, J. T. 2000. Arsenic, Its Clinical and Environmental Significance. *Journal of Trace Elements in Experimental Medicine*, **13** (1), 165-172.

Hirner, A. V., Feldmann, J., Krupp, E., Grumping, R., Goguel, R., & Cullen, W. R. 1998. Metal(Loid)Organic Compounds in Geothermal Gases and Waters. *Organic Geochemistry*, **29** (5-7), 1765-1778.

Hirner, A. V., Krupp, R. E., Gainsford, A. R., & Staerk, H. 1990. Metal-Organic Associations in Sediments .2. Algal Mats in Contact with Geothermal Waters. *Applied Geochemistry*, **5** (4), 507-513.

Hole, J. K., Bromley, C. J., Stevens, N. F., & Wadge, G. 2007. Subsidence in the Geothermal Fields of the Taupo Volcanic Zone, New Zealand from 1996 to 2005 Measured by INSAR. *Journal of Volcanology and Geothermal Research*, **166** (3-4), 125-146.

Houghton, J. L., Shanks, W. C., & Seyfried, W. E. 2004. Massive Sulfide Deposition and Trace Element Remobilization in the Middle Valley Sediment-Hosted Hydrothermal System, Northern Juan De Fuca Rdge. *Geochimica Et Cosmochimica Acta*, **68** (13), 2863-2873.

Huang, H., Shu, S. C., Shih, J. H., Kuo, C. J., & Chiu, I. D. 1998. Antimony Trichloride Induces DNA Damage and Apoptosis in Mammalian Cells. *Toxicology*, **129** (2-3), 113-123.

Hunt, T., Glover, R., & Wood, C. 1994. Waimangu, Waiotapu, and Waikite Geothermal Systems, New Zealand: Background and History. *Geothermics*, **23** (5-6), 379-400.

Hunt, T. M. 1998. Recent Developments in the New Zealand Geothermal Industry. *Energy Sources*, **20** (8), 777-786.

Huxham, J. 1777. *Medical and Chemical Observations Upon Antimony*, London, Hinton, J., 78 pp.

Iwashita, M. & Shimamura, T. 2003. Long-Term Variations in Dissolved Trace Elements in the Sagami River and Its Tributaries (Upstream Area), Japan. *The Science of The Total Environment*, **312** (1-3), 167-179.

Jābir ibn Ḥayyān 1678. The works of Geber, the most famous Arabian prince and philosopher of the investigation and perfection of the philosophers-stone. Printed for William Cooper, London, 302pp.

Jain, D. V. S. & Banerjee, A. K. 1961. On the Structure of Antimonates. *Journal of Inorganic & Nuclear Chemistry*, **19** (1-2), 177-179.

Jenkins, R. O., Forster, S. N., & Craig, P. J. 2002. Formation of Methylantimony Species by an Aerobic Prokaryote: Flavobacterium Sp. *Archives of Microbiology*, **178** (4), 274-278.

Jones, C.A., Nimick, D.A., McCleskey, R.B. 2004. Relative Effect of Temperature and pH on Diel Cycling of Dissolved Trace Elements in Prickly Pear Creek, Montana. *Water Air and Soil Polution*, **153** (1-4), 95-113.

Jones, B., Renaut, R. W., & Konhauser, K. O. 2005. Genesis of Large Siliceous Stromatolites at Frying Pan Lake, Waimangu Geothermal Field, North Island, New Zealand. *Sedimentology*, **52** (6), 1229-1252.

Jones, B., Renaut, R. W., & Rosen, M. R. 2001. Biogenicity of Gold- and Silver-Bearing Siliceous Sinters Forming in Hot (75 ^{O}C) Anaerobic Spring-Waters of Champagne Pool, Waiotapu, North Island, New Zealand. *Journal of the Geological Society*, **158** 895-911.

Jones, J. C. 1912. The Occurrence of Stibnite at Steamboat Springs, Nevada. *Science*, **35** (907), 775-776.

Kalac, P. & Svoboda, L. 2000. A Review of Trace Element Concentrations in Edible Mushrooms. *Food Chemistry*, **69** (3), 273-281.

Kawamoto, Y. & Morisawa, S. 2003. The Distribution and Speciation of Antimony in River Water, Sediment and Biota in Yodo River, Japan. *Environmental Technology*, **24** (11), 1349-1356.

Kirkland, D., Whitwell, J., Deyo, J., & Serex, T. 2007. Failure of Antimony Trioxide to Induce Micronuclei or Chromosomal Aberrations in Rat Bone-Marrow after Sub-Chronic Oral Dosing. *Mutation Research-Genetic Toxicology and Environmental Mutagenesis*, **627** (2), 119-128.

Kissling, W. M. & Weir, G. J. 2005. The Spatial Distribution of the Geothermal Fields in the Taupo Volcanic Zone, New Zealand. *Journal of Volcanology and Geothermal Research*, **145** (1-2), 136-150.

Knechtenhofer, L. A., Xifra, I. O., Scheinost, A. C., Fluhler, H., & Kretzschmar, R. 2003. Fate of Heavy Metals in a Strongly Acidic Shooting-Range Soil: Small-Scale Metal Distribution and Its Relation to Preferential Water Flow. *Journal of Plant Nutrition and Soil Science-Zeitschrift Fur Pflanzenernahrung Und Bodenkunde*, **166** (1), 84-92.

Kolpakova, N. N. 1982. Laboratory and Field Studies of Ionic Equilibria in the Sb_2S_3-H_2O-H_2S System. *Geochemistry International*, **19** 46-54.

Kozlov, E. D. 1982. *Migration of Antimony and Mercury in Hydrothermal Solutions Based on Experimental Data (in Russian)*, Unpublished Ph.D. thesis, Institute of Mineralogy, Geochemistry and Crystallochemistry of Rare Elements, Moscow.

Krachler, M., Burow, M., & Emons, H. 1999. Biomonitoring of Antimony in Environmental Matrices from Terrestrial and Limnic Ecosystems. *Journal of Environmental Monitoring*, **1** (5), 477-481.

Krachler, M., Emons, H., Barbante, C., Cozzi, G., Cescon, P., & Shotyk, W. 2002. Inter-Method Comparison for the Determination of Antimony and Arsenic in Peat Samples. *Analytica Chimica Acta*, **458** (2), 387-396.

Krauskopf, K. B. 1979. *Introduction to Geochemistry*, 2nd Edition. Tokyo, McGraw-Hill Kogakusha Ltd., 617 pp.

Kristmannsdottir, H. 1989. Types of Scaling Occurring by Geothermal Utilization in Iceland. *Geothermics*, **18** (1-2), 183-190.

Krupp, E., Browne, P. R. L., Henley, R. W., & Seward, T. M. 1986. *Rotokawa Geothermal Field*. In R. W. Henley & J. W. Hedenquist & P. J. Roberts, Guide to the Active Epithermal (Geothermal) Sysytems and Precious Metal Deposits of New Zealand, Monograph Series on Mineral Deposits, Volume 26, Gebruder Borntraeger, Berlin, Stuttgart. 47-55.

Krupp, R. E. 1988. Solubility of Stibnite in Hydrogen-Sulfide Solutions, Speciation, and Equilibrium-Constants, from 25 to 350 °C. *Geochimica Et Cosmochimica Acta*, **52** (12), 3005-3015.

Krupp, R. E. 1990a. As(III) and Sb(III) Sulfide Complexes - an Evaluation of Stoichiometry and Stability from Existing Experimental-Data - Comment. *Geochimica Et Cosmochimica Acta*, **54** (11), 3239-3240.

Krupp, R. E. 1990b. As(III) and Sb(III) Sulfide Complexes - an Evaluation of Stoichiometry and Stability from Existing Experimental-Data - Response. *Geochimica Et Cosmochimica Acta*, **54** (11), 3245-3245.

Krupp, R. E. & Seward, T. M. 1987. The Rotokawa Geothermal System, New Zealand - an Active Epithermal Gold-Depositing Environment. *Economic Geology*, **82** (5), 1109-1129.

Krupp, R. E. & Seward, T. M. 1990. Transport and Deposition of Metals in the Rotokawa Geothermal System, New-Zealand. *Mineralium Deposita*, **25** (1), 73-81.

Lam, C. W. Y. 1981. Ecological Studies of Phytoplankton in the Waikato River and Its Catchment. *New Zealand Journal of Marine and Freshwater Research*, **15** (1), 95-103.

Leblanc, G. A. & Dean, J. W. 1984. Antimony and Thallium Toxicity to Embryos and Larvae of Fathead Minnows (*Pimephales Promelas*). *Bulletin of Environmental Contamination and Toxicology*, **32** (5), 565-569.

Legmann, H. & Sullivan, P. 2003. *The 30 MW Rotokawa I Geothermal Project after Five Years of Operation*. 2003, International Geothermal Conference IGC-2003, Reykjavik, Iceland.

Leicester, H. M. & Klickstein, H. S. 1952. *A Source Book in Chemistry, 1400-1900*, 1st Edition. New York, McGraw-Hill, 554 pp.

Leleyter, L. & Probst, J.-L. 1999. A New Sequential Extraction Procedure for the Seciation of Particulate Trace Elements in River Sediments. *International Journal of Environmental Analytical Chemistry*, **73** 109-128.

Leonard, A. & Gerger, G. B. 1996. Mutagenicity, Carcinogenicity and Teratogenicity of Antimony Compounds. *Mutation Research-Reviews in Genetic Toxicology*, **366** (1), 1-8.

Leuz, A. K., Monch, H., & Johnson, C. A. 2006. Sorption of Sb(III) and Sb(V) to Goethite: Influence on Sb(III) Oxidation and Mobilization. *Environmental Science & Technology*, **40** (23), 7277-7282.

Li, X. D. & Thornton, I. 1993. Arsenic, Antimony and Bismuth in Soil and Pasture Herbage in Some Old Metalliferous Mining Areas in England. *Environmental Geochemistry and Health*, **15** (2-3), 135-144.

Li, Y.-H., Burkhardt, L., Buchholtz, M., O'Hara, P., & Santschi, P. H. 1984. Partition of Radiotracers between Suspended Particles and Seawater. *Geochimica Et Cosmochimica Acta*, **48** 2011-2019.

Lintschinger, J., Michalke, B., Schulte-Hostede, S., & Schramel, P. 1998. Studies on Speciation of Antimony in Soil Contaminated by Industrial Activity. *International Journal of Environmental Analytical Chemistry*, **72** (1), 11-25.

Lloyd, E. F. 1959. The Hot Springs and Hydrothermal Eruptions of Waiotapu. *New Zealand Journal of Geology and Geophysics*, **2** 141-176.

Lloyd, J. R. & Oremland, R. S. 2006. Microbial Transformations of Arsenic in the Environment: From Soda Lakes to Aquifers. *Elements*, **2** (2), 85-90.

Lovell, J. S., Meyer, W. T., & Atkinson, D. 1983. Surface Geochemistry at Roosevelt Springs, Utah. *Journal of Geochemical Exploration*, **19** (1-3), 345-346.

Lynch, B. S., Capen, C. C., Nestmann, E. R., Veenstra, G., & Deyo, J. A. 1999. Review of Subchronic/Chronic Toxicity of Antimony Potassium Tartrate. *Regulatory Toxicology and Pharmacology*, **30** (1), 9-17.

Maeda, S., Fukuyama, H., Yokoyama, E., Kuroiwa, T., Ohki, A., & Naka, K. 1997. Bioaccumulation of Antimony by *Chlorella Vulgaris* and the Association Mode of Antimony in the Cell. *Applied Organometallic Chemistry*, **11** (5), 393-396.

Magadza, C. H. D. 1979. Physical and Chemical Limnology of Six Hydroelectric Lakes on the Waikato River, 1970-72. *New Zealand Journal of Marine and Freshwater Research*, **13** (4), 561-572.

McCallum, R. I. 2005. Occupational Exposure to Antimony Compounds. *Journal of Environmental Monitoring*, **7** (12), 1245-1250.

McComb, K. A., Craw, D., & McQuillan, A. J. 2007. ATR-IR Spectroscopic Study of Antimonate Adsorption to Iron Oxide. *Langmuir*, **23** (24), 12125-12130.

McDowall, R. M. 1996. Volcanism and Freshwater Fish Biogeography in the Northeastern North Island of New Zealand. *Journal of Biogeography*, **23** (2), 139-148.

McLaren, S. J. & Kim, N. D. 1995. Evidence for a Seasonal Fluctuation of Arsenic in New-Zealand's Longest River and the Effect of Treatment on Concentrations in Drinking-Water. *Environmental Pollution*, **90** (1), 67-73.

Meinema, H. A. & Noltes, J. G. 1972. Investigations on Organoantimony Compounds 6. Preparation and Properties of Thermally Stable Dialkylantimony(V) Compounds of Types $R_2Sb(OrR')_3$, $R_2Sb(OAc)_3$ and $R_2Sb(O)OH$. *Journal of Organometallic Chemistry*, **36** (2), 313.

Meyer, J., Schmidt, A., Michalke, K., & Hensel, R. 2007. Volatilisation of Metals and Metalloids by the Microbial Population of an Alluvial Soil. *Systematic and Applied Microbiology*, **30** (3), 229-238.

Migdisov, A. A. & Bychkov, A. Y. 1998. The Behaviour of Metals and Sulphur During the Formation of Hydrothermal Mercury-Antimony-Arsenic Mineralization, Uzon Caldera, Kamchatka, Russia. *Journal of Volcanology and Geothermal Research*, **84** (1-2), 153-171.

Mighty River Power. 2001. *Taupo Waikato Resource Consents Assessment of Environmental Effects*. Mighty River Power, 251 pp.

Migon, C. & Mori, C. 1999. Arsenic and Antimony Release from Sediments in a Mediterranean Estuary. *Hydrobiologia*, **392** (1), 81-88.

Ministry of Health. 2005. *Drinking-Water Standards for New Zealand 2005*. Wellington, 181 pp.

Morgan, G. T. & Davies, G. R. 1926. Antimonial Analogues of the Cacodyl Series. *Proceedings of the Royal Society of London. Series A, Containing Papers of a Mathematical and Physical Character*, **110** (755), 523-534.

Mori, C., Orsini, A., & Migon, C. 1999. Impact of Arsenic and Antimony Contamination on Benthic Invertebrates in a Minor Corsican River. *Hydrobiologia*, **392** (1), 73-80.

Mountain, B. W. *Life in Hot Springs*. Te Ara - the Encyclopedia of New Zealand. 2007. Accessed:28March,2008,http://www.teara.govt.nz/EarthSeaAndSky/HotSpringsAndGeothermalEnergy/LifeInHotSprings/4/ENZ-Resources/Standard/2/en

Müller, K., Daus, B., Morgenstern, P., & Wennrich, R. 2007. Mobilization of Antimony and Arsenic in Soil and Sediment Samples – Evaluation of Different Leaching Procedures. *Water, Air, & Soil Pollution*, **183** (1), 427-436.

Murata, T., Kanao-Koshikawa, M., & Takamatsu, T. 2005. Effects of Pb, Cu, Sb, In and Ag Contamination on the Proliferation of Soil Bacterial Colonies, Soil Dehydrogenase Activity, and Phospholipid Fatty Acid Profiles of Soil Microbial Communities. *Water, Air, & Soil Pollution*, **164** (1 - 4), 103-118.

Murciego, A. M., Sanchez, A. G., Gonzalez, M. A. R., Gil, E. P., Gordillo, C. T., Fernandez, J. C., & Triguero, T. B. 2007. Antimony Distribution and Mobility in Topsoils and Plants (*Cytisus Striatus, Cistus Ladanifer and Dittrichia Viscosa*) from Polluted Sb-Mining Areas in Extremadura (Spain). *Environmental Pollution*, **145** (1), 15-21.

Newman, D.K., Beveridge, T. J., Morel, F.M.M. 1997. Precipitation of arsenic trisulfide by *Desulfotomaculum auripigmentum*. *Applied and Environmental Microbiology*, **63**(5), 2022-2028

Newton, P. E., Bolte, H. F., Daly, I. W., Pillsbury, B. D., Terrill, J. B., Drew, R. T., Bendyke, R., Sheldon, A. W., & Rubin, L. F. 1994. Subchronic and Chronic Inhalation Toxicity of Antimony Trioxide in the Rat. *Fundamental and Applied Toxicology*, **22** (4), 561-576.

Nimick, D. A., Moore, J. N., Dalby, C. E., & Savka, M. W. 1998. The Fate of Geothermal Arsenic in the Madison and Missouri Rivers, Montana and Wyoming. *Water Resources Research*, **34** (11), 3051-3067.

Nordstrom, D. K. 2004. All Acid Waters Are Not Equal: Biological Differences between Yellowstone's Acid Waters and Acid Mine Waters. *Geochimica Et Cosmochimica Acta*, **68** (11), A264-A264.

Nordstrom, D. K., Ball, J. W., & McCleskey, B. R. 2005. *Ground Water to Surface Water: Chemistry of Thermal Outflows in Yellowstone National Park*. In W. P. Inskeep & T. R. McDermott, Geothermal Biology and Geochemistry in Yellowstone National Park, Thermal Biology Institute, Montana State University, Bozeman. 73-94.

Nordstrom, D. K., McCleskey, R. B., & Ball, J. W. 2004. Processes Governing Arsenic Geochemistry in Thermal Waters of Yellowstone National Park. *Geochimica Et Cosmochimica Acta*, **68** (11), A262-A262.

Nriagu, J. O. 1989. A Global Assessment of Natural Sources of Atmospheric Trace-Metals. *Nature*, **338** (6210), 47-49.

O'Shea, B., Jankowski, J., & Sammut, J. 2007. The Source of Naturally Occurring Arsenic in a Coastal Sand Aquifer of Eastern Australia. *Science of The Total Environment*, **379** (2-3), 151-166.

Oelkers, E. H., Sherman, D. M., Ragnarsdottir, K. V., & Collins, C. 1998. An EXAFS Spectroscopic Study of Aqueous Antimony(III)-Chloride Complexation at Temperatures from 25 to 250 ^{0}C. *Economic Geology*, **151** 21-27.

Oremland, R. S. 1989. Present-Day Biogeochemical Activities of Anaerobic Bacteria and Their Relevance to Future Exobiological Investigations. *Advances in Space Research*, **9** (6), 127-136.

Oremland, R. S., Dowdle, P. R., Hoeft, S., Sharp, J. O., Schaefer, J. K., Miller, L. G., Blum, J. S., Smith, R. L., Bloom, N. S., & Wallschlaeger, D. 2000. Bacterial Dissimilatory Reduction of Arsenate and Sulfate in Meromictic Mono Lake, California. *Geochimica Et Cosmochimica Acta*, **64** (18), 3073-3084.

Oremland, R. S. & Stolz, J. F. 2003. The Ecology of Arsenic. *Science*, **300** (5621), 939-944.

Oremland, R. S. & Taylor, B. F. 1978. Sulfate Reduction and Methanogenesis in Marine Sediments. *Geochimica Et Cosmochimica Acta*, **42** (2), 209-214.

Pahlavanpour, B., Thompson, M., & Thorne, L. 1981. Simultaneous Determination of Trace Amounts of Arsenic, Antimony and Bismuth in Herbage by Hydride Generation and Inductively Coupled Plasma Atomic-Emission Spectrometry. *Analyst*, **106** (1261), 467-471.

Parkhurst, D. & Appelo, C. A. J. 1999. *User's Guide to Phreeqc (Version 2) - a Computer Program for Speciation, Batch-Reaction, One-Dimensional Transport and Inverse Geochemical Calculations*. U. G. Survey, Water Resources Investigations Report 99-4259. 326 pp.

Pauling, L. 1933. The Formulas of Antimonic Acid and the Antimonates. *Journal of the American Chemical Society*, **55** 1895-1900.

Phoenix, V. R., Renaut, R. W., Jones, B., & Ferris, F. G. 2005. Bacterial S-Layer Preservation and Rare Arsenic-Antimony-Sulphide Bioimmobilization in Siliceous Sediments from Champagne Pool Hot Spring, Waiotapu, New Zealand. *Journal of the Geological Society*, **162** 323-331.

Planer-Friedrich, B., Lehr, C., Matschullat, J., Merkel, B. J., Nordstrom, D. K., & Sandstrom, M. W. 2006. Speciation of Volatile Arsenic at Geothermal Features in Yellowstone National Park. *Geochimica Et Cosmochimica Acta*, **70** (10), 2480-2491.

Planer-Friedrich, B., London, J., McCleskey, R. B., Nordstrom, D. K., & Wallschlager, D. 2007. Thioarsenates in Geothermal Waters of Yellowstone National Park: Determination, Preservation, and Geochemical Importance. *Environmental Science & Technology*, **41** (15), 5245-5251.

Polmear, I. J. 1998. *Metallurgy of the Elements*. In N. C. Norman, Chemistry of Arsenic, Antimony and Bismuth, 1st Edition, Thomson Science, London. 483*ff*.

Pope, J. G. 2004. *Trace Element Geochemistry in the Waiotapu Geothermal Area and Waiotapu Catchment, New Zealand*, School of Environmental Science and Management, Unpublished Ph.D. Thesis, Southern Cross University

Pope, J. G., Brown, K. L., & McConchie, D. M. 2005. Gold Concentrations in Springs at Waiotapu, New Zealand: Implications for Precious Metal Deposition in Geothermal Systems. *Economic Geology*, **100** (4), 677-687.

Pope, J. G., McConchie, D. M., Clark, M. D., & Brown, K. L. 2004. Diurnal Variations in the Chemistry of Geothermal Fluids after Discharge, Champagne Pool, Waiotapu, New Zealand. *Chemical Geology*, **203** (3-4), 253-272.

Qi, C. C., Liu, G. J., Chou, C. L., & Zheng, L. Q. 2008. Environmental Geochemistry of Antimony in Chinese Coals. *Science of the Total Environment*, **389** (2-3), 225-234.

Quentel, F. & Filella, M. 2002. Determination of Inorganic Antimony Species in Seawater by Differential Pulse Anodic Stripping Voltammetry: Stability of the Trivalent State. *Analytica Chimica Acta*, **452** (2), 237-244.

Ravengai, S., Love, D., Mabvira-Meck, M., Musiwa, K., & Moyce, W. 2005. Water Quality in an Abandoned Gold Mining Belt, Beatrice, Sanyati Valley, Zimbabwe. *Physics and Chemistry of the Earth*, **30** (11-16), 826-831.

Raymond, J., Williams-Jones, A. E., & Clark, J. R. 2005. Mineralization Associated with Scale and Altered Rock and Pipe Fragments from the Berlin Geothermal Field, El Salvador; Implications for Metal Transport in Natural Systems. *Journal of Volcanology and Geothermal Research*, **145** (1-2), 81-96.

Reed, M. & Palandri, J. L. 1998. *Soltherm Database: A Compilation of Thermodynamic Data from 25 to 300 ^{O}C for Aqueous Species, Minerals and Gases (Version Soltherm.Joh Dated 4/98)*. E. University of Oregon, OR., pp.

Reed, M. H. 1982. Calculation of Multicomponent Chemical Equilibria and Reaction Processes in Systems Involving Minerals, Gases and an Aqueous Phase. *Geochimica et Cosmochimica Acta*, **46** (4), 513-528.

Reid, F. 1983. Origin of the Rhyolitic Rocks of the Taupo Volcanic Zone, New-Zealand. *Journal of Volcanology and Geothermal Research*, **15** (4), 315-338.

Reyes, A. G., Trompetter, W. J., Britten, K., & Searle, J. 2002. Mineral Deposits in the Rotokawa Geothermal Pipelines, New Zealand. *Journal of Volcanology and Geothermal Research*, **119** (1-4), 215-239.

Ritchie, J. A. 1961. Arsenic and Antimony in Some New Zealand Thermal Waters. *New Zealand Journal of Science*, **4** (2), 218-229.

Robinson, B., Duwig, C., Bolan, N., Kannathasan, M., & Saravanan, A. 2003. Uptake of Arsenic by New Zealand Watercress (*Lepidium Sativum*). *Science of the Total Environment*, **301** (1-3), 67-73.

Robinson, B., Outred, H., Brooks, R., & Kirkman, J. 1995a. The Distribution and Fate of Arsenic in the Waikato River System, North Island, New Zealand. *Chemical Speciation and Bioavailability*, **7** (3), 89-96.

Robinson, B. H., Brooks, R. R., Outred, H. A., & Kirkman, J. H. 1995b. Mercury and Arsenic in Trout from the Taupo Volcanic Zone and Waikato River, North-Island, New-Zealand. *Chemical Speciation and Bioavailability*, **7** (1), 27-32.

Rybach, L. 2003. Geothermal Energy: Sustainability and the Environment. *Geothermics*, **32** (4-6), 463-470.

Sakamoto, H., Kamada, M., Yonehara, N. 1988. The Contents and Distribution of Arsenic, Antimony and Mercury in geothermal waters. *Bulletin of the Chemical Society of Japan*, **61** (10), 3471-3477

Schemel, L. E., Cox, M. H., Runkel, R. L., & Kimball, B. A. 2006. Multiple Injected and Natural Conservative Tracers Quantify Mixing in a Stream Confluence Affected by Acid Mine Drainage near Silverton, Colorado. *Hydrological Processes*, **20** (13), 2727-2743.

Schippers, A. & Sand, W. 1999. Bacterial Leaching of Metal Sulfides Proceeds by Two Indirect Mechanisms via Thiosulfate or via Polysulfides and Sulfur. *Appl. Environ. Microbiol.*, **65** (1), 319-321.

Scott, B. J. 1994. Cyclic Activity in the Crater Lakes of Waimangu Hydrothermal System, New Zealand. *Geothermics*, **23** (5-6), 555-572.

Seward, T. M. & Sheppard, D. 1986. *Waimangu Geothermal Field*. In R. W. Henley & J. W. Hedenquist & P. J. Roberts, Guide to the Active Epithermal (Geothermal) Systems and Precious Metal Deposits of New Zealand, Monograph Series on Mineral Deposits, Volume 26, Gebruder Borntraeger, Berlin, Stuttgart. 81-91.

Shaw, P. 1747. *A Philosophical and Chymical Analysis of Antimony: Giving a Rational Account of the Nature, Principles, and Properties of That Celebrated Drug*, 2nd Edition. London, Joseph Davidson, 90 pp.

Sheppard, B. S., Shen, W.-L., Caruso, J. A., Heitkemper, D. T., & Fricke, F. L. 1990. Elimination of the Argon Chloride Interference on Arsenic Speciation in Inductively Coupled Plasma Mass Spectrometry Using Ion Chromatography. *Journal of Analytical Atomic Spectrometry*, **5** 431-435.

Sheppard, D. 1986. *Ngawha Geothermal Field*. In R. W. Henley & J. W. Hedenquist & P. J. Roberts, Guide to the Active Epithermal (Geothermal) Systems and Precious Metal Deposits of New Zealand, 1st, Monograph Series on Mineral Deposits, Volume 26, Gebruder Borntraeger, Berlin, Stuttgart. 185-192.

Shikina, N. D. & Zotov, A. V. 1996. Stoichiometry of the Neutral Antimony Hydroxo Complex (in Russian). *Geokhimiya*, **N12** 1242-1244.

Shikina, N. D. & Zotov, A. V. 1999. Solubilty of Stibnite (Sb_2S_3) in Water and Hydrogen Sulfide Solutions at Temperature of 200-300 ^{O}C under Vapor-Saturated Conditions and a Pressure of 500 Bars. *Geochemistry International*, **37** 82-86.

Shotyk, W., Cheburkin, A. K., Appleby, P. G., Fankhauser, A., & Kramers, J. D. 1996. Two Thousand Years of Atmospheric Arsenic, Antimony, and Lead Deposition Recorded in an Ombrotrophic Peat Bog Profile, Jura Mountains, Switzerland. *Earth and Planetary Science Letters*, **145** (1-4), E1-E7.

Shotyk, W. & Krachler, M. 2007. Contamination of Bottled Waters with Antimony Leaching from Polyethylene Terephthalate (PET) Increases Upon Storage. *Environmental Science & Technology*, **41** (5), 1560-1563.

Shotyk, W., Krachler, M., & Chen, B. 2006. Contamination of Canadian and European Bottled Waters with Antimony from Pet Containers. *Journal of Environmental Monitoring*, **8** (2), 288-292.

Sillen, L.G. & Martel, A. E. 1964. *Stability constants of metal-ion complexes*. 2nd edition, London, Chemical Society, 754pp.

Simmons, S. F., Stewart, M. K., Robinson, B. W., & Glover, R. B. 1994. The Chemical and Isotopic Compositions of Thermal Waters at Waimangu, New-Zealand. *Geothermics*, **23** (5-6), 539-553.

Skalbeck, J. D., Shevenell, L., & Widmer, M. C. 2002. Mixing of Thermal and Non-Thermal Waters in the Steamboat Hills Area, Nevada, USA. *Geothermics*, **31** (1), 69-90.

Skinner, B. J. & Porter, S. C. 1987. *Physical Geology*, New York, John Wylie & Sons Inc., 750 pp.

Skirnisdottir, S., Hreggvidsson, G.O., Holst, O., Kristjansson, J.K. 2001. Isolation and Characterization of a Mixotrophic Sulfur-Oxidizing Thermus scotoductus. *Extremophiles,* 5(1), 45-51.

Smith, C. L., Ficklin, W. H., & Thompson, J. M. 1987. Concentrations of Arsenic, Antimony, and Boron in Steam and Steam Condensate at the Geysers, California. *Journal of Volcanology and Geothermal Research*, **32** (4), 329-341.

Smith, L. M., Craig, P. J., & Jenkins, R. O. 2002. Formation of Involatile Methylantimony Species by *Clostridium Sp*. *Chemosphere*, **47** (4), 401-407.

Smith, P. 2006. *Waikato River Water Quality Monitoring Programme: Data Report 2005.* Environment Waikato, Technical Report 2006/34. 60 pp.

Spycher, N. F. & Reed, M. H. 1989a. As(III) and Sb(III) Sulfide Complexes - an Evaluation of Stoichiometry and Stability from Existing Experimental-Data. *Geochimica Et Cosmochimica Acta*, **53** (9), 2185-2194.

Spycher, N. F. & Reed, M. H. 1989b. Evolution of a Broadlands-Type Epithermal Ore Fluid Along Alternative P-T Paths - Implications for the Transport and Deposition of Base, Precious, and Volatile Metals. *Economic Geology*, **84** (2), 328-359.

Spycher, N. F. & Reed, M. H. 1990a. As(III) and Sb(III) Sulfide Complexes - an Evaluation of Stoichiometry and Stability from Existing Experimental-Data - Reply. *Geochimica Et Cosmochimica Acta*, **54** (11), 3241-3243.

Spycher, N. F. & Reed, M. H. 1990b. As(III) and Sb(III) Sulfide Complexes - an Evaluation of Stoichiometry and Stability from Existing Experimental-Data - Response. *Geochimica Et Cosmochimica Acta*, **54** (11), 3246-3246.

Stauffer, R. E. & Thompson, J. M. 1984. Arsenic and Antimony in Geothermal Waters of Yellowstone National Park, Wyoming, USA. *Geochimica Et Cosmochimica Acta*, **48** (12), 2547-2561.

Stewart, C. *Geothermal Energy*. Te Ara - the Encylopedia of New Zealand. 2006, Accessed: 9 June,2008,http://www.TeAra.govt.nz/EarthSeaAndSky/HotSpringsAndGeothermalEnergy/GeothermalEnergy/en

Stolz, J. F. & Oremland, R. S. 1999. Bacterial Respiration of Arsenic and Selenium. *Fems Microbiology Reviews*, **23** (5), 615-627.

Stumm, W. & Morgan, J. 1996. *Aquatic Chemistry*, 3rd Edition. New York, John Wiley & Sons Inc., 1022 pp.

Summers, A. O. & Silver, S. 1978. Microbial Transformations of Metals. *Annual Review of Microbiology*, **32** 637-672.

Takayanagi, K. 2001. Acute Toxicity of Waterborne Se(IV), Se(VI), Sb(III), and Sb(V) on Red Seabream (Pargus Major). *Bulletin of Environmental Contamination and Toxicology*, **66** (6), 808-813.

Tate, C. M., McKnight, D. M., & Broshears, R. E. 1996. Using Lithium (Li^+) as a Conservative Tracer Does Not Prevent Algal Uptake of Phosphate in an Acid Mine Drainage Stream (Reply to the Comment by Stewart and Kszos). *Limnology and Oceanography*, **41** (1), 191-192.

Thanabalasingam, P. & Pickering, W. F. 1990. Specific Sorption of Antimony(Iii) by the Hydrous Oxides of Mn, Fe, and Ai. *Water Air and Soil Pollution*, **49** (1-2), 175-185.

Thomson, S.C. 1925. Antimonyall Cups: Pocula Emetica or Calices Vomitorii. *Proceedings of the Royal Society of Medicine*, **19** (9), 123-128.

Tighe, M., Ashley, P., Lockwood, P., & Wilson, S. 2005a. Soil, Water, and Pasture Enrichment of Antimony and Arsenic within a Coastal Floodplain System. *Science of the Total Environment*, **347** (1-3), 175-186.

Tighe, M., Lockwood, P., & Wilson, S. 2005b. Adsorption of Antimony(V) by Floodplain Soils, Amorphous Iron(III) Hydroxide and Humic Acid. *Journal of Environmental Monitoring*, **7** (12), 1177-1185.

Tighe, M., Lockwood, P., Wilson, S., & Lisle, L. 2004. Comparison of Digestion Methods for ICP-OES Analysis of a Wide Range of Analytes in Heavy Metal Contaminated Soil Samples with Specific Reference to Arsenic and Antimony. *Communications in Soil Science and Plant Analysis*, **35** (9-10), 1369-1385.

Timperley, M. H. & Huser, B. A. 1996. Inflows of Geothermal Fluid Chemicals to the Waikato River Catchment, New Zealand. *New Zealand Journal of Marine and Freshwater Research*, **30** (4), 525-535.

Todar, K. 2008. *Todar's Online Textbook of Bacteriology*. University of Wisconsin, Accessed: 16 June, 2008, http://textbookofbacteriology.net/nutgro.html

Torma, A. & Gabra, G. 1977. Oxidation of Stibnite by *Thiobacillus ferrooxidans*. *Antonie van Leeuwenhoek*, **43** (1), 1-6.

Trois, C., Marcello, A., Pretti, S., Trois, P., & Rossi, G. 2007. The Environmental Risk Posed by Small Dumps of Complex Arsenic, Antimony, Nickel and Cobalt Sulphides. *Journal of Geochemical Exploration*, **92** (1), 83-95.

Tylenda, C. A. & Fowler, B. A. 2007. *Antimony*. In G. F. Nordberg & B. A. Fowler & M. Nordberg & L. T. Friberg, Handbook on the Toxicology of Metals, 3rd Edition, Elsevier Inc., 1024*ff*.

Ujiie-Mikoshiba, M., Imai, N., Terashima, S., Tachibana, Y., & Okai, T. 2006. Geochemical Mapping in Northern Honshu, Japan. *Applied Geochemistry*, **21** (3), 492-514.

United States Environmental Protection Agency. *Consumer Factsheet On: Antimony*. 2005, Accessed: 15 November, 2005, http://www.epa.gov/safewater/dwh/c-ioc/antimony.html

Valentinus, B. 1678. *His Triumphant Chariot of Antimony*, London, Dorman Newman, 160 pp.

Valli, V. E., Poon, R., Chu, I., Gupta, S., & Thomas, B. H. 2000. Subchronic/Chronic Toxicity of Antimony Potassium Tartrate. *Regulatory Toxicology and Pharmacology*, **32** (3), 337-338.

van der Krogt, P. *Stibium Antimony*. Elementymology & Elements Multidict. 2005, Accessed: 5 May, 2005, http://elements.vanderkrogt.net/elem/sb.html

Van der sloot, H. A., Hoede, D., & Wijkstra, J. 1989. Trace Oxyanions and Their Behavior in the Rivers Porong and Solo, the Java Sea and the Adjacent Indian-Ocean. *Netherlands Journal of Sea Research*, **23** (4), 379-386.

Van Hinsberg, V. J., Zinngrebe, E., de Wijs, C. J., & Vriend, S. P. 2003. A New Model for Sb Deposition in the French Massif Central Based Upon Thermodynamic Modeling of the Mineralizing Fluid. *Journal of Geochemical Exploration*, **78-9** 75-79.

Vant, B. & Smith, P. 2004. *Trends in River Water Quality in the Waikato Region, 1987–2002*. Environment Waikato, Technical Report 2004/02. 40 pp.

Wang, C. Y. 1952. *Antimony: Its Geology, Metallurgy, Industrial Uses and Economics*, 3rd Edition. London, Charles Griffin, 170 pp.

Ward, K. 2007. *Mineral Precipitation in the Rotokawa Geothermal Power Station: Implications for the Formation of Low Sulphidation Epithermal Deposits*, Department of Geology, Unpublished MSc thesis, University of Auckland, Auckland.

Warnock, D. W., Delves, H. T., Campell, C. K., Croudace, I. W., Davey, K. G., Johnson, E. M., & Sieniawska, C. 1995. Toxic Gas Generation from Plastic Mattresses and Sudden-Infant-Death-Syndrome. *Lancet*, **346** (8989), 1516-1520.

Webster-Brown, J. G. & Lane, V. 2005a. *Modeling Seasonal Arsenic Behaviour in the Waikato River, New Zealand*. In Advances in Arsenic Research: Integration of Experimental and Observational Studies and Implications for Mitigation, American Chemical Society Symposium Series, Volume 915, American Chemical Society, Washington. 253-266.

Webster-Brown, J. G. & Lane, V. 2005b. *The Environmental Fate of Geothermal Arsenic in a Major River System, New Zealand*. 2005, World Geothermal Congress, Antalya, Turkey.

Webster-Brown, J. G. & Webster, K. S. 2000. *Trace Metals in the Waikato River*. E. S. a. Research, Report CO3081. 62 pp.

Webster-Brown, J. G., Webster, K. S., & Lane, V. 2000. *Arsenic in the Waikato River: An Update*. 2000, 22nd New Zealand Geothermal Workshop, Auckland, New Zealand.

Webster, J. G. 1987. Thiosulphate in Surficial Geothermal Waters, North Island, New Zealand. *Applied Geochemistry*, **2** (5-6), 579-584.

Webster, J. G. 1990. The Solubility of As_2S_3 and Speciation of As in Dilute and Sulfide-Bearing Fluids at 25 ^{O}C and 90 ^{O}C. Geochimica Et Cosmochimica Acta, 54 (4), 1009-1017.

Webster, J. G. 1994. Trace-metal Behaviour in Oxic and Anoxic Ca-Cl Brines of the Wright Valley Drainage, Antarctica. Chemical Geology 112, 255-274

Webster, J. G. & Nordstrom, D. K. 2003. *Geothermal Arsenic*. In A. H. Welch & K. G. Stollenwerk, Arsenic in Ground Water, Kluwer Academic Publishers, Boston. 475*ff*.

Wedepohl, H. K. 1995. The Composition of the Continental Crust. *Geochimica et Cosmochimica Acta*, **59** (7), 1217-1232.

Weissberg, B. G. 1969. Gold-Silver Ore-Grade Precipitates from New Zealand Thermal Waters. *Economic Geology*, **64** (1), 95-108.

Weissberg, B. G., Browne, P., & Seward, T. M. 1979. *Ore Metals in Active Geothermal Systems*. In H. L. Barnes, Geochemistry of Hydrothermal Ore Deposits, Second, John Wiley & Sons, New York. 798*ff*.

Wenzel, W. W., Kirchbaumer, N., Prohaska, T., Stingeder, G., Lombi, E., & Adriano, D. C. 2001. Arsenic Fractionation in Soils Using an Improved Sequential Extraction Procedure. *Analytica Chimica Acta*, **436** (2), 309-323.

Westerhoff, P., Prapaipong, P., Shock, E., & Hillaireau, A. 2008. Antimony Leaching from Polyethylene Terephthalate (PET) Plastic Used for Bottled Drinking Water. *Water Research*, **42** (3), 551-556.

Wilson, N. J., Craw, D., & Hunter, K. 2004a. Antimony Distribution and Environmental Mobility at an Historic Antimony Smelter Site, New Zealand. *Environmental Pollution*, **129** (2), 257-266.

Wilson, N. J., Craw, D., & Hunter, K. 2004b. Contributions of Discharges from a Historic Antimony Mine to Metalloid Content of River Waters, Marlborough, New Zealand. *Journal of Geochemical Exploration*, **84** (3), 127-139.

Wilson, N. J., Webster-Brown, J., & Brown, K. 2007. Controls on Stibnite Precipitation at Two New Zealand Geothermal Power Stations. *Geothermics*, **36** (4), 330-347.

Wilson, W. E. & Thomssen, R. W. 1985. Steamboat Springs. *Mineralogical Record*, **16** (1), 25-31.

Wood, P. C. 1994. Aspects of the Geology of Waimangu, Waiotapu, Waikite and Reporoa Geothermal Systems, Taupo Volcanic Zone, New Zealand. *Geothermics*, **23** (5-6), 401-421.

Wood, S. A., Crerar, D. A., & Borcsik, M. P. 1987. Solubility of the Assemblage Pyrite-Pyrrhotite-Magnetite-Sphalerite-Galena-Gold-Stibnite-Bismuthinite-Argentite-Molybdenite in H_2O-NaCl-CO_2 Solutions from 200 ^{O}C to 350 ^{O}C. *Economic Geology*, **82** (7), 1864-1887.

Xu, Y., Schoonen, M. A. A., Nordstrom, D. K., Cunningham, K. M., & Ball, J. W. 1998. Sulfur Geochemistry of Hydrothermal Waters in Yellowstone National Park: I. The Origin of Thiosulfate in Hot Spring Waters. *Geochimica Et Cosmochimica Acta*, **62** (23-24), 3729-3743.

Xu, Y., Schoonen, M. A. A., Nordstrom, D. K., Cunningham, K. M., & Ball, J. W. 2000. Sulfur Geochemistry of Hydrothermal Waters in Yellowstone National Park, Wyoming, USA. II. Formation and Decomposition of Thiosulfate and Polythionate in Cinder Pool. *Journal of Volcanology and Geothermal Research*, **97** (1-4), 407-423.

Zakaznova-Herzog, V. P. & Seward, T. M. 2006. Antimonous Acid Protonation/Deprotonation Equilibria in Hydrothermal Solutions to 300 ^{O}C. *Geochimica Et Cosmochimica Acta*, **70** (9), 2298-2310.

Zotov, A. V., Shikina, N. D., & Akinfiev, N. N. 2003. Thermodynamic Properties of the Sb(III) Hydroxide Complex $Sb(OH)_{3(aq)}$ at Hydrothermal Conditions. *Geochimica Et Cosmochimica Acta*, **67** (10), 1821-1836.

APPENDIX I:
MODELLING DATA

DATABASE AMENDMENTS

SOLVEQ DATABASE

Database edition: Soltherm.h05

Stibnite 339.69 4 -6.00 2 2.00 24 3.00 6 3.00 1

Stibnite -57.026 -52.503 -45.749 -41.096 -37.907 -35.858 -34.901 -35.580 NW/Z-W

Stibnite -0.62509E+02 0.24133E+00-0.93029E-03 0.21939E-05-0.25082E-08

MINTEQ V.4 DATABASE

Database edition: minteq.v4.dat 794 2006-02-27 21:06:22Z dlpark

Stibnite
Sb2S3 + 6H2O = 2Sb(OH)3 + 3H+ + 3HS-
log_k -57.78
delta_h 293.78 kJ

WATCH INPUT CHEMISTRY

	Unit	Well Nine	Well Twelve	Rotokawa
Flash Point	^oC	198	193	225
Pressure	bar_G	14.1	13.3	27.7
Temperature $_{Water}$	^oC	22.0	21.0	14.0
Enthalpy	kJ/kg	931	987	1560
pH $_{Water}$		7.71	7.83	6.03
CO_2 $_{Water}$	mg/kg	330	300	69.0
H_2S $_{Water}$	mg/kg	17.8	15.8	16.6
NH_3 $_{Water}$	mg/kg	85.0	64.0	5.20
SiO_2 $_{Water}$	mg/kg	479	479	948
B $_{Water}$	mg/kg	977	997	18.9
Na $_{Water}$	mg/kg	882	899	402
K $_{Water}$	mg/kg	87.0	87.0	116
Mg $_{Water}$	mg/kg	0.1	0.07	0.00
Ca $_{Water}$	mg/kg	6.80	5.90	0.710
F $_{Water}$	mg/kg	2.40	2.50	3.60
Cl $_{Water}$	mg/kg	1350	1370	747
SO_4 $_{Water}$	mg/kg	28.0	22.0	4.70
Gas/Condensate	L/kg	4.30	3.03	0.574
Gas collection temp	^oC	25.0	25.0	25.0
pH_{gas}		0.00	0.00	0.00
H_2 $_{Gas}$	% volume	7.08	8.98	11.3
CH_4 $_{Gas}$	% volume	73.6	84.4	61.5
N_2 $_{Gas}$	% volume	19.3	6.64	27.2
CO_2 $_{Condensate}$	g/kg	181	155	20.7
H_2S $_{Condensate}$	g/kg	1.55	1.27	0.788
NH_3 $_{Condensate}$	mg/kg	0.539	0.492	0.034

SOLVEQ/CHILLER INPUT CHEMISTRY

BRINE	Rotokawa	Ngawha Well Nine	Ngawha Well Twelve
Temperature (^oC)	225	198	193
pH (Unitless)	6.20	6.72	6.88
H_2O	1.00×10^{-1}	1.00×10^{-1}	1.00×10^{-1}
Cl	2.14×10^{-2}	3.81×10^{-2}	3.90×10^{-2}
SO_4	4.98×10^{-5}	2.92×10^{-4}	2.31×10^{-4}
CO_2	2.15×10^{-3}	1.45×10^{-2}	1.28×10^{-2}
H_2S	3.30×10^{-4}	5.83×10^{-4}	5.13×10^{-4}
SiO_2	1.60×10^{-2}	7.98×10^{-3}	8.03×10^{-3}
Ca	1.80×10^{-5}	1.70×10^{-4}	1.48×10^{-4}
Mg		4.11×10^{-6}	2.92×10^{-6}
K	3.02×10^{-3}	2.23×10^{-3}	2.24×10^{-3}
Na	1.78×10^{-2}	3.84×10^{-2}	3.94×10^{-2}
F	1.93×10^{-4}	1.27×10^{-4}	1.33×10^{-4}
Sb	7.85×10^{-6}	2.13×10^{-5}	2.27×10^{-5}
As	2.42×10^{-5}		
NH_4	2.74×10^{-4}	4.22×10^{-3}	3.27×10^{-3}
H_3BO_3	1.78×10^{-3}	9.05×10^{-2}	9.29×10^{-2}

Note: Units in mg/kg unless otherwise stated

CONDENSATE	Rotokawa	Ngawha
Temperature (°C)	224	197
pH (Unitless)	4.95	5.06
H_2O	1.00×10^{-1}	1.00×10^{-1}
Cl	5.82×10^{-9}	7.24×10^{-11}
SO_4	-5.86×10^{-7}	-7.27×10^{-6}
HCO_3	6.49×10^{-3}	1.42×10^{-2}
HS	3.75×10^{-4}	3.32×10^{-4}
F	1.97×10^{-7}	7.55×10^{-9}
NH_4	2.64×10^{-5}	1.59×10^{-4}

Note: Units in mg/kg unless otherwise stated

PHREEQC INPUT CHEMISTRY

	Alum Lake	Lake Ohakuri
Temperature (°C)	35	19.1
pH (Unitless)	2.5	6.9
pe (Unitless)	4	4
Redox	S(-2)/S(6)	S(-2)/S(6)
O_2	0.56	2.8
CO_3		9.0
Cl	631	19 Charge
HS	2.18	0.024
SO4	473	9.5
Ca		5.9
Mg		3.3
NO_3		2.3
Na	0 Charge	1400
Fe		0.29
Mn		0.22
Sb	0.005	0.0015
As	1.5	0.057

Note: Units in mg/kg unless otherwise stated

APPENDIX II:
RESULTS FROM NATURAL SYSTEMS

WAI-O-TAPU

GENERAL CHEMISTRY DATA

SUMMER Site	Distance (m)	Time	Light (Lux)	Temperature (°C)	DO mg/L	pH	Conductivity mS/cm	Li µg/kg	H_2S mg/kg	SO_4 mg/kg	Cl mg/kg
WT 2	30	8:45 a.m.	75100	22.2	7.10	7.13	3.34	10500	< 0.05	146	2150
		10:45 a.m.	118000	27.8	5.65	7.03	7.29	10300	0.27	147	2150
		12:40 p.m.	133000	32.0	5.13	6.84	8.19	10600	0.51	254	2220
		2:05 p.m.	115000	33.7	5.36	6.84	8.21	9490	1.02	183	2250
		3:15 p.m.	96800	34.1	6.40	6.69	7.92	10600	0.61	163	2230
WT 3	150	9:05 a.m.	14800	17.3	8.19	7.42	5.73	10900	< 0.05	138	2090
		11:05 a.m.	113000	27.8	5.93	7.21	7.46	10400	0.53	149	2200
		12:55 p.m.	121000	31.2	5.60	7.08	8.39	10000	0.88	174	2290
		2:20 p.m.	121000	33.3	5.15	7.10	8.49	10500	1.07	168	2280
		3:30 p.m.	99600	31.9	5.70	7.15	8.02	11300	0.31	161	2270
WT 5	205	9:25 a.m.	37600	15.4	7.93	4.68	5.88	10800	0.93	223	2330
		11:20 a.m.	104000	23.1	7.13	3.89	7.55	11000	0.33	247	2460
		1:05 p.m.	124000	33.3	6.27	3.80	8.98	10900	0.42	257	2650
		2:30 p.m.	40500	32.1	5.78	3.99	9.71	12800	0.35	257	2820
		3:40 p.m.	49200	30.4	6.54	4.24	9.65	13600	< 0.05	264	2820
WT 6	225	9:40 a.m.	20200	21.9	6.91	2.54	4.19	4420	0.57	358	682
		11:40 a.m.	111000	26.8	6.71	2.50	4.72	3760	< 0.05	353	835
		1:20 p.m.	109000	30.1	6.34	2.53	5.13	5270	0.38	393	973
		2:40 p.m.	121000	31.8	6.28	2.50	4.97	3260	< 0.05	356	932
		3:55 p.m.	96600	29.9	7.27	2.51	4.95	5430	0.22	383	890

SUMMER Site	Distance (m)	Time	Light (Lux)	Temperature (°C)	DO mg/L	pH	Conductivity mS/cm	Li µg/kg	H_2S mg/kg	SO_4 mg/kg	Cl mg/kg
WT 7	260	9:55 a.m.	94600	24.1	6.60	2.53	4.46	4170	0.79	372	648
		11:50 a.m.	125000	30.4	5.56	2.52	5.00	3850	0.79	367	783
		1:30 p.m.	126000	33.7	5.36	2.51	3.74	4400	0.79	419	722
		2:45 p.m.	111000	34.0	5.56	2.49	5.17	4530	0.65	350	632
		4:00 p.m.	97200	32.4	6.21	2.48	5.06	3640	0.65	359	820
WT 8	320	10:25 a.m.	112000	32.9	0.18	2.44	4.42	2810	3.91	473	609
		12:05 p.m.	117000	33.0	0.39	2.43	4.46	2600	1.53	464	585
		1:50 p.m.	118000	34.5	0.68	2.45	4.62	2850	2.09	472	631
		3:00 p.m.	110000	35.0	0.56	2.45	4.63	3140	2.18	479	660
		4:15 p.m.	91400	34.7	0.84	2.45	4.63	3170	2.18	477	652

WINTER Site	Distance (m)	Time	Light (Lux)	Temperature (°C)	DO mg/L	pH	Conductivity mS/cm	Li µg/kg	H_2S mg/kg	SO_4 mg/kg	Cl mg/kg
WT 1	24	8:45 a.m.	4270	6.0	6.84	6.68	2.09	10800	0.11	96	2370
		10:00 a.m.	7500	4.7	8.27	5.28	4.48	10400	< 0.05	103	2360
		11:10 a.m.	18800	8.0	7.56	4.78	4.79	9810	< 0.05	115	2360
		1:15 p.m.	23400	9.4	6.25	5.05	4.96	9450	0.62	147	2390
		2:50 p.m.	16500	9.8	6.87	4.24	4.97	10700	0.16	203	2500
		4:05 p.m.	5450	9.5	6.92	3.92	5.00	11300	0.53	163	2400
WT 2	30	9:05 a.m.	5600	6.7	9.71	4.80	3.05	10700	0.73	118	2340
		10:15 a.m.	7830	7.1	8.81	5.03	4.73	10100	< 0.05	125	2370
		11:20 a.m.	18400	8.9	8.59	5.41	4.91	9340	< 0.05	120	2380
		1:05 p.m.	26400	9.9	8.34	4.35	4.90	10400	0.56	198	2440
		2:40 p.m.	18100	10.1	8.04	4.17	4.96	11400	< 0.05	209	2440
		3:55 p.m.	6230	9.4	8.20	4.17	4.91	10900	0.36	190	2440
WT 3	150	9:15 a.m.	4230	4.5	10.7	4.66	2.71	9700	1.76	116	2300
		10:25 a.m.	7590	3.9	9.54	5.26	4.67	9290	< 0.05	122	2340
		11:30 a.m.	15600	5.4	9.23	5.30	4.83	10100	0.52	154	2340
		12:55 p.m.	19700	6.4	9.03	4.06	4.70	11100	< 0.05	206	2370
		2:30 p.m.	14100	7.1	8.81	3.76	4.83	10700	< 0.05	232	2420
		3:45 p.m.	6490	6.6	8.65	3.52	4.91	10100	< 0.05	263	2430

WINTER Site	Distance (m)	Time	Light (Lux)	Temperature (°C)	DO mg/L	pH	Conductivity mS/cm	Li µg/kg	H_2S mg/kg	SO_4 mg/kg	Cl mg/kg
WT 4	200	9:25 a.m.	4840	2.2	10.8	5.08	2.45	9120	0.76	151	2270
		10:35 a.m.	11000	2.9	10.0	4.49	4.60	10300	0.16	150	2260
		12:00 p.m.	14800	4.2	9.63	3.65	4.63	10700	< 0.05	189	2260
		12:45 p.m.	19300	5.1	9.12	3.55	4.58	9960	< 0.05	201	2280
		2:20 p.m.	16500	6.1	8.65	3.44	4.76	9140	< 0.05	219	2300
		3:30 p.m.	7480	6.3	8.47	3.24	4.81	10200	< 0.05	245	2300
WT 6	225	9:45 a.m.	4710	15.0	7.77	2.39	2.95	1650	< 0.05	485	398
		11:00 a.m.	12800	16.3	7.50	2.39	3.21	1670	< 0.05	494	389
		11:40 a.m.	16100	15.3	7.65	2.42	3.04	1620	< 0.05	475	390
		12:30 p.m.	16000	16.2	7.22	2.41	3.01	1430	< 0.05	496	389
		2:00 p.m.	13200	16.4	7.30	2.39	2.99	1320	< 0.05	490	378
		3:10 p.m.	9650	15.4	7.11	2.40	2.97	1480	< 0.05	482	385
WT 9	-20	9:35 a.m.	1020	16.0	6.04	2.51	2.85	1440	< 0.05	472	374
		10:45 a.m.	1160	16.0	6.04	2.39	3.43	1550	< 0.05	488	373
		11:50 a.m.	1530	16.9	5.76	2.39	2.98	1470	0.11	487	374
		12:35 p.m.	1850	17.1	5.75	2.30	2.98	1400	0.11	480	375
		2:10 p.m.	2150	17.3	5.61	2.37	2.89	1330	< 0.05	487	376
		3:20 p.m.	1250	16.2	5.19	2.39	2.90	1350	< 0.05	485	377

METALLOID DATA

SUMMER Site	Distance (m)	Time	Sb^{III} µg/kg	Sb_{diss} µg/kg	Sb_{total} µg/kg	As^{III} µg/kg	As_{diss} µg/kg	As_{total} µg/kg
WT 2	30	8:45 a.m.	12.2	98.7	98.0	n/m	5690	7300
		10:45 a.m.	13.2	71.8	114	n/m	6470	7650
		12:40 p.m.	8.0	76.0	141	n/m	6790	8070
		2:05 p.m.	14.0	83.1	174	n/m	6590	8140
		3:15 p.m.	6.3	84.5	127	n/m	6570	7460
WT 3	150	9:05 a.m.	9.0	153	182	n/m	6080	6180
		11:05 a.m.	27.5	160	159	n/m	6560	7580
		12:55 p.m.	17.4	168	166	n/m	6860	8170
		2:20 p.m.	25.6	180	181	n/m	7040	8030
		3:30 p.m.	9.9	118	129	n/m	6590	7380
WT 5	205	9:25 a.m.	2.1	37.0	92.1	n/m	6150	7620
		11:20 a.m.	2.4	63.9	119	n/m	6660	7730
		1:05 p.m.	3.5	60.4	135	n/m	7550	9350
		2:30 p.m.	3.6	111	123	n/m	8380	10500
		3:40 p.m.	2.8	96.0	109	n/m	8170	10000
WT 6	225	9:40 a.m.	0.4	10.0	33.1	n/m	2040	2280
		11:40 a.m.	0.9	20.4	34.4	n/m	2070	2280
		1:20 p.m.	1.8	36.2	49.5	n/m	2290	3120
		2:40 p.m.	2.5	35.0	42.7	n/m	2200	2700
		3:55 p.m.	1.5	32.6	41.5	n/m	2250	2780
WT 7	260	9:55 a.m.	0.1	3.8	15.9	n/m	2050	2180
		11:50 a.m.	0.2	9.0	21.2	n/m	2100	2400
		1:30 p.m.	1.6	17.5	29.4	n/m	2170	2560
		2:45 p.m.	1.7	17.9	30.6	n/m	2070	2250
		4:00 p.m.	0.2	11.0	14.7	n/m	2000	2370
WT 8	320	10:25 a.m.	< 0.2	< 0.2	4.0	n/m	272	1000
		12:05 p.m.	< 0.2	< 0.2	3.9	n/m	310	1070
		1:50 p.m.	< 0.2	< 0.2	6.8	n/m	767	1340
		3:00 p.m.	< 0.2	< 0.2	6.5	n/m	1070	1340
		4:15 p.m.	< 0.2	< 0.2	6.0	n/m	820	1270

WINTER Site	Distance (m)	Time	Sb^{III} µg/kg	Sb_{diss} µg/kg	Sb_{total} µg/kg	As^{III} µg/kg	As_{diss} µg/kg	As_{total} µg/kg
WT 1	24	8:45 a.m.	4.8	14.9	65.1	4900	5670	5330
		10:00 a.m.	8.5	27.9	55.0	4600	5110	4820
		11:10 a.m.	29.3	46.2	59.6	4280	5540	5600
		1:15 p.m.	36.7	72.3	76.9	3620	5920	5820
		2:50 p.m.	114	153	301	2930	7780	8190
		4:05 p.m.	7.6	76.7	94.3	3450	5950	5920
WT 2	30	9:05 a.m.	14.6	44.7	72.2	3740	5960	5890
		10:15 a.m.	53.1	67.7	87.1	3070	5810	5810
		11:20 a.m.	48.4	62.1	85.6	2930	6080	5830
		1:05 p.m.	35.1	142	173	4220	6540	6420
		2:40 p.m.	93.6	154	160	4040	6400	6200
		3:55 p.m.	39.5	96.9	127	4380	6130	6130

WINTER Site	Distance (m)	Time	Sb^{III} µg/kg	Sb_{diss} µg/kg	Sb_{total} µg/kg	As^{III} µg/kg	As_{diss} µg/kg	As_{total} µg/kg
WT 3	150	9:15 a.m.	40.2	56.9	75.1	3400	5890	6090
		10:25 a.m.	80.3	109	130	1990	6330	6320
		11:30 a.m.	56.3	123	116	2820	6180	6190
		12:55 p.m.	97.0	163	176	1370	6220	6280
		2:30 p.m.	116	194	207	1900	6410	6470
		3:45 p.m.	112	184	213	1040	6570	6430
WT 4	200	9:25 a.m.	3.0	37.8	71.4	2800	5870	5750
		10:35 a.m.	2.7	44.4	78.7	2530	5780	5980
		12:00 p.m.	50.4	98.6	118	1470	6090	6110
		12:45 p.m.	56.8	114	125	1340	6330	6060
		2:20 p.m.	57.5	116	136	1260	6250	6250
		3:30 p.m.	75.6	119	151	984	6300	6510
WT 6	225	9:45 a.m.	0.2	1.3	2.0	81	251	316
		11:00 a.m.	0.4	1.0	1.8	68	208	290
		11:40 a.m.	0.5	1.9	3.3	78	269	347
		12:30 p.m.	0.4	1.5	2.4	64	233	293
		2:00 p.m.	0.3	1.3	1.8	58	227	253
		3:10 p.m.	0.5	2.2	2.4	59	236	294
WT 9	-20	9:35 a.m.	< 0.2	< 0.2	0.3	41	220	225
		10:45 a.m.	< 0.2	< 0.2	0.4	40	245	241
		11:50 a.m.	< 0.2	< 0.2	0.3	42	214	226
		12:35 p.m.	< 0.2	< 0.2	0.3	42	228	236
		2:10 p.m.	< 0.2	< 0.2	0.3	44	219	242
		3:20 p.m.	< 0.2	< 0.2	0.2	45	204	236

WAIMANGU

GENERAL CHEMISTRY DATA

JANUARY Site	Distance (m)	Time	Light (Lux)	Temperature (°C)	DO mg/L	pH	Conductivity mS/cm	Li µg/kg	H_2S mg/kg	SO_4 mg/kg	Cl mg/kg
WM 1	30	10:30 a.m.	95400	46.0	4.59	5.99	4.08	3150	<0.2	240	675
		11:50 a.m.	102000	46.6	4.96	6.04	4.05	3110	<0.2	238	676
		1:10 p.m.	29100	47.5	5.41	6.02	4.10	3400	<0.2	223	675
		2:20 p.m.	126000	47.0	4.76	5.99	4.09	3640	<0.2	228	675
		3:40 p.m.	121000	49.5	4.63	5.91	4.11	3310	<0.2	233	681
WM 2	130	10:10 a.m.	83200	33.4	4.71	6.15	4.08	3410	<0.2	253	674
		11:35 a.m.	48200	45.3	5.32	6.16	4.08	3130	<0.2	243	674
		12:55 p.m.	133000	43.8	6.25	6.30	4.04	3350	<0.2	231	663
		2:10 p.m.	123000	46.9	5.86	6.21	4.05	3710	<0.2	241	666
		3:30 p.m.	124000	44.8	5.31	6.17	4.12	3600	<0.2	237	685
WM 3	270	9:50 a.m.	7860	44.6	4.65	6.47	4.00	3260	<0.2	230	653
		11:25 a.m.	5920	47.5	5.29	6.46	4.04	2940	<0.2	228	663
		12:40 p.m.	8610	45.7	5.62	6.71	3.91	3130	<0.2	204	629
		1:50 p.m.	117000	48.7	5.58	6.65	3.96	3310	<0.2	233	642
		3:15 p.m.	86500	48.7	5.17	6.56	3.99	3540	<0.2	216	650
WM 4	285	9:30 a.m.	5380	46.2	4.73	6.50	3.89	3400	<0.2	226	626
		11:10 a.m.	7000	47.9	5.22	6.61	3.93	3140	<0.2	228	626
		12:30 p.m.	11400	47.6	5.44	6.77	3.91	3300	<0.2	223	630
		1:40 p.m.	93200	46.8	5.50	6.68	4.02	3600	<0.2	229	632
		3:00 p.m.	97100	47.5	4.95	3.11	4.96	4810	<0.2	301	745
WM 5	510	9:15 a.m.	10600	46.7	4.92	6.70	3.88	3350	<0.2	226	621
		10:50 a.m.	117000	48.3	5.54	6.77	4.11	3150	<0.2	229	682
		12:20 p.m.	124000	46.4	5.86	6.94	3.95	3220	<0.2	228	639
		1:30 p.m.	118000	48.7	5.64	6.95	4.00	3510	<0.2	237	653
		2:45 p.m.	98400	48.8	5.99	6.18	4.11	3930	<0.2	247	682

FEBRUARY Site	Distance (m)	Time	Light (Lux)	Temperature (°C)	DO mg/L	pH	Conductivity mS/cm	Li µg/kg	H_2S mg/kg	SO_4 mg/kg	Cl mg/kg
WM 5	510	11:29 a.m.	n/m	52.6	7.10	6.47	4.14	3570	n/m	218	623
WM 6	930	11:03 a.m.	n/m	46.7	4.01	7.70	3.73	3450	n/m	221	615
WM 7	1120	10:41 a.m.	n/m	34.8	5.34	7.80	1.81	2020	n/m	150	301
WM 8	1330	10:19 a.m.	n/m	36.9	5.16	7.54	1.92	1900	n/m	159	345
WM 9	1870	9:44 a.m.	n/m	21.9	5.94	7.06	1.30	1700	n/m	131	266
WB	1710	10:04 a.m.	n/m	21.0	6.07	6.53	0.57	343	n/m	139	64.5

AUGUST Site	Distance (m)	Time	Light (Lux)	Temperature (°C)	DO mg/L	pH	Conductivity mS/cm	Li µg/kg	H_2S mg/kg	SO_4 mg/kg	Cl mg/kg
WM 1	30	12:30 p.m.	n/m	44.0	10.20	6.00	3.52	2750	n/m	262	721
WM 3	270	12:10 p.m.	n/m	43.2	9.49	6.69	3.26	2530	n/m	241	657
WM 5	510	11:45 a.m.	n/m	43.9	7.20	6.92	3.27	2250	n/m	236	657
WM 6	930	11:20 a.m.	n/m	40.6	7.46	7.89	3.11	2420	n/m	233	637
WM 7	1120	11:00 a.m.	n/m	28.0	8.57	7.67	1.21	1480	n/m	138	263
WM 8	1330	10:40 a.m.	n/m	29.4	7.90	7.69	1.28	1410	n/m	135	270
WM 9	1870	9:50 a.m.	n/m	13.6	7.78	7.07	1.06	1600	n/m	123	281
WB	1710	10:20 a.m.	n/m	18.6	9.46	6.94	0.49	232	n/m	145	49.8

METALLOID DATA

JANUARY Site	Distance (m)	Time	Sb^{III} µg/kg	Sb_{diss} µg/kg	Sb_{total} µg/kg	As^{III} µg/kg	As_{diss} µg/kg	As_{total} µg/kg
WM 1	27	10:30 a.m.	1.5	14.5	15.9	n/m	674	781
		11:50 a.m.	1.5	13.9	16.5	n/m	694	774
		1:10 p.m.	1.5	13.1	16.1	n/m	746	759
		2:20 p.m.	1.5	12.5	15.7	n/m	752	792
		3:40 p.m.	1.3	12.7	15.6	n/m	636	776
WM 2	127	10:10 a.m.	1.5	16.3	16.2	n/m	697	741
		11:35 a.m.	1.5	15.4	16.3	n/m	708	780
		12:55 p.m.	1.5	15.5	16.4	n/m	672	812
		2:10 p.m.	1.4	15.4	15.8	n/m	837	835
		3:30 p.m.	1.3	14.7	15.4	n/m	652	760
WM 3	267	9:50 a.m.	1.1	13.1	15.5	n/m	686	695
		11:25 a.m.	1.2	13.4	16.1	n/m	615	761
		12:40 p.m.	1.2	13.2	15.3	n/m	639	738
		1:50 p.m.	1.2	12.8	15.5	n/m	641	682
		3:15 p.m.	0.5	12.7	15.4	n/m	681	702
WM 4	285	9:30 a.m.	1.3	14.1	15.4	n/m	738	747
		11:10 a.m.	1.2	14.3	15.7	n/m	652	666
		12:30 p.m.	1.3	14.1	15.7	n/m	636	658
		1:40 p.m.	1.2	13.4	15.4	n/m	683	725
		3:00 p.m.	0.4	9.9	10.8	n/m	910	943
WM 5	507	9:15 a.m.	1.3	13.9	14.9	n/m	618	661
		10:50 a.m.	1.3	15.0	15.4	n/m	592	631
		12:20 p.m.	1.4	15.0	15.7	n/m	593	668
		1:30 p.m.	1.4	14.9	15.7	n/m	693	723
		2:45 p.m.	1.1	13.8	15.0	n/m	733	789

FEBRUARY Site	Distance (m)	Time	Sb^{III} µg/kg	Sb_{diss} µg/kg	Sb_{total} µg/kg	As^{III} µg/kg	As_{diss} µg/kg	As_{total} µg/kg
WM 5	510	11:29 a.m.	n/m	16.0	16.1	n/m	648	649
WM 6	930	11:03 a.m.	n/m	15.9	16.4	n/m	560	614
WM 7	1120	10:41 a.m.	n/m	8.8	8.8	n/m	331	372
WM 8	1330	10:19 a.m.	n/m	9.9	10.1	n/m	376	404
WM 9	1870	9:44 a.m.	n/m	2.7	2.7	n/m	232	240
WB	1710	10:04 a.m.	n/m	3.5	3.4	n/m	67.3	68.7

AUGUST Site	Distance (m)	Time	Sb^{III} µg/kg	Sb_{diss} µg/kg	Sb_{total} µg/kg	As^{III} µg/kg	As_{diss} µg/kg	As_{total} µg/kg
WM 1	30	12:30 p.m.	0.8	21.5	21.2	19.1	761	759
WM 3	270	12:10 p.m.	0.9	19.9	19.6	25.4	691	686
WM 5	510	11:45 a.m.	0.9	19.1	18.9	21.3	677	700
WM 6	930	11:20 a.m.	0.7	18.8	18.5	17.9	680	683
WM 7	1120	11:00 a.m.	0.3	9.3	9.2	8.8	294	298
WM 8	1330	10:40 a.m.	0.4	10.6	10.4	15.8	310	317
WM 9	1870	9:50 a.m.	0.1	4.4	4.5	5.8	211	207
WB	1710	10:20 a.m.	0.0	3.8	3.8	1.1	63.2	62.1

APPENDIX III:
RESULTS FROM RECEIVING ENVIRONMENTS

AQUEOUS DATA

WAIOTAPU STREAM DATA

SUMMER	Distance	Temp	DO	pH	Cond	Li	SO_4	Cl	Sb^{III}	Sb_{diss}	Sb_{tot}	As^{III}	As_{diss}	As_{tot}
Site	km	°C	mg/L		µS/cm	µg/kg	mg/kg	mg/kg	µg/kg	µg/kg	µg/kg	µg/kg	µg/kg	µg/kg
WK	20	43.1	5.56	4.64	1860	2150	129	322	n/m	34.5	33.1	n/m	774	833
WS 2	18	30.0	7.17	5.49	802	884	97.7	142	n/m	8.0	8.3	n/m	39.2	98.0
WS 3	12	24.1	8.54	6.37	567	626	67.9	106	n/m	5.0	5.0	n/m	43.5	88.3
WS 4	9	23.7	8.55	6.41	541	589	67.5	108	n/m	4.6	4.6	n/m	61.4	85.2
WS 5	6	21.9	6.51	6.12	464	603	54.5	85.5	n/m	3.9	3.9	n/m	51.6	86.9
MK	14	15.6	8.97	6.32	75.9	13.1	3.2	6.5	n/m	< 0.2	< 0.2	n/m	3.2	3.8

WINTER	Distance	Temp	DO	pH	Cond	Li	SO_4	Cl	Sb^{III}	Sb_{diss}	Sb_{tot}	As^{III}	As_{diss}	As_{tot}
Site	km	°C	mg/L		µS/cm	µg/kg	mg/kg	mg/kg	µg/kg	µg/kg	µg/kg	µg/kg	µg/kg	µg/kg
HK	24	32.0	7.50	3.10	910	697	150	94.9	< 0.2	4.4	4.9	3.4	40.5	146
WO	24	13.0	9.35	6.23	96.4	29.4	16.4	7.9	< 0.2	4.1	4.7	6.7	39.0	134
WK	20	39.0	6.48	3.76	1580	4640	117	302	< 0.2	5.2	6.3	6.9	40.5	149
WS 1	21	26.3	8.01	3.33	785	615	116	132	< 0.2	6.2	7.6	7.7	30.5	204
WS 2	18	24.6	7.47	5.35	652	852	100	140	0.3	9.7	11.2	13.1	52.5	210
WS 3	12	19.2	7.74	6.22	500	591	71.1	106	1.6	7.3	10.3	13.9	204	253
WS 4	9	17.9	7.50	6.51	350	445	63.6	92.9	3.3	38.9	38.3	41.6	631	718
WS 5	6	16.1	7.28	6.66	351	336	53.0	74.5	< 0.2	5.3	5.8	15.6	96.0	131
WS 6	3	15.1	7.15	6.70	341	350	50.0	68.4	< 0.2	< 0.2	< 0.2	0.8	2.4	2.5

WAIKATO RIVER DATA

SUMMER '06 Site	Distance km	Temperature °C	DO mg/kg	pH	Conductivity µS/cm	Li µg/kg	Sb_{diss} µg/kg	Sb_{tot} µg/kg	As_{diss} µg/kg	As_{tot} µg/kg
WR 1	1	20.7	n/m	7.74	122.3	47.0	0.4	0.3	9.1	9.9
WR 2	13	23.6	n/m	8.10	171.1	161	1.2	1.2	26.1	27.4
WR 3	40	23.0	n/m	7.30	191.4	137	1.1	1.1	22.3	23.4
WR 4a	49	21.7	n/m	7.20	213.0	167	1.5	1.4	20.9	22.9
WR 5	79	22.5	n/m	7.20	176.3	148	1.1	1.0	21.1	21.9
WR 6	105	22.4	n/m	7.20	156.9	113	0.8	0.8	17.8	19.4
WR 8	155	21.3	n/m	6.95	168.6	118	0.9	0.9	20.7	21.6
WR 10	205	21.0	n/m	7.05	166.8	110	0.9	0.8	21.5	21.9
WR 12	250	20.0	n/m	7.13	162.9	130	0.8	0.9	19.2	20.8

WINTER '06 Site	Distance km	Temperature °C	DO mg/kg	pH	Conductivity µS/cm	Li µg/kg	Sb_{diss} µg/kg	Sb_{tot} µg/kg	As_{diss} µg/kg	As_{tot} µg/kg
WR 1	1	11.0	9.85	7.33	118	45.9	0.2	0.2	10.3	10.9
WR 2	13	12.0	11.8	7.42	138	93.1	0.3	0.3	24.2	24.7
WR 3	40	11.8	11.0	7.06	138	90.8	0.3	0.5	18.5	21.5
WR 4	62	12.0	10.2	6.96	144	94.1	0.5	0.4	18.9	18.3
WR 5	79	12.3	9.34	7.02	159	110	0.6	0.7	25.4	27.5
WR 6	105	12.3	8.61	7.02	159	99.1	0.6	0.6	20.7	25.7
WR 7	130	12.2	9.02	7.03	137	90.0	0.4	0.3	16.9	n/m
WR 8	155	12.2	10.2	7.10	137	89.3	0.6	0.6	17.6	17.3
WR 9	180	11.7	9.96	7.17	142	83.6	0.6	0.6	17.1	18.9
WR 10	205	11.4	9.93	7.18	140	84.4	0.6	0.6	17.8	17.8
WR 11	225	11.4	10.8	7.17	145	91.0	0.4	0.4	16.5	17.5
WR 12	250	11.0	11.0	6.79	148	68.9	0.4	0.5	13.4	12.6
WR 13	288	11.4	8.77	6.86	131	33.8	0.4	0.3	5.4	8.3

SUMMER '07	Distance	Temperature	DO	pH	Conductivity	Li	Sb_{diss}	Sb_{tot}	As_{diss}	As_{tot}
Site	km	°C	mg/kg		µS/cm	µg/kg	µg/kg	µg/kg	µg/kg	µg/kg
WR 1	1	21.8	8.5	6.80	111	43.1	0.3	0.3	8.0	8.3
WR 2	13	24.4	10.8	7.71	150	106	1.0	1.0	25.3	26.6
WR 3	40	23.2	8.6	6.89	161	133	1.0	1.1	26.5	31.9
WR 4	62	23.0	7.9	6.59	150	103	0.9	1.1	22.3	31.9
WR 5	79	22.7	9.5	6.89	156	126	1.0	1.1	24.6	26.4
WR 6	105	23.5	10.4	7.94	153	121	1.0	0.9	24.7	20.9
WR 7	130	22.4	9.0	6.78	152	113	0.9	0.9	22.7	24.4
WR 8	155	23.3	10.1	7.11	161	136	1.0	1.0	23.4	26.5
WR 9	180	22.7	9.2	6.86	154	112	0.9	0.9	22.7	25.1
WR 10	205	22.2	8.3	6.97	156	132	0.8	0.9	23.5	24.5
WR 11	225	21.6	8.3	6.83	155	120	0.8	0.8	22.9	24.8
WR 12	250	21.3	8.6	7.04	155	125	0.8	0.9	22.5	23.9
WR 13	288	21.7	8.8	6.86	156	117	0.7	0.8	19.4	20.9

WINTER '07	Distance	Temperature	DO	pH	Conductivity	Li	Sb_{diss}	Sb_{tot}	As_{diss}	As_{tot}
Site	km	°C	mg/kg		µS/cm	µg/kg	µg/kg	µg/kg	µg/kg	µg/kg
WR 1	1	11.8	10.4	6.79	86.0	49.5	0.2	0.3	9.4	9.9
WR 2	13	14.8	12.1	6.73	146	158	1.1	1.1	45.6	45.3
WR 3	40	14.7	9.86	6.42	162	181	1.0	1.1	35.8	42.3
WR 4	62	13.4	9.96	6.56	146	163	0.9	1.0	26.2	37.7
WR 5	79	13.2	11.3	6.69	130	134	0.7	0.9	25.3	31.6
WR 6	105	12.7	10.5	6.71	116	122	0.6	0.6	20.9	23.0
WR 7	130	12.3	10.4	6.71	110	92.3	0.4	0.5	16.5	18.7
WR 8	155	12.9	12.6	6.81	108	86.7	0.4	0.5	16.6	17.6
WR 9	180	11.8	10.8	6.65	105	86.4	0.4	0.5	14.6	16.3
WR 10	205	11.9	10.3	6.70	106	93.1	0.4	0.4	14.5	16.5
WR 11	225	11.9	11.1	6.48	107	90.6	0.4	0.5	13.4	16.0
WR 12	250	11.9	8.62	6.32	92.4	45.8	0.1	0.2	5.3	6.9
WR 13	288	12.5	8.77	6.19	107	44.4	0.2	0.2	4.4	6.4

LAKES

LAKE	Depth m	Temp °C	DO mg/kg	pH	Conductivity µS/cm	Na mg/kg	K mg/kg	Mg mg/kg	Ca mg/kg	Cl mg/kg	SO_4 mg/kg	NO_3 mg/kg	H_2S mg/kg
Ohakuri	0	19.9	8.22	7.27	174	n/m	n/m	n/m	n/m	24.7	10.7	2.6	< 0.02
	20	19.3	7.63	7.16	183	n/m	n/m	n/m	n/m	25.3	11.2	3.6	< 0.02
	25	18.8	6.43	6.77	168	n/m	n/m	n/m	n/m	n/m	n/m	n/m	n/m
	30	18.5	3.31	6.62	153	20.3	3.3	3.3	5.9	n/m	n/m	n/m	n/m
	35	18.0	3.10	6.81	153	n/m	n/m	n/m	n/m	n/m	n/m	n/m	n/m
	40	19.1	2.78	6.90	151	n/m	n/m	n/m	n/m	19.1	9.5	2.3	0.024
Maraetai	0	18.9	7.64	7.24	155	n/m	n/m	n/m	n/m	20.4	9.7	1.4	< 0.02
	20	18.3	8.01	7.38	154	n/m	n/m	n/m	n/m	20.4	9.5	3.2	< 0.02
	40	18.4	8.01	7.60	139	n/m	n/m	n/m	n/m	18.5	8.2	3.4	< 0.02
Arapuni	0	21.5	7.81	7.81	154	n/m	n/m	n/m	n/m	19.4	9.8	1.6	< 0.02
	20	21.1	7.71	7.51	153	n/m	n/m	n/m	n/m	18.9	9.6	1.4	< 0.02
	40	21.0	7.60	7.46	155	n/m	n/m	n/m	n/m	18.9	9.6	1.5	< 0.02

LAKE	Depth m	Sb_{diss} µg/kg	Sb_{tot} µg/kg	As_{diss} µg/kg	As_{tot} µg/kg	Li µg/kg	Fe_{diss} µg/kg	Fe_{tot} µg/kg	Mn_{diss} µg/kg	Mn_{tot} µg/kg
Ohakuri	0	1.5	1.5	48.9	52.7	163	68.2	128	2.5	23.2
	20	1.5	1.5	53.4	56.0	164	66.3	131	4.1	27.5
	40	0.9	1.2	57.3	138	124	292	1730	217	271
Maraetai	0	1.1	1.1	41.0	42.3	130	51.4	80.9	2.5	11.7
	20	1.1	1.1	42.6	44.1	120	40.8	101	1.7	17.2
	40	0.9	0.9	38.1	39.3	104	53.5	136	9.9	25.1
Arapuni	0	0.9	0.9	38.5	39.6	103	37.5	74.2	3.3	16.1
	20	0.9	0.9	37.8	39.1	106	42.7	101	2.3	17.4
	40	0.9	0.9	39.1	39.6	115	42.7	92.9	2.6	19.0

TUAKAU

Month	Temperature °C	DO mg/kg	pH	Conductivity µS/cm	Flow m^3/s	Li µg/kg	Sb_{diss} µg/kg	Sb_{tot} µg/kg	As_{diss} µg/kg	As_{tot} µg/kg
Feb-06	24.7	7.02	7.30	126	367	77.5	0.4	0.4	14.9	18.0
Mar-06	20.9	9.43	8.48	161	293	88.7	0.3	0.3	21.5	21.7
Apr-06	21.7	7.81	7.74	153	269	96.9	0.5	0.5	18.0	20.6
May-06	18.8	7.72	7.02	140	624	65.7	0.6	0.5	12.8	14.2
Jun-06	12.8	7.48	7.00	119	575	52.0	0.2	0.2	9.0	10.9
Jul-06	14.7	8.49	7.12	129	472	62.7	0.3	0.2	12.9	15.3
Aug-06	13.0	9.19	7.11	151	524	72.7	0.3	0.3	13.7	15.9
Sep-06	14.8	10.3	7.31	123	477	56.5	0.3	0.3	9.3	13.9
Oct-06	16.3	8.43	7.14	123	496	64.6	0.3	0.4	11.3	18.8
Nov-06	18.0	8.41	7.59	127	426	79.7	0.4	0.4	18.4	24.7
Dec-06	18.7	8.55	7.41	113	453	82.7	0.3	0.3	17.4	23.6
Jan-07	18.7	9.13	6.64	145	262	83.4	0.4	0.3	19.5	22.7
Feb-07	22.7	9.17	7.18	160	284	114	0.5	0.5	22.3	24.1
Mar-07	23.5	9.50	7.90	163	290	114	0.6	0.7	24.6	29.3
Apr-07	20.5	8.27	7.40	151	247	75.2	0.8	0.7	17.8	20.8
May-07	17.3	8.89	7.08	152	246	103	0.5	0.4	19.0	20.8
Jun-07	14.9	10.1	5.72	138	284	119	0.9	1.0	25.9	26.0
Jul-07	11.7	11.1	5.51	119	469	80.0	0.6	0.8	16.1	15.6
Aug-07	11.5	8.17	6.23	101	817	50.5	0.2	0.2	5.1	6.7
Sep-07	13.7	9.92	6.29	122	375	74.4	0.4	0.4	10.9	12.9
Oct-07	15.9	11.3	7.32	114	403	76.5	0.5	0.4	13.5	14.9
Nov-07	16.1	8.51	7.03	111	489	62.8	0.4	0.4	11.2	14.7
Dec-07	20.5	7.67	7.60	154	253	96.7	0.6	0.6	24.4	28.0
Jan-08	Data missing				170	99.2	0.8	0.8	28.5	30.9

SEDIMENT DATA

WAIOTAPU STREAM

SUMMER '07 SPM Site	Distance km	Sb mg/kg	As mg/kg	Fe wt %	Mn wt %
WK	20	178	1040	1.30	< 60
WS 2	18	74.0	4050	8.05	< 60
WS 3	12	31.6	1560	9.14	< 60
WS 4	9	25.1	1440	8.84	284
WS 5	6	27.3	1230	9.62	527
MK	14	1.7	5.1	8.06	965

WINTER '07 SPM Site	Distance km	Sb mg/kg	As mg/kg	Fe wt %	Mn wt %
HK	24	27.2	3320	4.32	< 60
WO	24	12.9	18	3.97	< 60
WK	20	270	5360	5.25	< 60
WS 1	21	448	15400	8.56	< 60
WS 2	18	110	10500	6.74	< 60
WS 3	12	43.4	7710	8.55	261
WS 4	9	12.4	5290	7.51	373
WS 5	6	25.5	3110	5.92	477
WS 6	3	6.7	2150	4.52	425

BED SEDIMENT Site	Distance km	Sb mg/kg	As mg/kg	Fe wt %	Mn mg/kg
WO	24	0.9	41.6	2.39	200
WK	20	205	775	5.66	< 60
WS 2	18	49.5	3460	7.72	80.4
WS 3	12	21.4	1150	3.48	210
WS 4	9	14.5	1050	2.97	267
WS 5	6	16.3	1000	2.38	220
WS 6	3	4.8	680	1.54	346

WAIMANGU

SUMMER '07 Site	Distance km	Sb mg/kg	As mg/kg	Fe wt %	Mn wt %
WM 7	930	< 2.0	< 5.0	1.42	0.11
WM 8	1120	< 2.0	220	2.33	0.18
WM 9	1870	6.8	25.8	0.98	0.15
WB	1710	5.8	11.9	0.79	0.03

WINTER '07 Site	Distance km	Sb mg/kg	As mg/kg	Fe wt %	Mn wt %
WM 1	30	22.6	160	1.43	<0.10
WM 3	270	16.8	234	1.85	<0.10
WM 5	510	23.9	189	1.88	<0.10
WM 6	930	14.8	99.4	1.66	<0.10
WM 7	1120	18.8	135	4.66	0.10
WM 8	1330	33.3	135	4.92	0.13
WM 9	1870	18.8	219	3.41	0.47
WB	1710	9.3	16.8	1.79	<0.10

WAIKATO RIVER

SUMMER '07 SPM Site	Distance km	Sb mg/kg	As mg/kg	Fe wt %	Mn wt %
WR 1	1	2.5	46.3	1.52	< 0.06
WR 2	13	7.9	124	1.32	< 0.06
WR 3	40	10.1	731	2.08	< 0.04
WR 4	49	11.8	1080	3.73	0.10
WR 5	79	7.1	331	2.52	0.19
WR 6	105	4.7	186	1.57	0.18
WR 7	130	3.8	424	2.38	0.45
WR 8	155	2.9	335	2.72	0.50
WR 9	180	4.0	359	2.04	0.49
WR 10	205	1.1	341	1.67	0.26
WR 11	225	4.0	400	2.89	0.62
WR 12	250	2.6	218	3.02	0.59
WR 13	288	1.9	193	2.84	0.43

WINTER '07 SPM Site	Distance km	Sb mg/kg	As mg/kg	Fe wt %	Mn wt %
WR 1	1	2.1	148	4.42	< 0.16
WR 2	13	10.8	62.6	1.08	< 0.04
WR 3	40	27.3	4450	8.17	< 0.08
WR 4	49	35.5	4760	10.8	0.06
WR 5	79	28.6	2580	7.48	0.18
WR 6	105	14.3	1340	6.02	0.22
WR 7	130	5.3	549	4.61	0.40
WR 8	155	11.1	469	4.75	0.29
WR 9	180	5.0	270	3.60	0.20
WR 10	205	5.1	198	4.01	0.21
WR 11	225	5.2	180	3.98	0.19
WR 12	250	2.0	43.2	4.59	0.16
WR 13	288	2.7	49.5	4.06	0.10

BED SEDIMENT Site	Distance km	Sb mg/kg	As mg/kg	Fe wt %	Mn wt %
WR 1	1	1.1	11.3	2.71	0.03
WR 2	13	0.6	8.9	0.91	0.02
WR 3	40	2.6	64.3	1.94	0.05
WR 4	49	4.9	335	1.60	0.06
WR 5	79	8.3	383	4.17	0.15
Maraetai	100	6.7	264	3.35	0.14
WR 6	105	6.7	225	2.87	0.17
WR 7	130	2.4	209	2.54	0.25
WR 8	155	3.3	194	2.59	0.27
WR 9	180	5.6	78.9	1.78	0.06
WR 10	205	1.4	208	2.60	0.11
WR 11	225	1.4	52.6	2.82	0.08
WR 12	250	1.2	42.3	3.07	0.18
WR 13	288	3.3	71.6	2.66	0.11
WR 14	300	0.8	106	2.67	0.19
WR 15	325	1.9	48.9	2.68	0.11

PLANTS

Type	Location	Sb mg/kg	As mg/kg
Waimangu algae	WM 1	25.3	738
	WM 3	31.3	2330
	WM 5	12.3	529
Lake macrophyte	Taupo	0.1	22
	Aratiatia	0.3	52
	Ohakuri	0.3	105
	Whakamaru	0.7	210
	Maraetai	0.5	520
	Waipapa	0.1	478
	Arapuni	0.2	455
	Karapiro	0.1	215

TUAKAU

Month	Sb mg/kg	As mg/kg	Fe wt %	Mn wt %
Aug-06	2.0	245	4.51	0.29
Sep-06	1.4	184	3.39	0.17
Oct-06	1.2	211	4.56	0.20
Nov-06	1.8	353	4.90	0.38
Dec-06	1.8	222	3.36	0.27
Jan-07	1.0	111	1.79	0.18
Feb-07	1.0	84.3	1.35	0.14
Mar-07	2.6	204	2.32	0.37
Apr-07	1.3	175	2.65	0.19
May-07	2.6	181	3.89	0.22
Jun-07	2.1	106	2.01	0.17
Jul-07	2.8	218	4.19	0.26
Aug-07	1.4	63.8	4.20	0.16
Sep-07	1.1	229	4.48	0.20
Oct-07	2.1	201	3.72	0.28
Nov-07	1.3	110	4.38	0.13
Dec-07	1.6	216	4.50	0.36
Jan-08	1.2	100	1.64	0.20
WR 15 (Jun-07)	0.8	72.5	2.11	0.08

APPENDIX IV:
ADSORPTION EDGE RESULTS

SB^V DATA

Season	pH	Sb in solution µg/kg	Adsorbed Sb %
Winter	2.66	6.7	37
	3.18	7.3	32
	3.59	8.7	18
	4.11	9.6	10
	4.68	9.9	7
	5.54	10.3	4
	6.34	10.4	2
	6.35	10.4	2
	7.03	10.5	2
	7.06	10.6	1
	7.81	10.4	2
	8.70	10.1	5
	9.46	10.6	0
	9.94	10.4	2
Spring	2.58	6.6	33
	3.02	6.4	36
	3.54	7.6	24
	4.02	8.4	16
	4.62	9.4	6
	5.55	9.8	2
	5.89	9.9	1
	6.27	9.9	1
	6.45	9.9	1
	6.81	10.0	0
	7.10	10.0	0
	7.14	10.0	0
	8.23	10.0	0
	8.70	10.0	0
	8.90	10.0	0
	9.92	9.9	1
	10.52	9.9	1

Note: Temperature = 25 ^oC, SPM = 100 mg/kg, Sb = 10 µg/kg

SB^{III} DATA

pH	Sb in solution µg/kg	Adsorbed Sb %
6.91	3.3	68
6.58	3.1	70
6.57	2.8	72
6.52	2.8	72
6.25	2.6	75
6.15	2.3	77
5.51	1.9	81
4.88	2.0	81
4.55	2.0	81
3.95	1.8	82
3.35	1.7	84

Note: Temperature = 25 °C, SPM = 100 mg/kg, Sb = 10 µg/kg

TIME EXPERIMENT

	Days	Sb in solution µg/kg	Adsorbed Sb %
pH 3	0	10.2	4
	1	6.7	38
	2	6.4	40
	3	5.2	52
	5	4.6	57
	7	4.4	59
	10	4.6	57
pH 7	0	10.7	0
	1	10.5	0
	2	10.4	2
	3	10.4	3
	5	10.3	4
	7	10.0	6
	10	9.5	11

Note: Temperature = 25 °C, SPM = 100 mg/kg, Sb = 10 µg/kg

APPENDIX V:
LAKE MAPS

Presented below are topographic maps for the three lakes for which depth profiles were taken, all adapted from the NZ 260 1:50 000 series. Approximate sampling sites are marked as blue circles.

LAKE OHAKURI

LAKE ARAPUNI

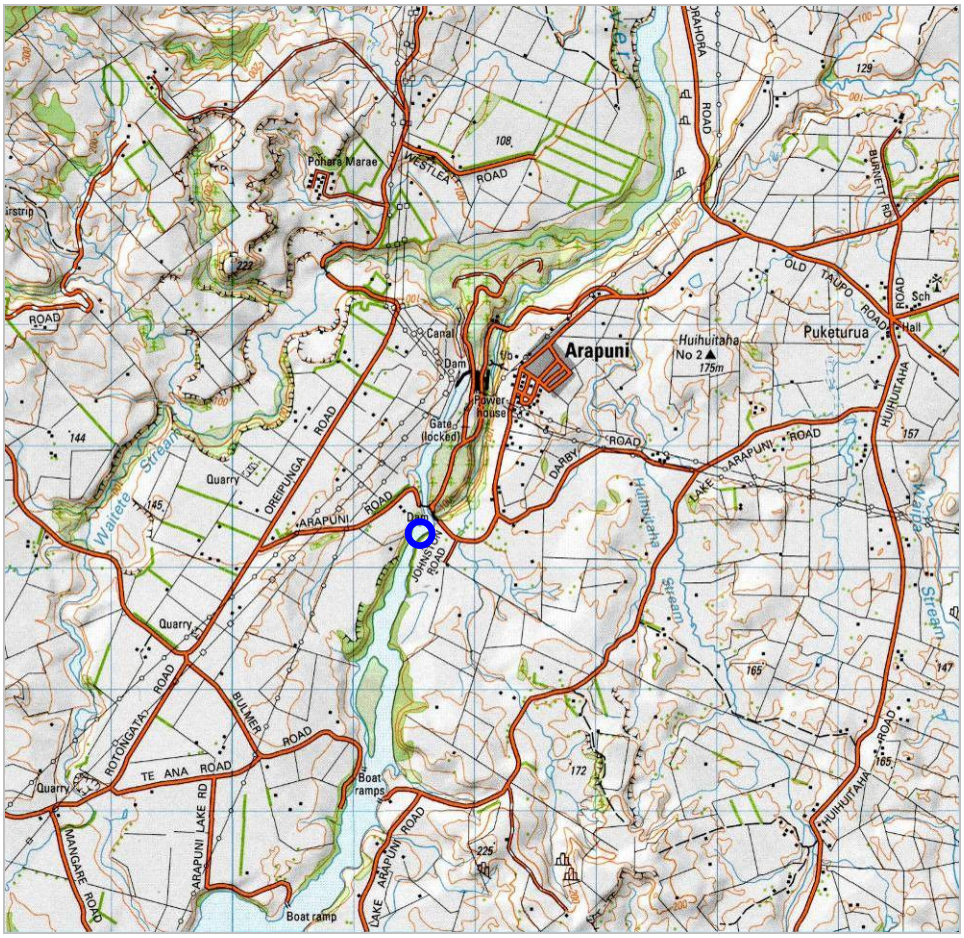

LAKE MARAETAI

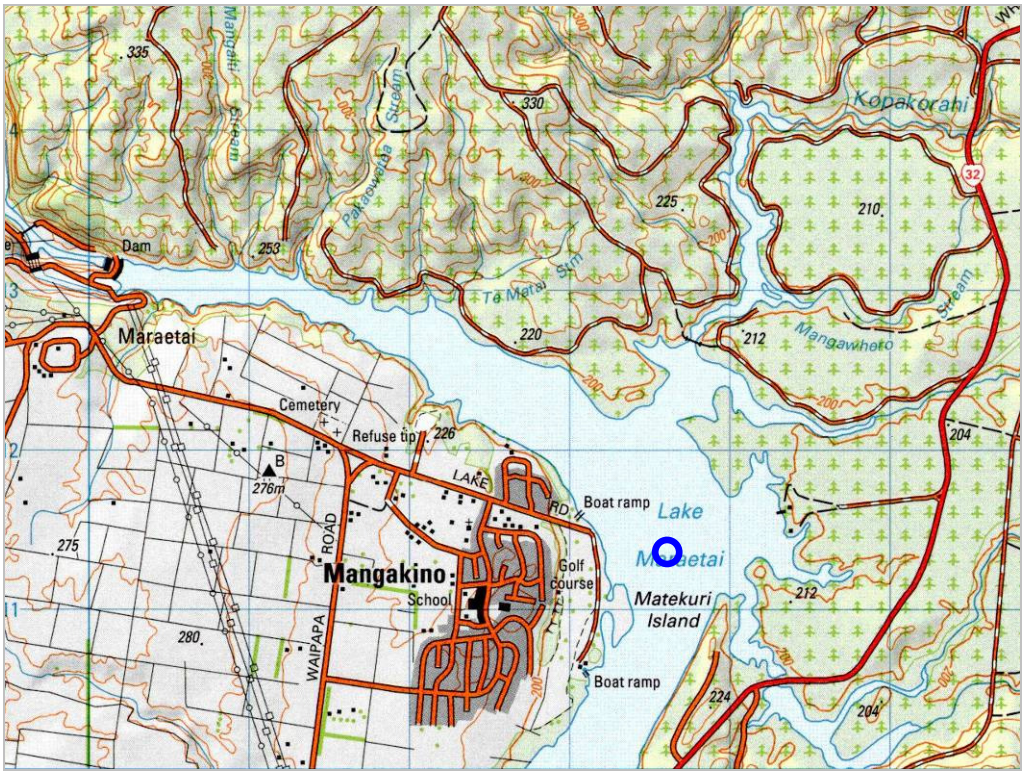

INDEX

LIST OF FIGURES

LIST OF TABLES

LIST OF PLATES